

TL  
242  
.T27

DOT HS-801-969

# CRASHWORTHINESS OF THE SUBCOMPACT VEHICLE

Contract No. DOT-HS-113-3-746

August 1976

Final Report

PREPARED FOR:

U.S. DEPARTMENT OF TRANSPORTATION

National Highway Traffic Safety Administration

Washington, D.C. 20590

Document is available to the public through  
the National Technical Information Service,  
Springfield, Virginia 22161.

The opinions, findings, and conclusions expressed in this publication are those of the authors and not necessarily those of the National Highway Traffic Safety Administration.

1. Report No. DOT HS-801 969		2. Government Accession No.		3. Recipient's Catalog No.	
4. Title and Subtitle Crashworthiness of the Subcompact Vehicle.				5. Report Date August 1976	
				6. Performing Organization Code	
7. Author(s) Richard B. Tanner,				8. Performing Organization Report No. DOT-HS-113-3-746	
9. Performing Organization Name and Address Minicars, Inc. 35 La Patera Lane Goleta, California 93017				10. Work Unit No. (TRAIS)	
				11. Contract or Grant No. DOT HS-113-3-746	
12. Sponsoring Agency Name and Address Department of Transportation National Highway Safety Administration Washington, D.C. 20590				13. Type of Report and Period Covered Final Report 6/73 -- 10/75	
				14. Sponsoring Agency Code	
15. Supplementary Notes					
16. Abstract <p>This study examined the crashworthiness of subcompact vehicles both analytically and experimentally. The analytical studies included statistical accident analysis and dynamic response modeling. Experimental testing to determine baseline performance consisted of ten dynamic impacts at various angles and velocities. The 1974 production Pinto sedan provided adequate crashworthiness for 40 mph BEV aligned frontal impacts, 30 mph BEV offset and oblique frontal impacts, and 12 mph BEV side impacts.</p> <p>A modified design was developed which improved the crashworthiness in the most significant modes. Specifically, the modified design provides safety in the frontal aligned mode to at least 50 mph BEV, in the offset and oblique modes to at least 50 mph, and in the side impact mode to at least 30 mph.</p> <p>The modified design relies on extensive use of foam-filled sheetmetal sections throughout the vehicle. The all-directional nature of volumetric structures provides good energy management in all impact modes. At the same time, the weight of the vehicle was increased only 5.3% over the baseline vehicle.</p>					
17. Key Words Crashworthiness Structural Stiffness Subcompact vehicle Foam filled sheet metal Volumetric managment			18. Distribution Statement Document is available to the public through the National Technical Information Service, Springfield, Virginia 22161		
19. Security Classif. (of this report) Unclassified		20. Security Classif. (of this page) Unclassified		21. No. of Pages 300	22. Price



## TABLE OF CONTENTS

	<u>Page</u>
1.0 Program Description and Executive Summary . . . . .	1.1
1.1 Conclusions . . . . .	1.1
1.2 Background . . . . .	1.3
1.3 Task Description . . . . .	1.5
1.4 Method of Approach . . . . .	1.10
1.4.1 Evaluation of the Problem . . . . .	1.10
1.4.2 The State of the Art . . . . .	1.14
1.4.3 Conceptualization of Possible Designs . . . . .	1.17
1.4.4 Development and Verification of the Final Modifications . . . . .	1.18
1.5 Program Highlights . . . . .	1.19
2.0 Mathematical Studies . . . . .	2.1
2.1 Accident Analysis . . . . .	2.2
2.1.1 Introduction . . . . .	2.2
2.1.2 Methodology . . . . .	2.2
2.1.3 Interpretation of Results . . . . .	2.24
2.2 Compatibility Analysis . . . . .	2.25
2.2.1 Introduction . . . . .	2.25
2.2.2 Methodology . . . . .	2.26
2.2.3 Compatibility of the Unmodified 1974 Pinto Sedan . . . . .	2.36
2.2.4 Study of Restraint Modifications . . . . .	2.48
2.2.5 Study of the Compatibility of Modified Subcompact Vehicles . . . . .	2.52
2.2.6 Conclusions and Recommendations . . . . .	2.59
2.3 Study of Finite Element Techniques to Develop Force Deflection Characteristics . . . . .	2.62
2.3.1 Introduction . . . . .	2.62
2.3.2 Methodology . . . . .	2.63
2.3.3 Description of Models . . . . .	2.65
2.3.4 Discussion of Model I Run . . . . .	2.70
2.3.5 Discussion of Model II Run . . . . .	2.70
2.3.6 Conclusions and Recommendations . . . . .	2.73
3.0 Frontal Impact Crashworthiness . . . . .	3.1
3.1 Summary and Introduction . . . . .	3.1
3.1.1 Summary . . . . .	3.1
3.1.2 Introduction . . . . .	3.2
3.2 Evaluation of the Design . . . . .	3.3
3.2.1 Design Approach . . . . .	3.3

TABLE OF CONTENTS (Cont'd)

	<u>Page</u>
3.2.2	Rigidization of the Compartment. . . . . 3.10
3.2.3	Alternate Energy Absorbers . . . . . 3.16
3.2.4	Evaluation of Linear Absorber System . . 3.25
3.2.5	Evaluation of Volumetric Structures. . . 3.31
3.3	Frontal Barrier Impact. . . . . 3.50
3.3.1	Baseline Impacts . . . . . 3.50
3.3.1.1	20 mph Frontal Aligned Barrier Baseline Test, 01 . . . . . 3.50
3.3.1.2	40 mph Frontal Aligned Barrier Baseline Test, 02 . . . . . 3.55
3.3.1.3	30 mph Frontal Aligned Barrier Baseline Test, 03 . . . . . 3.58
3.3.1.4	50 mph Frontal Aligned Barrier Baseline Test, 09 . . . . . 3.61
3.3.1.5	Discussion of Baseline Tests. . 3.64
3.3.2	Evaluation Tests . . . . . 3.69
3.3.2.1	50 mph Frontal Aligned Barrier Evaluation Test, E1 . . . . . 3.69
3.3.2.2	50 mph Frontal Aligned Barrier Evaluation Test, E1A. . . . . 3.73
3.4	Frontal Aligned Subcompact-to-Standard Impacts. 3.82
3.4.1	80 mph Frontal Aligned Large Car to Small Car Baseline Test, 08. . . . . 3.82
3.4.2	80 mph Frontal Aligned Large Car to Small Car Evaluation Test, E25 . . . . . 3.85
3.4.3	Comparison of Results. . . . . 3.90
3.5	Oblique Barrier Impact - 50 mph . . . . . 3.90
3.5.1	50 mph 30° Oblique Barrier Baseline Test, 10 . . . . . 3.90
3.5.2	45 mph 30° Oblique Frontal Barrier Evaluation Test, E15 . . . . . 3.97
3.5.3	50 mph 30° Oblique Frontal Barrier Evaluation Test, E24 . . . . . 3.100
3.6	Offset Subcompact-to-Standard Impacts . . . . . 3.103
3.6.1	80 mph Frontal Offset Large Car to Small Car Baseline Test, 06. . . . . 3.103
3.6.2	70 mph Frontal Offset Large Car to Small Car Evaluation Test, E17 . . . . . 3.109
3.6.3	80 mph Offset Large Front to Small Front Evaluation Test, E21 . . . . . 3.109

TABLE OF CONTENTS (Cont'd)

	<u>Page</u>
3.7 Subcompact-to-Standard Vehicle Oblique Impact, 04 . . . . .	3.117
4.0 Side Impact Crashworthiness . . . . .	4.1
4.1 Evolution of Design . . . . .	4.2
4.1.1 Design Approach . . . . .	4.2
4.1.2 Final Design of the Side Structure . . . . .	4.6
4.1.3 Development Testing . . . . .	4.9
4.1.3.1 Introduction . . . . .	4.9
4.1.3.2 Static Crush Tests . . . . .	4.11
4.1.3.3 Dynamic Tests . . . . .	4.13
4.2 Front-to-Side Impact . . . . .	4.16
4.2.1 30 mph 270° Large Front to Small Side Baseline Test, 05 . . . . .	4.16
4.2.2 30 mph 370° Large Front to Small Side Evaluation Test, E9 . . . . .	4.23
4.2.3 Evaluation of Results . . . . .	4.23
4.3 Side Pole Impact . . . . .	4.26
4.3.1 20 mph Side Pole Evaluation Tests, E3 and E3A . . . . .	4.26
4.3.2 Evaluation of Results . . . . .	4.32
4.4 Front-to-Side Oblique Impact . . . . .	4.32
4.4.1 30 mph 300° Small Front to Small Side Baseline Test, E22 . . . . .	4.32
4.4.2 30 mph 300° Oblique Large Front to Small Side Evaluation Test, E19 . . . . .	4.36
4.4.3 30 mph 300° Large Front into Small Side Evaluation Test, E20 . . . . .	4.40
4.4.4 30.4 mph 300° Modified Front into Modified Small Side Evaluation Test, E23 . . . . .	4.43
5.0 Rear Impact Condition . . . . .	5.1
5.1 Evolution of Design . . . . .	5.1
5.1.1 Design Goal . . . . .	5.1
5.1.2 Final Design of Modified Rear Structure . . . . .	5.2
5.2 60 mph Large Front to Small Rear Baseline Test, 07 . . . . .	5.4
6.0 Bumper Subsystem . . . . .	6.1
6.1 Evolution of Design . . . . .	6.1
6.1.1 Design Approach . . . . .	6.1
6.1.2 Design of the Low-Speed Energy Absorbers . . . . .	6.3
6.1.3 Design of Bumper . . . . .	6.6
6.2 Evaluation Tests . . . . .	6.9
6.2.1 10 mph Bumper Test, D6 . . . . .	6.9
6.2.2 40 mph Front Pole Test, E2 . . . . .	6.9



Figure No.	Page No.	Title
1.1	1.6	Subcompact Cars as a Fraction of Vehicle Population
1.2	1.12	Accident Analysis Methodology
1.3	1.13	Societal Cost by Clock Position for 1975
1.4	1.16	TENMASS Model Correlation Subcompact Vehicle 1975 Pinto and 1968 Plymouth
2.1	2.6	Frontal Fixed Object
2.2	2.7	Side Fixed Object
2.3	2.8	Primary Rollover
2.4	2.9	Car-to-Car Head On
2.5	2.10	Car-to-Car Side Collisions
2.6	2.11	Car-to-Car Rear End
2.7	2.14	Societal Cost Versus AMA Injury Scale
2.8	2.15	Frontal Fixed Object
2.9	2.16	Side Fixed Object
2.10	2.17	Primary Rollover
2.11	2.18	Vehicle To Vehicle Frontal
2.12	2.19	Vehicle To Vehicle Side
2.13	2.20	Vehicle To Vehicle Rear
2.14	2.21	Societal Costs in 10 mph Ranges for Various Types of Involvement
2.15	2.22	Cumulative Societal Costs for Various Types of Involvement
2.16	2.23	Cumulative Societal Costs for Various Accident Types
2.17	2.28	Two Car Model
2.18	2.29	Typical Force Displacement (F- $\delta$ ) Data
2.19	2.31	TENMASS Model Correlation Subcompact Vehicle
2.20	2.32	TENMASS Model Correlation Full Sized Vehicle
2.21	2.34	ABAG Correlations
2.22	2.39	Critical Velocity Curve for 1974 Pinto Sedan
2.23	2.44	Comparison of BEV Definitions vs. Minimum Critical Speed for 1974 Pinto
2.24	2.45	Overall Force-Displacement Characteristics for Unmodified 1974 Pinto Impacting Car 1 at 100 mph Closing Velocity
2.25	2.51	Critical Closing Velocities for Restraint Deployment Times of .010, .025, and .040 Seconds
2.26	2.55	Critical Closing Velocity Comparison - Modified vs. Unmodified Pinto
2.27	2.56	Pinto Compartment Pulse - 100 mph Into Vehicle 5
2.28	2.57	Pinto Compartment Pulse - 100 mph Into Vehicle 1
2.29	2.58	Pinto Compartment Pulse - 100 mph Into Vehicle 7
2.30	2.66	Bent Cantilever Beam
2.31	2.67	Pinto Foreframe, Model I
2.32	2.68	Pinto Foreframe Structure and Attachment Points
2.33	2.69	Pinto Foreframe, Model II
2.34	2.72	ANSYS Model II
3.1	3.6	Exterior Dimensions of Stock 1974 Pinto Sedan

LIST OF ILLUSTRATIONS (Cont'd)

Figure No.	Page No.	Title
3.2	3.7	Interior Dimensions of Stock 1974 Pinto Sedan
3.3	3.8	Required Modifications of Pinto Geometry for Frontal Impacts
3.4	3.9	Required Modifications of Pinto Geometry for Side Impacts
3.5	3.11	Candidate Force Deflection Curves for Frontal Impact
3.6	3.12	Selected Force-Deflection Curve Modified Subcompact Vehicle
3.7	3.15	Enlarged Rocker Panel Cross-Section
3.8	3.17	Energy Absorber Concepts
3.9	3.18	Behavior of Plastic Hinge
3.10	3.21	Energy Absorber Concepts
3.11	3.26	Production Subframe
3.12	3.28	Concept for Crushable Front End Energy Management System
3.13a	3.29	1/6 Scale Model of Tubular Front Structure
3.13b	3.30	Post Test View of Scale Model
3.15	3.32	Acceleration Pulse of Full Scale Crushable Tube Front Structure (D3)
3.16	3.37	Volumetric Hood Modifications
3.17	3.38	Front Lower Structure for Test Article D4
3.18	3.40	Lower Front Structure for Test Article D5
3.19	3.42	Crash Pulse (D4)
3.20	3.43	D5 Crash Pulse
3.21	3.44	Section View of Modified Upper Structure
3.22	3.46	Modified Pinto Structure
3.23	3.53	Baseline Test No. 001
3.24	3.56	Baseline Test No. 002
3.25	3.59	Baseline Test No. 003
3.26	3.62	Baseline Test No. 009
3.27	3.65	Static and Dynamic Crush of Baseline Pinto as Function of Velocity
3.28	3.66	Peak Acceleration of Baseline Pinto as Function of Velocity
3.29	3.67	Maximum Pitch of Baseline Pinto as Function of Velocity
3.30	3.68	Trunk Acceleration of Baseline Frontal Barrier Tests 01, 02, 03, 09
3.31	3.71	Photographic Coverage of Evaluation Test E1
3.32	3.74	Trunk Acceleration of Test E1 vs. Desired Pulse and Simulation
3.33	3.76	Photographic Coverage of Evaluation Test E1A
3.35	3.80	Photographic Coverage of Evaluation Test E1B
3.36	3.86	Photographic Coverage of Test E25
3.37	3.89	Chest and Vehicle Acceleration for 80 mph Large Car - Modified Pinto Impacts

LIST OF ILLUSTRATIONS (Cont'd)

Figure No.	Page No.	Title
3.38	3.91	Trunk Acceleration of 80 mph Aligned Large Car to Small Car Tests 08 and E25
3.39	3.94	Photographic Coverage of Baseline Test 10
3.40	3.96	Trunk Accelerations of 30° Barrier Tests 10, E15, and E24
3.41	3.98	Photographic Coverage of Test E15
3.42	3.101	Photographic Coverage of Test E24
3.43	3.105	Photographic Coverage of Barrier Test 06
3.44	3.108	Trunk Acceleration for Offset Large Car to Small Car Tests 06, E17, E21
3.45	3.110	Photographic Coverage of Test E17
3.46	3.113	Photographic Coverage of Test E21
3.47	3.118	Photographic Coverage of Baseline Test 07
4.1	4.3	Typical Side Pole Impact Damage
4.2	4.8	Door Modifications
4.3	4.10	Compartment Modifications
4.4	4.12	Static Force Displacement for Baseline 74 Pinto Side Structure
4.5	4.14	Side Pole Crush Test D7
4.6	4.15	Side Crush Test D11
4.7	4.18	Dynamic Side Pole Tests D1 and D2
4.8	4.21	Photographic Coverage of Baseline Test 05
4.9	4.24	Photographic Coverage of Test E9
4.10	4.27	Compartment Accelerations for 90° Front to Side Tests 05 and E9
4.11	4.30	Photographic Coverage of Test E3A
4.12	4.34	Damage to Struck Car, E22
4.13	4.35	Baseline and Evaluation Tests of Side Structure
4.14	4.37	Photographic Coverage of Test E19
4.15	4.41	Photographic Coverage of Test E20
4.16	4.45	Photographic Coverage of Test E23
5.1	5.3	Rear Modifications
5.2	5.6	Photographic Coverage of Baseline Test 07
6.1	6.4	Friction Pad Bumper Energy Absorber
6.2	6.5	Coil Type Bumper Energy Absorber
6.3	6.7	Friction Pad Energy Absorber Test Data
6.4	6.8	Alternative Bumper Designs
6.5	6.10	Photographic Coverage of Test E2
6.6	6.14	Frontal Acceleration For Frontal Pole Test E2

LIST OF TABLES

Table No.	Page No.	Title
1.1	1.15	Baseline Tests
1.2	1.20	Development Tests
1.3	1.21	Evaluation Test List
1.4	1.22	Test Vehicle Configuration
2.1	2.33	Comparison of Simulation and Test for Aligned Frontal 80 mph Impact
2.2	2.37	Vehicles Used in the Study
2.3	2.38	Results of Phase 1 Study
2.4	2.43	Critical Closing Velocities
2.5	2.49	Results of Phase 2 Study
2.6	2.54	Results of Phase 3 Study
2.7	2.71	Finite Element Model of the Pirto Foreframe
3.1	3.13	Pulse Selections for Modified Compatible Subcompact
3.2	3.24	Energy Absorber Crush Test Data
3.3	3.34	Tests of Candidate Volumetric Structures
3.4	3.36	Comparison of Test Articles D4 and D5
3.5	3.52	Baseline Test Data Frontal Barrier Test
3.6	3.70	Baseline and Modified Test Data Frontal Barrier Impact
3.7	3.79	Peak Longitudinal Acceleration of E1, E1A, E1B, 09
3.8	3.84	Baseline and Modified 80 mph Front to Front
3.9	3.93	Baseline and Modified Oblique Frontal Barrier Test Data
3.10	3.104	Baseline and Modified Test Data Offset Subcompact Front to Large Sedan Front
3.11	3.120	Baseline Test Data (Test 04) 30° Oblique Large Sedan Front to Subcompact Front
4.1	4.5	Front End Crush Force of Various Vehicles in the Traffic Mix
4.2	4.17	Baseline and Modified Test Data Side Pole Impact Development Tests
4.3	4.20	Baseline Test Data 270° Large Front to Small Side Impact
4.4	4.29	Development and Evaluation Test Data Side Pole Impact
4.5	4.33	Baseline and Modified Test Data, 300° Front to Side Impact
5.1	5.5	Baseline Test Results Front to Rear Impact
6.1	6.12	Evaluation Test Data Frontal Pole Impact

## 1.0 PROGRAM DESCRIPTION AND EXECUTIVE SUMMARY

### 1.1 Conclusions

The Subcompact Car Crashworthiness Program, documented by this final report, was an extensive and ambitious project covering all phases of the auto safety problem from the structural point of view. As such it is difficult to summarize in a few words the insights and understandings gained during the program as well as the physical achievements of the actual design hardware. This summary must necessarily suffer from sins of omission; the reader is referred to the body of the report for complete details.

1. The crashworthiness of a subcompact car (1974 Pinto sedan) was improved for the most significant accident modes.
  - a. The frontal barrier critical velocity (top survivable impact velocity) was increased from 40 mph to at least 50 mph.
  - b. The oblique frontal barrier critical velocity was increased from 30 mph to at least 50 mph.
  - c. The aligned head-on large car to small car critical closing velocity was increased from 65 mph to at least 80 mph (50 BEV for the small car).
  - d. The offset head-on large car to small car critical closing velocity was increased from 50 mph to at least 80 mph (50 BEV).
  - e. The square-on large front to small side critical closing velocity was increased from 15 mph to at least 30 mph.
  - f. The oblique small front to small side critical closing velocity was increased from 12 mph to at least 30 mph.
  - g. It is anticipated that the proposed design changes have increased the capability in the large front to small rear impacts from 30 mph to 50 mph.
2. The greatest societal benefit is obtained by improving the restraint systems. Both the analytical compatibility study and the baseline testing indicated the critical closing velocity or BEV is limited by the performance of the restraint rather than by that of the structure. Thus the restraint system must be improved before structural improvements can affect the societal cost.

3. Assuming adequate restraints, the structural improvements should be directed toward improvements for oblique frontal impacts and for square-on and oblique side impacts. These accident modes represent significant proportions of the societal cost, yet the current production vehicle structures are best suited to handle only purely longitudinal impacts. Three design changes are necessary to produce the desired impact mode capability:
  - a. The compartment must be rigidized longitudinally across the door opening.
  - b. A significant portion of the energy management structure must be insensitive to the direction of loading.
  - c. The primary side load path must be at the same height as the impacting bumper.
4. Standard writing efforts should be directed towards improvements in crashworthiness which result in the greatest reduction of societal cost. Specifically, specifications concerning the longitudinal rigidity of the passenger compartment and the relative height of bumpers and rocker panels would be valuable in protecting occupants during high speed frontal and side impacts. In addition, a frontal oblique barrier criterion is needed to supplement the present pure frontal barrier standard.
5. The subcompact car crashworthiness program was essentially a research and development effort. The highest priority was to satisfy the design goals specified in the contract while maintaining an awareness of such items as producibility, customer acceptance, and subsystem integration. The attempt to insure satisfaction of the design goals resulted in an overdesign. This contract should be followed by a study to determine the minimum design modifications which would adequately satisfy the design specifications. Such a program should be empirically based, with modifications introduced one at a time and tested at each step. Highest priority should be given to door modifications and to providing energy management material above the wheel well and alongside the engine compartment.

## 1.2 Background

The National Highway Traffic Safety Administration of the Department of Transportation has, since its inception, conducted and funded studies aimed at reducing the societal costs of highway accidents. The agency's overall program provides for research into all phases of the highway safety problem. As one part of the total effort, a number of investigations have been undertaken into the crashworthiness of various vehicles and vehicle elements. Until recently these studies were addressed to improving the crashworthiness of standard size vehicles. The problem of crashworthiness of small vehicles had been approached in only a few studies. Notable among these were "Frontal and Side Impact Crashworthiness - Compact Cars" (DOT-HS-257-2-461) and "Basic Research in Crashworthiness" (DOT-HS-800-818). None of this previous work, however, is directly applicable to the unique problem of subcompact vehicle crashworthiness due to reduced crush and stroking distance.

In order to fill this gap, NHTSA, in July 1973, awarded Contract DOT-HS-113-3-746, entitled "Crashworthiness of Subcompact Vehicles," to Minicars, Inc., Goleta, California. The work was performed under the technical direction of Mr. Glen F. Brammeier, the Contract Technical Manager, and under contract administration of Mrs. Evelyn Wright, the Contracting Officer.

The importance of vehicle crashworthiness in the overall safety program cannot be overstated. Crashworthiness can be defined as the ability of the vehicle to provide a survivable environment throughout the crash. Many separate factors are implicitly included in this definition of crashworthiness, including:

1. Limitation of occupant accelerations.
2. Limitation of hard surface intrusion into the occupants' living space.
3. Prevention of occupant ejection.
4. Elimination of lethal projectiles.
5. Provision for post-impact escape.
6. Prevention of post-impact fires.

Of these items, the two most troublesome are limitation of occupant acceleration and the limitation of intrusion. Control of these two factors is sufficient to provide a major reduction in the societal cost of accidents.

The small car presents several major difficulties to the improvement of crashworthiness not present in larger vehicles. These difficulties are related to the obvious difference in volume and mass between subcompact and standard cars. First, the small size allows much less room to provide efficient energy management. Second, in collisions with other vehicles, the mass differential causes a larger velocity change in the smaller car.

The lack of space creates a problem because absorbing crash energy over short stroking distance necessitates high acceleration levels. Conversely, to limit accelerations at a given velocity, it is necessary to increase the crush distance, which increases the possibility of intrusion into the passenger compartment. The small size of the subcompact requires a compromise between these two factors.

The effect of unequal mass is best illustrated by an example. A car weighing 2,700 pounds and traveling at 40 mph impacts a car weighing 4,400 pounds and going the other way at 40 mph. The velocity change for the small car will be

$$\Delta V_S = (V_S + V_L) \frac{M_L}{M_S + M_L} = (40+40) \frac{4400}{2700 + 4400} = 49.6 \text{ mph,}$$

while for the large car it is

$$\Delta V_L = (40+40) \frac{2700}{2700 + 4400} = 30.4 \text{ mph,}$$

when  $M_L$  = mass of large car,  
 $M_S$  = mass of small car,  
 $M_L$  = velocity of large car, and  
 $V_S$  = velocity of small car.

It is apparent from these calculations that a small car is at a serious disadvantage in the real world of traffic accidents. The traffic mix of large and small cars guarantees accidents between discrepant sizes. The number

of such accidents, and thus the societal cost, will depend upon the percentage of each vehicle type in the overall mix.

The small car has been in use in America since the very beginning of automotive travel. The number of subcompact cars has steadily grown since the introduction of small foreign cars after the second World War. Since 1960 the American public has generally accepted small cars and increasingly used them. In particular, the desirability of the small car was recently and graphically emphasized by the energy crisis and the resulting economic inflation. Figure 1.1 graphs the number of small cars in the traffic mix from 1970 projected to the year 1985. Extrapolating the growth wave indicates that subcompact cars will become a major portion of the vehicle population in a few short years. As the number of small cars increases, their percentage involvement in accidents increases and they become a major factor in the overall societal cost of accidents, especially during the transitional period of the greatest number of crashes between large and small cars, but also beyond this period into the time when small cars predominate. It is to the credit of NHTSA that they have anticipated the increased usage of subcompact vehicles, and realized the urgent need to provide a crashworthy structure for such vehicles.

### 1.3 Task Description

The stated purpose of the contract was "to develop crashworthy structures for subcompact vehicles which will protect the occupants in impacts of all types in a cost-effective, production-feasible, and weight-controlled manner." The key phrasing that distinguishes this contract is "protect the occupants" and "impacts of all types." The first phrase implies that the design criterion for the structure is to protect the occupant. The survival of the structure itself after the crash is of little importance if it has satisfied the primary objective of protecting the occupant. A definition of crashworthiness based on occupant protection implicitly introduces restraint performance into the system. The early stage of this contract accounted for restraint performance in a subjective manner. After contract amendment number three, an improved passive

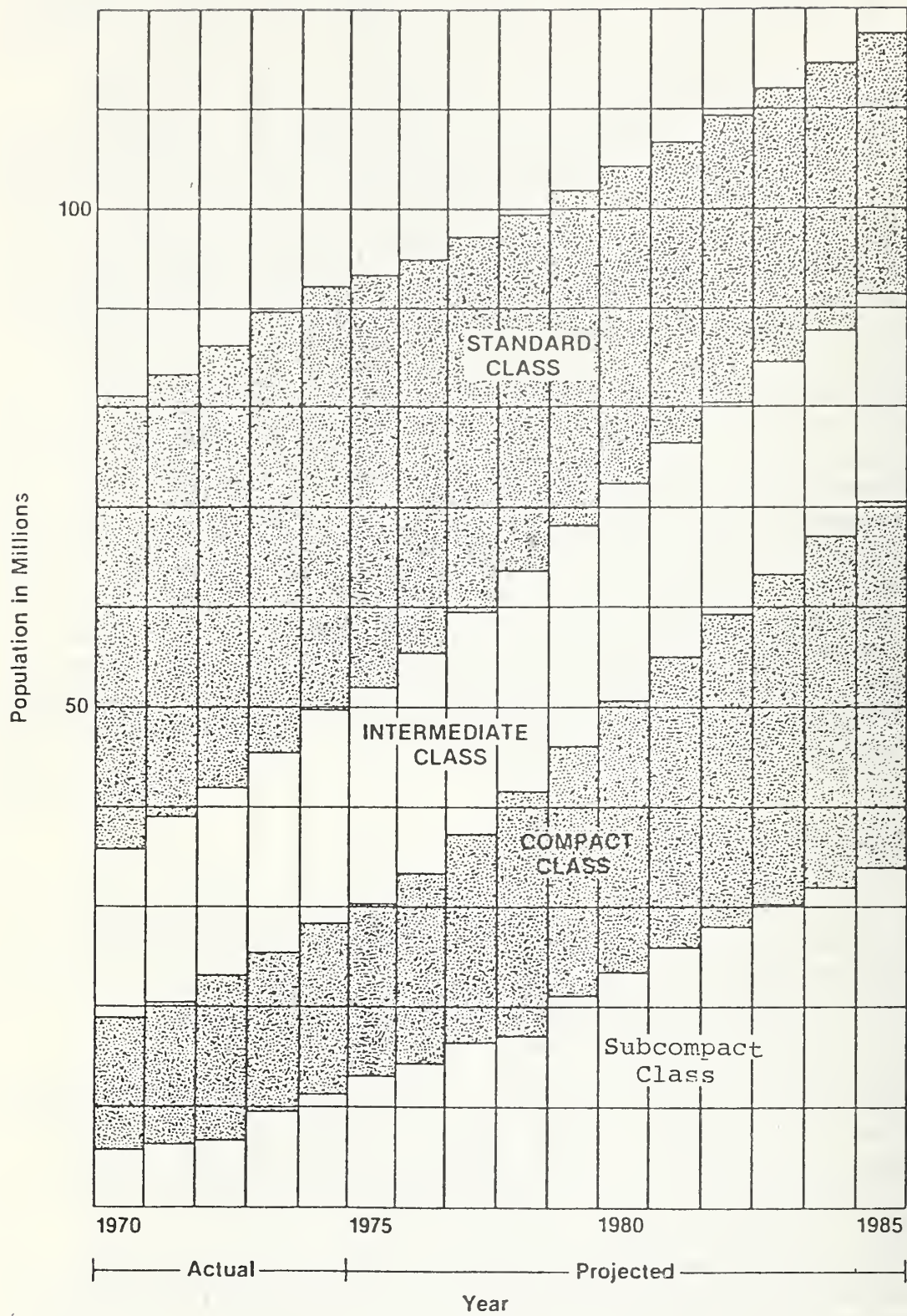


FIGURE 1.1 SUBCOMPACT CARS AS A FRACTION OF VEHICLE POPULATION

restraint system was integrated into the vehicle and crashworthiness measured directly by occupant response. Details of the restraint system were presented in the reports of contracts DOT-HS-113-3-742 "Development of Advanced Passive Restraint System for Subcompact Car Drivers," and DOT-HS-4-00917 "Inflatable Belt Development for Subcompact Car Passengers." Actual occupant data is included in this report where it is applicable and is a defined item of the contract.

The phrase which includes "impacts of all types" into the contract is vital to the development of an efficient structural design. Accident statistics show that oblique and offset impacts constitute the major portion of the real world accidents and societal costs. Acting on this conclusion and using a broad interpretation of "impacts of all types," Minicars has expanded the specified design goals for the structure to include both offset and oblique frontal impacts and oblique side impacts, crash modes not specified by the contract. To develop such a structure required thoughtful compromise of performance in some modes for improvements in other accident modes. Rather than pursue the greater possibility of reduction in any one crash mode, our design goal was to achieve the greatest reduction in the societal cost of accidents.

The specific objectives to be achieved under the contract were defined as follows:

1. To analyze current structure and proposed structural modifications for subcompact vehicles for their applicability in the highway environment.
2. To advance the development of impact energy absorption and/or distribution devices or concepts for subcompact vehicles while considering the overall mix of accident and vehicle types commonly encountered on the highway.
3. To verify and demonstrate the improved performance of the developed subcompact vehicle by testing and computer simulation under a wide range of conditions.
4. To provide data to support the development of structural standards.

To accomplish these objectives, four tasks were specified. The first task required the formulation of a Plan of Work and Methodology. This was strictly an organizational task and was completed and approved prior to commencement of work on the functional tasks.

The second task provided for collection of data on the baseline vehicle. Minicars selected the 1974 Pinto sedan as the baseline vehicle. Baseline data was collected primarily by a series of tests, both static and dynamic, conducted on production vehicles. Static data provided force/deformation information for use in the mathematical dynamic response model, while dynamic tests were used to provide insight into the behavior of the vehicle during actual crash environments and to correlate and correct the mathematical dynamic model. The dynamic crashes also provide a data base for evaluation of the modified vehicle. Information about weights, center of gravity, inertias, etc. for the baseline Pinto was obtained from the Ford Motor Company. Particular results of baseline investigations are presented in detail in the report section dealing with the particular subsystem; e.g., the baseline behavior of the front structure is given in Section 3, Frontal Impact Crashworthiness.

The third task defined the mathematical analysis required for the program. Three distinct analyses were required:

1. Analysis of available accident data to define the frequency of accident types.
2. Analysis of the compatibility of the subcompact vehicle with other cars in the traffic mix.
3. Analysis to determine the force/deflection characteristic required for each load path, and to support the design of components to produce desired characteristics.

The first two of these subtasks are reported in detail in Section 2. Analysis of the design is presented in each section dealing with the particular subsystem.

The final task of the program was the development of a structurally improved subcompact vehicle. Several concepts for each subsystem were selected. These were reviewed for this applicability to energy management, weight efficiency, and producibility. The most promising of these were selected for further development. The final selection processes included both analytical evaluation and developmental testing to produce a final design. After the design was finalized, a series of vehicles were modified and prepared for system testing. The evaluation tests were conducted and the data analyzed both for critical evaluation of the success of the design and to assist in recommendations for design improvements. During the course of the contract, several design improvements were recommended and incorporated into the contract by modification number 3. The details of each subsystem design development are presented separately in Sections 3, 4, 5, and 6 of this report.

The contract design goals were specified in Task 4. The crashworthiness goals included the following:

I. Front Crashes

- a. 50 mph frontal flat barrier impact.
- b. 50 mph frontal flat pole impact.
- c. 100 mph frontal car-to-car impact with baseline, modified, and large cars.

II. Side Crashes

- a. 20 mph side pole impact.
- b. 40 mph side impact by baseline, modified, and large cars.

III. Rear Crashes

- a. 50 mph rear impact by a large car.

Other design goals included limited weight increase, limited size increase, no-damage, low-speed impact capability, fuel system safety, and operational considerations.

All of the crashworthiness design goals were satisfied and verified by either full scale testing, scale model testing,

or computer analysis. The final weight increase was 132 pounds for the final design. Of this amount, 47 pounds was due to raising the body of the vehicle and should not be included in the evaluation of the modifications. The resulting weight of 85 pounds results in a percentage increase of 3.5 percent, which is well within the specified limit of 120 percent. The final length was 105 percent of the baseline, and the width did not increase.

In addition to the contractual goals, Minicars in conjunction with the CTM selected the following impact conditions as desirable design goals for the real world accident environment.

1. 50 mph, 30°\* oblique barrier impact.
2. 80 mph, 30° oblique vehicle-to-vehicle impact with a large car.
3. 80 mph, 50 percent offset, vehicle-to-vehicle impact with a large car.
4. 40 mph, 300° oblique large car into the modified side structure.

The modified vehicle met or exceeded all of these additional requirements.

#### 1.4 Method of Approach

Minicars presented its approach to the problem of crashworthiness of subcompact vehicles in the Plan of Work and Methodology. Our purpose there was to provide a thorough, logical, systematic evaluation of the problem, the state of the art, and the possible solutions, and provide for complete design development and verification.

##### 1.4.1 Evaluation of the Problem

The current crashworthiness problem consists of two parts: 1) the nature of the accidents occurring in the real world, and 2) design of present production automobiles. The

---

\*The angle of impact is measured clockwise from the forward direction of the longitudinal axis.

first step in evaluating the problem was a study of the available accident data to determine the predominant velocity, location, and angle of impact. The primary data bases for the accident analysis were the National Safety Council<sup>1</sup>, the Cornell Level II file<sup>2</sup>, and the Multi Disciplinary Accident Investigation (MDAI) file<sup>3</sup>. The methodology of the analysis is outlined in Figure 1.2. National Safety Council figures provided the total number of accidents, injuries, and fatalities. The Cornell Level II file was then used to separate the data by accident mode, e.g., frontal fixed object, etc. Next the MDAI file was used to determine the number of injuries and fatalities in each accident mode for 10 mph velocity ranges. The MDAI file also provided the distribution of the degree of injury for a given accident mode and velocity range. This information, combined with the average societal cost for each injury level as obtained from the "Societal Cost of Motor Vehicle Accidents,"<sup>4</sup> determined the average cost per injury in each accident mode and velocity range. Multiplying the average cost per injury by the number of injuries gives the total societal cost in each accident mode and velocity range. The final results are summarized in Figure 1.3.

The second part of the problem evaluation consisted of a mathematical study and full scale testing of the compatibility of production subcompact vehicles with other vehicles. The purpose of this study and testing was to develop a relationship between the mass of the "other" vehicle (the vehicle which is assumed to collide with the subject subcompact) and a critical closing velocity. The critical velocity was defined as the lowest velocity which would cause either an occupant stroke of 20 inches or a vehicle crush limit of 45 inches for the subcompact vehicle. These values were chosen as typical maximums attainable in subcompact cars. The occupant was defined as a 50th percentile male. The mathematical study was conducted using a non-linear lumped mass dynamic model with a total of ten mass points and nineteen force-displacement curves, which correspond to springs in a linear model. These are obtained from static crush data of the vehicles and represent the principle load

# ACCIDENT ANALYSIS

## Source of Information

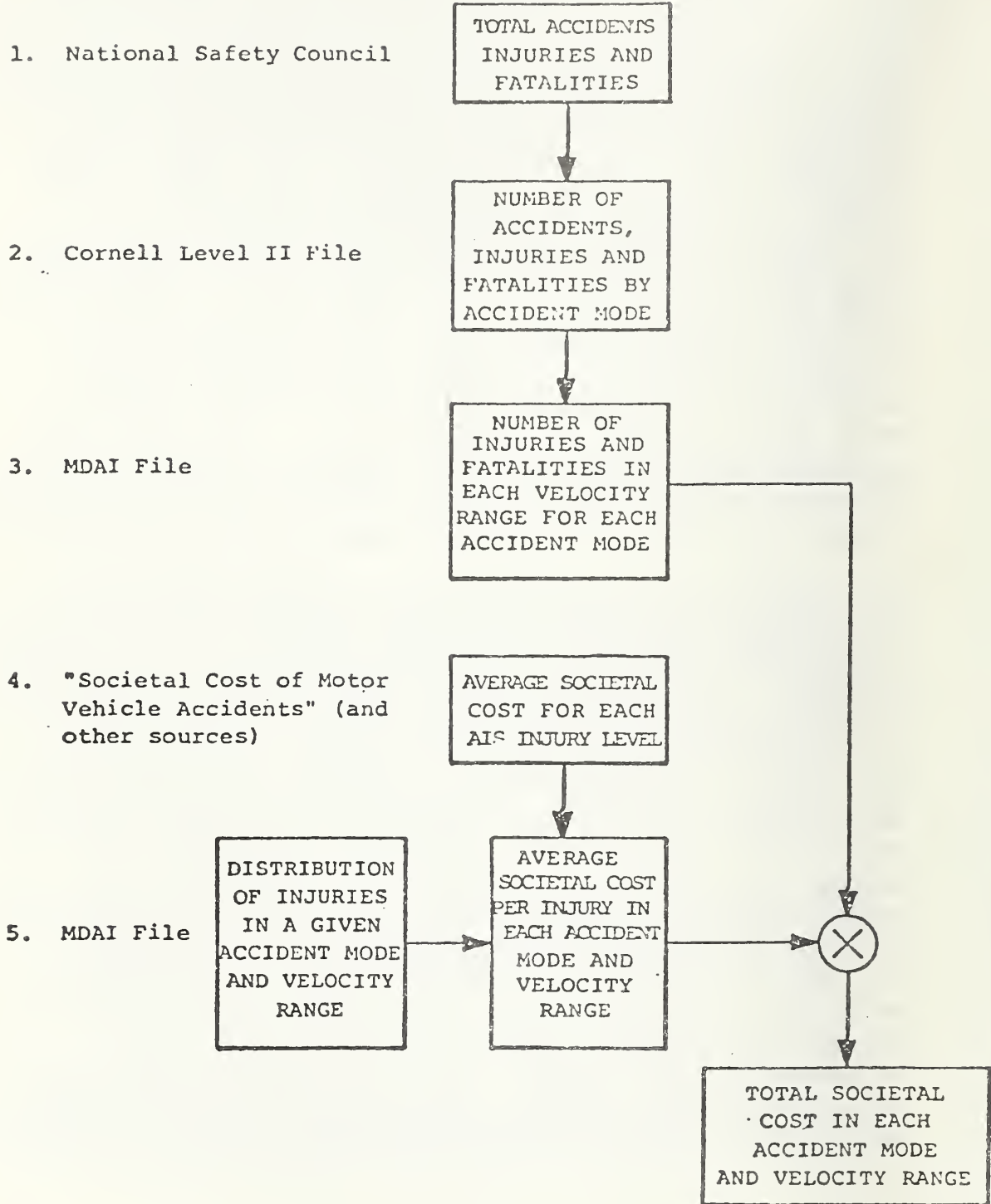


FIGURE 1.2 ACCIDENT ANALYSIS METHODOLOGY

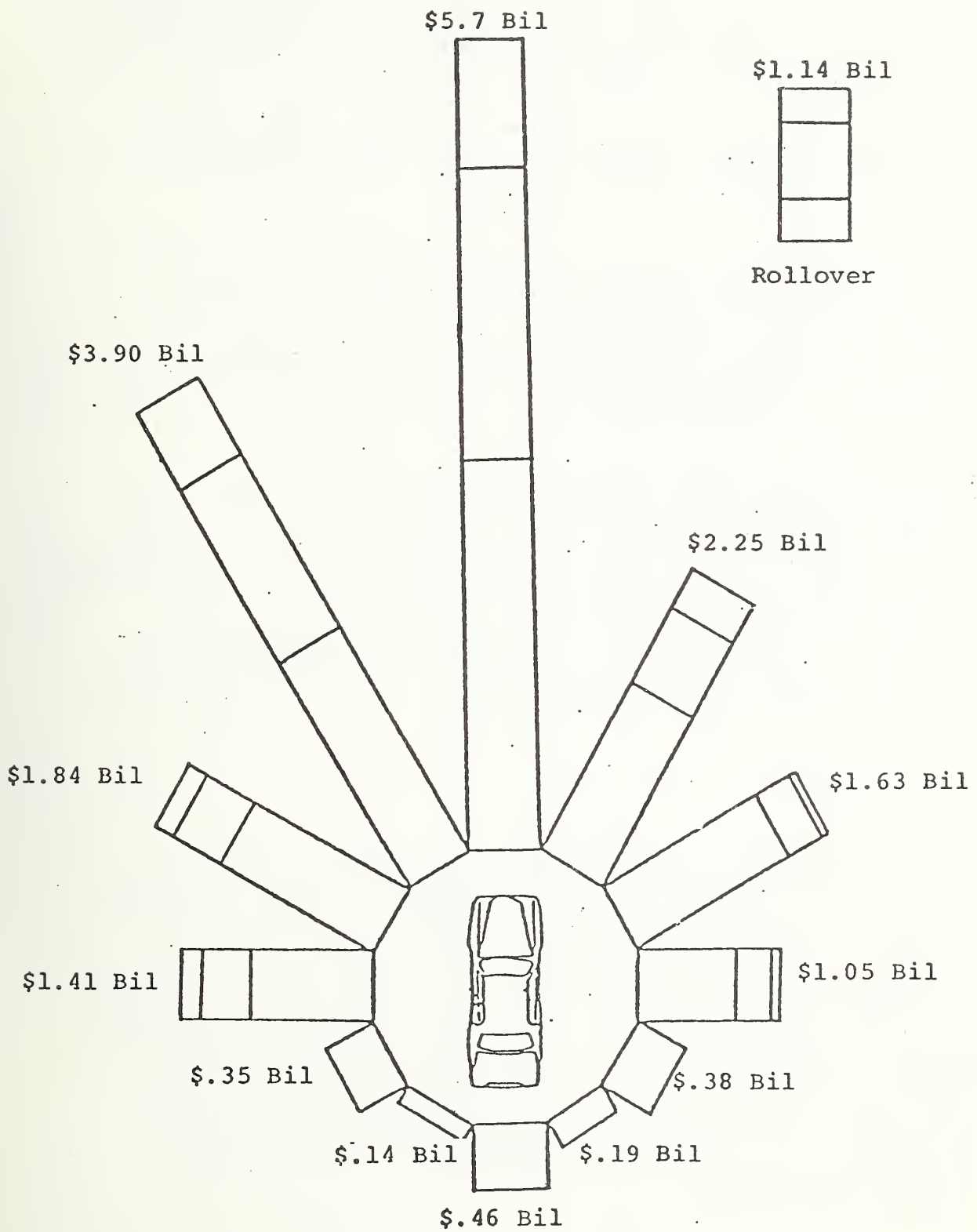


FIGURE 1.3 SOCIETAL COST BY CLOCK POSITION FOR 1975

paths through the vehicle front structure. Initial velocity conditions were applied to the masses and a time step integration was used to calculate the dynamic response. The results of the modeling were correlated with baseline test data as shown in Figure 1.4.

The baseline full scale dynamic testing consisted of 11 tests as listed in Table 1.1. The complete baseline test plan is presented in Appendix A.

The results of the baseline tests established a survivable frontal barrier impact velocity of 40 mph (assuming advanced restraint systems). The frontal oblique and offset conditions were much less favorable, with a maximum velocity established at 30 mph. The baseline capacity in side impacts was 12 mph.

As a result of the baseline tests and the accident analysis, the design emphasis was placed on oblique and offset impacts for both front and side while the square-on frontal and rear impact design goals were de-emphasized. The frontal aligned mode was de-emphasized since the baseline Pinto behaved well, especially considering its weight classification. The rear structure was considered less important since the accident analysis showed this accident mode to have a low societal cost.

#### 1.4.2 The State of the Art

Previous safety vehicle design studies have resulted in designs which were either extremely heavy or provided unidirectional crush characteristics. One type of design which has received much attention is the use of plastic hinges as energy absorbers. This design requires all the energy absorption to occur at ends of the members with the members themselves acting as incompressible links. As a result, the absorbed energy per pound of material is very low, creating a heavy structure. The subcompact vehicle cannot accommodate a significant increase in weight, thus eliminating a plastic hinge structural design.

TABLE 1.1 BASELINE TESTS

<u>Test No.</u>	<u>Description</u>	<u>Velocity (mph)</u>	<u>Test Location</u>	<u>Date of Report</u>
01	1974 Pinto, frontal barrier	20	Minicars	Dec. 1974 Progress Report
02	1974 Pinto, frontal barrier	40	Minicars	Dec. 1974 Progress Report
03	1974 Pinto, frontal barrier	30	Minicars	April 1974 Progress Report
04	1974 Pinto to 1968 Plymouth Fury 4-door, 30° Oblique	80	Dynamic Science	Jan. 1974 Separate Report
05	1968 Fury front into 1974 Pinto side, 270° (T-crash)	30	Minicars	Sept. 1974 Progress Report
06	1974 Pinto to 1968 Fury, front- to-front 50% offset	80	Dynamic Science	Jan. 1974 Separate Report
07	1968 Fury front to 1974 Pinto rear	60	Dynamic Science	Jan. 1974 Separate Report
08	1968 Fury to 1974 Pinto, front- to-front aligned	80	Dynamic Science	Jan. 1974 Separate Report
09	1974 Pinto, frontal barrier	50	Minicars	June 1974 Progress Report
10	1974 Pinto, frontal barrier, 30° oblique	50	Minicars	June 1974 Progress Report
E22	1974 Pinto front to 1974 Pinto side, 300°	30	Minicars	August 1975 Progress Report

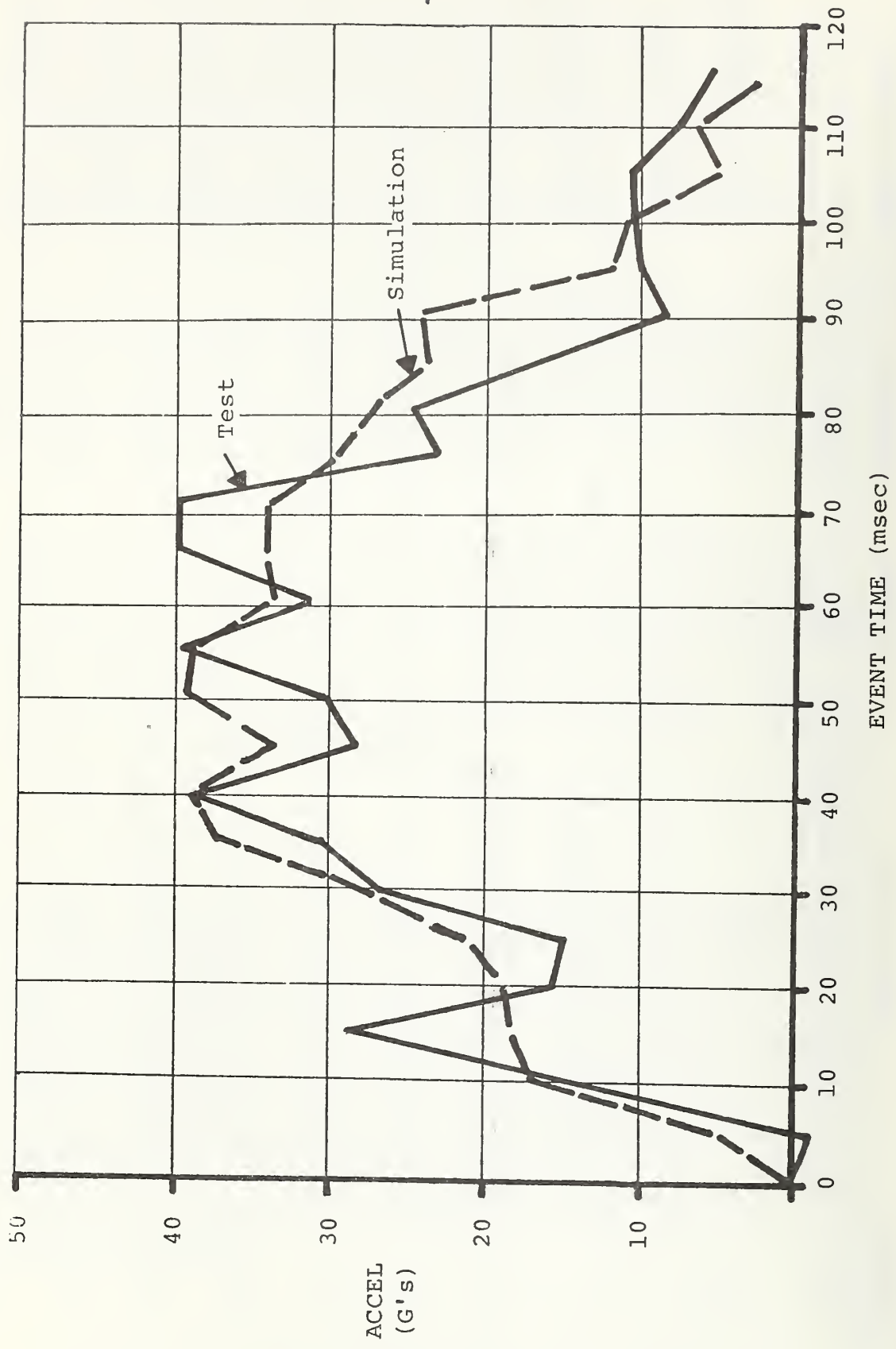


FIGURE 1.4 TENMASS MODEL CORRELATION SUBCOMPACT VEHICLE  
 1974 Pinto and 1968 Plymouth

The second most prominent type of design utilizes progressive crush or displacement of axial members. Such designs include hydraulic cylinders, round or square hollow crush tubes, and linear low density structures such as honeycomb cylinders. These designs are much more efficient than the plastic hinge frame. However, they are only appropriate for loads directly along the member. This design deficiency limits their usefulness, because if they are longitudinally aligned, then they are beneficial only in frontal aligned impacts, which constitute a small portion of the real world accidents; if several are used in different alignments, the system becomes too heavy.

The state of the art in design of safe side structures has emphasized either door beams inside the doors or extensive support structure for the door posts. The door beams require massive latches and hinges to develop and transmit high membrane loads. The post supports are theoretically more efficient, but they infringe on the occupant space. Both designs neglect the real problem of the mismatch of front bumper height to rocker panel height. If this mismatch can be avoided, the side structure design is greatly simplified.

All of the results of previous safety vehicle studies were used as guides in the development of the subcompact car modifications. Knowledge of the successes and failures of previous designs was instrumental in the selection of concepts and an overall design approach.

#### 1.4.3 Conceptualization of Possible Designs

After the review of the state of the art, a variety of possible design concepts was formulated for each vehicle subsystem. These concepts included improvements in previous energy management systems as well as new concepts.

The use and improvement of previous designs were considered, since familiar concepts generally are more acceptable than new ones. This is particularly true when considering the

relative producibility of the structures. Several front structure designs were fabricated and tested prior to selection of a final design approach. The front structure concepts considered included round and square crush tubes supported to improve oblique impact capability, honeycomb crush tubes, uncontained foam structures, and foam-filled sheetmetal volumes. The development tests, including both scale model and full scale dynamic tests, proved the greater efficiency of the foam-sheetmetal combination. The ability of this design to absorb energy from oblique impacts and the inherent weight efficiency of foam provide an optimum structure for automobile safety.

One of the basic modifications attempted in this program was the rearrangement of the passenger compartment geometry. The rocker panels and tunnel were raised, head-to-windshield distance was increased, and more room was provided for energy management structure. For ease of fabrication, these modifications were achieved by raising the entire passenger compartment with respect to the drive system. A final production design would require new styling to increase consumer acceptance of these changes.

Relatively few design concepts were generated for the side structure or rear structure, due to the outstanding success of the early designs. The results of the front end studies helped eliminate many possible concepts and oriented the design to foam and sheetmetal volumes. For the side structure, the door was enlarged and filled with foam in the lower portion, and lateral floor members were added under the front and rear seats. The rear design combined a foam-filled rear deck with three filled longitudinal members. Development tests of both these concepts verified their suitability and use as final designs.

#### 1.4.4 Development and Verification of the Final Modifications

After review and selection of design concepts, the final design phase of the contract began. The results of the

last development test were incorporated into the design and a final iteration of the design cycle was completed. (Table 1.2 describes the development test series.) This included dynamic response model runs and completion of shop drawings for fabrication of the test articles. Altogether 14 test vehicles were fabricated for use in 15 evaluation tests. The design was frozen for the last five tests. The weight of the final modified vehicle was increased 5.5% (estimated 3.5% for a production vehicle) over the baseline Pinto. Appendix B represents the final weight analysis.

Table 1.3 lists the series of evaluation tests performed under the contract. The evaluation test plan is presented in Appendix C. The actual configuration of each test article is listed in Table 1.4. The actual results of the tests are covered in detail in the particular section discussing the design (Sections 3, 4, and 5). The final configuration met or exceeded all of the requirements of the program.

#### 1.5 Program Highlights

The subcompact crashworthiness program, as conceived by NHTSA and executed by Minicars, was a basic research and development project. The goal was to determine the critical impact conditions and provide a crashworthy vehicle structure for those conditions. The results of the project have illuminated the following major points:

1. In real world accident environment, offset and oblique frontal collisions at the eleven and one o'clock positions predominate.
2. The best total design is that design which will lead to the greatest reduction in the societal cost of accidents in the future. Therefore performances in the various crash modes must be traded off against each other according to the societal cost incurred in each mode. In particular, to satisfy the offset and oblique frontal impact conditions, aligned frontal crashworthiness must be treated as a part of the whole frontal problem.

TABLE 1.2 DEVELOPMENT TESTS

<u>Test No.</u>	<u>Test Type</u>	<u>Test Article</u>	<u>Test Fixture</u>	<u>Velocity (mph)</u>	<u>Date (Week of)</u>
D.1	Dynamic	Precrashed 1972 Pinto	Large Sled	20	Jan. 14
D.2	Dynamic	Precrashed 1972 Pinto - Modified	Large Sled	20	Jan. 21
D.3	Dynamic	Frontal Modified 1974 Pinto Configuration "A"	Tow Motor	40	Mar. 11
D.4	Dynamic	Frontal Modified 1974 Pinto Configuration "C"	Tow Motor	40	April 1
D.5	Dynamic	Frontal Modified 1974 Pinto Configuration "B"	Tow Motor 30° barrier	40	April 15
D.6	Dynamic	Bumper EA Units	Small Sled	10	Jan. 29
D.7	Static Crush	1972 Pinto Compartment (Side Pole)	Crusher	N/A	April 15
D.8	Dynamic	Modified Rear Structure	Tow Motor	35	April 22
D.9	Dynamic	Front Modified 1974 Pinto with bumper	Tow Motor	10	May 6
D.10	Static	Modified Upper Structure	Crusher	N/A	April 29
D.11	Static	1972 Pinto Compartment	Crusher	N/A	May 13

Note: Material tests and basic component behavior tests are not assigned test numbers. They are performed on an "as required" basis.

TABLE 1.3 EVALUATION TEST LIST

<u>Test No.</u>	<u>Description</u>	<u>Velocity (mph)</u>	<u>Test Location</u>	<u>Date of Report</u>
E1	Frontal Barrier	50	Minicars	Aug. 1974 Progress Report
E1A	Frontal Barrier	50	Minicars	Aug. 1974 Progress Report
E1B	Frontal Barrier	50	Minicars	Nov. 1974 Progress Report
E2	Frontal Pole	40	Minicars	Oct. 1974 Progress Report
E3	Side Pole	20	Minicars	Sept. 1974 Progress Report
E3A	Side Pole	20	Minicars	Sept. 1974 Progress Report
E9	270° Front to Side	30	Minicars	Sept. 1974 Progress Report
E15	30° Oblique Barrier	45	Minicars	Sept. 1974 Progress Report
E17	50% Offset Large to Small	70	Dynamic Science	Sept. 1974 Progress Report
E19	300° Oblique Front to Side	30	Minicars	Oct. 1974 Progress Report
E20	300° Oblique Front to Side	30	Minicars	June 1975 Progress Report
E21	50% Offset Large to Small	80	Dynamic Science	July 1975 Progress Report
E23	300° Aggressivity	30	Minicars	Aug. 1975 Progress Report
E24	30° Oblique Barrier	50	Minicars	Aug. 1975 Progress Report
E25	Aligned Large to Small	80	Dynamic Science	April 1975 Progress Report

TABLE 1.4 TEST VEHICLE CONFIGURATION

Modification*	Test Vehicle														
	E1	E1A	E1B	E2	E3	E9	E15	E17	E19	E20	E21	E23	E24	E25	
1. Friction EA Unit with 12 inch slider bars	X	X	X	X						X	X	X	X	X	
2. Friction EA Unit with 18 inch slider bars	X	X	X	X						X	X	X	X	X	
3. Bumper support frames - .063 thick	X	X	X	X						X	X	X	X	X	
4. Bumper support frames - .083 thick	X	X	X	X						X	X	X	X	X	
5. Inner fender panels															
6. Head															
7. Vertical Toe Board															
8. Sloping Toe Board															
9. A Post Reinforcement															
10. A Post Fender Section															
11. Mid Compartment Lateral															
12. B Post Lateral															
13. Enlarged Rocker Panel															
14. Enlarged Tunnel															
15. Tunnel Stiffeners															
16. Modified Doors															
17. Stabilized Rear Quarter															
18. Breakaway Engine Mounts															
19. Breakaway Transmission Mounts															
20. Collapsible Driveline															
21. Foam Filled Plenum, 5 lb.															
22. Foam Filled Plenum, 2 lb.															
23. Forward Fender Box (5 lb. foam)															
24. Forward Fender Box (2 lb. foam)															
25. Aluminum Bumper															
26. Modified Aft Frame															
27. B Post Gusseted															
28. B Post Closed and Foamed															

\*Description of specific modification is given in Section 3.2.6, 4.1.2 and 5.1.2.

3. The societal cost of side impacts warrants extensive structural modifications in that area. On the other hand, rear impact statistics will not justify significant structural changes aft of the B post.
4. The design developed under this contract is strictly a research design. The structure must be optimized and productionized under future efforts.
5. To provide a crashworthy vehicle, the structures and the restraints must be a compatible system. Inclusion of the restraints on the later evaluation tests verified the accuracy of this concept.

As noted in Section 1.4.1, the accident statistics show a relatively high total societal cost for impacts in the eleven and one o'clock positions. These two locations combined have about equal the societal cost to the twelve o'clock position. It is apparent that a crashworthy vehicle must deal with these offset and oblique impacts. Present production vehicles and many of the proposed safety cars are oriented to head-on barrier crashes; they provide good characteristics for zero degree impacts. Their structures tend to be unidirectional, with the strength primarily along the axis of the vehicle. Under offset or oblique impacts, there is little structural stiffness to absorb the energy of impact. The problem is to provide good energy absorption for oblique impacts without adversely affecting the crashworthiness in frontal impacts. This problem is well illustrated by the 1974 Pinto sedan. This vehicle performed quite well up to 40 mph for aligned frontal impacts in the baseline tests. However, both offset and oblique baseline tests showed very serious passenger compartment intrusions at equivalent velocities. Survivable velocity for these modes is estimated to be 30 mph. It would have been possible to perform minor modifications to the Pinto structure and satisfy the specified frontal impact goals of the contract, but the intent of the contract necessitated a crashworthy structure for all critical accident modes.

The modifications required to satisfy the offset and oblique impact modes naturally affected the behavior of the vehicle during frontal crashes. If the basic structure, the stub frames, firewall, and driveline were unchanged, the addition of oblique structure would make the vehicle too stiff frontally. Thus, it was necessary to modify the entire front structure, replacing it with an omnidirectional volumetric energy absorbing structure. The subframes were redesigned to provide a more predictable failure mode, the engine and driveline were provided with breakaway mounts and free travel distances to preclude them from acting as a load path, and finally the hood and fenders were stiffened with foam to carry load from any direction.

Side impacts have been shown to produce an extremely significant portion of the societal cost of accidents. Today's cars, with their low planar aspect ratios (width divided by length), are vulnerable to all types of side impacts. There is little space available for energy absorbing structures. The door beams installed in production cars and proposed in some safety vehicles are not effective. The support structures required to transmit lateral loads to the door frame are necessarily very heavy and weight-inefficient. Minicars has chosen a more efficient technique of providing lateral support across the width of the car in the floor, with only a longitudinal brace at the top of the A post. Such a structure is weight and energy efficient but requires a specified maximum height for bumpers of other cars. If the present bumper regulations are met, and the bumper does not override the sill, then the design developed under this contract will significantly lower the societal cost of side impacts. The actual design used foam-filled rocker panels and lateral members, as well as filled lower portions of the door. The evaluation tests have completely validated this concept of a crashworthy side structure.

The contract specified a rear impact goal of 50 mph, and a structural modification was designed to provide this protection. The accident analysis, on the other hand, showed that societal costs of rear accidents justified only small expenditure for the rear modification. It was obvious that any modification directed at a 50 mph goal would exceed the justified expense and would not be an economical change. Based on these results, the rear structure mode was not tested in the evaluation series of tests. The rear barrier development test, D8 (see Table 2.1), proved the basic concept and contrasted dramatically with the baseline rear impact test.

It is important to emphasize that the "Crashworthiness of Subcompact Vehicles" contract was a research and development effort. The design developed has been proven to be technically feasible. There is still a tremendous gap between the results of this work and a full production vehicle. The next major effort should be directed towards optimization of the design. As in all engineering projects, the first designs are based on conservative assumptions and are "over-designed" to ensure proper performance of the concept. The second stage is to remove some of the conservatism and to optimize the structure based on the previous test results. In the case of the Pinto, the next effort should be to see how little modification is really necessary. In both the side structure and the front structure, it may be possible to use standard production hardware in place of the extensively modified design reported here. Such items as the shape of the door, the tunnel modifications, and the hood alteration must be investigated to determine their effectiveness. In addition, much research into the behavior of foam and foam-filled structures under dynamic loading is required. The third stage of the development of a crashworthy subcompact car should be the productionizing of the design. It is always possible to change the engineering design to facilitate production and not adversely affect the performance. The overall questions concerning the use of volumetric structures can be answered in general terms

prior to the third stage, but the details of true productionizing must be postponed. The results of a well planned program will be a readily acceptable, safer vehicle with little increase in cost and weight.

The last major point demonstrated during the course of this contract is that structures and restraints must be designed as a system. The ultimate in protection of the occupant can only be achieved if the structure and the restraints complement each other. The difficulty in tailoring a structure to provide a precisely defined crash pulse has been illustrated in this work and in many other projects. When considering oblique and offset impacts, the difficulty is magnified many times. It may be possible in the future to analytically predict a crash pulse without either static or dynamic test data, but for the present the only believable pulses must be based on test data. Since the design of the restraint system is based upon the crash pulse, a restraint system optimized to an unrealistic pulse will have difficulty when used in the real vehicle. The answer to this problem is to develop the restraint concurrently with the structure, accounting for pulse shapes as they are determined by test.

To summarize the program highlights, the modified design developed by Minicars provides a technically feasible concept for crashworthy vehicles. The structure has been placed where the accident analysis predicts the greatest benefit. The optimization stage will answer many questions concerning the novel approach of the design.

The Minicars RSV Phase II study will also further the development of the foam-filled sheet metal design concept. The structure for that vehicle relies heavily on the preliminary work conducted under this contract.

## 2.0 MATHEMATICAL STUDIES

The mathematical studies delineated in Task 3 of the contract were separated into three subtasks. The first subtask was to analyze the available accident data to determine the societal cost of the various accident modes (Appendix D). This information shows how much can justifiably be spent on each required structural modification. The second mathematical study helped to determine the compatibility of the subcompact, both production and modified, with other vehicles in the highway environment (Appendix E). The final subtask was an attempt to use finite element analysis to predict the static force-displacement behavior of the structural members (Appendix F). This effort was conducted by the Jet Propulsion Laboratory of Pasadena, California.

The results of the accident analysis indicates that significant societal cost is incurred in the eleven o'clock and one o'clock accident modes. The total societal cost in these two modes exceeds the cost for the frontal aligned accidents. Therefore a crashworthy vehicle design must satisfy both offset and oblique impact modes. On the other hand, the rear impact statistics showed relatively little societal cost at high velocities, thus allowing de-emphasis of that accident mode.

The compatibility study investigated the survivable impact velocity for the baseline Pinto sedan as a function of the weight of the other vehicle in the collision. The safe velocity was limited by the occupant restraint performance rather than by the structural crashworthiness. The second phase of the study considered the effect of improved restraint systems, with the results indicating higher survivable velocities as the restraint deployment time decreased. The final phase of the study investigated possible structural modifications to provide a more suitable force deflection characteristic.

The JPL finite element effort was directed at analytically determining the force deflection characteristics of the primary load path through the vehicle. The study showed promising results for the forward frame element. However, on recommendation of the CTM the effort was terminated after these preliminary studies. The potential of the technique has been demonstrated and awaits additional funding to fully develop the methodology.

## 2.1 Accident Analysis

### 2.1.1 Introduction

The accident analysis undertaken as part of Task 3 of this contract is one of the most comprehensive studies of the subject to date. A new and unique approach for interpretation of the existing data was developed. The same techniques have subsequently been extended and applied by Minicars to other DOT contracts. They have also been used to support investigations by automobile insurance companies. The analysis combined accident data from all available sources using the best and most reliable features of each file to complement the other data files. The primary data sources were:

1. The National Safety Council.
2. Cornell Level II Accident File.
3. Multi-Disciplinary Accident Investigation File.
4. Department of Transportation, Preliminary Report on "Societal Cost of Motor Vehicle Accidents."

### 2.1.2 Methodology

In this accident analysis, we have attempted to determine the types of accidents resulting in the greatest cost to

society. We have concerned ourselves only with injury (including fatal) accidents and the cost associated with injury to the occupants of vehicles involved. We have neglected property damage costs because they are relatively small (about 29% of all accident costs) and are not necessarily resolved by modifications made to improve crashworthiness. As a way of quantifying the negative aspects of injuries and fatalities, we have used the concept of societal cost. This concept is extremely useful because the activities to which this analysis will be applied -- such as safety modifications to cars -- are themselves partly defined in terms of how much cost they add to the car. For comparison purposes (cost/benefit), guides such as this analysis must also use monetary terms. In addition, societal costs provide a method of weighting the relative importance of various levels of injury.

The methodology used in the accident analysis was presented in Figure 1.2. Referring to this figure, we can follow the analysis step by step.

- Step 1: The total number of accidents, injuries, and fatalities is obtained based on the estimate by the National Safety Council.
- Step 2: The total number of injuries and fatalities is divided among the accident modes using the Cornell Level II accident file.
- Step 3: The distribution of injuries with impact velocity for the various accident modes is obtained using the MDAI file with the results of Step 2. This distribution is stored for use in Step 7.
- Step 4: The societal cost for each injury level is determined based on the American Medical Association Abbreviated Injury Scale (AIS). A value of \$200,000 or 6,000 man days is the cost of a fatality. Cost of other injury levels follow a cubic curve to \$240,000 for a permanently disabling injury.
- Step 5: The MDAI file is used to determine the number and level of injuries in a mode-velocity range cell.

Step 6: The average cost per injury in a mode-velocity cell is calculated by combining Steps 4 and 5. The formula is:

$$\text{Cost/Injury} = \frac{\sum_{i=1}^{10} n_i \times \text{cost}_i}{N}$$

where  $n_i$  = number of injuries at level  $i$   
 $\text{cost}_i$  = cost of injury at level  $i$   
 $N$  = total number of injuries.

Step 7: The total societal cost of accidents for each mode-velocity cell is determined by multiplying the number of injuries in a particular velocity range by the average cost per injury in that range.

Let us consider each of these steps in detail. In Steps 1 and 2 we first divide the accident population into accident modes by area of involvement and type of object struck (i.e., front-to-front, front-to-side, etc.). The total number of injuries and fatalities, as estimated by the National Safety Council, is divided among the accident modes (1972 data) using the Cornell Level II accident file. This file (for 1971 and 1972) consists of over 29,000 vehicle involvements recorded from the Buffalo, New York area. It contains a similar ratio between rural and urban accidents as the national average, so it can be thought of as a good statistical sample of accidents nationwide. The similarity of the National Safety Council's "disabling-beyond-the-day-of-the-accident injury" and a level 1 or greater on the AMA-AIS injury scale indicates that the two million National Safety Council injuries corresponds to the number of Level 1-5 injuries nationwide.

Step 3 is necessary because safety modifications which will eliminate injuries tend to be most effective over a particular velocity range. To complete this step, we need information on how injuries and their resulting cost vary with velocity. The only accident file which records impact velocity and AIS injury level is the Multi-Disciplinary Accident Investigation file (MDAI). The MDAI file tends to be biased toward severe accidents, i.e., ones in which there is injury. It contains over 5,000

injury involvements out of nearly 6,000 total occupant involvements. The MDAI file would not be useful for, say, the distribution of accidents by velocity, but can be of use to determine the distribution of injuries by velocity. It should be noted that the impact velocity recorded in the MDAI file is an estimate of the true impact velocity and, though made by trained professional accident investigators, is still open to question. However, it is more accurate than the police-estimated velocity recorded in some accident files.

In this analysis we took velocity to be the relative velocity between a vehicle and the object impacted. For the vehicle-to-vehicle case, the velocity was taken to be one-half the closing velocity. The velocity in the primary rollover (single vehicle rollover) case is the velocity of the vehicle just prior to the initiation of the roll. The distribution of injuries by 10-mile-per-hour range for the various accident modes, as determined from the MDAI file, is shown in Figures 2.1 through 2.6.

Step 4, determining the cost associated with various injuries, is perhaps the most difficult part of the accident analysis. It is, at best, a tenuous procedure and problems of what to include in the cost of an injury are open to interpretation. Medical costs are certainly not the only "costs" of an injury. Including time lost from work might make the estimate more realistic, but still does not include any costs associated with the pain and suffering of an injury. These "costs" are by far the hardest to quantify and most open to subjective considerations. In this accident analysis, we used the injury and fatality costs presented in the Department of Transportation preliminary report "The Societal Cost of Motor Vehicle Accidents."<sup>4</sup> The report only includes direct costs such as medical costs and time lost from work, and makes no attempt to quantify pain and suffering or to put an intrinsic value on human life. The societal cost of a death is placed at the value of wages lost and medical bills incurred. This should present a conservative estimate of the negative aspects of injuries

DISTRIBUTION OF INJURIES BY VELOCITY RANGE

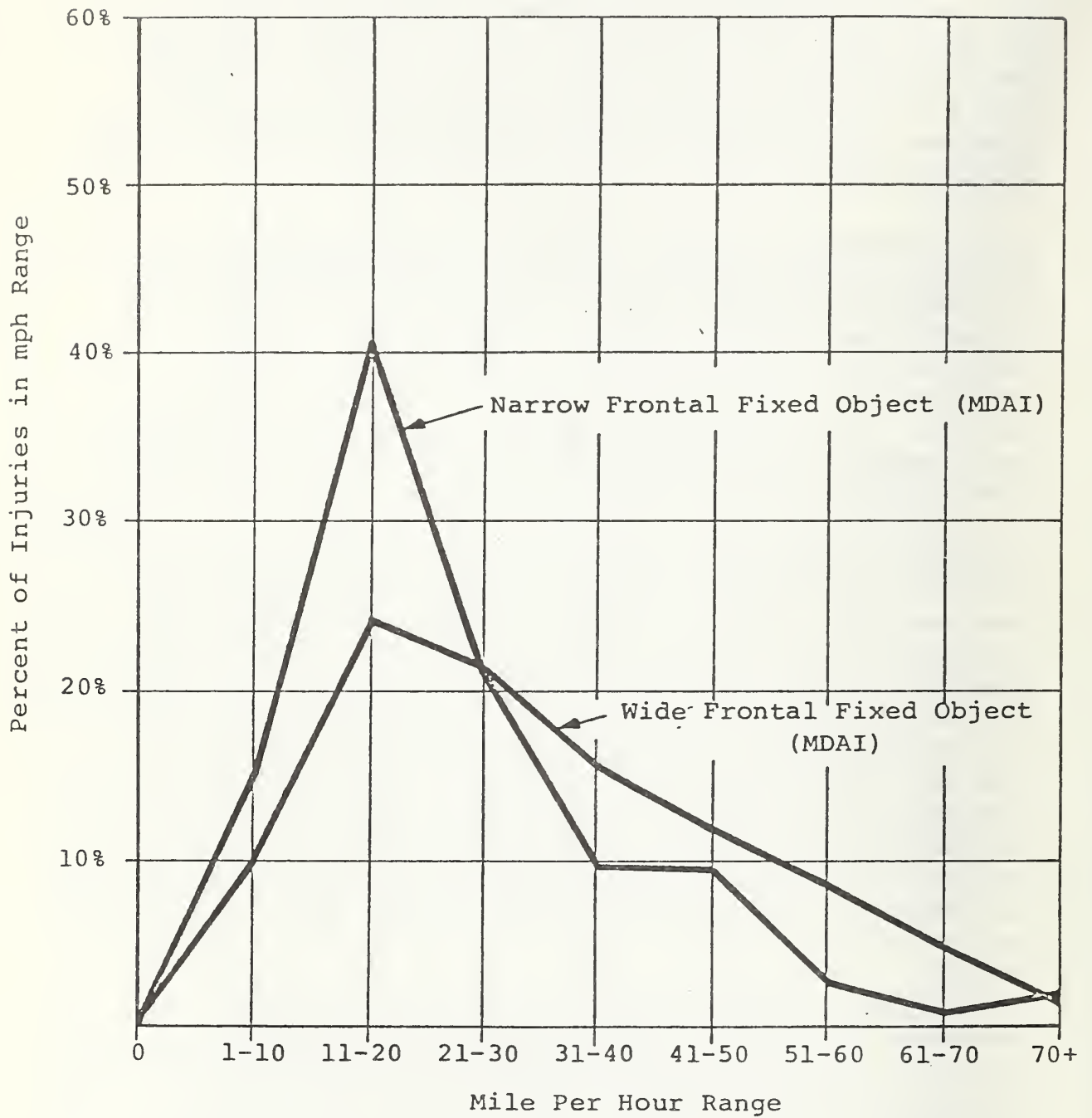


FIGURE 2.1 FRONTAL FIXED OBJECT

# DISTRIBUTION OF INJURIES BY VELOCITY RANGE

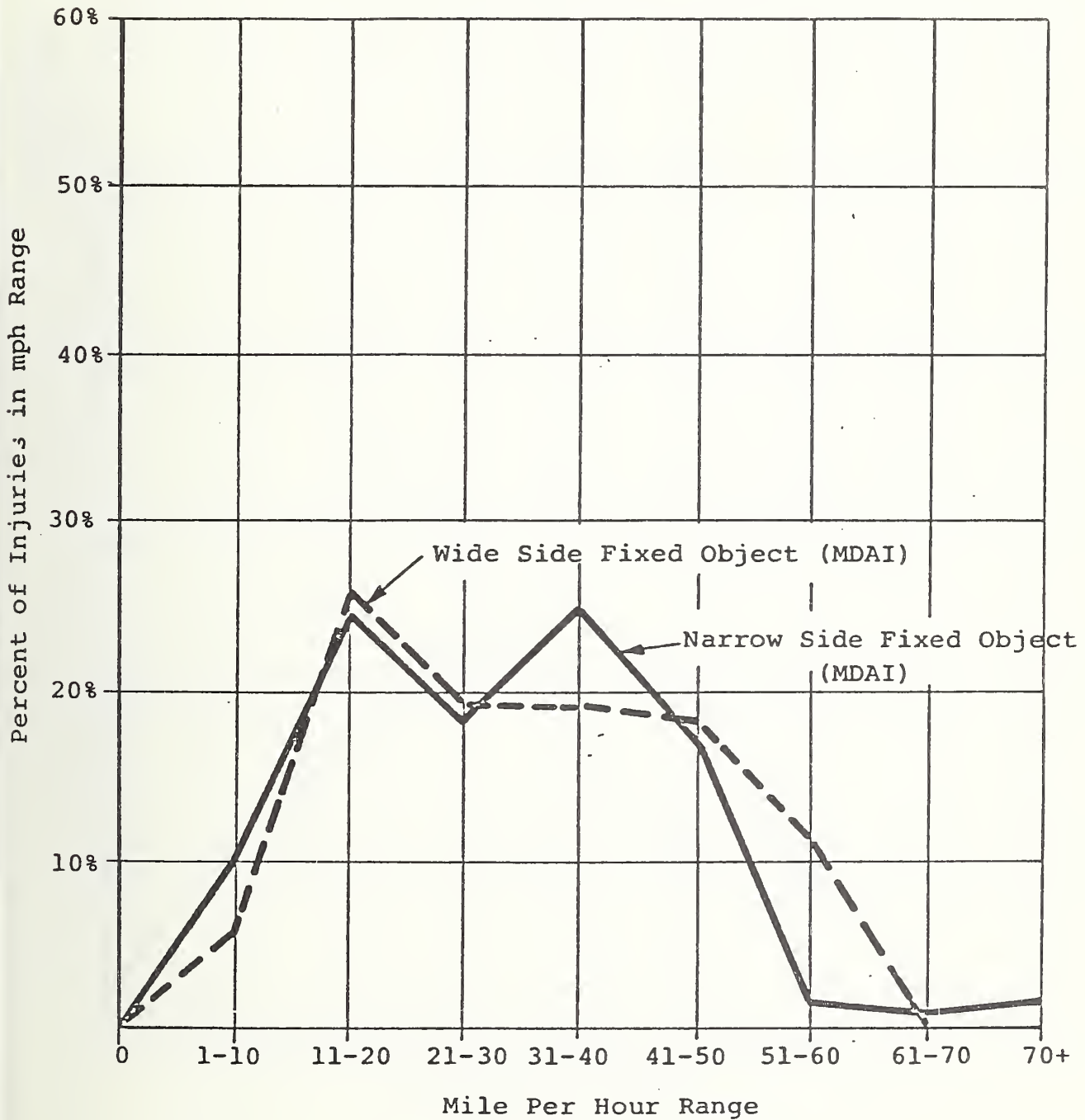


FIGURE 2.2 SIDE FIXED OBJECT

DISTRIBUTION OF INJURIES BY VELOCITY RANGE

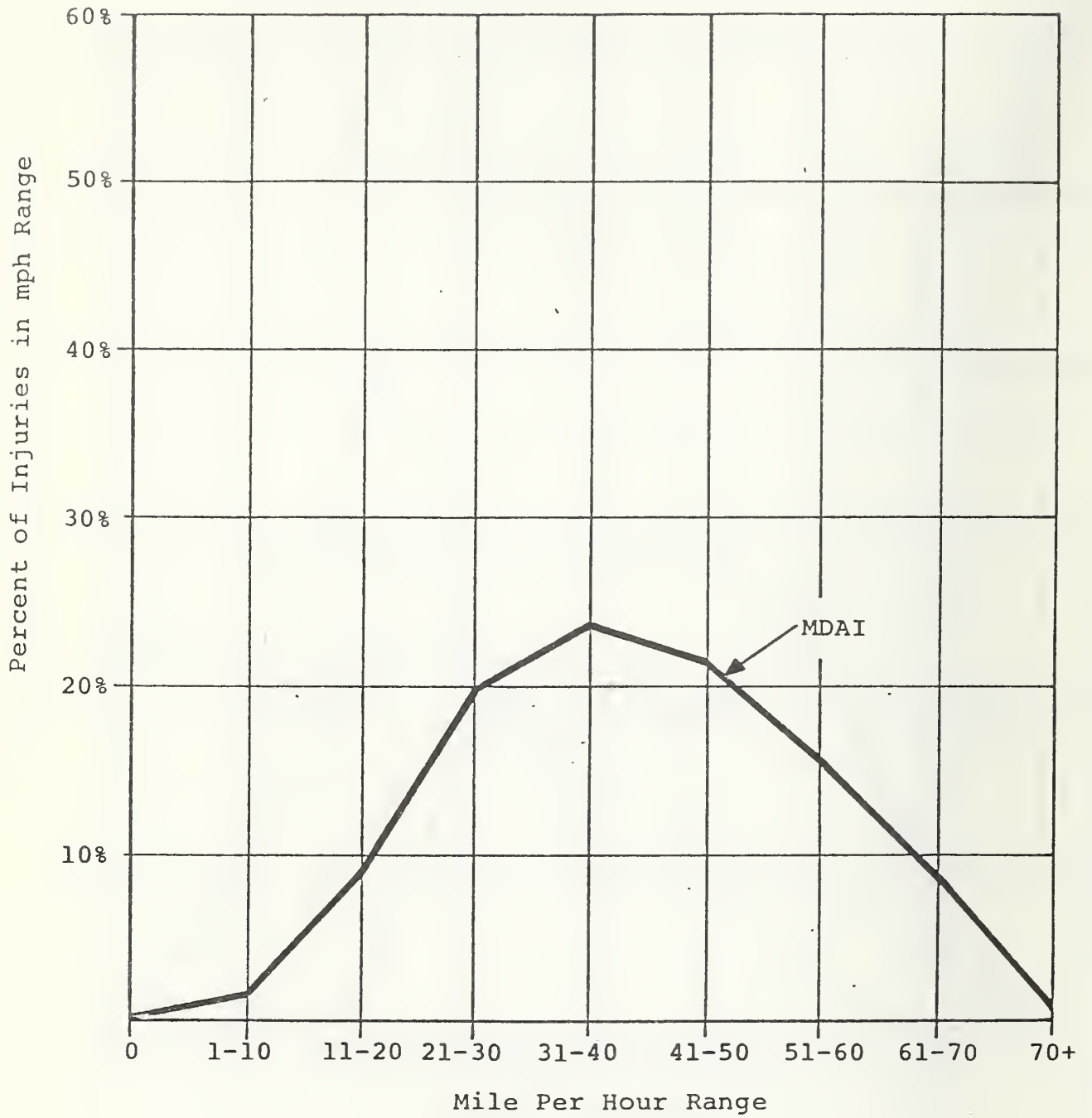


FIGURE 2.3 PRIMARY ROLLOVER

# DISTRIBUTION OF INJURIES BY VELOCITY RANGE

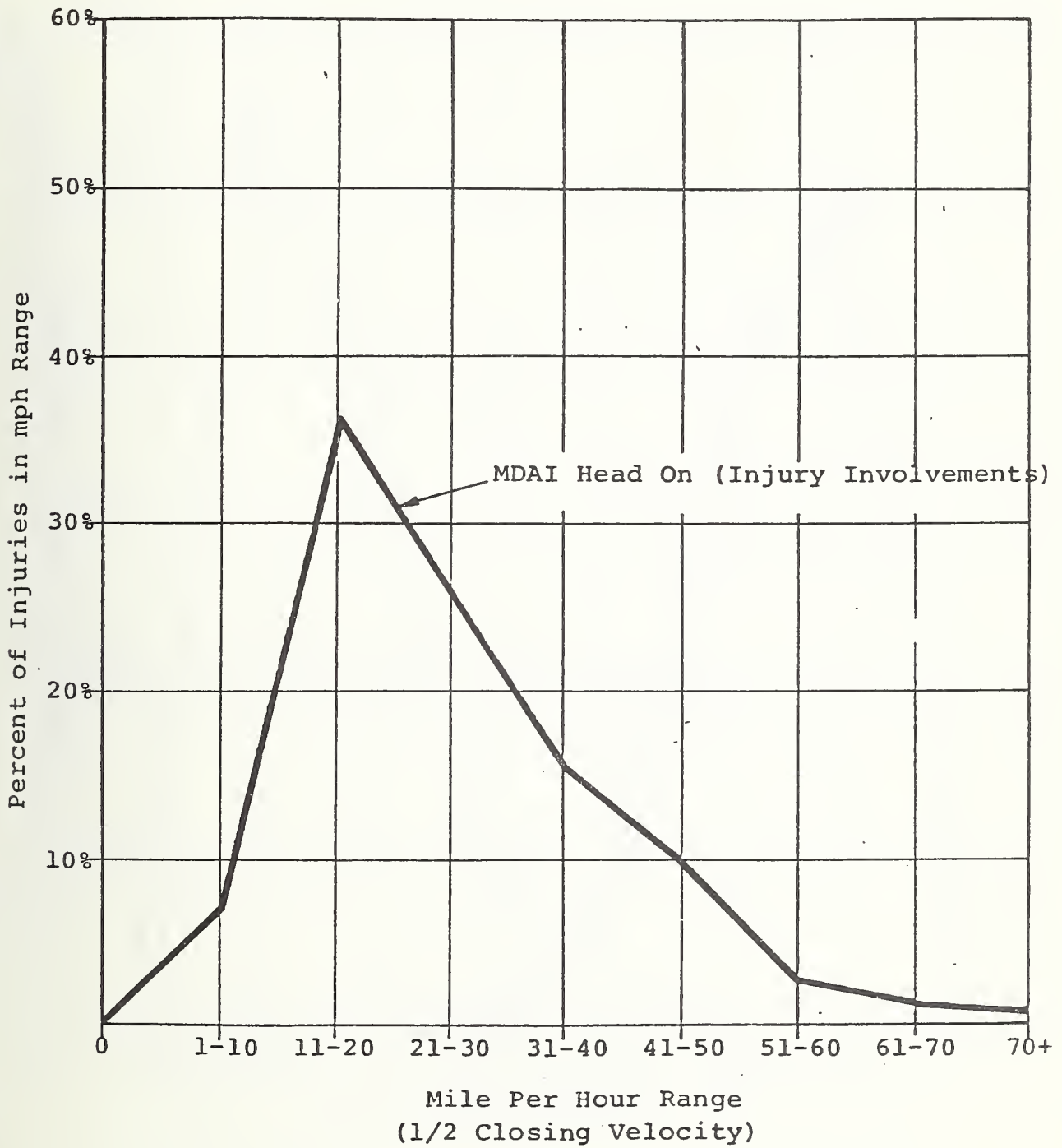


FIGURE 2.4 CAR-TO-CAR HEAD ON

DISTRIBUTION OF INJURIES BY VELOCITY RANGE

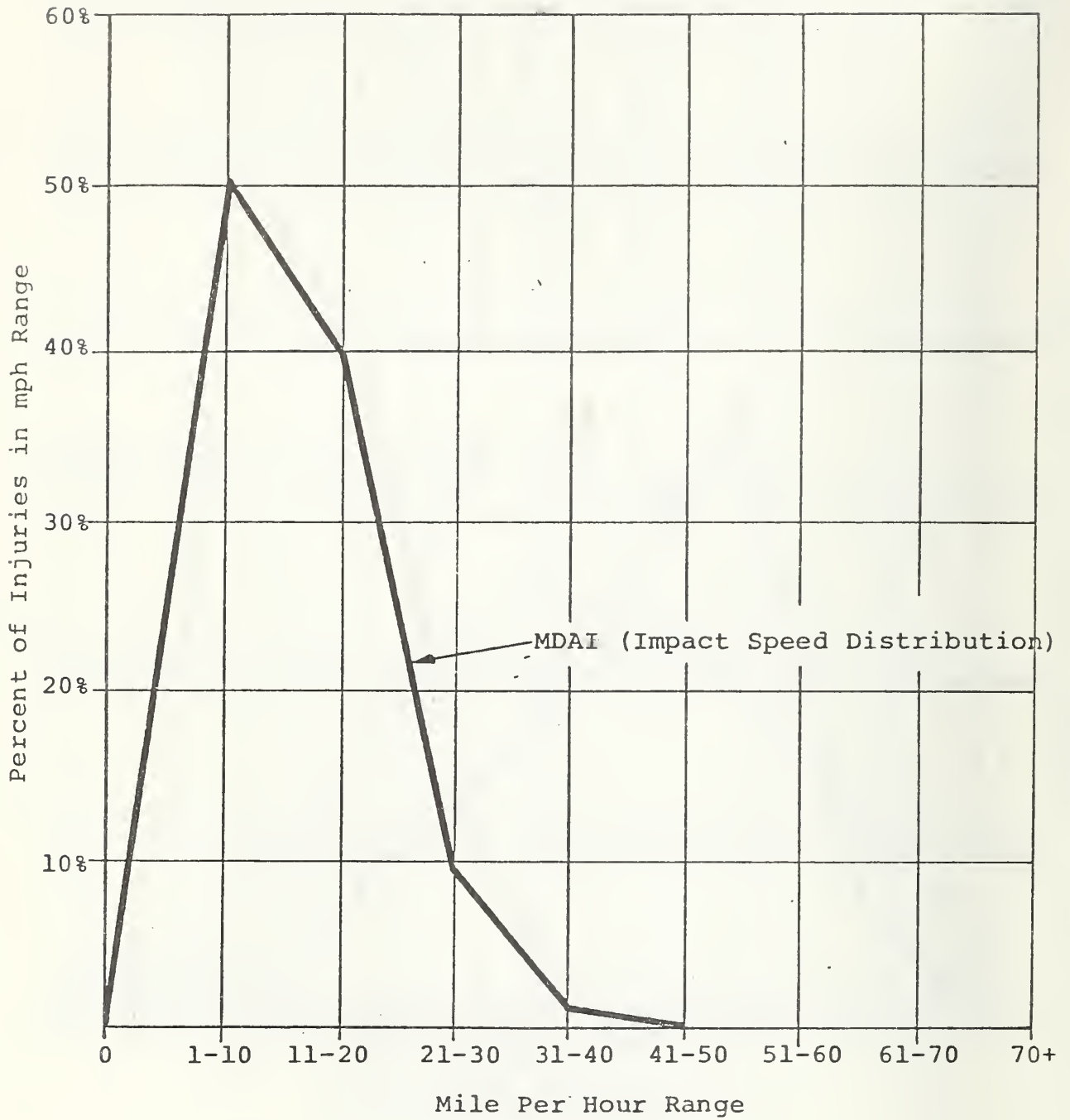


FIGURE 2.5 CAR-TO-CAR SIDE COLLISIONS

# DISTRIBUTION OF INJURIES BY VELOCITY RANGE

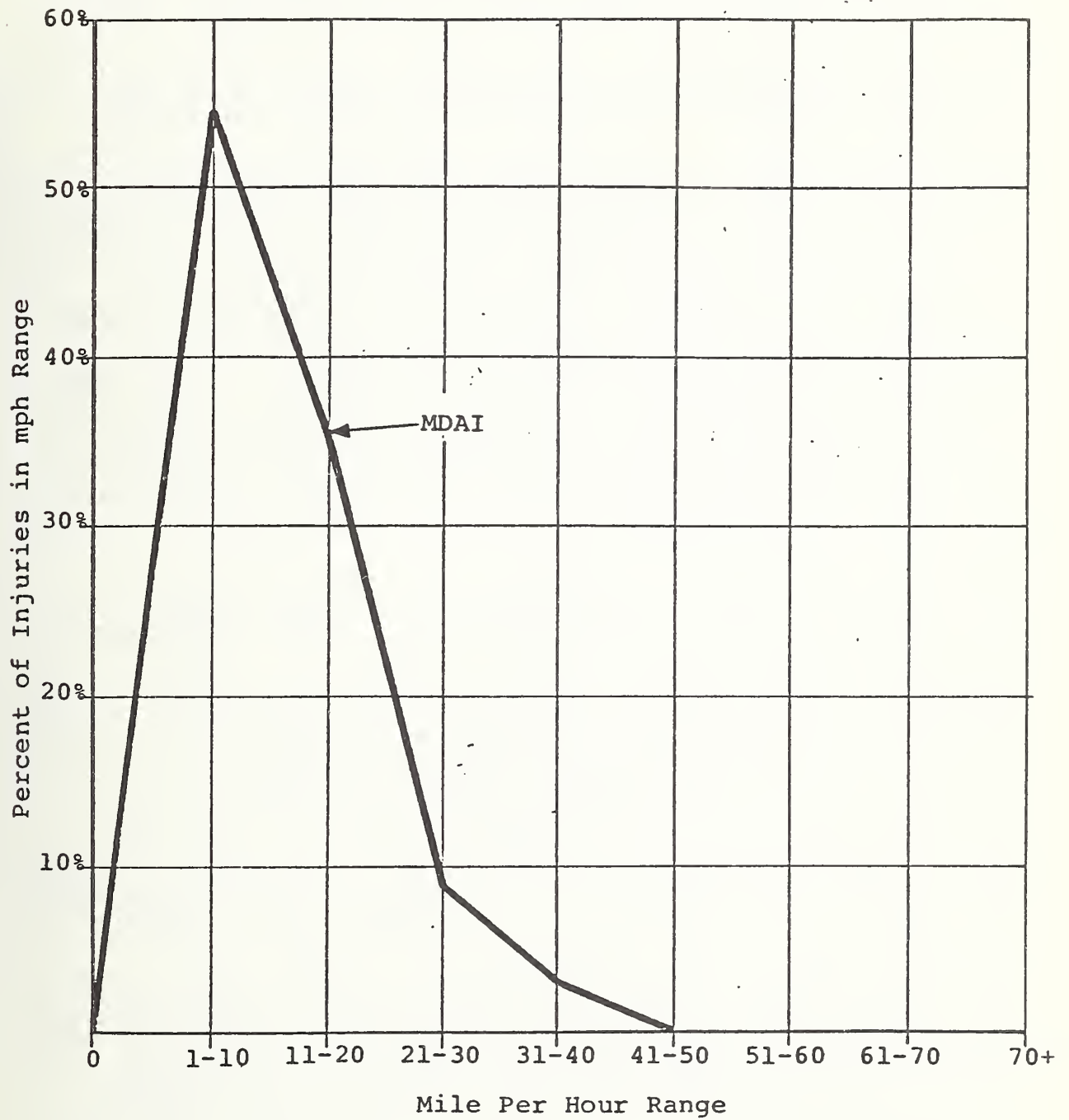


FIGURE 2.6 CAR-TO-CAR REAR END

and fatalities, and what it is worth spending to alleviate them. Unfortunately, injury levels recorded by accident investigators are not those used in "The Societal Cost of Motor Vehicle Accidents," so a method was devised to assign a societal cost to an injury scale used by accident investigators.

The American Medical Association Abbreviated Injury Scale (AIS) was chosen as a reliable representation of the level of injury suffered in accidents. In those accident files where it is used, the assigning of an injury level is based on a doctor's judgment of the type of injury suffered. The Police Injury Scale, which is coded by police at the time of the accident, was felt to be less reliable. In accident files where both police and AIS injury levels are recorded, there does not seem to be a good correlation between the two scales. This might be expected, since the police scale is based on a subjective determination of injury and rated by police officers with limited medical knowledge, whereas the AIS scale is defined in terms of specific types of injury and rated by a medical doctor.

Having chosen the AIS injury scale, how much cost should one assign to each injury level on the scale? We used the figure of \$200,000 from "The Societal Cost of Motor Vehicle Accidents" as the cost of a fatality. Levels 6 through 9 on the AIS scale represent various levels of fatality and therefore are assigned a societal cost of \$200,000 (levels 7 through 9 represent more than one fatal injury). Injury levels 1 through 5 represent various levels of non fatal injury. Since each increment has a physical definition -- broken limb, laceration, etc. -- we can estimate cost by comparison to known costs of injuries. For instance, the railroad industry keeps careful track of work time lost due to injuries and defines injuries in physical terms, as does the AMA AIS. The Federal Railroad Administration publication Accident Bulletin No. 140<sup>5</sup> equates a fatality to 6,000 lost man days, with broken limbs, etc., having correspondingly lower costs in man days. Using the \$200,000 and 6,000 man days as a reference point, we can compute the cost of various AIS injury levels by simple ratios. The

cost is based on the ratio of man days lost to man days lost for a fatality times the societal cost of a fatality. Figure 2.7 shows the cost associated with various levels of injury on the AIS scale as calculated by this method. The curve, which turns out to be a "cubic" to Level 6, rises to \$240,000 just before Level 6 since that is the cost "The Societal Cost of Motor Vehicle Accidents" assigns to a permanently disabling injury.

Having established the relationship between injury level and cost, we can proceed to Step 5. The total number of injuries in each velocity range for a particular accident mode is just the total number of injuries in that mode times the probability of occurrence in that velocity range.

To determine the average cost per injury in a mode velocity range, Step 6, we sum over the AIS injury levels the number of injuries at each AIS injury level in the MDAI file (in the mode/velocity range) times the cost at that level divided by the total number of injuries in that mode/velocity range (in the MDAI file). In mathematical terms

$$\text{Avg. Cost/Injury} = \sum_{i=1}^9 \frac{n_i \times \text{cost}_i}{N} ,$$

where  $i$  = injury level,  
 $n_i$  = number of injuries at each level (in MDAI file),  
 $\text{cost}_i$  = cost of an injury at level  $i$ , and  
 $N$  = total number of injuries

Figures 2.8 through 2.13 show the average cost per injury for the various accident modes.

The final step, Step 7, is to determine the total cost in a particular mode/velocity range. This value is the total number of injuries in a mode/velocity range, from Step 3, times the average cost per injury from Step 6. The results are presented in Appendix D in tabular form. They are summarized in Figures 2.14 through 2.16. These figures are plots of the total societal cost of motor vehicle accidents as a function of velocity for frontal, side, and rear impact involvements.

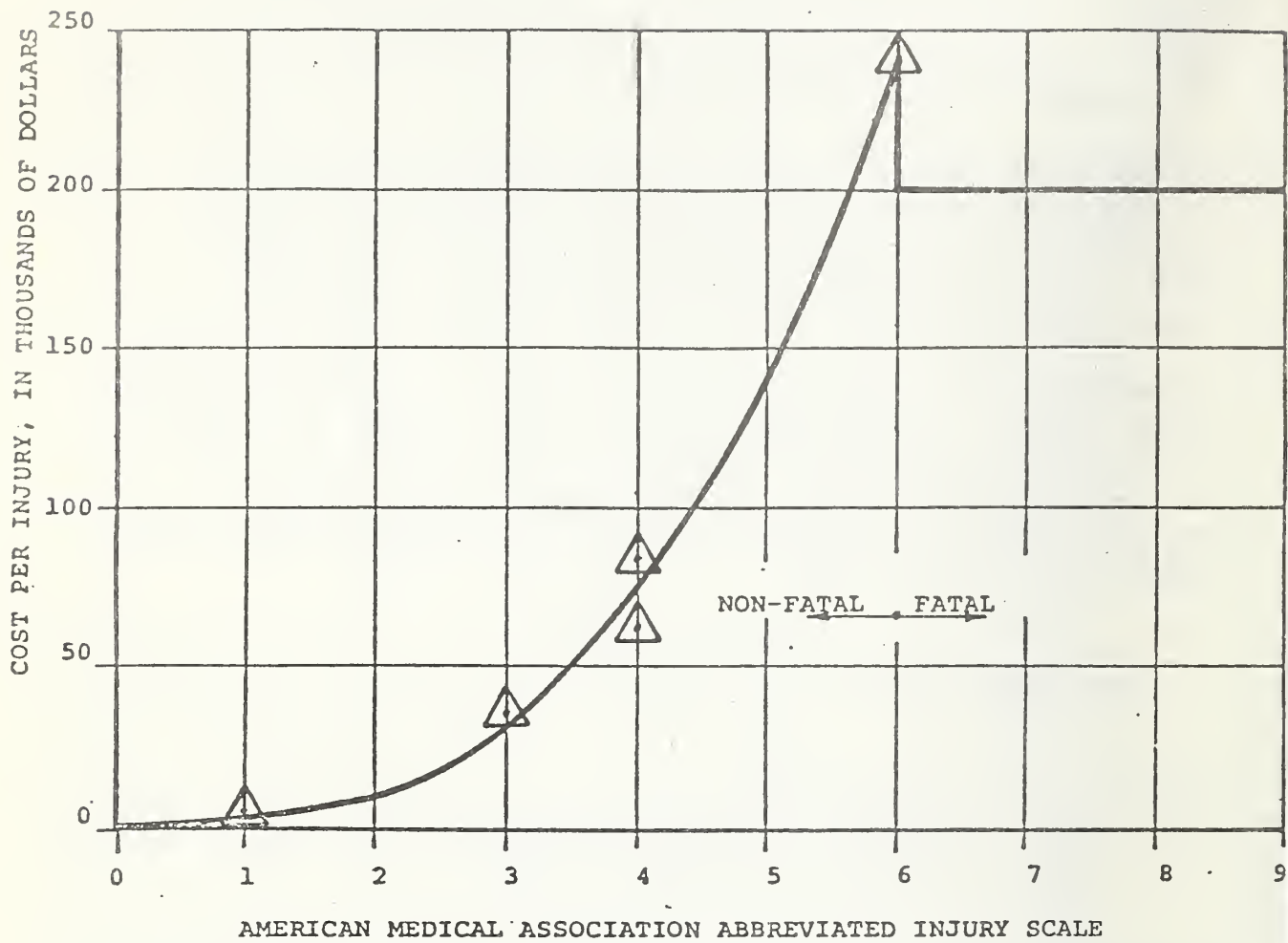


FIGURE 2.7 SOCIETAL COST VERSUS AMA INJURY SCALE

# AVERAGE COST PER INJURY

- △ Narrow (less than 16")
- Wide (greater than 16")

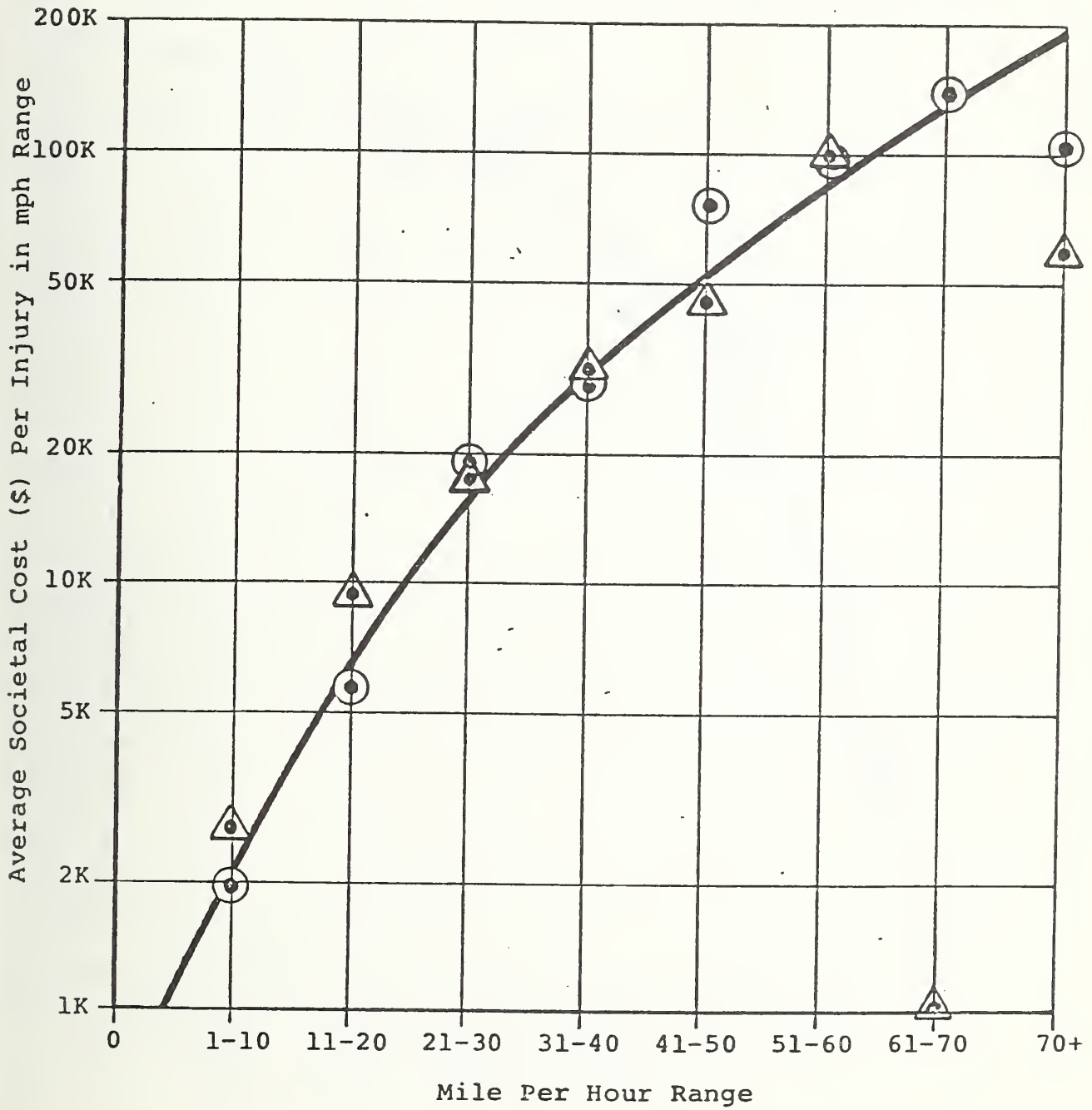


FIGURE 2.8 FRONTAL FIXED OBJECT

AVERAGE COST PER INJURY

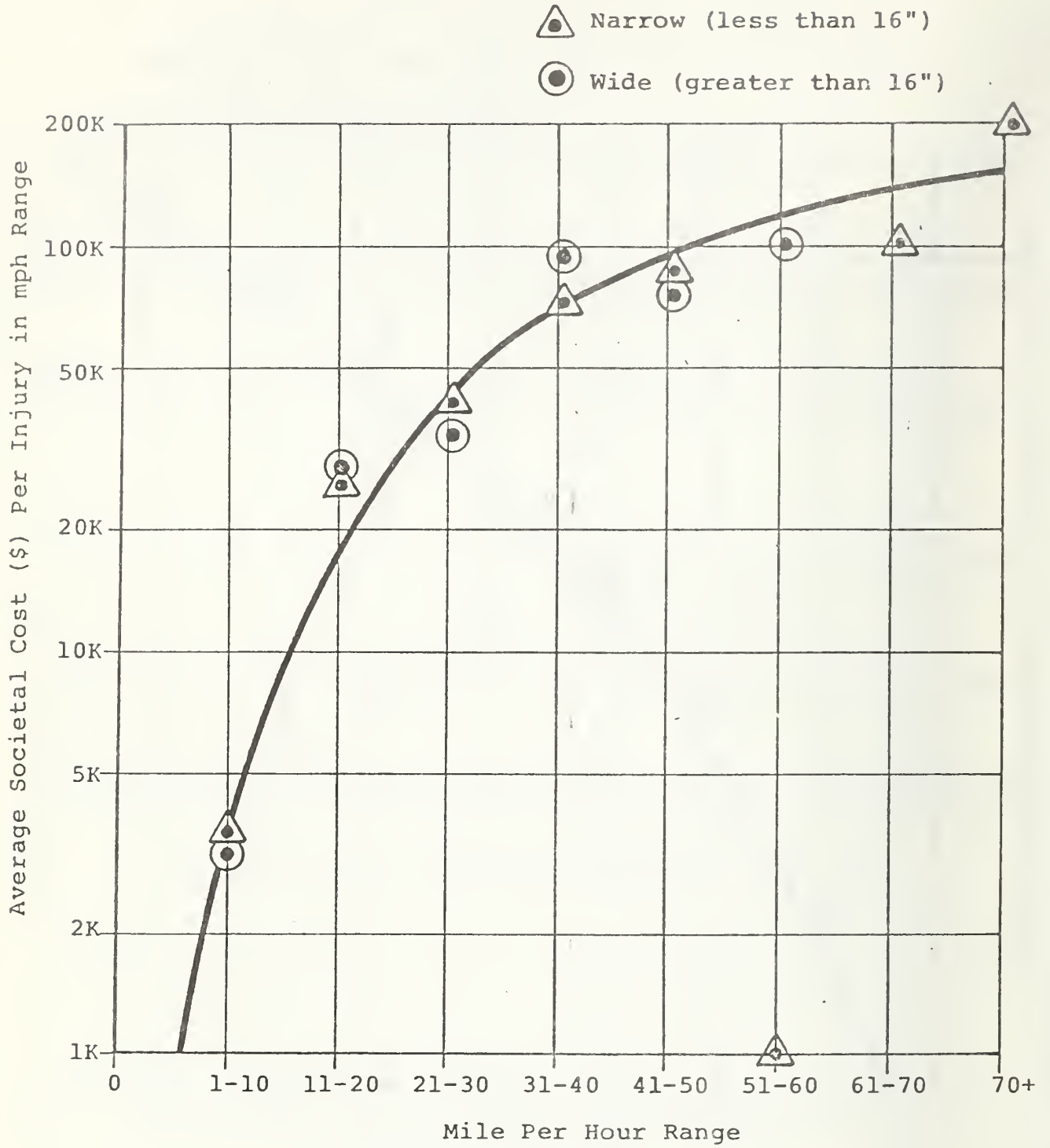


FIGURE 2.9 SIDE FIXED OBJECT

### AVERAGE COST PER INJURY

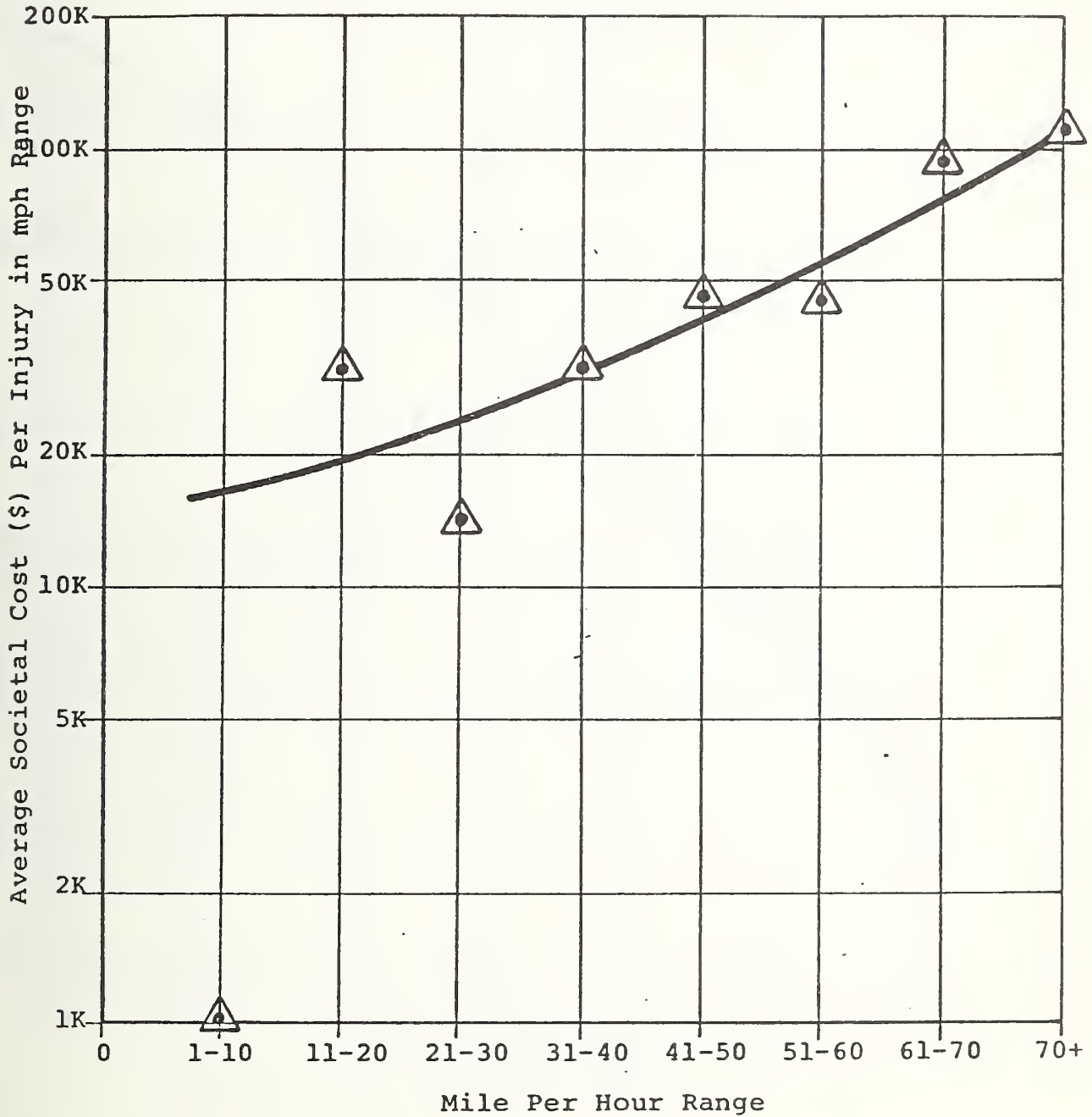


FIGURE 2.10 PRIMARY ROLLOVER

### AVERAGE COST PER INJURY

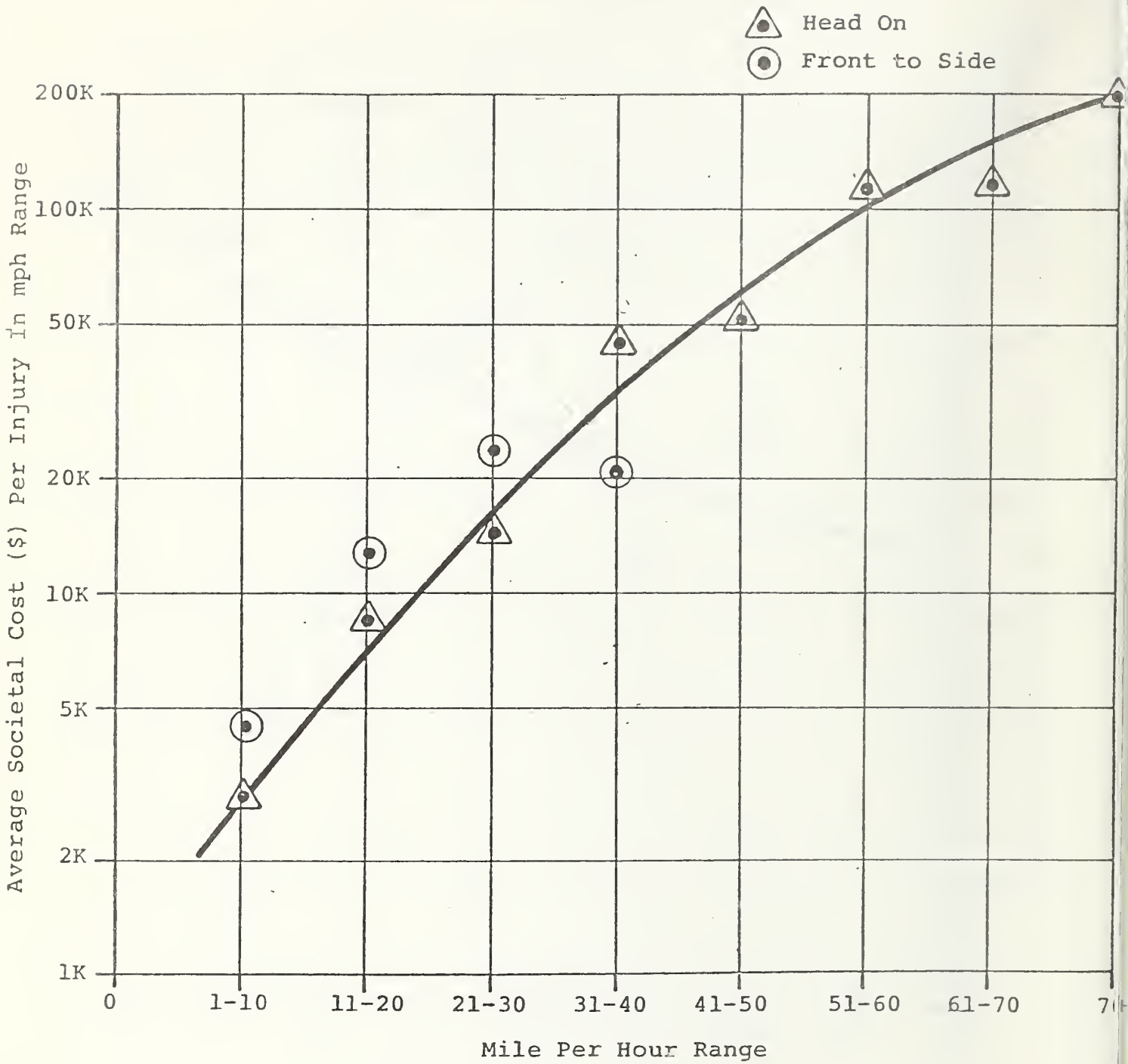


FIGURE 2.11 VEHICLE TO VEHICLE FRONTAL

AVERAGE COST PER INJURY

- △ Side to Front
- Sideswipe

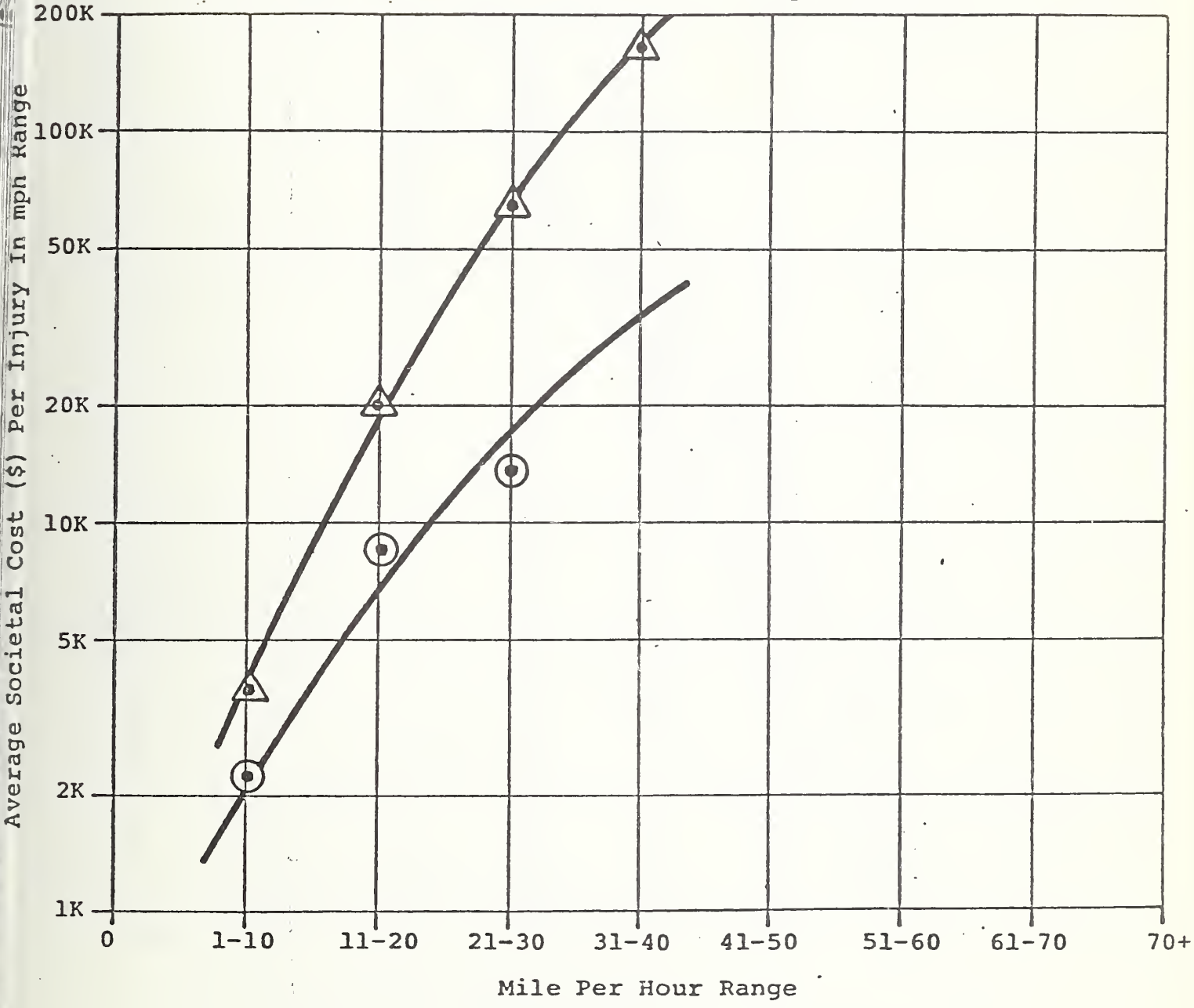


FIGURE 2.12 VEHICLE TO VEHICLE SIDE

AVERAGE COST PER INJURY

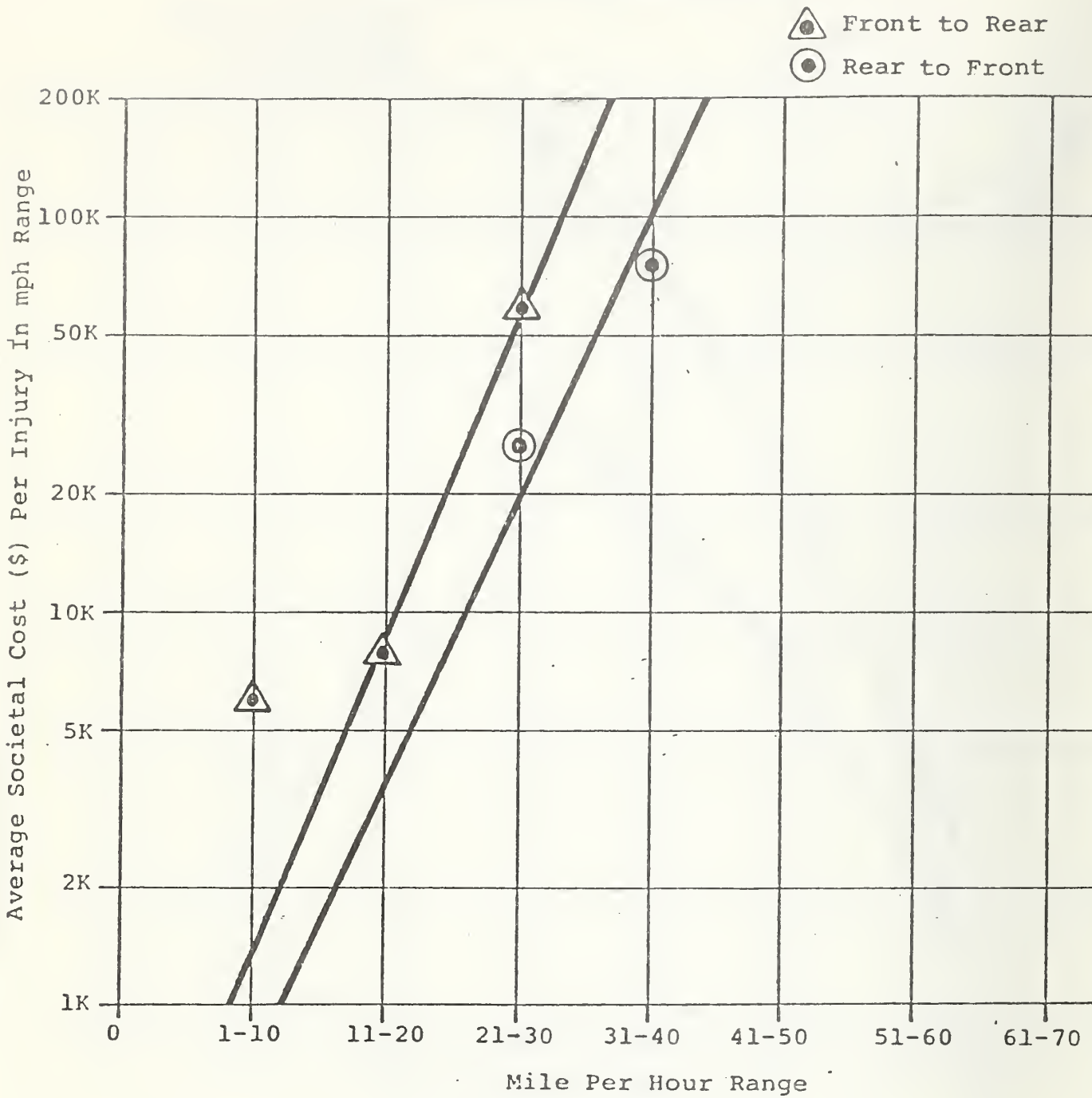


FIGURE 2.13 VEHICLE TO VEHICLE REAR

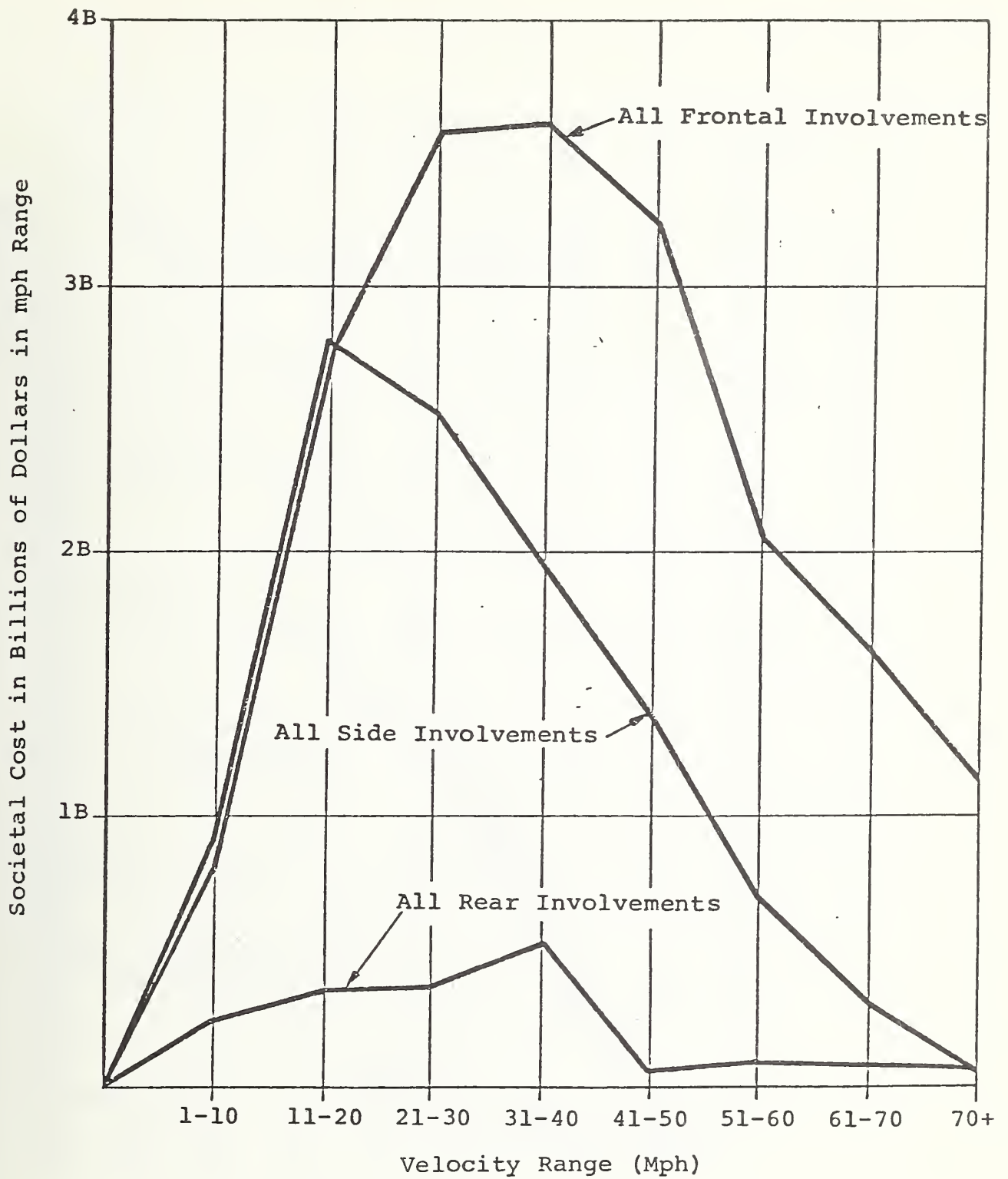


FIGURE 2.14 SOCIETAL COSTS IN 10 MPH RANGES FOR VARIOUS TYPES OF INVOLVEMENT

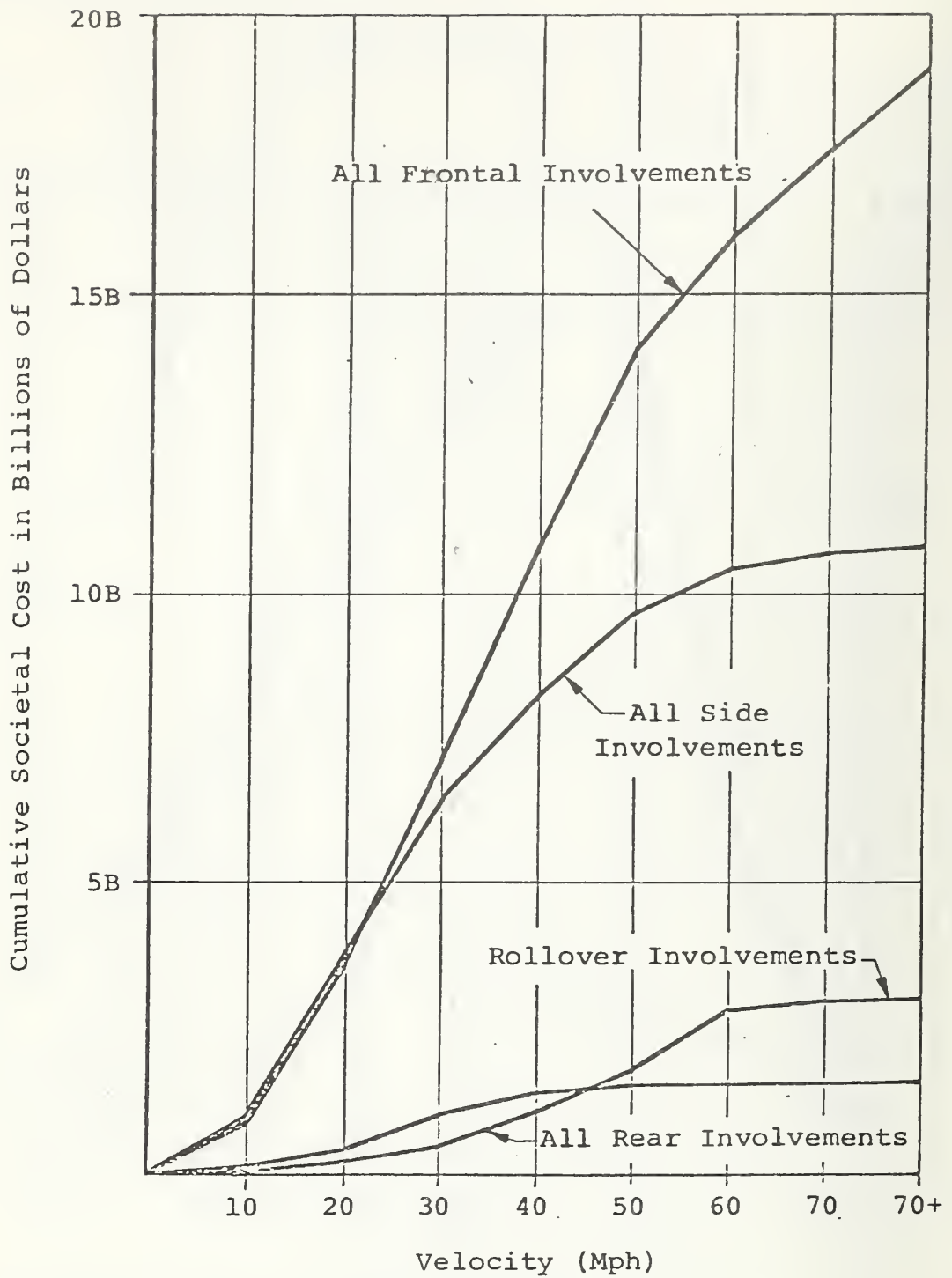


FIGURE 2.15 CUMULATIVE SOCIETAL COSTS FOR VARIOUS TYPES OF INVOLVEMENT

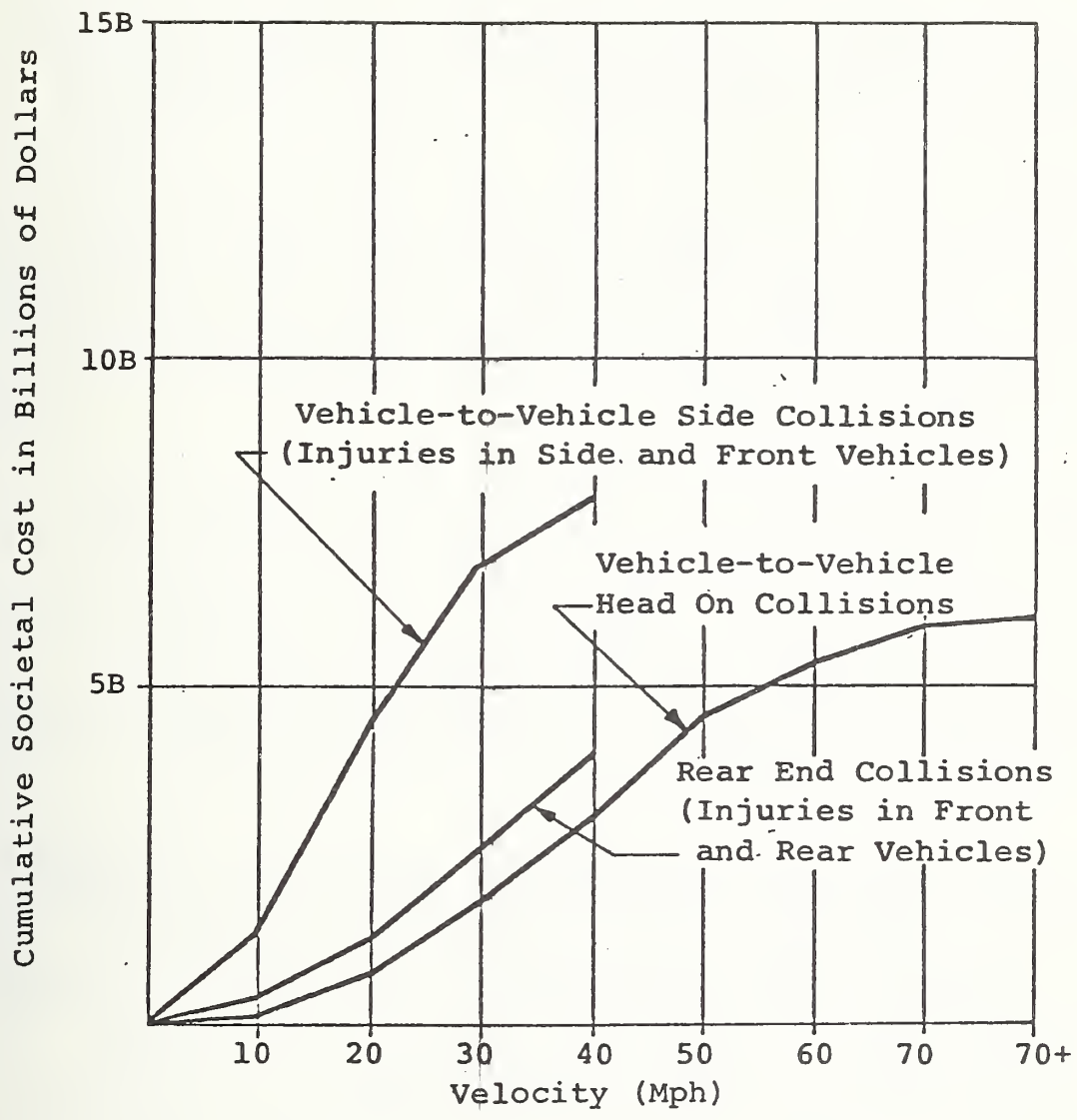


FIGURE 2.16 CUMULATIVE SOCIETAL COSTS FOR VARIOUS ACCIDENT TYPES

### 2.1.3 Interpretation of Results

The information in this analysis can be interpreted to give many interesting and useful results. For instance, what is it worth -- what societal cost will be saved -- to eliminate all casualties in frontal collisions to 50 mph, as is currently proposed? Since spending a dollar on a safety modification for an expected return of one dollar might seem unreasonable, we have assumed a 4:1 benefit/cost ratio. In other words, one-fourth the societal cost per vehicle represents what could justifiably be expended per vehicle to eliminate all injuries in a particular mode/velocity range. Maintaining a benefit/cost ratio of 4:1 not only makes the estimates of what could be spent in each mode to eliminate injuries conservative, but also allows for any uncertainty in the data.

Based on these results, priorities for the development of safety modifications to vehicles can be developed. One can see from the curves in Figure 2.15 that the front end involvements result in substantially greater costs than rear end involvements. Side impacts also represent significant societal cost. Rollover accidents account for a surprisingly large portion of the societal cost of accidents, especially considering their relative infrequency.

In this analysis we have attempted to quantify the benefit to society which would be realized by reducing the frequency of injuries and fatalities in a number of accident modes. We do not claim that the results presented here are exactly right or represent the only way to interpret the data. They do, however, provide a useful way of viewing the accident situation and do present a good estimate of the relative magnitude of various components of the accident population. To keep the analysis simple, we divided the accident population into a relatively few modes. However, if one wanted to decide what specific modifications should be made to, say, a vehicle's front end structure, a more detailed analysis of the accident population would be desired. The societal cost of these accidents will have a strong effect on what structural modifications are cost effective.

It should be mentioned that the accident analysis is based on the distribution of accidents as they exist today (or within the last few years). No attempt has been made to evaluate the effect of safety improvements such as seat belt shoulder harness interlock systems required under FMVSS 208. However, our analysis indicates that a large percentage of societal cost is incurred at velocities and in accident modes in which harnesses have limited effectiveness.

The current popularity of the small car will also have an influence on the societal cost of motor vehicle accidents. Safety improvements which cannot be justified for big cars may be necessary on small cars to compensate for the increased injury potential in a small car due to the unequal mass effects when impacting a heavier vehicle.

## 2.2 Compatibility Analysis

### 2.2.1 Introduction

The compatibility analysis constitutes the largest part of the mathematical studies. The purpose was three-fold. First, the study was required to determine the behavior of the baseline vehicles when impacting other vehicles in the traffic mix. In other words, we were to determine the compatibility of production subcompact structures with other size vehicles. Second, the effects of various restraint systems were investigated. And, third, the study was to determine an idealized structural modification and assess the effect on the compatibility of the subcompact vehicle. This would measure both the effectiveness of the energy management system and the aggressivity of the modified structure.

The complete report of the compatibility study is presented in detail in Appendix E. The reader who is interested in the detailed analysis is referred to that report. The purpose of section 2.2 is to summarize the method and results with emphasis on the logic of the study rather than the precise calculations.

The techniques used throughout the study are the results of several years of development by the entire auto safety community. Similar math models have been used by various investigators to study both frontal barrier and vehicle-to-vehicle impacts. In accordance with the specifications of Task 3, existing Minicars models were used rather than undertaking extensive development of new models. The unique feature of the subcompact vehicle compatibility study was the extent and variety of vehicles included. A total of nine different vehicles representing the four major U.S. manufacturers, model years 1971 to 1974, and weights from 2,520 pounds to 6,170 pounds were used.

In accordance with contractual design goals, the basic mode of impact investigated was a vehicle-to-vehicle, aligned, frontal crash. Effects of offset collisions, oblique collisions, and side and rear impacts were not considered. Each of the eight other vehicles was used to impact the subcompact vehicle. Thus the results of the study reflect the frontal compatibility of the subcompact car with most other weight, make, and age vehicles of the traffic mix.

The primary information obtained was the critical closing velocity for each pair of vehicles. The critical closing velocity is defined as the minimum relative velocity of two impacting vehicles which causes either the Pinto to crush 45 inches, or the occupant to stroke 20 inches. These are the typical maximum distances available in the subcompact. These limiting values were determined by actual measurement and subjective evaluation. The results and conclusions derived in the study must be considered in the light of these limits. Other crush or stroke limits may alter the results.

### 2.2.2 Methodology

The basic model used in the compatibility analysis was a lumped mass model with defined mass points connected by non-linear force couplings. The solution routine is a time step integration of the governing equations of motion. This model offers the best compromise between the elaborate finite element models and the simplistic

closed form solutions. The finite element (or continuous medium) models are expensive, time consuming, and, as yet, unproved in automobile impact studies. Current programs sponsored by NHTSA may soon provide workable finite element models of automobiles, but these are not yet available for general use. The closed form solutions generated in the early stages of auto safety work do not address either the problem complexity or the non-linear nature of the crash. It is the time step integration routine which allows for true consideration of the non-linear force deflection characteristics of the force couplings. The classic model used in the analysis is shown in Figure 2.17. The model itself and the solution procedure are described in very great detail in Appendix E and will not be repeated here.

The mass points shown in Figure 2.17 represent the major masses of the vehicles such as engine, passenger compartment, etc. The force couplings are the primary load paths through the vehicle. The force couplings are defined by force-deflection curves relating the force generated between two mass points to the relative displacement of the masses. These curves can be obtained by either calculation or static test. The curves used in the study of the production vehicles (Phase I) represent actual test data. The curves of the idealized subcompact structure (Phase III) were calculated values. A typical force deflection ( $F-\delta$ ) curve is shown in Figure 2.18.

It is the non linear nature of the  $F-\delta$  curves which requires the use of the time step integration routine. With this integration system, each progressive time step uses the results of the previous integrations as initial conditions. A special subroutine in use at Minicars provides for hysteresis action of the force couplings. The special routine also applies a velocity-dependent factor to the static crush behavior. This factor accounts for all velocity effects such as strain rate, etc.

The second phase of the study, the restraint effect analysis, used a model developed for airbag simulation, called ABAG19. It is basically a one-dimensional model of the driver torso

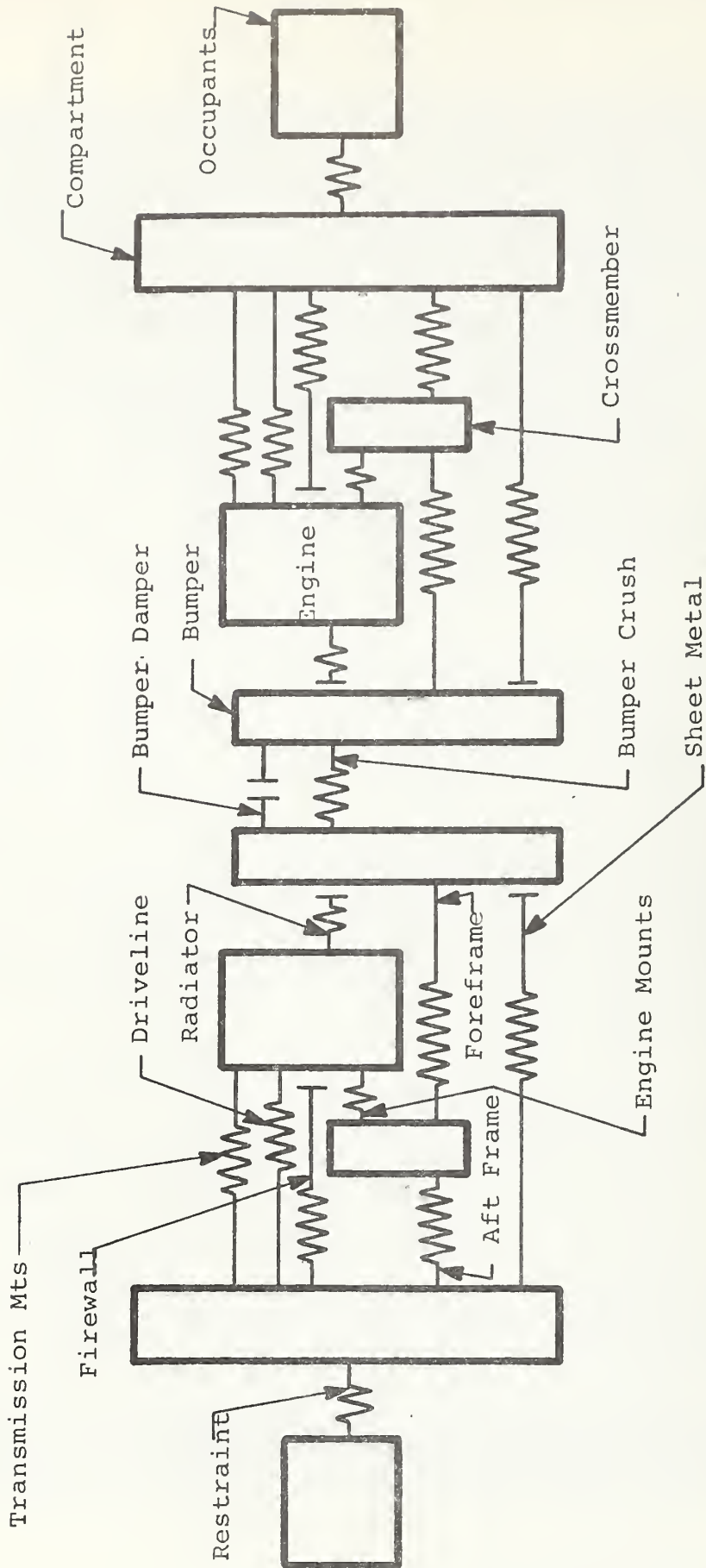


FIGURE 2.17 TWO CAR MODEL

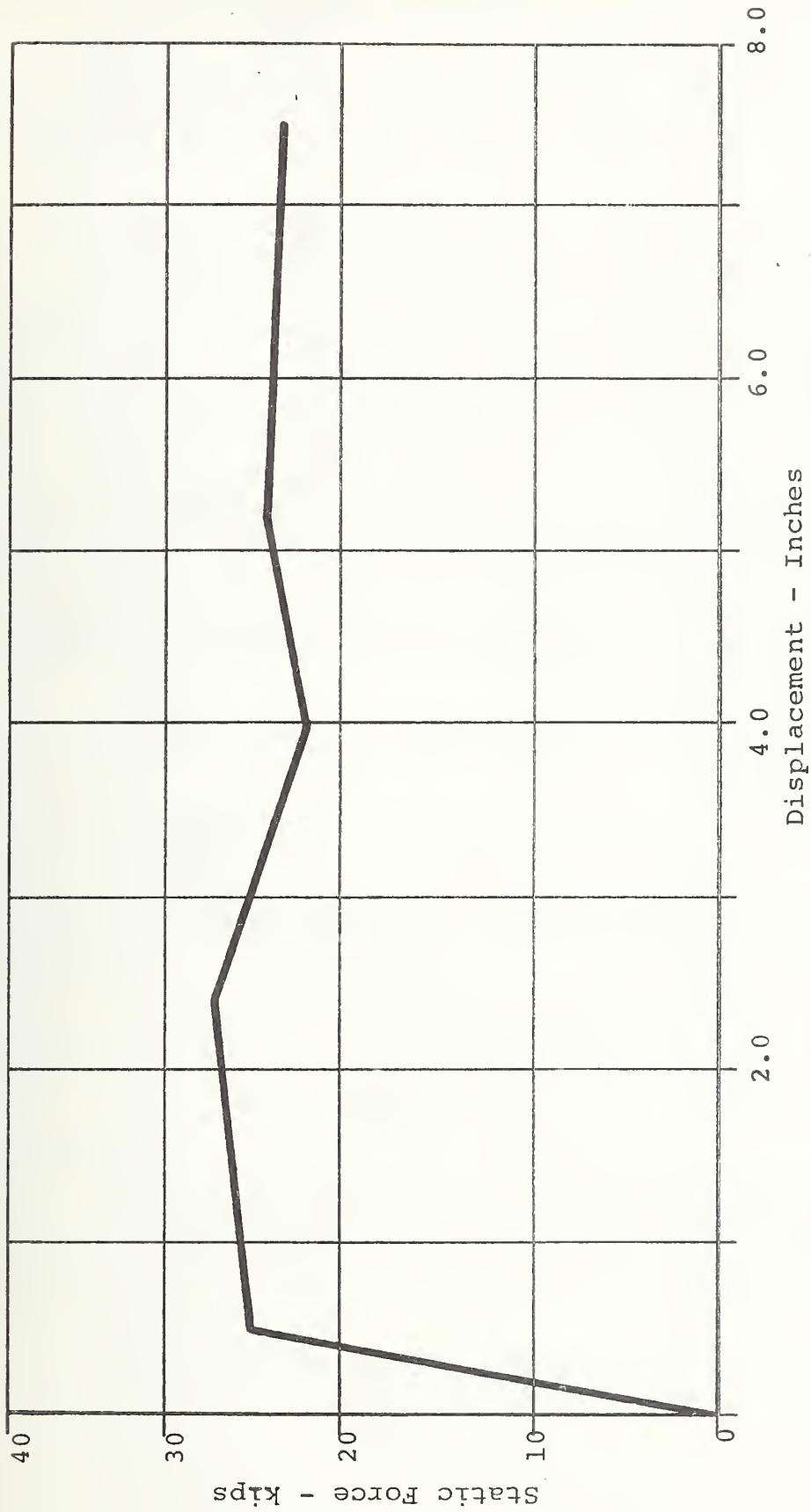


FIGURE 2.18 TYPICAL FORCE DISPLACEMENT (F- $\delta$ ) DATA

interacting with the airbag while the entire assembly is stroking toward the dash. This model uses the crush pulse determined by the vehicle model as input data. It also uses complete airbag data, airbag support data, size of occupant, and stroke of the restraint rear plane. The ABAG19 model uses the same solution routine as the vehicle impact model.

Both of the mathematical models were correlated with dynamic test data to verify the results. The TENMASS model was correlated with a frontal vehicle-to-vehicle impact between a 1968 Plymouth Fury and a 1974 Pinto. The nominal closing velocity was 80 mph. The acceleration time histories of both of the cars compared to the predicted values are shown in Figures 2.19 and 2.20. The comparisons were made at five millisecond intervals as this was the edit interval of computer run. Table 2.1 summarized the pertinent parameters of this bench mark crash. The ABAG correlations are shown in Figure 2.21. From the curves, it is apparent that both models provide reliable estimates of the dynamic behavior of the vehicles and occupants during impacts.

The methodology of the compatibility study is best summarized as follows:

#### Phase I - Study of Baseline Vehicles

1. Obtain force-deflection and geometrical data on the subject vehicles.
2. Prepare dynamic model using TENMASS and DYSIM.
3. Run program for 80 mph and 100 mph for each vehicle pair.
4. Interpolate or extrapolate to determine critical closing velocity. This is based on the defined limits of 45 inches of crush and 20 inches of occupant stroke.
5. Plot the resulting critical closing velocity as a function of "other" vehicle weight.

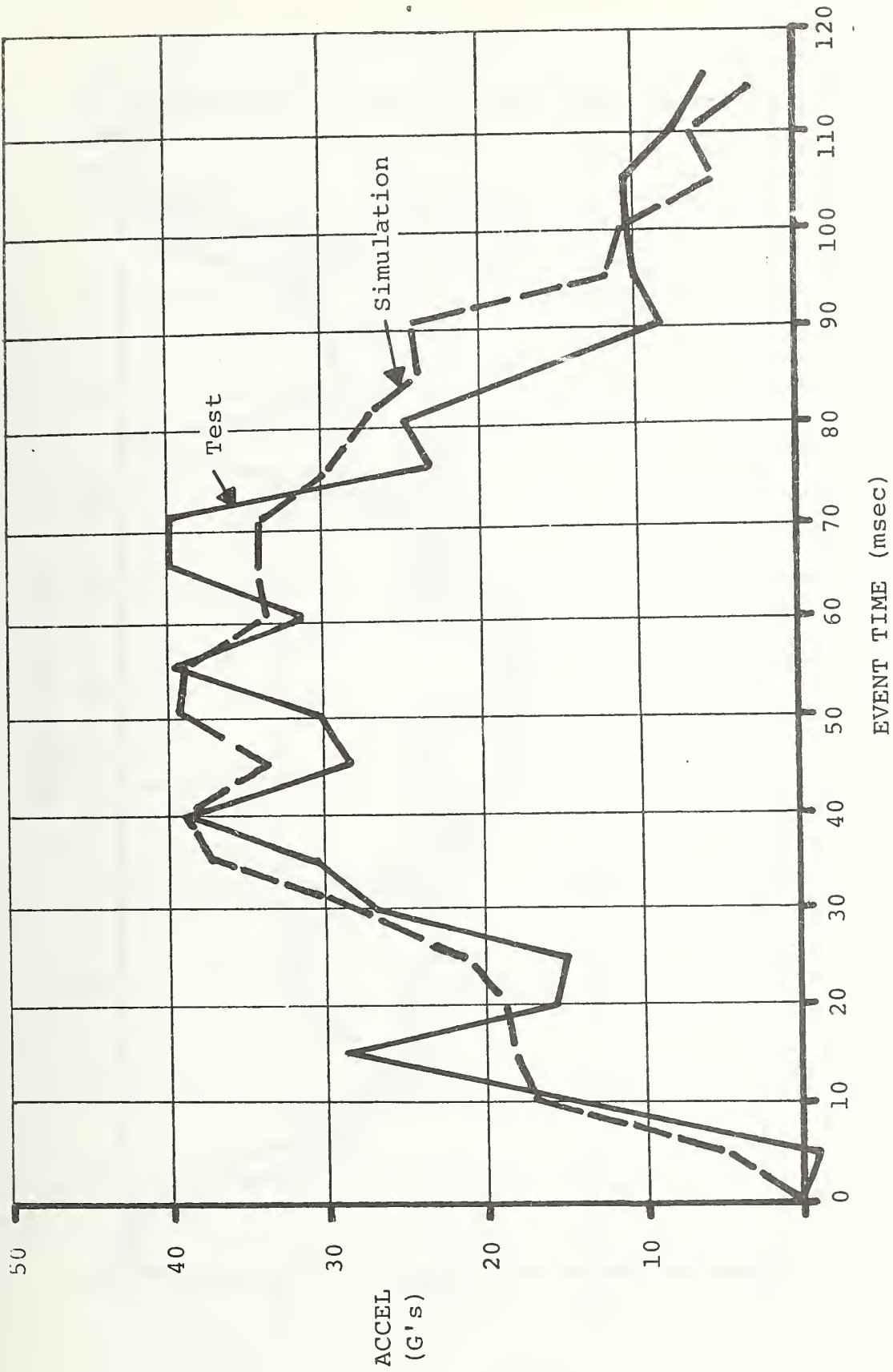


FIGURE 2.19 TENMASS MODEL CORRELATION SUBCOMPACT VEHICLE

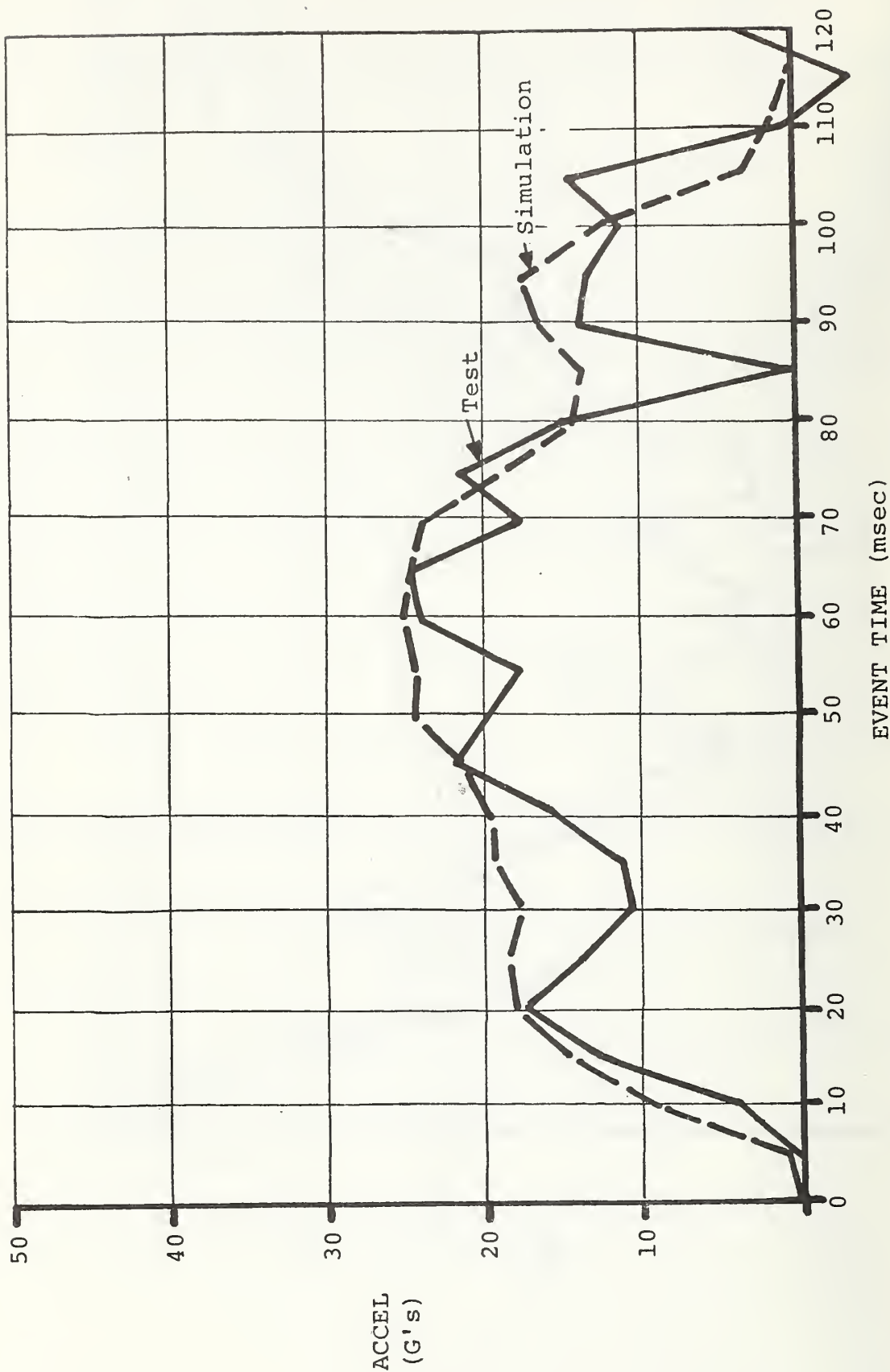
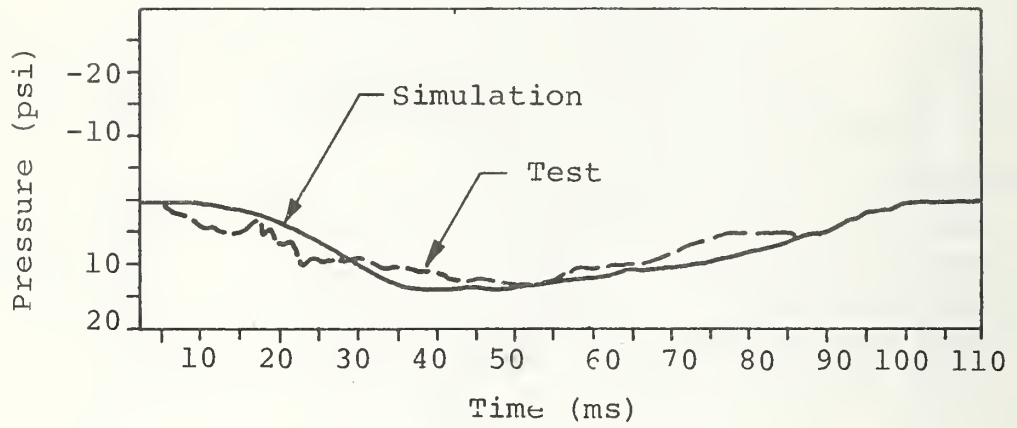


FIGURE 2.20 TENMASS MODEL CORRELATION FULL SIZED VEHICLE

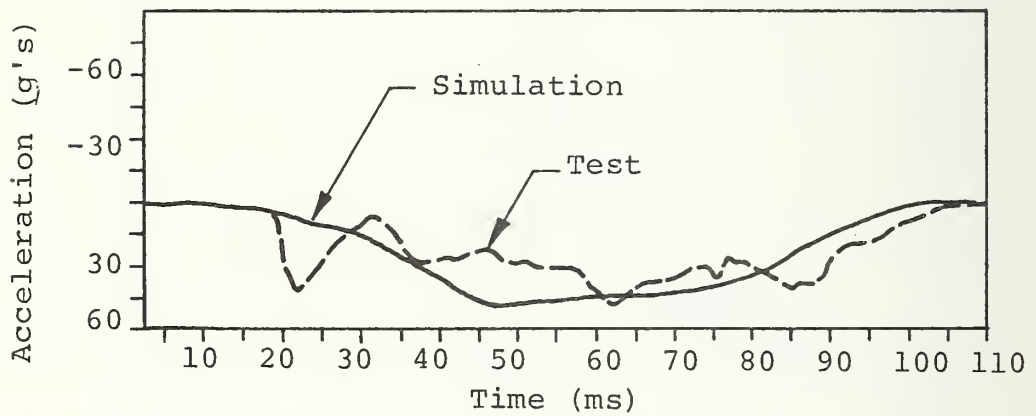
TABLE 2.1  
 COMPARISON OF SIMULATION AND TEST FOR  
 ALIGNED FRONTAL 80 MPH IMPACT

	<u>Simulation</u>	<u>Test</u>
<u>Large Car</u>		
Velocity (mph)	40	39.4
Static Crush (in)		18.0 average
Dynamic Crush	18.3	
Peak Acceleration (g's)	25.0	24.0
Pulse Duration (ms)	115	110
 <u>Small Car</u>		
Velocity (mph)	40	39.4
Static Crush (in)		41.0
Dynamic Crush	41.5	
Peak Acceleration (g's)	39.3	43.1
Pulse Duration	115	120

FIGURE 2.20 TENNASS MODEL CORRELATION FULL SIZED VEHICLE



a) Bag Pressure



b) Chest Acceleration

FIGURE 2.21 ABAG CORRELATIONS

## Phase II - Effect of Restraint Systems

1. Calculate a barrier equivalent velocity for each of the Phase I impacts. (For a discussion of barrier equivalent velocity, see Section 2.2.3.)
2. Use Phase I results to define the overall force-deflection characteristics for each impact.
3. Run ABAG19 for the conditions of 1 and 2 for a .025 second deployment time.
4. Take values of Step 3 as the critical occupant stroke for the remaining .010 second and .040 second deployment times. (Note: The discrepancy from the defined 20 inches is discussed in Appendix E.)
5. Rerun ABAG19 at various velocities until the critical stroking value was bracketed. Obtain critical BEV by interpolation.
6. Calculate critical closing velocity from the BEV momentum equation.

## Phase III - Effect of Structural Modification

1. Select four "other" vehicles to cover the complete weight range of the traffic mix.
2. Select the primary load paths in the Pinto which could be modified to produce an efficient crush. An efficient crush is one which maximizes the "ride down" of the occupant.
3. Select trial modifications and perform TENMASS computer runs for selected vehicles.
4. Repeat Step 3 until occupant stroking is satisfactory.

### 2.2.3 Compatibility of the Unmodified 1974 Pinto Sedan

The compatibility of the unmodified 1974 Pinto sedan was evaluated in aligned, frontal impacts with eight other vehicles and with another Pinto. Table 2.2 presents the vehicles used in this study. The purpose of the study was to determine the critical closing velocity for each type of vehicle and to seek a relationship between "other" vehicle weight and critical closing velocity.

In order to define and then determine the critical closing velocity, it was necessary to define the critical parameters of the study. Two parameters were selected.

1. The maximum crush available in the Pinto structure was 45 inches.
2. The maximum occupant stroke distance for a 50th percentile male occupant in the mid-seat position was 20 inches.

The 45 inches of crush represents 75 percent of the total distance from the bumper face to the A post. The 75 percent structural efficiency is typical of values found in automobile crash studies. The 20-inch occupant stroke represents the head to windshield distance for a 50th percentile occupant for the conditions listed above. The critical closing velocity is defined as the maximum velocity attainable prior to exceeding either of these parameters for the Pinto or Pinto occupant.

The dynamic response model was run for impact velocities selected to bracket the critical closing speed. The actual critical speed was obtained by linear interpolation between these velocities and is plotted in Figure 2.22. Table 2.3 summarizes the results of Phase I. The complete results of the study are presented in Appendix E.

Figure 2.22 shows a plot of the "other" vehicle weight as the abscissa and the critical closing velocity as the ordinate. Points for both restraint critical velocity

TABLE 2.2 VEHICLES USED IN THE STUDY

<u>Vehicle</u>	<u>Type</u>	<u>Year</u>	<u>Gross Weight</u>
1	Subcompact	1971	2500
2	Subcompact	1971	2570
3	Pinto	1974	2817
4	Subcompact	1972	2958
5	Compact	1971	3406
6	Compact	1974	3830
7	Intermediate	1973	4324
8	Standard	1974	5128
9	Pickup	1974	6170

TABLE 2.3 RESULTS OF PHASE 1 STUDY

<u>"Other"</u> <u>Car</u>	<u>Stock Pinto</u> <u>Restraint Stroke</u>		<u>Stock Pinto</u> <u>Crush</u>		<u>Critical Velocity</u>	
	<u>80 mph</u> <u>(in.)</u>	<u>100 mph</u> <u>(in.)</u>	<u>80 mph</u> <u>(in.)</u>	<u>100 mph</u> <u>(in.)</u>	<u>Restraint</u> <u>Limited</u> <u>(mph)</u>	<u>Crush</u> <u>Limited</u> <u>(mph)</u>
Vehicle 1	16.9	20.9	35.9	42.8	96	106
Vehicle 2	15.0	18.8	30.4	38.8	106	115
Pinto	14.8	18.0	32.2	41.9	112	106
Vehicle 4	18.1	23.6	38.2	47.1	86	95
Vehicle 5	18.8	26.0	39.4	49.1	83	92
Vehicle 6	16.5	21.2	36.8	49.0	96	94
Vehicle 7	20.4	28.6	41.5	51.1	80	87
Vehicle 8	21.2	31.0	43.8	54.1	78	82
Vehicle 9	20.1	31.1	40.7	53.3	79	87

- Critical Occupant Stroke Limit = 20 inches
- △ Critical Vehicle Crush Limit = 45 Inches

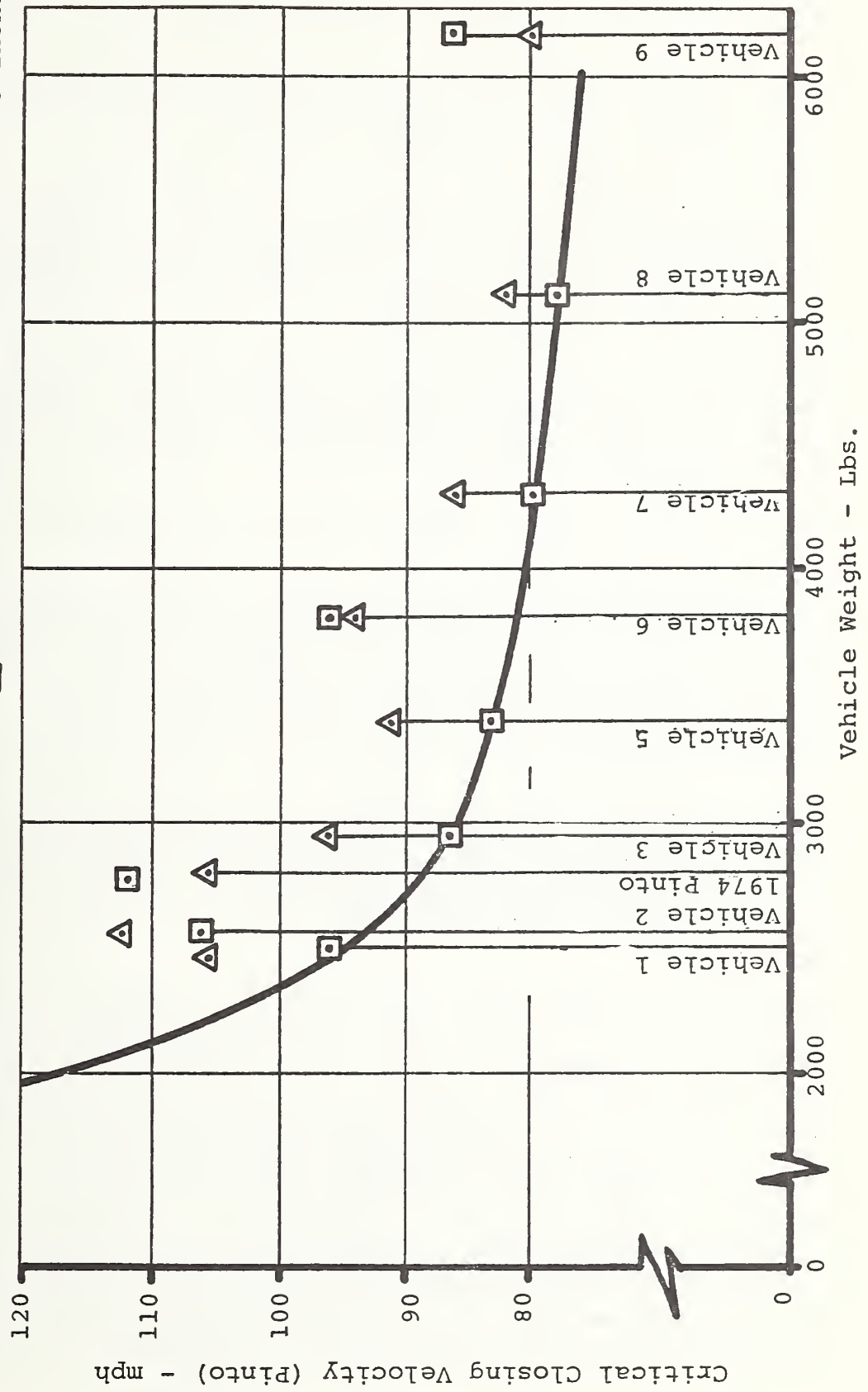


FIGURE 2.22 CRITICAL VELOCITY CURVE FOR 1974 PINTO SEDAN

and crush critical velocity are plotted for each impact. Three important results can be observed from the curve.

1. In most of the impacts the restraint-limited closing velocity was lower than the crush-limited closing velocity for the unmodified Pinto.
2. The actual critical closing velocity is highly dependent on the crush characteristics of the subject vehicle and is not necessarily a function of the other vehicle weight.
3. The curve representing the lower of the two critical closing velocities as a function of other vehicle weight is very nearly equivalent to an energy definition of BEV (discussed below).

Let us take up these three points one at a time.

The first point listed above indicates that improvement in the available occupant stroking distance could significantly increase the safety of the Pinto sedan. Such a change would amount to a geometrical rearrangement of the structure and would not increase the weight of the vehicle. The design modifications of the subcompact car crashworthiness program have provided up to 6 inches of extra occupant stroking distance. A further benefit from providing increased occupant stroking distance is that the occupant is farther back in the vehicle and is not as susceptible to intrusion.

It should be noted that the compatibility study was run with an "advanced" restraint system whose characteristics are shown in Appendix E. The characteristics of this restraint system are similar to the system developed under Contract No. DOT-HS-113-3-742, "Development of Advanced Passive Restraint System for Subcompact Car Drivers."<sup>6</sup> That they are fully realizable has been demonstrated in that contract. A production restraint system would have shown an even worse discrepancy between crush-limited and restraint-limited velocities. In the ideal vehicle, the two systems will be optimized so that both criteria produce the same critical velocity.

The second point listed above illustrates the difficulty in rational study of the automobile safety problem. Each vehicle-to-vehicle impact must be evaluated separately. It is possible to draw a minimum critical closing velocity curve which appears smooth. However, one cannot guarantee that vehicles not included in the study will have critical velocities that fall above that curve. Attempts by other investigators to relate crush characteristics to vehicle weight have been extremely useful in providing insight to the overall problem. However, a detailed analysis of the compatibility of a particular vehicle requires the true crush characteristics for a large variety of other vehicles. As the compatibility concept is extended around the perimeter of the car, the quantity of required data becomes enormous. Until the additional data is available, we must use engineering judgment and say the curve drawn in Figure 2.22 represents the critical closing velocity for a 1974 Pinto sedan as a function of other vehicle weight.

The critical closing velocities range from 95 mph for subcompacts of 2,520 pounds to 76 mph for 6,170-pound vehicles. These surprisingly large values are due to use of an advanced restraint system. The question now arises as to the relation of this curve to barrier test values.

There are two possible definitions of BEV. First, we can define BEV as the closing velocity which transfers an equivalent amount of momentum to the Pinto as would occur in a rigid barrier impact. For this case, the governing equation is

$$BEV_M = \left( \frac{M_2}{M_1 + M_2} \right) V_{CL}$$

Where  $M_1$  = the vehicle under study  
 $M_2$  = the "other" vehicle  
 $V_{CL}$  = the closing velocity of the vehicles

Second, the BEV could be defined as the closing velocity which transfers the same energy to the Pinto as would occur in a rigid barrier crash. For this case, the governing equation is

$$BEV_E = \left( \sqrt{\frac{M_2}{2(M_1 + M_2)}} \right) V_{CL}$$

Applying each of these definitions to the minimum curve in Figure 2.22 gives the BEV's shown in Table 2.4. Plotting these curves over the minimum critical velocity curve (Figure 2.23), it is seen that the energy BEV concept is valid within the limits of the study. Therefore, the energy definition of BEV would provide a better representation for the range of the data included in this study. But to conform to accepted procedure, we use  $BEV_M$  herein.

The curve drawn in Figure 2.23 reflects only the effect of the crash on the Pinto. If the effect on the other car has been considered, the critical closing velocity would decrease as the Pinto became the heavier vehicle. Therefore, the sharply increasing curve below 2,500 pounds does not realistically depict the overall crashworthiness and safety problem.

However, though this is generally true, this study has shown that it is difficult to set down rules based strictly on mass relationships that can reliably predict the performance of one car relative to another in all impacts. In matters of relative front end crush, peak accelerations, etc, one simply has to know the force deflection characteristics of the individual structural components of both vehicles to draw specific conclusions.

Figure 2.24 illustrates a case in point. Here we have the dynamic force deflection characteristics for a 2,500-pound vehicle impacting the 1974 Pinto. One might expect the lighter vehicle (Car 1) to crush more than the Pinto, but here the reverse is true. The foreframe and aftframe of the lighter vehicle are substantially stronger than those of the Pinto, thereby forcing the Pinto to absorb the majority of the crash energy. Thus, at least for this car-to-car impact at a closing velocity of 100 mph, the crush for the smaller car is substantially less than for the larger Pinto. Therefore, one would correctly draw the, perhaps, surprising conclusion that for a frontal impact between Car 1 and the Pinto, the lower-mass Car 1 will crush less than the Pinto.

TABLE 2.4 CRITICAL CLOSING VELOCITIES

<u>Weight</u>	<u>Minimum Critical Curve (Fig. 8) (mph)</u>	<u>Energy BEV (mph)</u>	<u>Momentum BEV (mph)</u>
2500	95	89.3	99.8
3000	86	85.3	91.0
3500	82	82.3	84.7
4000	80	80.0	80.0
4500	79	78.1	76.3
5000	78	76.6	73.4
5500	77	75.4	71.0
6000	76	74.3	69.0

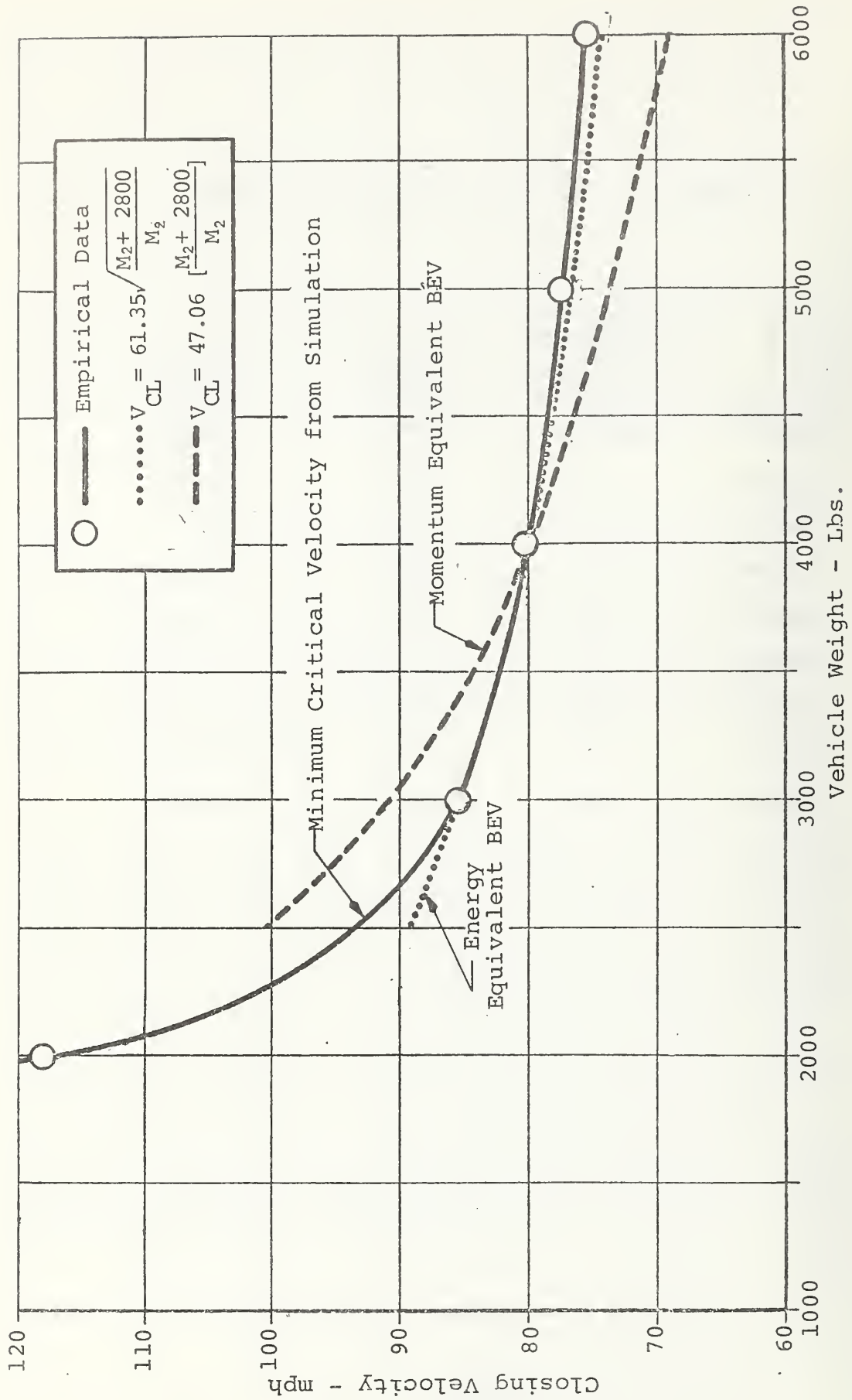


FIGURE 2.23 COMPARISON OF BEV DEFINITIONS VS. MINIMUM CRITICAL SPEED FOR 1974 PINTO

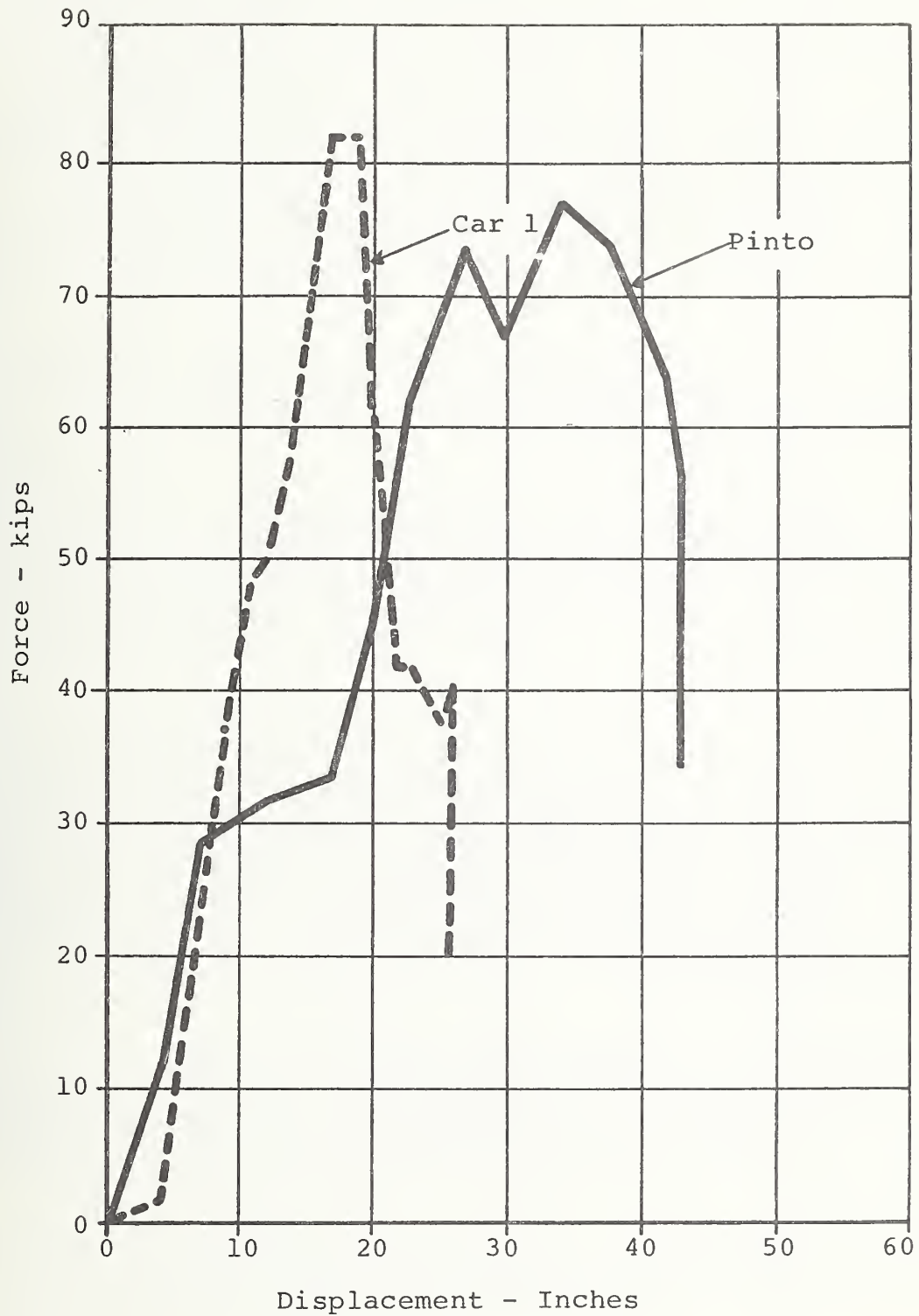


FIGURE 2.24 OVERALL FORCE-DISPLACEMENT CHARACTERISTICS FOR UNMODIFIED 1974 PINTO IMPACTING CAR 1 AT 100 MPH CLOSING VELOCITY

Even here, one has to be careful, for the relative amount of crush between the two cars for this closing velocity may change or even reverse at higher closing velocities. This can happen, for example, if the structural components of Car 1 (which are stronger than those of the Pinto up to some point in the crush of Car 1) would buckle catastrophically at further increase in load, while the Pinto becomes increasingly stiff. From this point on, further increases in the closing velocities between the two vehicles would cause Car 1 to crush more and more, absorbing an increasingly greater percentage of the total crash energy. This trend could continue to the point that at some high closing velocity the crush of Car 1 could actually exceed that of the Pinto, so that the trend noted for the original closing velocity of 100 mph is now reversed.

Thus, any general conclusion based solely on the mass ratio of the interacting cars that attempts to predict the relative crush or even relative peak accelerations between cars with the characteristics described above will be in error -- at least for certain closing velocities.

A further point: when two cars impact frontally, the crush history of the two vehicles is a function of the sudden force changes that occur between the two cars due to buckling, engine impact, firewall impingement, etc. This causes the overall crush history of the two cars to be composed of several small individual crush increments that occur primarily in one car or the other at any particular time.

For example, as the foreframe in one car buckles, practically all the crush takes place in this car until it, at some point in the impact, again becomes the harder car -- say, when its engine impacts the firewall. When this happens, then the other car crushes and the first car ceases crushing. This crush alternation back and forth between the cars means that at any particular time the velocity at which a major structural component is

crushing (neglecting the dynamic oscillation of the structural components that is superimposed upon the overall crush) is very nearly equal to the instantaneous closing velocity between the two cars. This fact has a very important effect on the force characteristic that is generated at the interface of the impacting cars. This is due to the effect that the rate of structural deformation has on the force required to generate that deformation, and is typical of materials that make up existing cars.

In car-to-car impacts, because of this fact, i.e., that structure is deforming at rates near the closing velocity between the two vehicles, we have the structure deforming at much higher rates of strain than in an "equivalent" barrier crash. Therefore, since we found in this study that the force required to crush a structural component is related linearly to strain rate, we have much higher forces generated in car-to-car impacts than in the "equivalent" barrier impacts.

For example, suppose two cars of equal mass impact head-on at a closing velocity of 100 mph. Suppose also that the strain rate factor varies linearly from 1.0 to 2.0 from 0 to 100 mph (this is the same strain rate relationship used in this study). This means for the first few inches Car A crushes at a strain rate of approximately 100 mph with a strain rate factor of 2.0 and a bumper force of 100 kips. However, Car A in an "equivalent" barrier crash at 50 mph would have an initial strain rate of 50 mph with a corresponding bumper force of 75 kips. Therefore, Car A experiences peak accelerations 25 percent greater in a car-to-car crash than it does in an "equivalent" barrier crash. Furthermore, the total crush is less in the car-to-car crash than in the barrier crash.

We bring up these points not to confuse the issue of crash compatibility, but merely to show that although general relationships that apply in a large percentage of cases can be derived, these are really only general trends. Therefore, any detailed conclusions one draws about the crash compatibility of two specific vehicles must rely on the individual force deflection characteristics of the structural components of the two cars and must differentiate between car-to-car crashes and "equivalent" barrier crashes.

#### 2.2.4 Study of Restraint Modifications

The next phase of the compatibility study addressed the question of the effect of restraint modification on the critical closing velocity. The restraint system used in Phase I was considered an advanced restraint system with the characteristics shown in Appendix E. In addition, and to make the restraint more representative of what might be attainable with a developmental restraint, we assumed the restraint was 75 percent stroke-efficient, so that stroke values attained with the computer simulations were divided by 0.75. Even with this "development" type of system, the minimum closing velocity was restraint-limited. It was felt that the appropriate parameter available for variation in the restraint system would be the deployment time of the restraint. The deployment time used in Phase I was .025 seconds. Two other deployment times, .010 and .040 seconds, were chosen as the values for the comparative restraint systems.

Computer simulations were run with .025, .010, and .040-second deployment times for all of the vehicles in the study. Table 2.5 and Figure 2.25 show the results of the Phase II study.

A 10-millisecond deployment could correspond to an inflatable belt system. Such a system represents the minimum deployment time attainable with any current deployable restraint system. Any time lower than .010 second requires a pre-impact sensing

TABLE 2.5 RESULTS OF PHASE 2 STUDY

RESTRAINT CRITICAL VELOCITY (MPH)

<u>Vehicle</u>	<u>Deployment Time .025 ms</u>	<u>Deployment Time .010 ms</u>	<u>Deployment Time .040 ms</u>
1	96	121	73
2	106	114	67
3	112	132	90
4	86	99	71
5	83	92	64
6	96	107	82
7	80	88	65
8	78	85	64
9	79	84	65

device. The 40-millisecond deployment time could be representative of an airbag restraint system for the passenger side of the compartment. Times longer than .040 second are unreasonably slow for an airbag system for impacts at speeds greater than 40 mph and are not included in the study.

A review of Figure 2.25 yields two significant observations.

1. As would be expected, the shorter restraint deployment time gives higher critical closing velocity.
2. The longer deployment time decreases the effect of the other vehicle weight on the total occupant stroke, since the occupant is restrained for a smaller percentage of the time when the vehicles are crushing.

The increase in critical velocity with decrease in deployment time is not a linear effect. There is greater benefit for a .015-second change from .040 to .025 than from .025 to .010.

The decrease in the effect of the other car weight is due to the decrease in the amount of ride down experienced by the occupant. For instance, if the deployment time exceeded 100 milliseconds, the vehicle would be stopped before the occupant hit the restraint. In this case, the mass of the impacting vehicle would have no effect on the restraint critical closing velocity.

There are many other parameters of the restraint system which could be studied to determine their effect on the critical closing velocity. The deployment time was selected as being the most appropriate to a structural crashworthiness contract. Such items as airbag size, knee restraint angle, etc. are better studied as part of a restraint contract. This study does illustrate that improvement in restraint systems will increase the critical closing velocity.

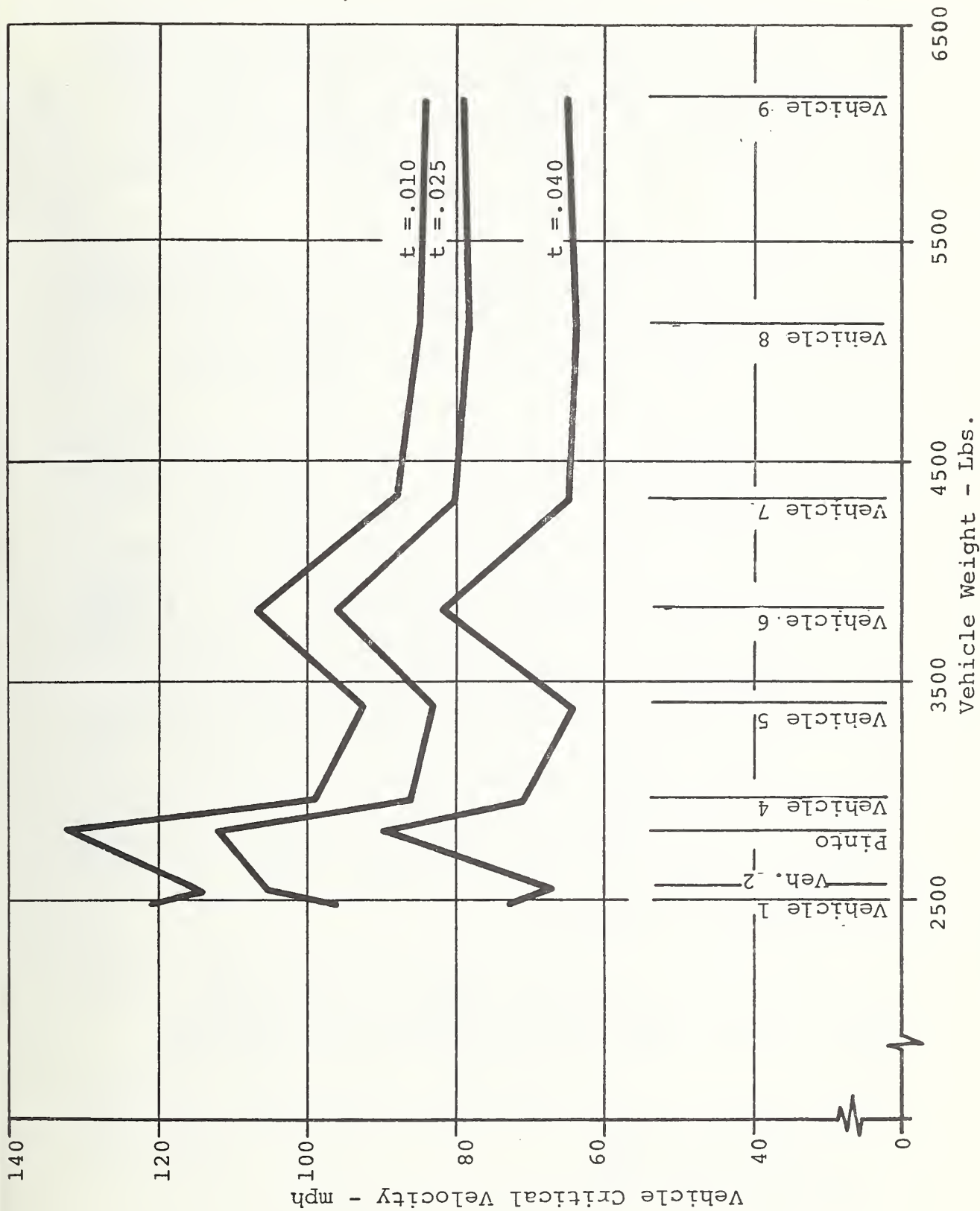


FIGURE 2.25 CRITICAL CLOSING VELOCITIES FOR RESTRAINT DEPLOYMENT TIMES OF .010, .025, AND .040 SECONDS

## 2.2.5 Study of the Compatibility of Modified Subcompact Vehicles

The main purpose of this phase of the study was to determine the structural changes which best improve the crash-worthiness of the subcompact vehicle. The effect of the modifications on the frontal impacts only was studied. No attempt was made to optimize the modifications for both front and side crashes. The restraint system parameters were the same as used in Phase I.

When considering only frontal impacts, it is possible to choose the proper combinations for the  $F-\delta$  characteristics of the individual structural front end components, such that the overall crash pulse of the vehicle is more "efficient." This "efficient" crash pulse maximizes the amount of occupant kinetic energy absorbed in "ride down," thus minimizing the energy required to be absorbed in the restraint itself, which, in turn, minimizes the interior stroke of the occupant. Such a crash pulse may be realized for a given available crush distance by designing the collapsing structural components in a way that results in a rapid onset to the "plateau" or steady state  $g$  level for the overall compartment. This  $g$  plateau should be as low as possible, consistent with not exceeding the allowable crush for the maximum velocity condition. This  $g$  level should remain at this level without large fluctuation either up or down until the vehicle comes to rest. Although it's not obvious from this brief discussion of this desirable type of crash pulse, such a pulse will have the maximum duration for a given overall front end crush. Structural components derived as optimum in the Mod 2 Pinto were chosen to contribute to this overall structural characteristic. The exact modifications are discussed in Appendix E.

A review of the load paths as defined in the front structure dynamic response model indicated that the best results would be obtained by modifying the following members:

1. sheetmetal,
2. forward stub frame,
3. aft stub frame, and
4. firewall.

These are the primary energy absorbing members. In the baseline impacts they absorb approximately 85 percent of the total energy of a barrier impact. The modifications included both decreasing the clearance and increasing the strength of the structures. In the case of the firewall, it was found beneficial to lower the strength of that member. Two attempts at modification were required before satisfactory results were obtained.

The compatibility study of the modified Pinto used four "other" vehicles selected from the Phase I study and chosen to cover the weight range of other cars in the traffic mix. These were vehicles 1, 5, 7, and 8 of the group shown in Table 2.2. The critical closing velocity for the Mod 2 Pinto was obtained as discussed in Section 2.2.3 for the Phase I study.

The results of the study are presented in Table 2.6 and plotted in Figure 2.26. The curves compare the critical closing velocity for the modified and unmodified Pintos. It is apparent that the critical closing velocity for the modified Pinto is still occupant stroke limited even though the structure has been optimized to have a more stroke efficient front end structure. However, the modified structure has decreased both the vehicle crush and the occupant stroking distance, thus increasing the critical velocity for both conditions. The net effect of modifying the structure was to raise the critical closing velocity by mathematically modeling a more stroke-efficient front end structure. All other aspects of the results of the modified Pinto compatibility study are similar to the results of the unmodified Pinto compatibility study. Figures 2.27, 2.28, and 2.29 present the compartment crush pulse for both the stock and modified Pintos at 100 mph closing velocity with three of the cars used in the study. Appendix E presents the complete results of the Phase III study.

The vehicle design resulting from the Phase III study was not used in the hardware development part of the contract. This study produces an optimized design for frontal accidents only, while the hardware must undergo various other crash modes.

TABLE 2.6 RESULTS OF PHASE 3 STUDY

MOD 2 PINTO  
CRITICAL VELOCITY - MPH

<u>Vehicle</u>	<u>Restraint Limited</u>	<u>Crush Limited</u>
1	124	High
5	102	117
7	103	106
8	93	97

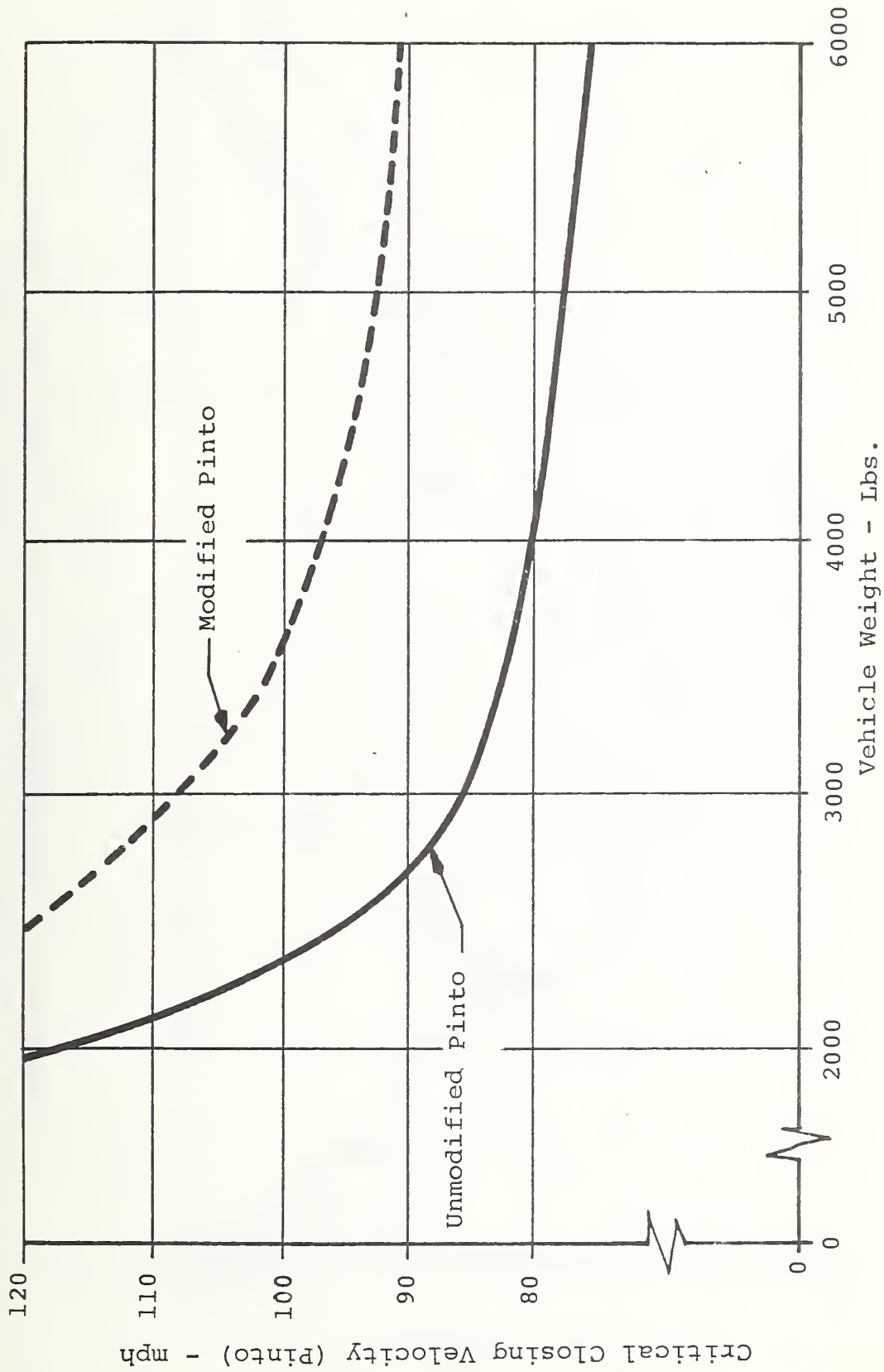


FIGURE 2.26 CRITICAL CLOSING VELOCITY COMPARISON -  
 MODIFIED VS. UNMODIFIED PINTO

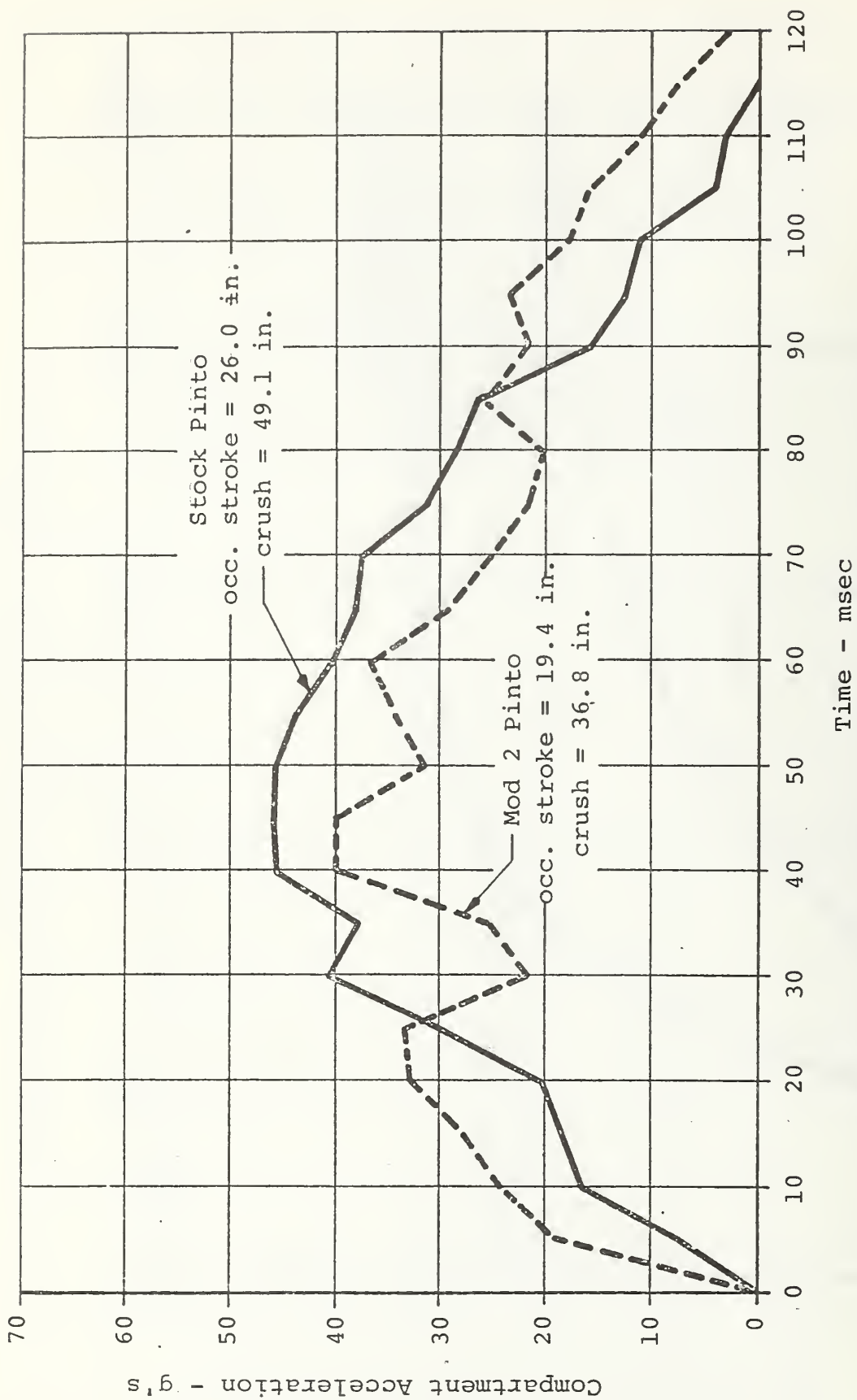


FIGURE 2.27 PINTO COMPARTMENT PULSE - 100 MPH INTO VEHICLE 5

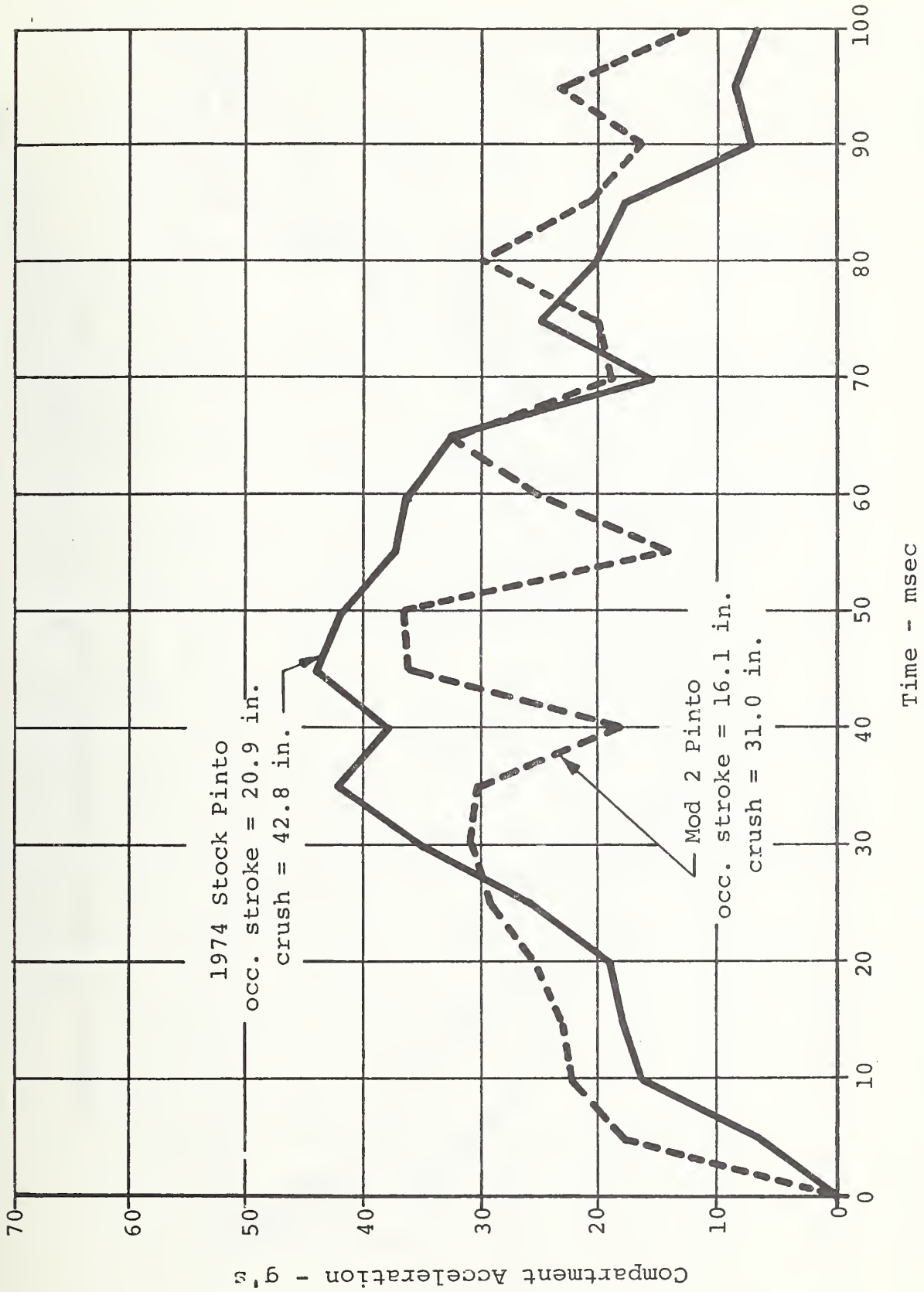


FIGURE 2.28 PINTO COMPARTMENT PULSE - 100 MPH INTO VEHICLE 1

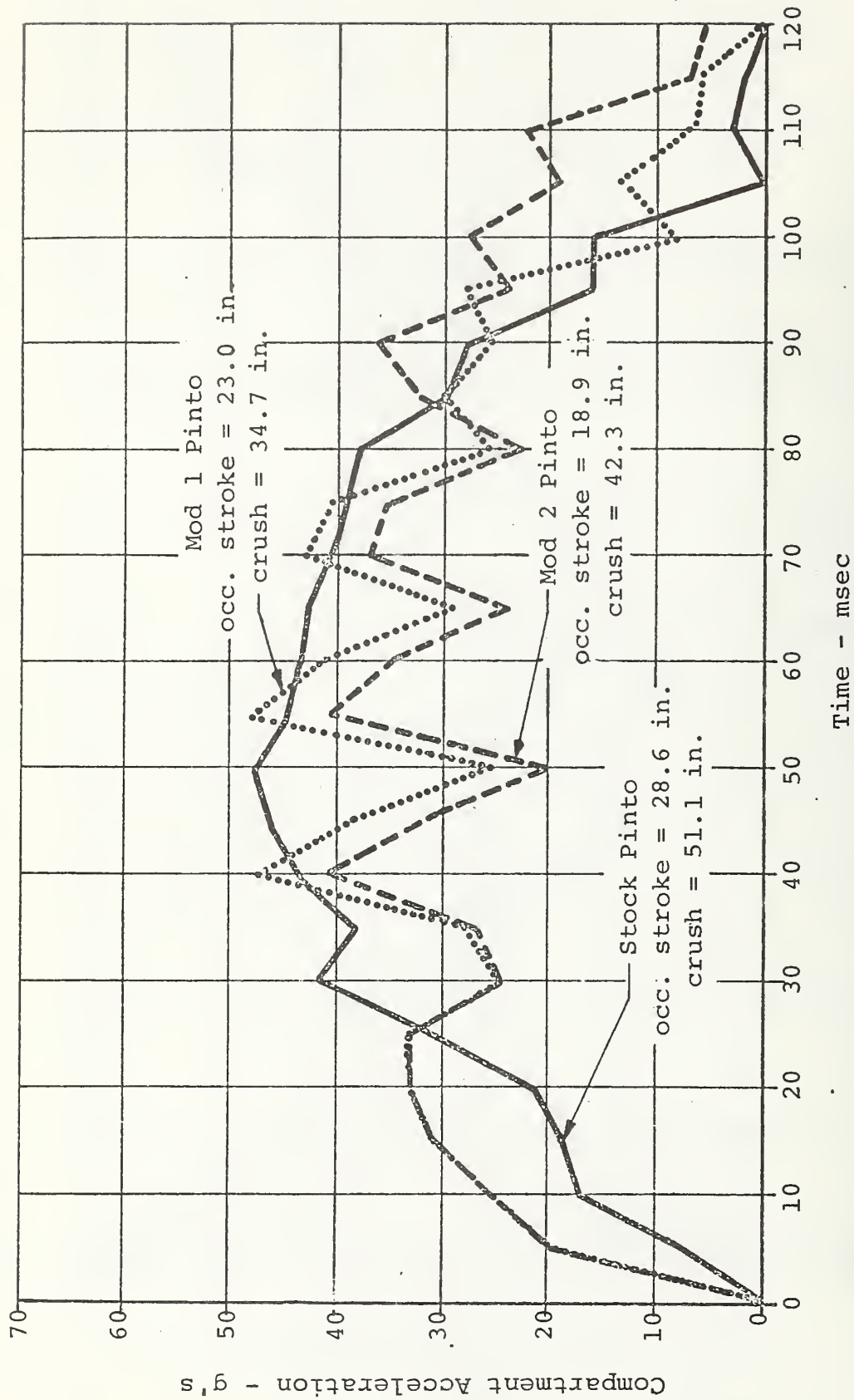


FIGURE 2.29 PINTO COMPARTMENT PULSE - 100 MPH INTO VEHICLE 7

## 2.2.6 Conclusions and Recommendations

The basic objectives of this study were:

1. To analyze how the baseline Pinto interacts in impacts with other vehicles in the traffic mix.
2. To determine the effect of proposed modifications on this interaction.
3. To provide data to support structural standards efforts.

In considering the conclusions reached by this study, it is essential to recognize the contractual limitations which were included. First, the analysis was limited to frontal, aligned impacts. No consideration was given to oblique, offset, side, or rear crashes. Second, the study was limited to nine "other" vehicles. These represent most manufacturers and the weight and age range of most of the vehicles in the present traffic mix. However, it is still possible for some other existing or future vehicle to distort the conclusions reached here.

Subject to these limitations, the study has shown the following conclusions:

1. Computer models can provide valuable information on a cost effective basis as to the likelihood of protecting occupants in any vehicle impacting any other vehicle in the traffic mix. Computer simulations of frontal aligned impacts for unequal mass collisions were tested and validated with excellent correlation.
2. In general, a minimum critical velocity relationship can be based on the concept of a barrier equivalent velocity for frontal aligned vehicle-to-vehicle accidents. However, the energy definition of BEV should be used, i.e.,

$$BEV_E = \left( \sqrt{\frac{M_2}{2(M_1 + M_2)}} \right) V_{CL}$$

Specific "other" vehicles may place above this curve, but it provides a measure of the effectiveness of the design of the subject vehicle in the current traffic mix.

3. The results associated with restraint and structural modifications are very sensitive to two critical parameters -- the assumed maximum crush distance of 45 inches and the assumed maximum occupant stroke distance for the 50th percentile male of 20 inches. These two parameters identify the critical closing velocity at which the occupant can be protected with an assumed advanced restraint similar to that developed under Contract DOT-HS-113-3-742. With the above assumptions, the critical closing velocity of the 1974 Pinto was restraint-limited, providing a  $BEV_E$  of 43 mph as a minimum. The structure itself would allow a critical  $BEV_E$  of 49 mph.
4. Restraint modifications indicate that the critical closing velocity for current airbag restraint deployment times of 40 milliseconds is lower and less dependent on the mass of the "other car" than faster-deploying restraints, as shown in Figure 2.25. As one reduces the deployment time to 10 milliseconds, the critical closing velocity increases, but at a declining rate.
5. In order to provide cost effective occupant protection, it is desirable to increase the assumed occupant stroking distance or decrease the assumed crush distance so that the critical closing velocity ( $BEV_E$ ) is the same for both structural and restraint criteria. This would amount to adding about 5 inches to the assumed 20 inches of occupant stroke, or decreasing the critical vehicle crush limit to about 40 inches.
6. A more efficient crash pulse is possible by reducing the spacing (clearances) between which various of the vehicle structural elements provide retarding forces. The study shows that no additional weight would need to be added to make the structure stronger earlier in

the event and weaker later; only a rearrangement or change of components is necessary. However, other studies have indicated that such efficient crash pulses must be compromised to limit side impact intrusion in the struck car and to provide pedestrian impact protection. These considerations were outside the scope of this study.

7. A configuration adjustment to increase the occupant stroking distance would require the minimum structural effort for a given increase in the critical closing velocity ( $BEV_E$ ). This has the same effect as improving the restraint system.
8. This study was not comprehensive enough to specify FMVSS data guidelines, since the effects of oblique, offset, side, and rear impacts were not considered. However, the results of this study do indicate that when such data is available, the most useful parameter which can be used to specify standards will be the overall structural force-crush characteristic for the particular accident mode.

#### Recommendations:

1. Static force deflection data provide valuable insight and support to structural standards efforts, at least in the frontal aligned accident mode. Collection and dissemination of this data should be encouraged.
2. It is vitally important to extend this study to other accident modes and thus obtain a complete compatibility analysis. In order to accomplish this extension, it is necessary to have or assume adequate crush test data for these other vehicle structural areas.
3. The structure should be designed to provide the most efficient crash pulse. Considering frontal aligned crashes only, such a pulse should maximize ride down of the occupant. The Mod 2 structure developed in Section 2.2.5 represents such an efficient structure, as shown in Figures 2.27, 2.28, and 2.29.

## 2.3 Study of Finite Element Techniques to Develop Force Deflection Characteristics

### 2.3.1 Introduction

One of the major limitations in the dynamic analysis of vehicle impacts has been the lack of adequate data on the crush characteristics of vehicles. The two predominant methods of dynamic analysis are:

1. Prepare a finite element model of the entire vehicle and conduct a dynamic structural analysis of the vehicle.
2. Prepare a lumped mass model of the vehicle and use prescribed force deflection properties as the mass couplings. The  $F-\delta$  properties are obtained by either static crush or by crude limit analysis.

Each of these methods has its advantages and disadvantages. The first is an extremely expensive technique in both manpower to prepare the model and computer time for the runs. Although the techniques for conducting a non-linear, dynamic finite element structural analysis are presently within the state of the art, they have not been proven successfully. Studies currently under way, sponsored by NHTSA, may prove the technical feasibility, but good accuracy will still be expensive.

The second method is relatively economical for model preparation and computer time, but requires an extensive library of force-deflection information. As was noted in Section 2.2, the  $F-\delta$  properties are completely individual for each vehicle. The Minicars data file of nine vehicles is one of the largest in existence, but still falls short of a satisfactory statistical sample. In addition, the  $F-\delta$  properties will change for every location and angle of impact. To obtain information for a significant number of vehicles at all locations and angles would require an expensive and lengthy test program.

Thus the dynamic analysis of vehicle impacts is in an untenable middle ground -- too expensive for an accurate prediction and too valuable to be ignored. As a solution to this dilemma, Minicars proposed to investigate the use of finite element analysis to predict component force-deflection characteristics. For instance, a finite element model of a foreframe could be prepared and analyzed for deformation from a variety of directions. The results would then be incorporated into a lumped mass model of an impact at a specified angle. The best of both the finite element technique and the lumped mass method could be obtained at a fraction of the cost of either individual method.

The work under this subtask was performed by the Jet Propulsion Laboratory of Pasadena, California. The original JPL proposal involved the extension of the JPL program IMAN<sup>7</sup> to include elastoplasticity effects. However, during the early stages of this work, it was recognized that extending IMAN was too large an effort, beyond the scope of the task. Therefore, the program IMAN was dropped from consideration. Then a broad and extensive survey of the available computer programs to assess their relative merits for crashwork was performed. The general-purpose program ANSYS<sup>8</sup> (Engineering Analysis System) was finally selected. An initial attempt to run a highly nonlinear sample problem of simple geometry proved to be highly successful. Subsequent runs were made on the Pinto foreframe with reasonable success. At this point, it was felt that although the effort showed considerable merit, the funds would best be used in the direct structural development task, and the program was terminated with the consent of the CTM.

### 2.3.2 Methodology

Under dynamic loading caused by impact, the state of stresses and deformations in the structure may be described by the theory of wave propagation. In automobile structures, the wave will induce structural nonlinearities in the form of geometrical and physical effects. The

geometrical nonlinearities may be described as the effect caused by large deformations, rotations, and large strains. Physical nonlinearities, on the other hand, are symptomatic of nonlinear elasticity and elastoplasticity associated with most materials. A step-by-step incremental procedure<sup>9</sup> is usually adopted for the solution of such nonlinear problems.

A number of relevant computer programs were reviewed to assess their suitability in relation to the development of component  $F$ - $\delta$  curves by finite element methods. The NASA general-purpose program NASTRAN was found unsuitable for the present work, since it does not have the required nonlinear analysis capability. Among the large number of programs reviewed for this purpose, two programs appeared to be most suitable for the analysis.

The first program ANSYS developed by Swanson Analysis, Inc., is a rather new but frequently used general-purpose program available to the public. The program will perform both static and dynamic analysis. Linear as well as nonlinear structures may be handled by the program. The "Incremental-Initial Strain" procedure is adopted for such analysis. For static analysis increments, the corresponding load-deformation characteristics are computed at each time step. Effects of elastoplasticity and large deformation are automatically included in the analysis. The program was found to be extremely easy and straightforward to use for the finite element data generation.

The general-purpose program MARC<sup>10</sup>, commercially available on the CDC computer system, was also thoroughly investigated in this connection. The MARC and ANSYS systems have similar capabilities, with the element capabilities in MARC being more sophisticated. However, the program was found to be somewhat complicated from the point of view of data preparation.

Another alternative would be to modify the program IMAN. The procedure of modification is based on a nodewise predictor-corrector fourth order Runge-Kutta technique in which only the relevant equations at each node are solved at one time, involving simple algebraic operations. The

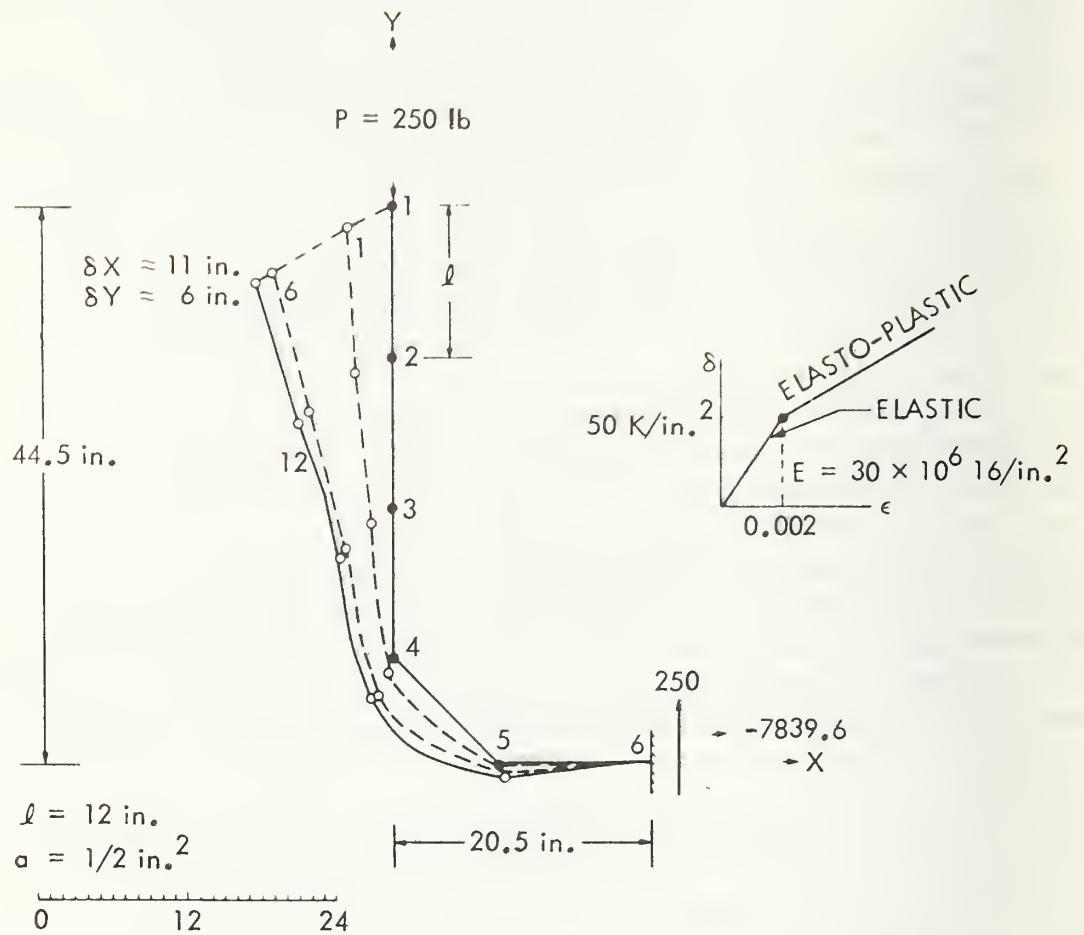
core storage requirements for the analysis are insignificant and the analysis is independent of matrix bandwidth or active columns. Consequently, problems of much larger size can be efficiently handled in-core, when compared with other procedures of such analysis. Although the procedure may prove most economical in the long run, funds were not available under the current contract to effect the modifications.

As a result, the program ANSYS was selected as the one most suitable for car crash analysis work. A brief discussion of the ANSYS solution methodology for static loadings is given in Appendix F.

### 2.3.3 Description of Models

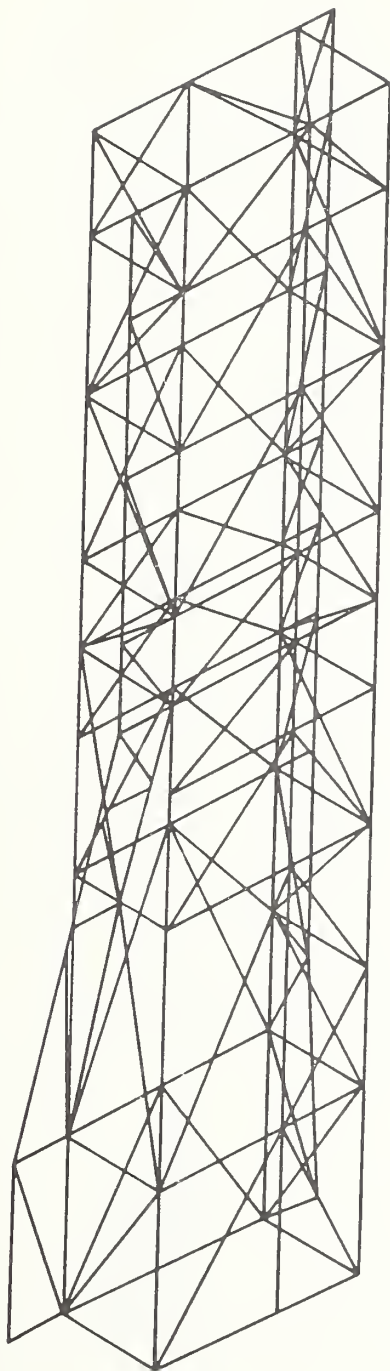
In an effort to check out the static nonlinear analysis capability, a simple bent cantilever beam (Figure 2.30) was analyzed by the program. The structure was idealized by 5 two-dimensional "elastoplastic" beam elements, being subjected to a load of 250 pounds as illustrated in the figure. Both forms of nonlinearities, i.e., geometric and material, were considered in the analysis. The deformed shape of the structure is shown in the figure, depicting substantial nodal deformations found to occur in the structure. A maximum elastoplastic stress of about 75,000 psi was recorded in element 5-6. The support reactions at the built-in end checked exceedingly well with the force and moment corresponding to the final deformed state of the structure.

The Pinto foreframe structure was discretized by the finite element technique, using plastic flat triangular shell elements, resulting ultimately in six degrees of freedom per node. A 3-dimensional view of the model (Model I) is shown in Figure 2.31, idealized by 137 such elements. The structure has 76 nodes altogether, and 456 equations are solved at each time step. The structure was assumed to be supported at its four attachment points with the engine mount shown in the attached drawing (Figure 2.32) as points A, B, C, and D. Loadings in the shape of incremental deformations were applied at nodes P and Q, simulating its attachment during actual static loading of the foreframe. Concurrently, a much simpler two-dimensional 9-element beam



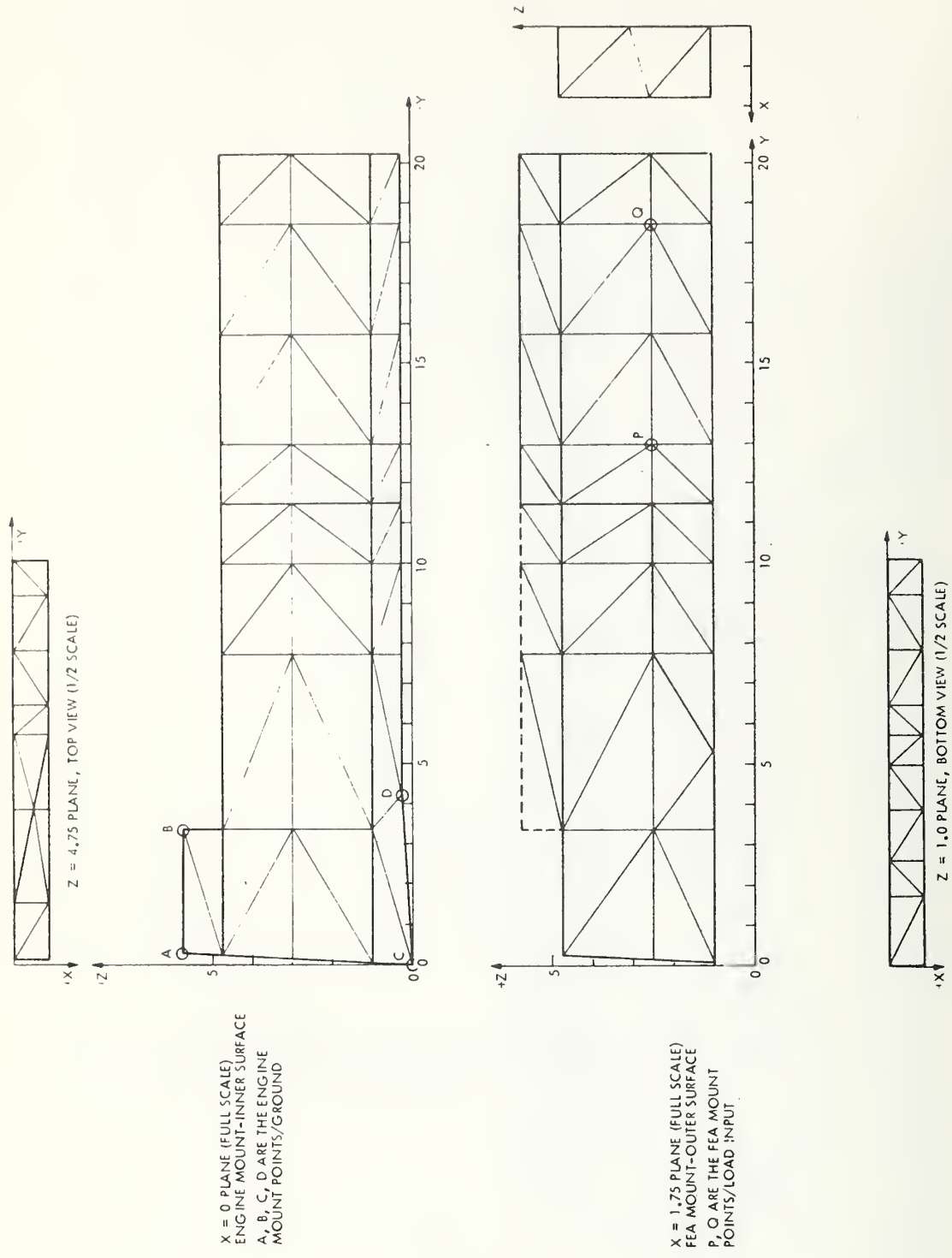
NOTE: INCREMENTAL INITIAL STRAIN APPROACH RESULTS USING 'ANSYS' PROGRAM

FIGURE 2.30 BENT CANTILEVER BEAM



ELEMENTS: 137  
NODES: 76

FIGURE 2.31. PINTO FOREFRAME, MODEL I



X = 0 PLANE (FULL SCALE)  
 ENGINE MOUNT-INNER SURFACE  
 A, B, C, D ARE THE ENGINE  
 MOUNT POINTS/GROUND

X = 1.75 PLANE (FULL SCALE)  
 FEA MOUNT-OUTER SURFACE  
 P, O ARE THE FEA MOUNT  
 POINTS/LOAD INPUT

FIGURE 2.32 PINTO FOREFRAME STRUCTURE AND ATTACHMENT POINTS

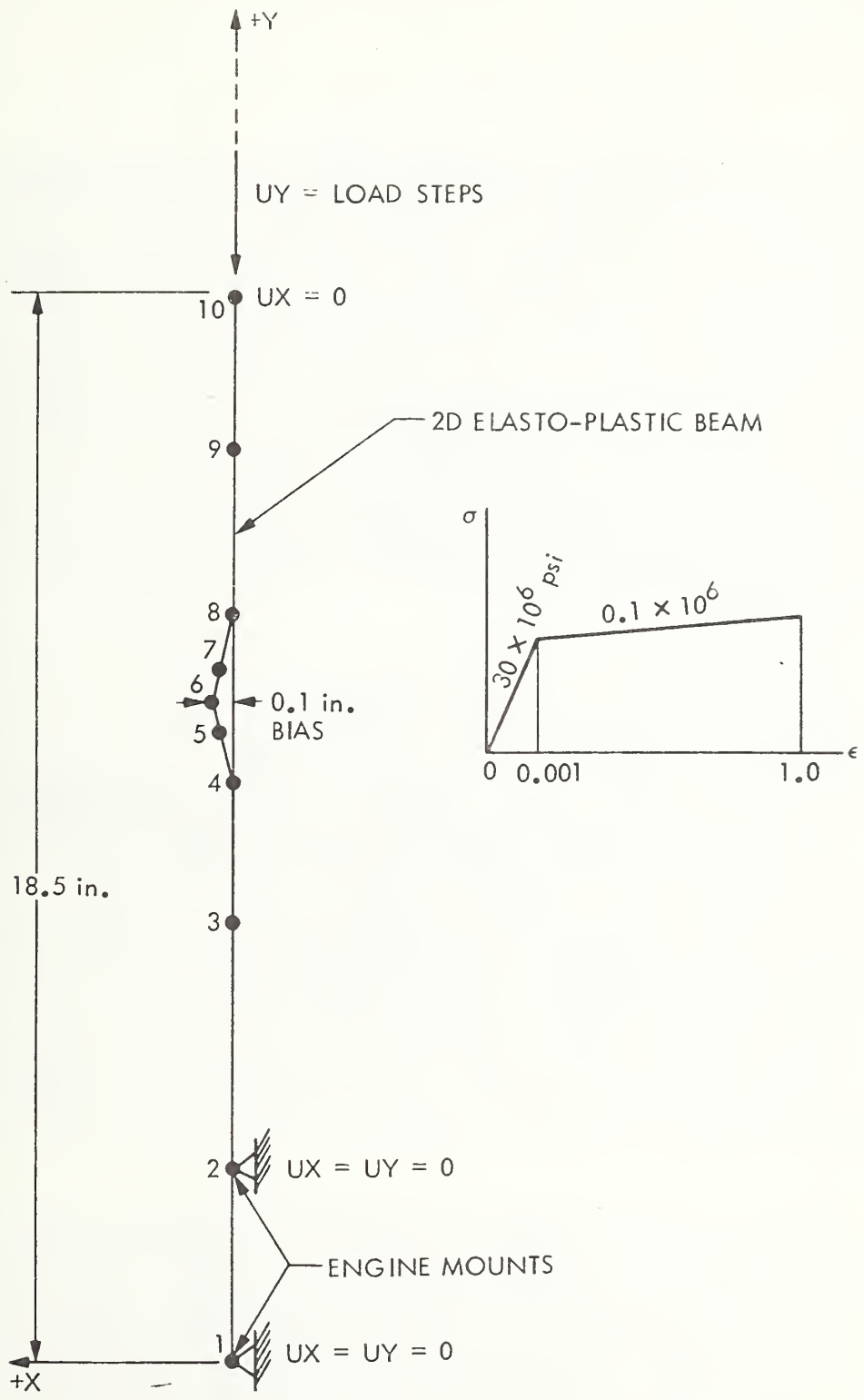


FIGURE 2.33 PINTO FOREFRAME, MODEL II

model (Figure 2.33) of the foreframe was analyzed in parallel to Model I. The input details of the models are listed in Table 2.7.

#### 2.3.4 Discussion of Model I Run

The ANSYS output converged in one iteration for an input displacement at the mount points of  $UY = 0.01$  inch. This resulted in a computed reaction force of  $FY = 2,400$  pounds. For the next load step of  $UY = 0.1$  inch, the solution iterated in oscillatory fashion, and the run was terminated without convergence. It seemed clear at this point that each iteration was rather costly (190 CPU sec/iteration = \$42/iteration @ CSC overnight rate). Since large numbers of iterations were expected to reach total input displacement of  $UY = 5.0$  inches, it was decided to create a simple two-dimensional beam model (Model II) to obtain the optimum set of parameters, which might later be useful in analyzing the Model I.

#### 2.3.5 Discussion of Model II Run

The Model II is a two-dimensional beam element approximation of the foreframe. Each element of the beam represents the corresponding cross sectional area, moment of inertia, and thickness of the foreframe sections. In order to initiate plastic collapse, a small geometric bias of 0.1 inch was given at the center of the beam (refer to Figure 2.33). Input displacements were increased from 0.01 inch to 2.25 inches in 14 steps. At each step, the solution was allowed to iterate up to 18 times until it converged within 5 percent convergence criteria. The convergence criteria relate to a comparison of the solution at the preceding iteration step.

A summary of the results of analyzing Model II is shown graphically in Figure 2.34 for the reaction forces ( $FY$ ) and the maximum lateral center deflection ( $UX$ ). Up to an input displacement of  $UY = 0.5$  inch, the reaction forces and the center deflection exhibited the expected phenomenon of plastic beam collapse. However, beyond  $UY = 0.75$  inch the solution tends to oscillate and eventually diverges.

TABLE 2.7  
FINITE ELEMENT MODEL OF THE PINTO FOREFRAME

	Model I	Model II
Element Type	3D elasto-plastic flat triangular shell	2D elasto-plastic beam
Number of Elements	137	9
Number of Nodes	76	10
Convergence Criteria	0.05	0.05
Boundary Condition	UX=UY=UZ=0 at engine mount points	Refer to Fig. 2.33
Material Property	Modulus = $30 \times 10^6$ psi for $0 \leq \epsilon < 0.001$ = $0.1 \times 10^6$ psi for $0.001 < \epsilon < 1.0$	

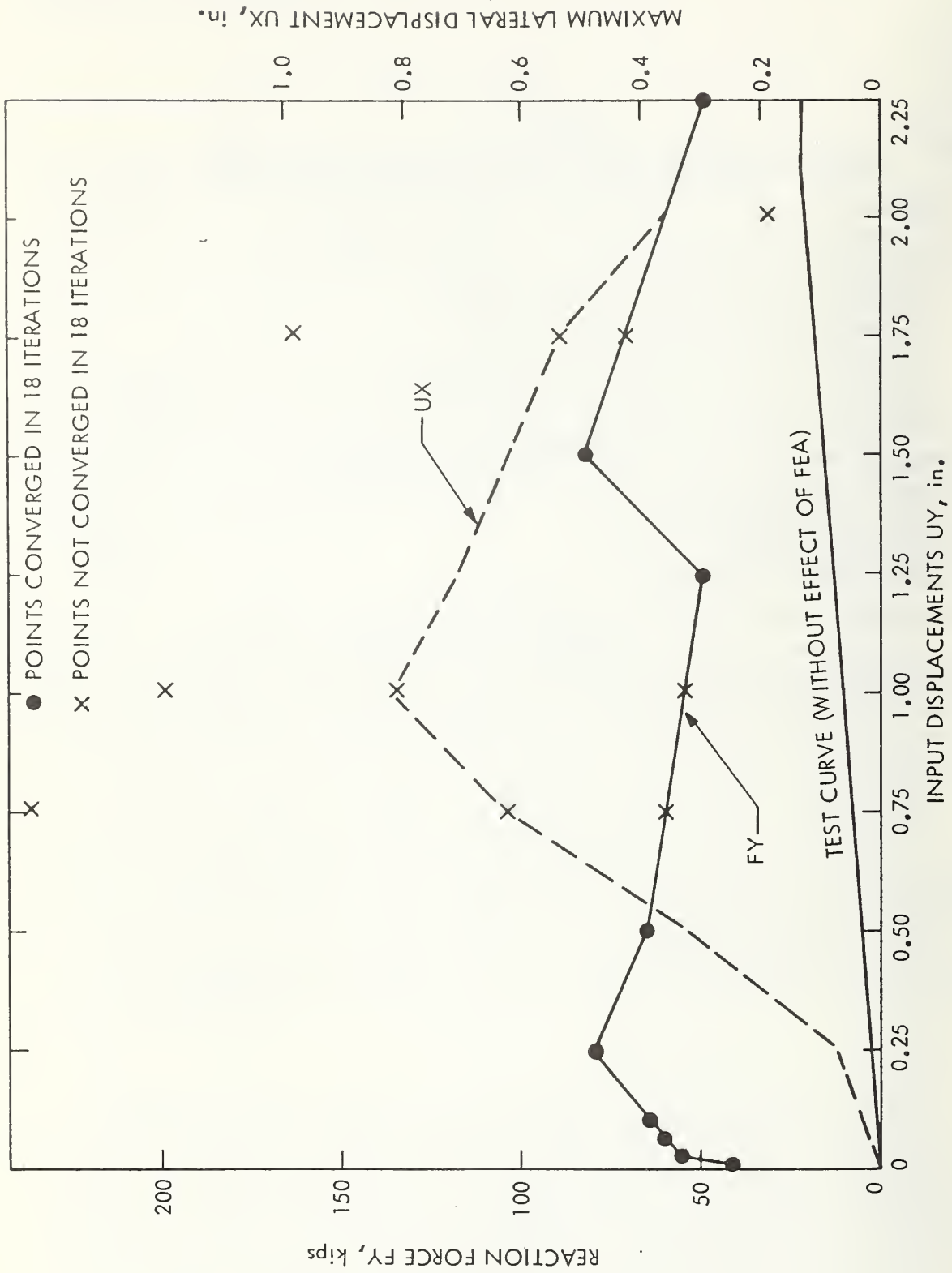


FIGURE 2.34 ANSYS MODEL II

### 2.3.6 Conclusions and Recommendations

Because of its rather new development and also due to the complexities involved in predicting non-linear structures behavior, any new non-linear analysis program will have to be used with caution. First of all, it is absolutely necessary to understand the underlying basic non-linear theory adopted by the program and, most importantly, its implications from the point of view of numerical stability. Only then may the user form the input data in the optimum manner, so that the numerical instabilities inherent in a relevant program may be avoided. Also, the user will have to exercise great caution in not violating the constraints usually associated with such programs.

Both models run in connection with the Pinto frame should yield far better results, provided the program may be used with greater skill and understanding. Thus, it is apparent from the basic ANSYS input data that the elastic curve is almost vertical in nature, in contrast to the almost horizontal elastic-plastic portion of the material curve. Unless special precautions are taken at the interface of the two portions of the curve, the analysis results will oscillate back and forth around the intersection point, finally resulting in divergence of computed results due to rounding errors. This is precisely what happened in connection with the two models of the Pinto foreframe analyzed by ANSYS. In retrospect, it is clear that much improved results could be obtained by appropriate smoothing of the interface portion of the elastic and the elastic-plastic curve. The resulting idealization of the curve will result in only slight deviation from the true results.

In addition to the above recommendation regarding handling of existing non-linear analysis programs, it is also strongly suggested that computer programs with the primary aim of solving the crashworthiness problem of automobiles be developed. Such a "special-purpose" program will not only be far more efficient than the existing general-purpose programs, but will be much more accurate and fool-proof.



## 3.0 FRONTAL IMPACT CRASHWORTHINESS

### 3.1 Summary and Introduction

#### 3.1.1 Summary

The front end structure of the baseline 1974 Pinto sedan was tested both statically and dynamically in a variety of accident modes. These tests showed that minor modifications would produce a satisfactory crashworthy front structure for frontal aligned crashes, but offset and oblique impacts required extensive changes in design. The modified front end design improved the survivable impact speed from 40 mph BEV to at least 50 mph BEV in the pure frontal barrier impact mode and the aligned two car impacts. For the offset and oblique barrier the BEV crashworthiness level was increased from 30 mph to at least 50 mph.

Several structural modification concepts were developed and tested. The most satisfactory of these concepts used foam filled sheet metal sections as energy absorbing members. The production hood and inner fender panels were removed and replaced with volumetric (foam filled sheet metal) structures. A volumetric section was located forward of the front wheel, and in addition the rear of the wheel well was enclosed and foam filled. The sub frames were replaced with rectangular tubes of controlled crush characteristics. The engine and transmission mounts and the driveline were replaced with load limiting breakaway design. The final design change for frontal impacts was to provide a compression strut as a longitudinal load path through the door.

The modified front structure was tested in a series of dynamic crashes in various crash modes and velocities. The majority of these tests included instrumented anthropomorphic dummies allowing the use of both intrusion and dummy survival criteria as the measure of satisfactory crashworthy behavior.

### 3.1.2 Introduction

This part of the program aimed at achieving crashworthiness of subcompact vehicles in frontal impacts in five mode-velocity combinations. Three were defined in the contract as:

1. 50 mph, frontal into flat barrier.
2. 50 mph, frontal into pole barrier.
3. 100 mph, frontal car-to-car (baseline, modified, and large car).

In addition, Minicars, with CTM concurrence, established the following goals:

4. 50 mph, 30° frontal oblique into flat barrier.
5. 80 mph, 50 percent frontal offset into large car.

The inclusion of goals 4 and 5 greatly complicated the frontal crashworthiness problem. However, the results of the accident analysis (Section 2.1) graphically illustrated the importance of these accident modes.

The design of the frontal crashworthy structure was a process of growth and change. First, a series of baseline tests was conducted to thoroughly evaluate the problem. Then, several design concepts were generated and evaluated. A "final" design was selected and evaluation testing initiated. As the test program progressed, several improvements in the "final" design were developed, primarily related to design goals 4 and 5. The design was eventually frozen, and a final series of evaluation tests was conducted. The final task was to compare test results of the modified vehicle with the baseline test results and with the design goals.

For convenience and continuity, this report will first discuss the evolution of the design. Then, each design goal and the final result will be discussed, in turn.

## 3.2 Evolution of the Design

### 3.2.1 Design Approach

The crashworthiness of a vehicle can be evaluated in a variety of ways. The two most common are the peak acceleration levels of the vehicle and/or the structural intrusion into the passenger compartment. Minicars has chosen to interpret these criteria in an alternate way. The acceleration of the occupant and the intrusion into his living space, or the space he actually occupies during the crash event, are the evaluation criteria used in the development of the modified subcompact vehicle design. In other words, the crashworthiness of a vehicle was measured in terms of the effect on the occupant, not the effect on the vehicle.

Improvements in crashworthiness can be obtained by modifying the structure in two ways. First, it is possible to rearrange the geometry of the existing structure, and second, one can replace existing structure with a more efficient design. The first technique has two significant advantages:

1. Little or no weight penalty is incurred by the rearrangement.
2. The basic producibility is not affected by these changes.

The only disadvantage is that marketability may be affected if gross modifications are chosen.

In view of the inherent advantages of the geometrical modifications, Minicars decided to maximize the crashworthiness improvement in this way and then make design changes in the structure, as required, to satisfy the goals.

Observations of crashed Pintos revealed the following geometrical problems with subcompact vehicles:

1. The distance from a 95th percentile male occupant's head to the windshield is 12 inches.

2. The engine is not crushable and yet has no room to move past the firewall.
3. The Pinto is low to the ground with little room for additional structure.
4. There is serious height mismatch between the hard structure (rocker panels) on the side and an impacting bumper.

Preliminary calculations, prior to establishment of the dynamic model, indicated that a total occupant travel of 55 inches would be required for protection in a 50-mph barrier crash. This total distance consists of the over-the-ground travel of the occupant compartment and the relative movement of the occupant with respect to the compartment. An examination of the Pinto showed that the maximum crush distance available would be 40 inches without intrusion into the compartment. Thus 15 inches is required between the occupant and the windshield. Therefore, the existing compartment did not have sufficient room in this dimension.

The total available crush distance of 40 inches could be obtained only if the engine were allowed to stroke at least 12 inches. The production vehicle had approximately 7 inches of clearance before the engine impacted the firewall. Since the firewall force deflection curve was unsuitable for proper crash pulses, the engine stroke distance had to be improved.

The upper portion of the existing front structure showed very poor load carrying capability -- it collapsed much more easily than the lower front structure, thus allowing excessive pitch to the vehicle. In order to increase the strength of the upper structure, it is necessary to place material above the wheel and below the fender line. This can only be accomplished by increasing the height of the vehicle.

The final geometrical problem concerns the side impact and will be discussed in detail in Section 4.0. It is only necessary to note here that a rational safety vehicle should have strong side structure at the same height as the impacting bumper.

The geometrical considerations are shown in Figures 3.1 through 3.4. Figure 3.1 shows the exterior dimensions of a Pinto sedan. Figure 3.2 presents the interior and occupant H-point dimensions. Figures 3.3 and 3.4 show the needed modifications in vehicle geometry.

The geometrical modifications can be achieved by altering the individual structural components. This is the method which would be used in production and would result in the most marketable vehicle. Since this was a research and development contract, funds were not available for this "ideal" solution. Instead, all of the objectives were obtained by the simple expedient raising of the body of the vehicle relative to the running gear and drive train.

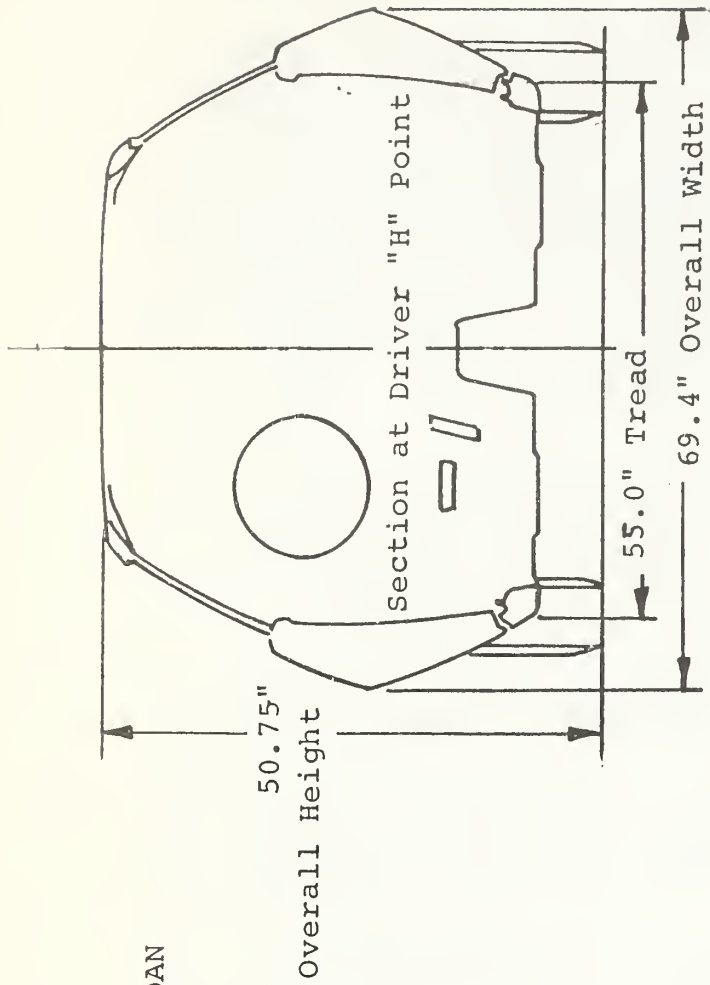
The second aspect of the front structure must now be considered. The proper force deflection characteristics for the modified vehicle must minimize the occupant stroke relative to the compartment. The final shape of the pulse is subject to four limiting conditions:

1. The no-damage bumper must stroke at not more than 10 g's.
2. The maximum rate of change of acceleration (jerk) must be less than 1500 g's/sec.
3. The maximum acceleration of the occupant must be less than 60 g's.
4. The maximum available crush distance of the front structure is 40 inches.

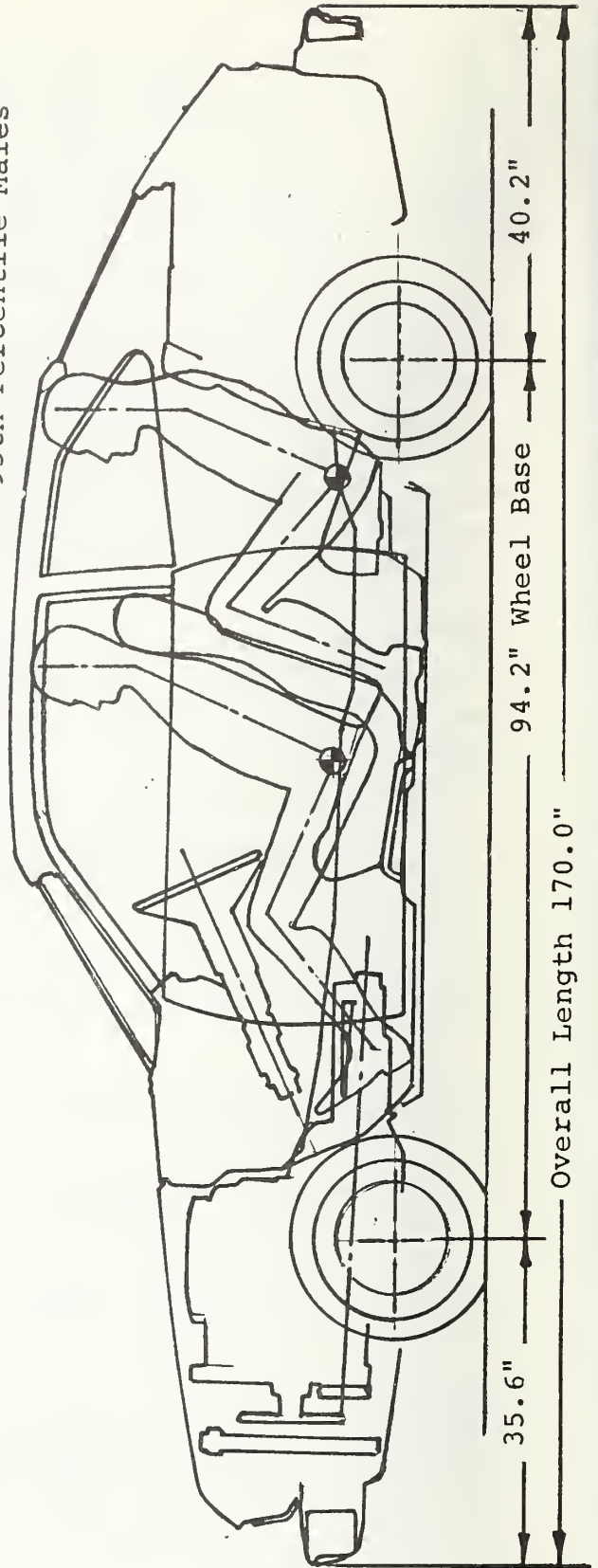
The limitations will appear in the force deflection curve as a low early plateau (Item 1), a linearly increasing portion (Item 2), a high level plateau (Item 3), and finally a rapidly increasing force curve (Item 4). The major values to be established were the length of the ramp, or initial rate of increase in acceleration, and level of the upper plateau.

1974 PINTO 2-DOOR BASE SEDAN

1/20 Full Size



95th Percentile Males



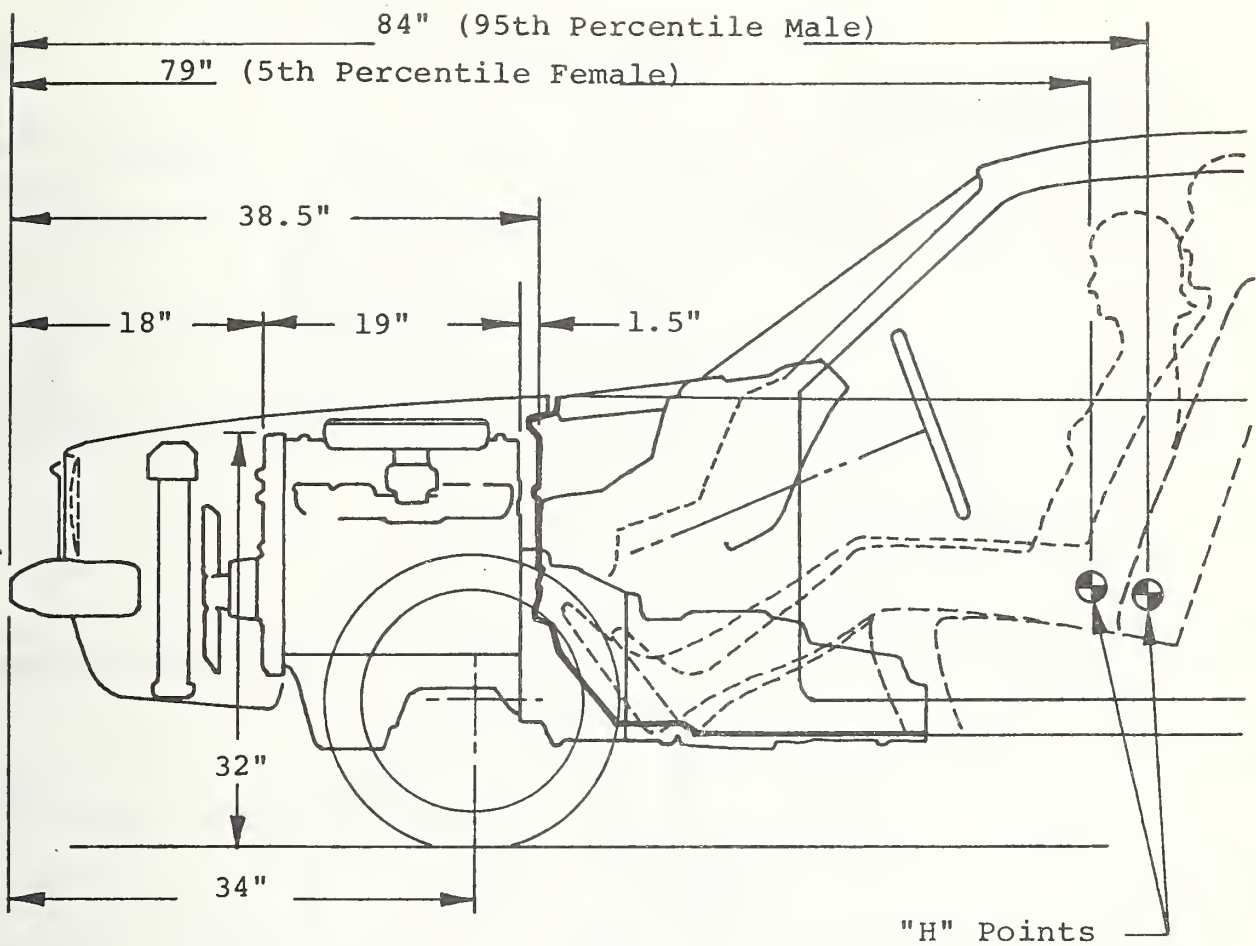


FIGURE 3.2 INTERIOR DIMENSIONS OF STOCK  
1974 PINTO SEDAN

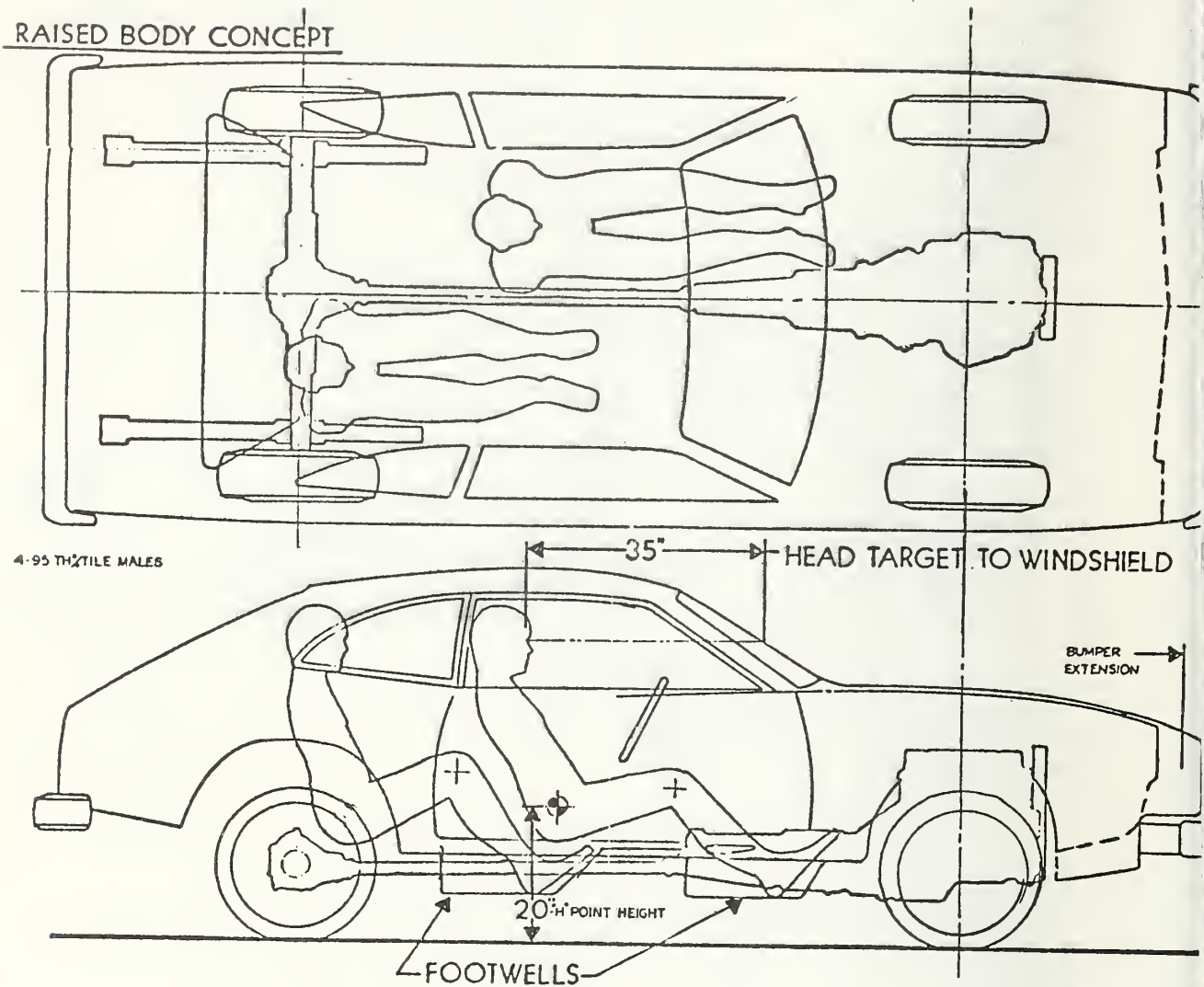


FIGURE 3.3 REQUIRED MODIFICATIONS OF PINTO GEOMETRY FOR FRONTAL IMPACTS

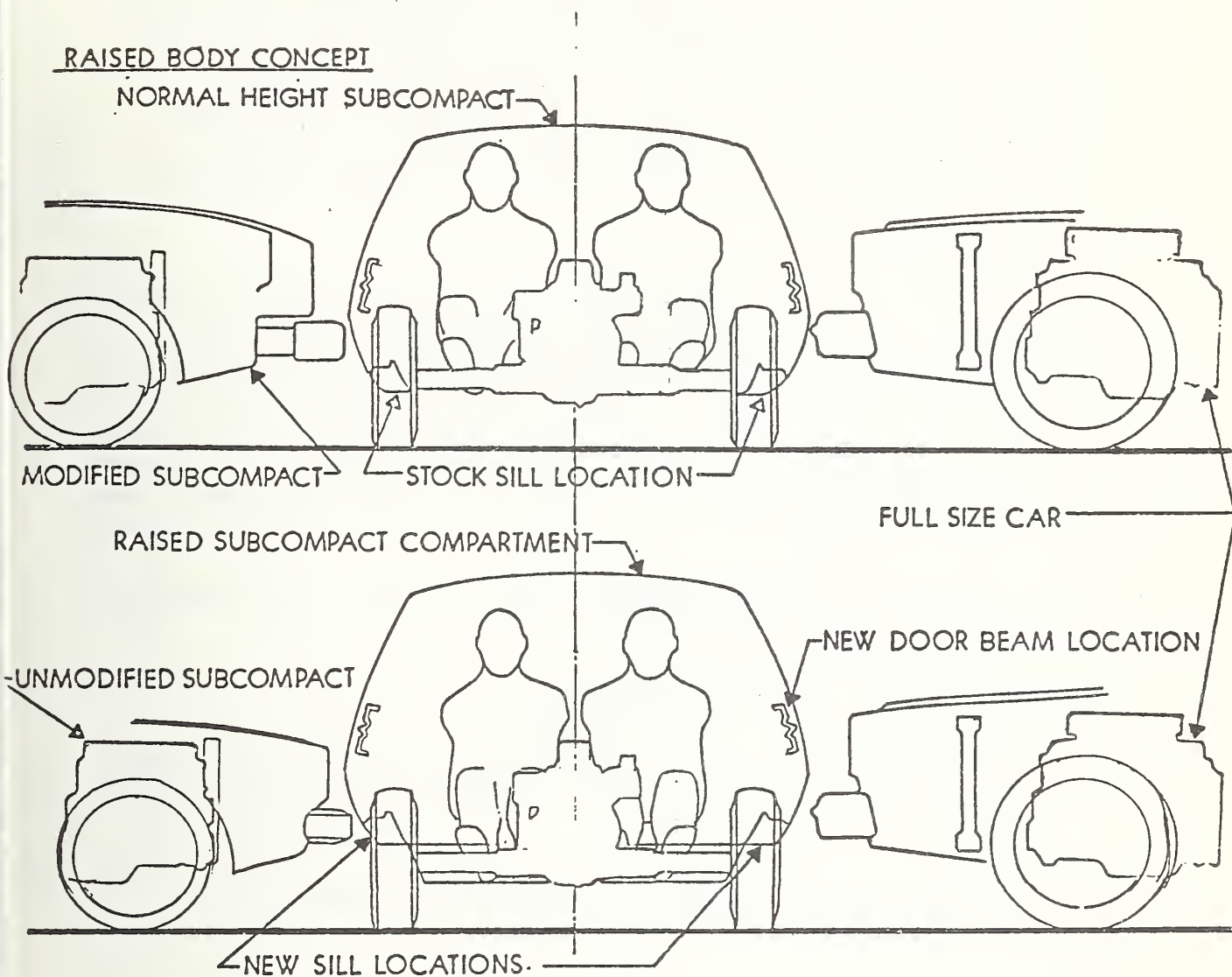


FIGURE 3.4 REQUIRED MODIFICATIONS OF PINTO GEOMETRY FOR SIDE IMPACTS

Figure 3.5 shows two candidate F- $\delta$  curves for the modified design, along with two representative curves for a standard size automobile. A computer analysis was conducted for various impact combinations of these curves, with the results presented in Table 3.1. The results show that the pulse shape which rises most quickly (within the jerk limitation) to its plateau exhibits the least crush and occupant stroke.

This result is to be expected, since with this pulse shape the driver torso reaches its peak g level as early as possible, and the greatest possible energy is absorbed via ride down. Also, the crash duration is longer, due to the lower plateau. Therefore, the optimum curve is one which rises as rapidly as the jerk level will allow to the lowest plateau consistent with the available crush distance in the car. Figure 3.6 shows the selected force/deflection curve.

In summary, the design approach was to modify the geometry of the structure to achieve the following results:

1. Allow more occupant stroke.
2. Provide engine stroke distance.
3. Provide room for upper structure above the wheel wells.
4. Raise the rocker panels to the height of an impacting bumper.

The structure itself was to be modified to produce the force deflection curve shown in Figure 3.6.

### 3.2.2 Rigidization of the Compartment

The final portion of the optimum crash pulse is a rapidly increasing force level beyond the allowable crush distance. This portion of the curve is necessary to limit the intrusion of hard structure into the living space of occupants. In essence, what is desired is a rigid structure, completely surrounding the occupant, to support the inertia loads generated during the impact without undergoing excessive deformation.

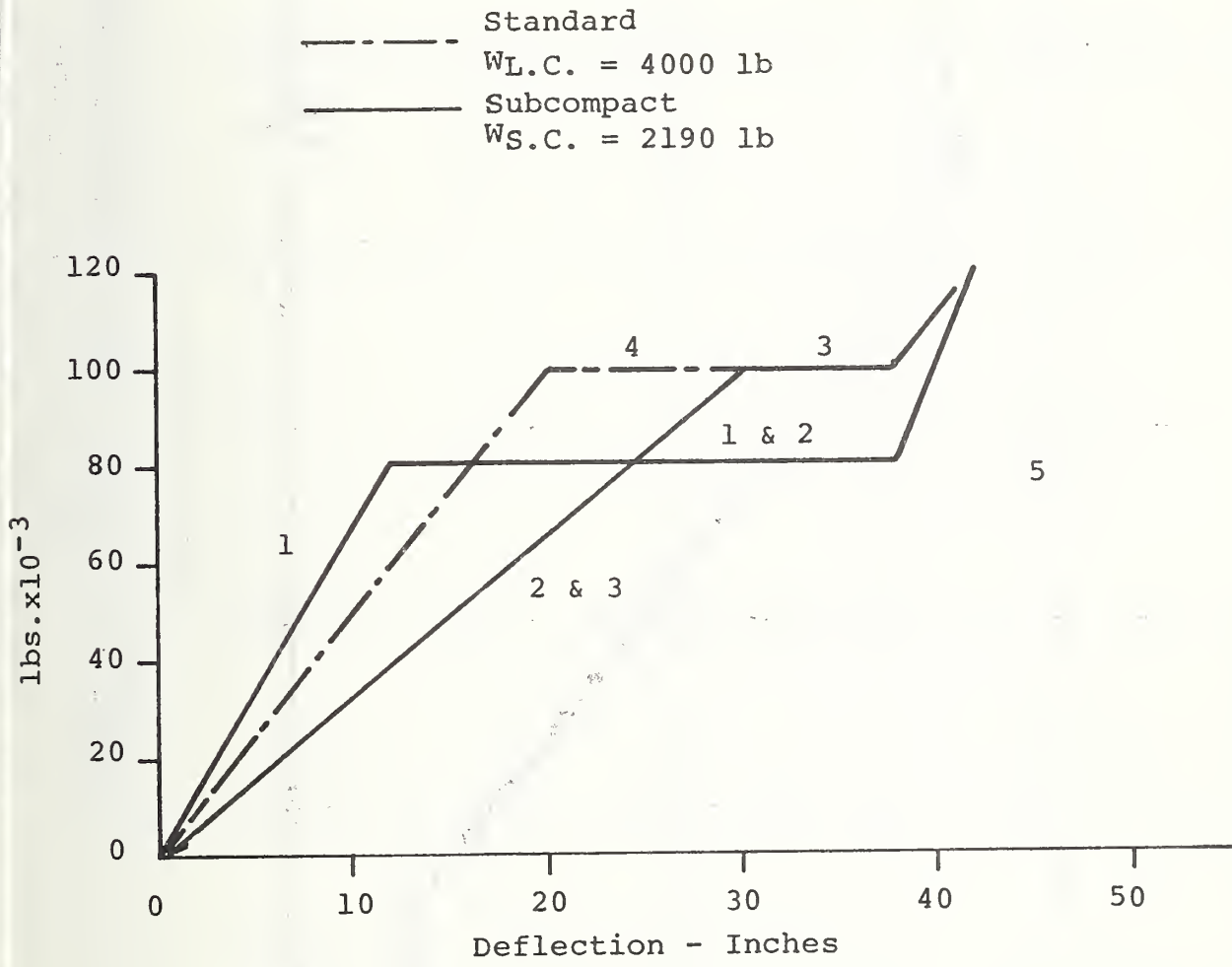


FIGURE 3.5 CANDIDATE FORCE DEFLECTION CURVES FOR FRONTAL IMPACT

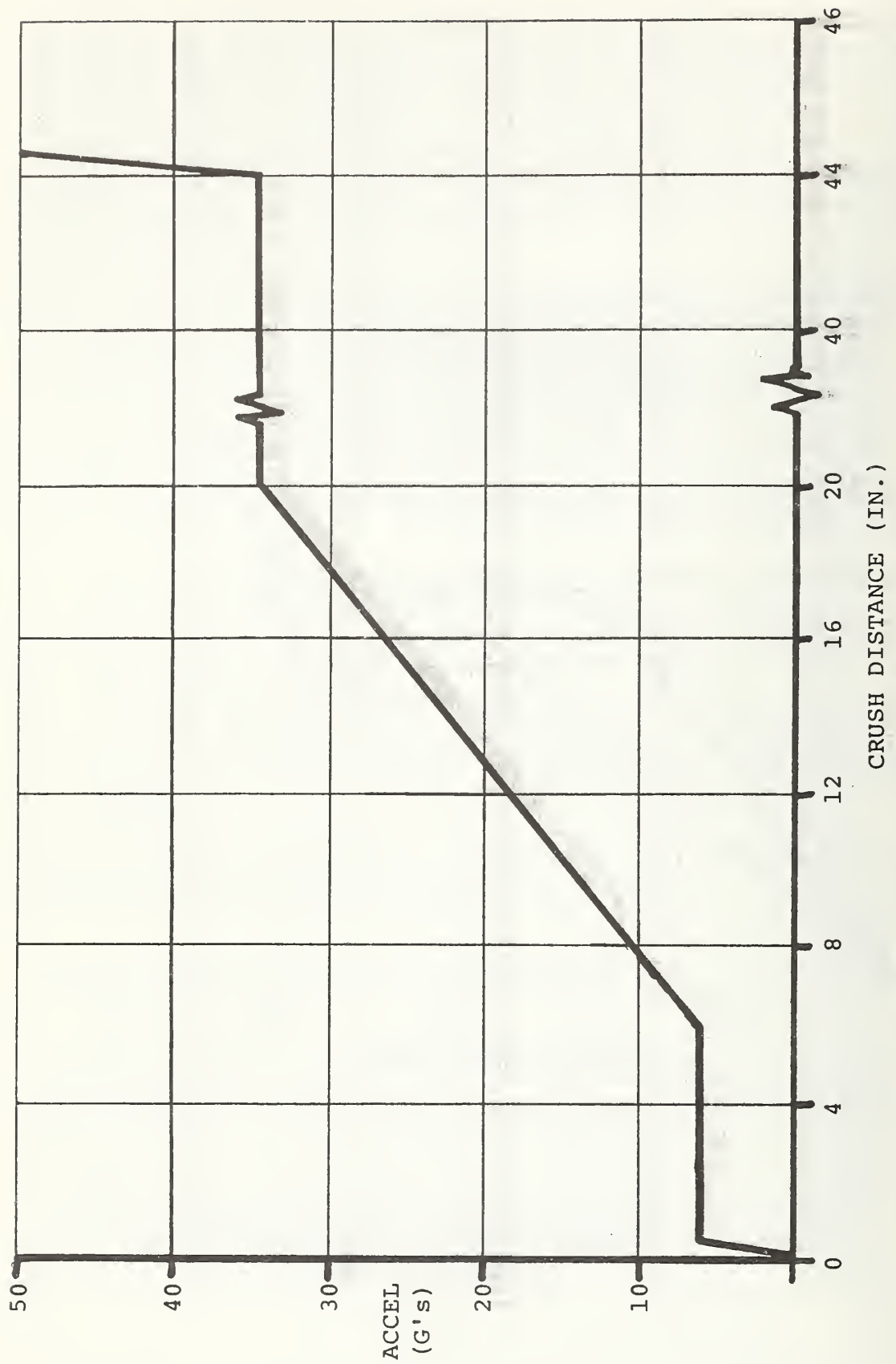


FIGURE 3.6 SELECTED FORCE-DEFLECTION CURVE  
MODIFIED SUBCOMPACT VEHICLE

TABLE 3.1 PULSE SELECTIONS FOR MODIFIED COMPATIBLE SUBCOMPACT

Computer Run No.	Subcompact Car Front End	Standard Car Front End	Subcompact Car Crush Inches	Standard Car Crush Inches	Total Driver Interior Stroke Inches	Peak Chest G's
1	80K - 12*	100K - 20	32.0	20.2	23.6	65.6 @ t = 60 msec
2	100K - 30	100K - 20	32.6	23.4	25.7	66.0 @ t = 65 msec
3	80K - 24	100K - 20	39.7	18.8	24.5	65.5 @ t = 65 msec
4	80K - 24	100K - 54**	25.9	46.6	22.3	64.8 @ t = 75 msec

\* 80K - 12 means a front end force-deflection characteristic that rises from zero to 80 kip in 12 inches and remains constant at the 80 kip level.

\*\* The 100K - 54 front end for the standard sized car roughly represents a 20-30 degree oblique frontal impact.

A review of the baseline Pinto structure revealed three areas of weakness in the compartment region. First, the door and door beam were not rigid enough to prevent collapse of the door opening. Second, the floor and tunnel structure could not carry the longitudinal inertia loads. And, finally, the toe board region could not support loads at the ends of the sub-frames. As a result of these weaknesses, the baseline Pintos exhibited failure of the compartment structure under only 30-mph barrier loads.

The rigidization of the door opening was accomplished by improving the longitudinal stiffness of the door itself. The production door beam was removed and replaced with a 2.5 inch x .065 inch steel tube extending from the upper A post hinge to the door latch mechanism on the B post. This member formed a compression strut supporting the upper portion of the A post across the door opening.

The floor and tunnel section was stiffened by a redesign of the tunnel including longitudinal hat section stiffeners on each side. In addition, the rocker panel was enlarged, as shown in Figure 3.7, and filled with 2 lb/ft<sup>3</sup> density foam.

The integrity of the toeboard region was enhanced by forming a box section and filling it with foam. The box section followed the original contour on the engine compartment side and formed a vertical plane on the occupant side. It extended the full width of the foot well, bridging between the tunnel and the rocker panel. A local stiffener was placed in the box to back up the sub-frame members where they intersected the toeboard.

The net effect of the passenger compartment changes was to force all crush to occur forward of the foot well-dash station. The area aft of the dash had to remain inviolate to allow maximum occupant stroking distance.

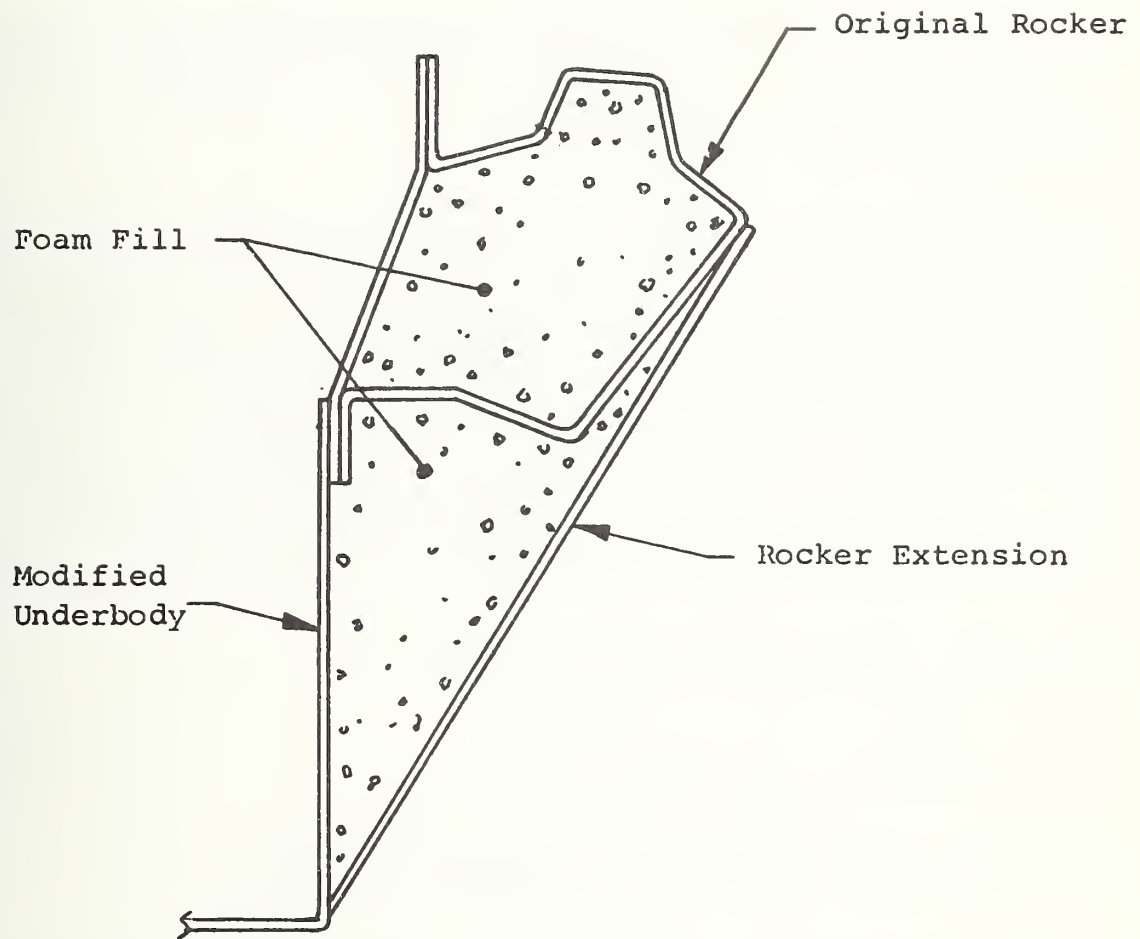


FIGURE 3.7 ENLARGED ROCKER PANEL CROSS-SECTION

### 3.2.3 Alternate Energy Absorbers

The problem of front end energy management systems has been studied under DOT auspices for several years. The subcompact vehicle geometry significantly increased the difficulty of the problem. This, combined with the addition of the offset and angular accidents, dictated a completely new evaluation of front end energy absorbers.

The primary systems developed previously were the following energy absorbers: (1) plastic hinge, (2) hydraulic cylinder, and (3) crushable tube structure. These concepts are pictured in Figure 3.8

The first method, plastic hinge structure (Figure 3.8a), provides excellent crashworthiness, but results in a heavy design. The weight increase is due to the inefficient utilization of the material. Only the small portion of the frame members at the location of the hinge participates in energy absorption. The remainder of the members behave elastically and do not absorb energy. Figure 3.9a illustrates the action. Figure 3.9b demonstrates the second disadvantage of the plastic hinge structures, i.e., the individual hinges are not constant force devices, but load decreases with increased deformation.

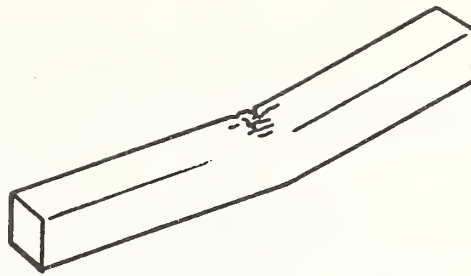
The force carried by a plastic hinge is

$$F = \frac{M_p}{d} \quad ,$$

where  $M_p$  = the plastic moment of section, and  
 $d$  = the offset of the applied force.

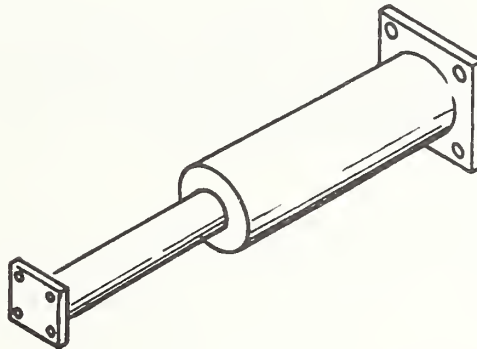
Since  $M_p$  is constant for any given section and  $d$  increases with collapse of the member, then the applied force must decrease. Referring to Figure 3.9a,

$$\delta = \text{collapse movement of point A} = \ell(1 - \cos\theta) \quad ,$$



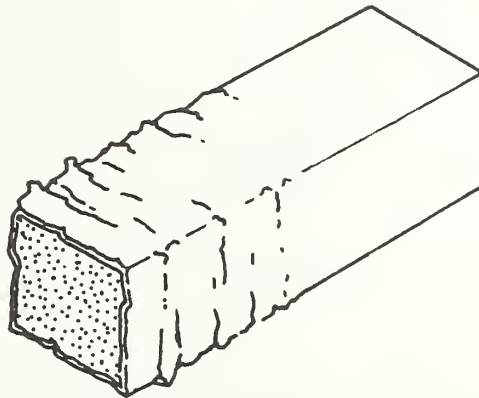
Stroke Efficiency - high  
Energy Density - low

a. Structural Tube with Plastic Hinge



Stroke Efficiency - low  
Energy density - fair

b. Hydraulic Cylinder Energy Absorber

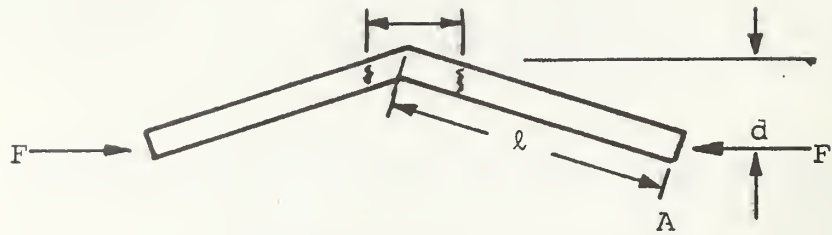


Stroke Efficiency - high  
Energy Density - high

c. Crush Tube Energy Absorber

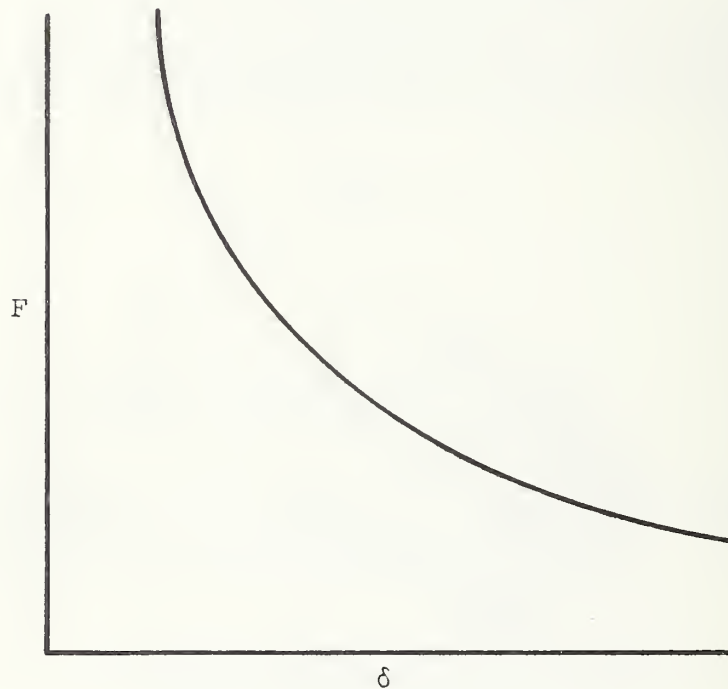
FIGURE 3.8 ENERGY ABSORBER CONCEPTS

Area of Plastic Hinge



$\ell = 1/2$  length of member  
 $d =$  affect of applied load  
 $F =$  applied loads

a. Efficiency of Plastic Hinges



b.  $F-\delta$  of a Plastic Hinge Member

FIGURE 3.9 BEHAVIOR OF PLASTIC HINGE

where  $\theta = \arcsin \frac{d}{\ell} = \arcsin \frac{M_p}{F\ell}$ ,

$$\cos\theta = \frac{\sqrt{(F\ell)^2 - M_p^2}}{F\ell}, \text{ and}$$

$$\delta = \ell \left( 1 - \frac{\sqrt{(F\ell)^2 - M_p^2}}{F\ell} \right).$$

The curve which is plotted in Figure 3.9a was verified by tests conducted under Contract DOT-HS-257-2-461. Such a force deflection curve will not provide the most efficient structure. One final disadvantage of plastic hinges is that they are truly achieved only with solid sections. With hollow members, the side walls collapse well before complete operation of the failure mechanism.

The use of hydraulic cylinders for front end energy management was pioneered in early experimental safety vehicle work where the emphasis was on "no damage" at high velocities. For this purpose, they were extremely useful, as they could provide large strokes and easy repositioning. They do, however, suffer from the disadvantages of high cost, heavy weight, low stroke efficiency, and linear actuation.

Hydraulic cylinders are normally precision hardware with a large amount of machining and assembly time. Even on a mass production basis, the long stroke cylinders would significantly increase the cost of automobiles. Secondly, since the loads on a front structure are relatively high, the cylinders must be able to carry high pressure and high column loading. To accomplish this elastically requires a heavy cylinder and piston, and back-up structure which is much heavier than existing frame structures.

The maximum stroke efficiency of a hydraulic unit is 50 percent since the cylinder and piston may not collapse. In actual practice, this efficiency will be lower due to fittings, end caps, etc. The limited allowable room in the subcompact vehicles seriously hampers the use of hydraulic cylinders as front end energy absorbers. As a final limitation, the hydraulic cylinders will absorb energy from one direction only. Thus oblique and offset accident modes cannot be accommodated by these unidirectional devices.

The third category of energy absorber used in previous designs is the crushable or collapsing tube. This system is the most efficient, most economical, and lightest of the designs. Its major drawback is the unidirectional nature of the stroke. In the past, devices have consisted of either round or square seamless metal tubes designed to form progressive local buckles down their length. Additional collapsing mechanisms were considered under this contract. Altogether, the following five types of crushable energy absorbers were investigated:

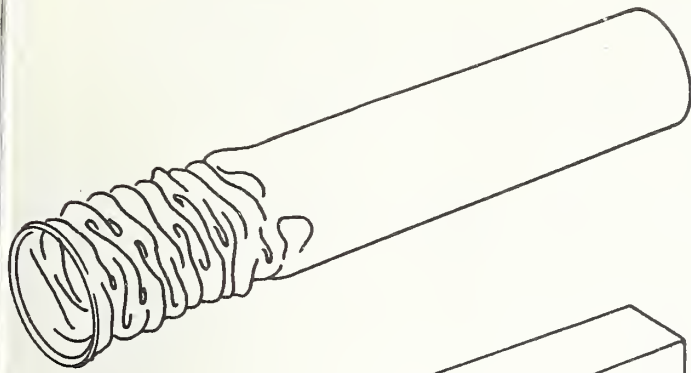
1. Hollow circular metal tubes.
2. Hollow rectangular metal tubes.
3. Foam-filled circular metal tubes.
4. Aluminum "tubecore."
5. Foam-filled aluminum honeycomb.

Figure 3.10 shows these five alternate energy absorber concepts.

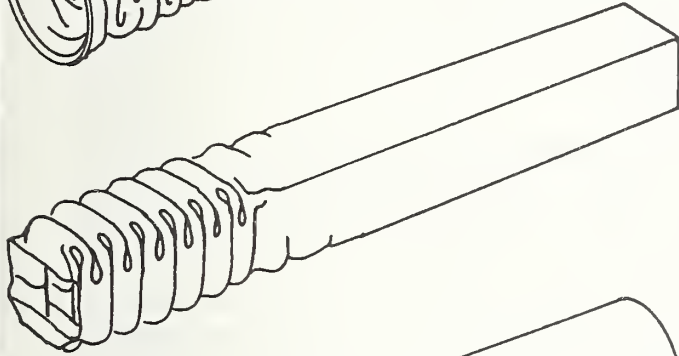
The use of hollow round circular tubes as energy absorbers predates the auto safety effort. The aerospace industry has long been aware of the high efficiency of circular collapsing tubes. The particular designs considered for the subcompact front end were based on the scale model studies<sup>11</sup> conducted at Stanford Research Institute. Candidate hollow circular metal tubes for use in the design were:

1. A 3.5 inch x .08 inch aluminum tube
2. A 4.5 inch x .08 inch aluminum tube

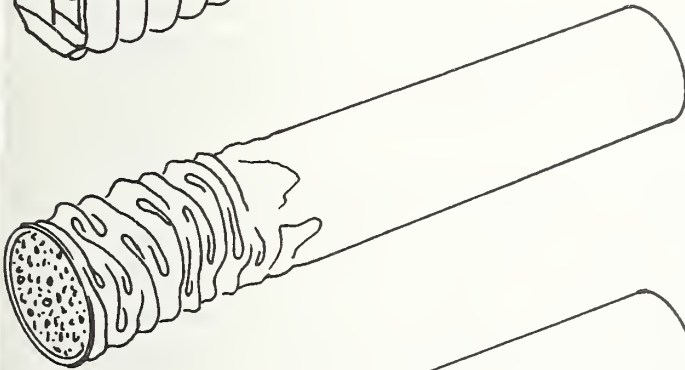
The exact behavior of a collapsing tube is difficult to predict analytically. The empirical approach, either scale model or full scale, will yield the most reliable load deflection behavior. Round tubes are especially difficult to analyze, since they may form either the extensional ring mode or the inextensional multi-lobe mode.



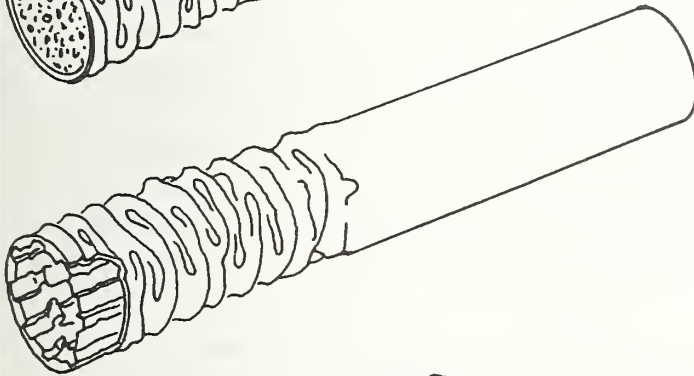
a) Round Hollow Tube



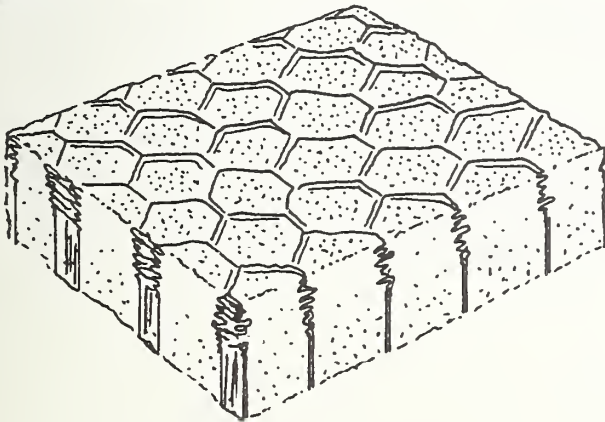
b) Square Hollow Tube



c) Foam Filled Hollow Tube



d) Aluminum Tube Core



e) Honeyfoam

FIGURE 3.10 ENERGY ABSORBER CONCEPTS

The SRI model was a 0.75 diameter by .022 thick aluminum tube giving a load of 405 pounds. Scaling this up from a 1/6 model gave a force level 15,000 pounds for a 4.5 diameter by .132 thick 6061-0 aluminum tube. The available 4.5x.08 tube should yield a force level of 7000 pounds. The smaller diameter tube (3.5x.08) would be expected to have a crush load of 4000 pounds. Although the round tubes are the most efficient geometrical form, they are not the most practical for automobile structures. Automatic positioning and joining of such members requires a great deal of development work.

This leads directly to the second type of absorber, the hollow rectangular metal tube. For this geometry, the buckle is always inextensional with adjoining sides buckling in and out alternately (Figure 3.10b). Analysis of rectangular tubes has been considered in detail in SAE paper 740040. However, it is still necessary to rely on empirical data for good design of collapsing rectangular sections.

The rectangular tubes considered included both steel and aluminum. They were 2 inch x 4 inch or 2 inch x 5 inch, with thicknesses ranging from .063 inch to .125 inch. The results of the static crush tests are presented in Table 3.2. The actual load-deflection curves are shown in Appendix G. Stroke efficiencies of 75 percent are obtained with these devices. They are light, having the approximate shape and size of the standard subframe structure, and economical, since standard production techniques can be used. Minicars ultimately selected a rectangular section (2 x 4 x .083 inch steel) as the bumper support member in the lower structure.

The third linear absorber considered was a foam-filled circular metal tube. The standard crush tube was filled with pour-in-place polyurethane foam. The concept was to rigidize the tube and increase the collapse strength to provide a more weight efficient structure. The concept was scale model tested at SRI and found to be far too stiff for application to automobile structures. Obtaining the correct force level required a thinner tube than is

commercially available. Although this concept was rejected, the tests did verify the basic applicability of foam and metal combination structures.

The fourth concept, "tubecore," is a commercially available energy absorber developed for the aerospace industry. It is made by rolling corrugated aluminum sandwich material around a circular mandrel. The corrugations run parallel to the axis of the cylinder. The device offers a well-defined, square wave force deflection characteristic. However, the cost, even in production quantities, is quite high. The absorber itself has a skin, which would decrease the weight efficiency of the device.

The final linear energy absorber considered as a Minicars concept for combining the best qualities of honeycomb and foam, which was named "honeyfoam." A section of ACG-3/4 - .003 honeycomb was filled with 2 lb/ft<sup>3</sup> polyurethane foam, and test specimens were cut from the block. The ACG-3/4 - .003 is a commercial grade aluminum honeycomb with 3/4-inch cells made from .003-inch thick material. A total of eight 3 inch x 3 inch x 6 inch specimens were statically crushed with nominal crush loads of 100 psi. This is compared to the individual crush levels of constituents of 25 psi for the foam and 50 psi for the honeycomb. All of the specimens were tested with the load parallel to the cell axis of the honeycomb.

A parallel effort to the above tests was a series of five dynamic tests of aluminum honeyfoam samples. The test specimens were 6 x 6 x 12 inches, mounted on a 200-pound sled and impacted at various velocities from 9.5 mph to 24.8 mph. The specimens were formed by bonding together two 6-inch cubes. In the first three specimens, the blocks were bonded directly. In the last two tests, a thin aluminum sheet was bonded between the blocks. The results of the tests are presented in Table 3.2b. The material behaved extremely well during dynamic impact test, showing little rebound or disintegration.

TABLE 3.2 ENERGY ABSORBER CRUSH TEST DATA

## 3.2a Rectangular Tube Crush Test Data

<u>Shape</u>	<u>Material</u>	<u>Preformed</u>	<u>Peak Load</u> lb.	<u>Average Load</u> lb.
2 x 5 x .125	6063-T52 AL	No	32,400	≈14,000
2 x 5 x .125	6063-T52 AL	No	38,400	Specimen Buckled
2 x 4 x .083	1010 Steel	No	34,500	≈13,000
2 x 4 x .083	1010 Steel	Yes	26,400	≈11,000
2 x 4 x .063	1010 Steel	Yes	14,500	≈9,000

## 3.2b Dynamic Honeyfoam Test Data

<u>Specimen</u>	<u>Velocity</u> (mph)	<u>Crush Distance</u> (ins)	<u>Average Crush</u> (psi)
1	24.8	10.0	137
2	9.5	1.5	134
3	18.0	7.5	96
4	17.8	6.1	115
5	11.1	1.8	152

The variation in average crush loads is due to the different crush depths. Comparison of static and dynamic data show approximately a 30 percent dynamic factor. Honeyfoam was not used in the final design due to the high cost of production. It may prove feasible in the future in areas requiring high strength, light weight absorbers.

#### 3.2.4 Evaluation of Linear Absorber System

In order to fully evaluate the concept of a tabular front end energy management system, a full scale test vehicle was fabricated and tested. The design of the trial structure was based primarily on the use of round aluminum crushable tubes as described in Section 3.2.3.

The load path selection for a crushable tube front energy absorber is dictated by the operational requirements of the automobile. The structure must support the bumper, engine, and front suspension. It must extend from the firewall to the bumper and not interfere with the power system or wheel turning geometry. The only available space which satisfies all of these requirements is the area occupied by the production subframe, two longitudinal parallel members running on each side of the engine, inboard of the front wheel. Figure 3.11 shows these members. The results of the baseline tests indicated that production Pintos exhibit excessive pitch in frontal barrier impacts. The pitch is due to lack of adequate structure above the center of gravity of the vehicles. To improve the pitch performance, additional crush tubes were located in the upper portion of the fender area, extending from the upper A posts to the headlamps. These four tubes represent the basic load paths of the crushable tube design.

Since Minicars had added the oblique and offset impact as design goals, it was necessary to deal with the uni-directional nature of the crush tubes. To provide lateral support, two diagonal crush tubes were added, running from the upper fenders to the center of the firewall. The

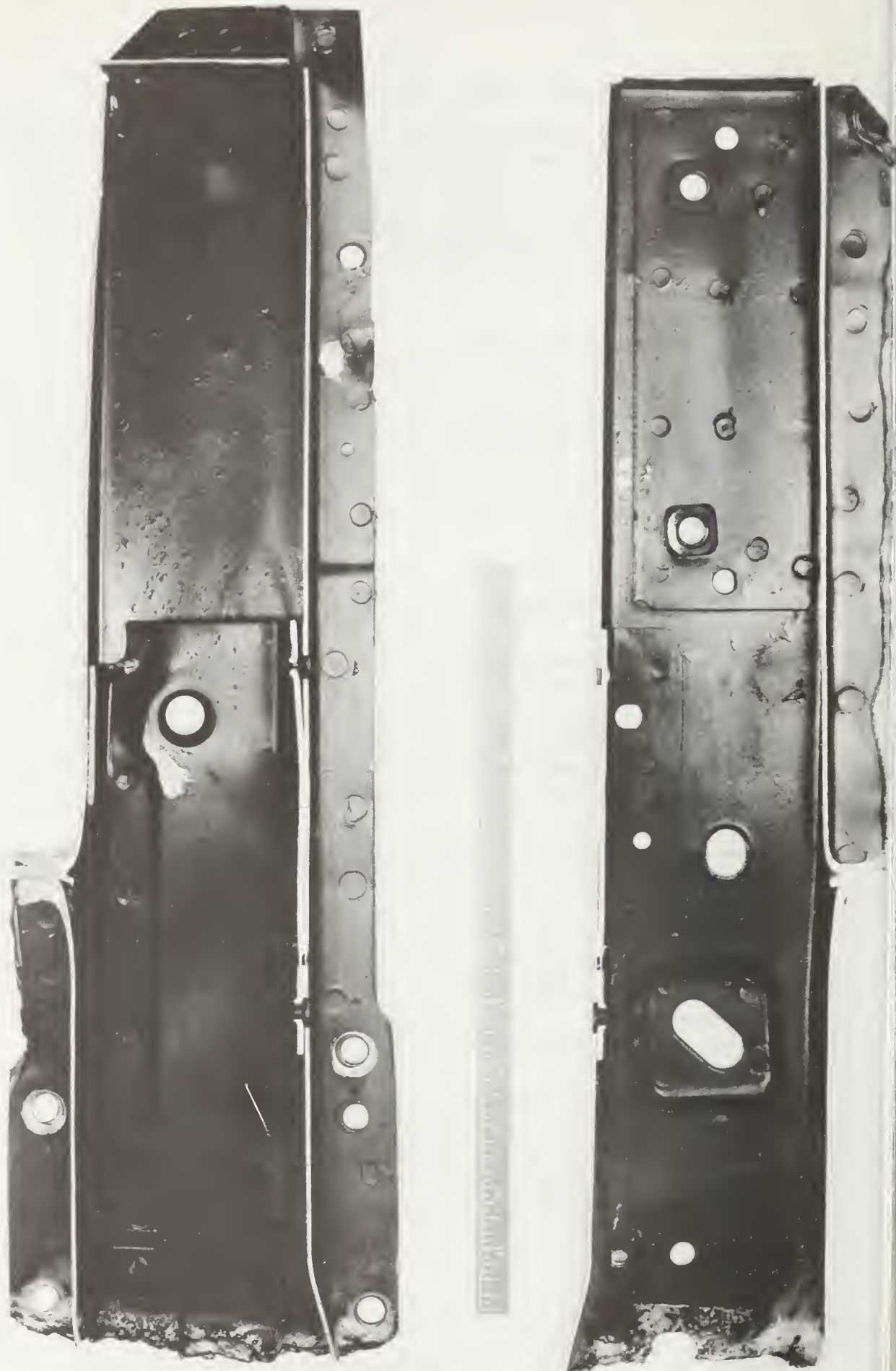


FIGURE 3.11 PRODUCTION SUBFRAME  
3.26

entire front end was tied together with an aluminum channel yoke. Figure 3.12 shows the configuration of the crushable tube front end energy management system.

A 1974 production Pinto was modified for use as the test vehicle. The production forward frame members were disengaged from the body sheetmetal at the firewall, toeboard, and underbody area; 6-inch deep footwells were inserted, and the forward frame members reattached to them. The forward frame members were cut off at the engine cross member.

The crushable tubes selected from the available energy absorbing concepts were hollow aluminum tubes. The upper longitudinal struts were 4.5 x .080 inch 6061-0 aluminum. The lower struts were 4.5 x .125 inch 6061-T6 aluminum. The diagonal struts were 3 x .080 inch 6061-0 aluminum. The tube dimensions were selected based on scale model tests conducted by Stanford Research Institute under a separate NHTSA contract.

The upper frame members were tied to the A post at the upper door hinge. The A post is supported by a compression strut in the modified door running from the upper hinge on the A post to the latch mechanism on the B post.

Concurrent with the development of the full scale test vehicle, Stanford Research Institute constructed and tested a one-sixth scale model of a similar front end structure. The model, as shown in Figure 3.13, was composed of four aluminum struts, foam-filled and mounted to a solid compartment. The forward ends of the tubes were secured by an aluminum yoke. The bumper and its short stroke energy absorption units were mounted forward of the yoke. Tension ties were used to stabilize the structure. The model was tested at 50 mph into a 30° oblique barrier. The post-test picture of the model shows the completely unacceptable behavior of the structure. The filled struts proved to be too rigid to allow progressive collapse, failing instead by beam-column action. The higher force levels induced by the rigid structure caused complete failure of the model. It was apparent from this test that foam-filling the tubes increases the collapse load far more than predicted by

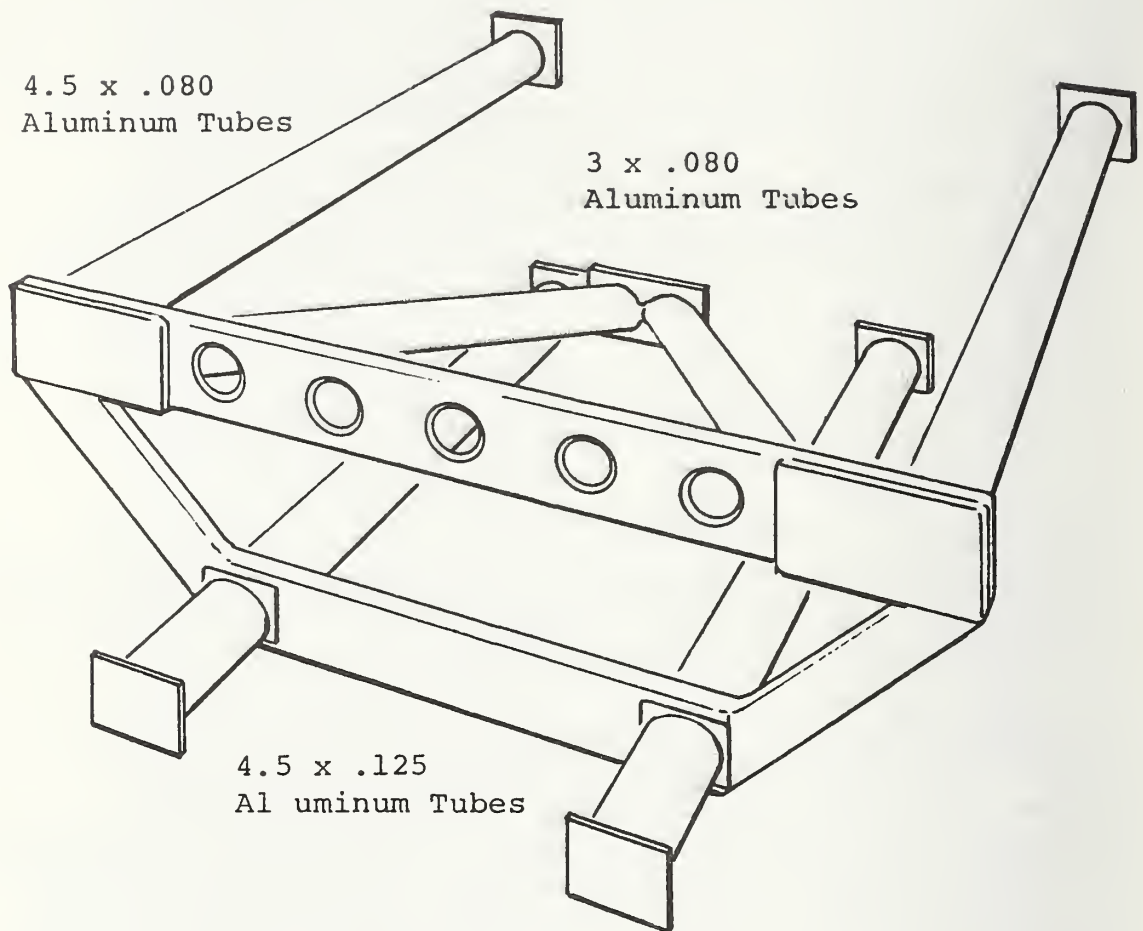
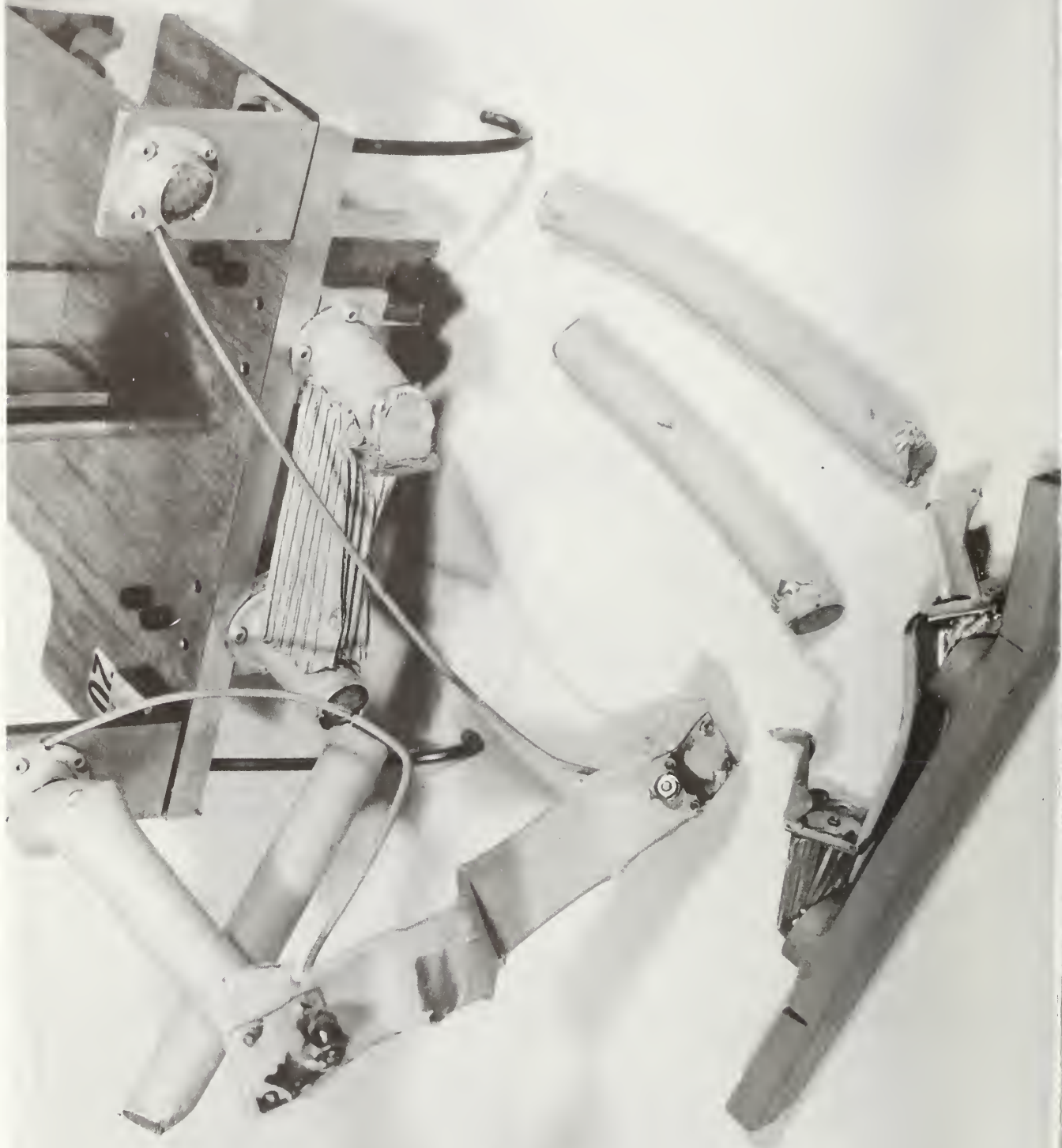


FIGURE 3.12 CONCEPT FOR CRUSHABLE FRONT END  
ENERGY MANAGEMENT SYSTEM



FIGURE 3.13a 1/6 SCALE MODEL OF TUBULAR FRONT STRUCTURE



combining the strength of the foam alone and the unfilled tube. The acceleration pulse from this test is presented in Figure 3.14.

In light of the poor results of the SRI scale model at 50 mph, the full scale vehicle was tested at 40 mph into a frontal barrier. It was hoped that a test at the lower speed and perpendicular barrier would define a lower bound on the performance of the design. However, the failure exhibited by the structural components during the test did not agree with the mode predicted prior to test. The lower round aluminum tubes supporting the bumper started to form the crush mode as predicted, but after two lobes developed, the tube penetrated the firewall and then buckled. The upper W strut was pulled down by the collapse of the lower tubes and bent at the line of the firewall. This was a bending failure and not crippling or buckling. The crash pulse from the test (D3) is shown in Figure 3.15. The design produced a long low crush pulse, ramping up to 23 g's in 40 milliseconds. These tests clearly indicated that tubular structures are not the proper method of energy management. Though it may be possible to solve the problems of tubular structures for the aligned frontal impact, their use for oblique impacts is severely limited.

### 3.2.5 Evaluation of Volumetric Structures

In accordance with Minicars' original proposal, the primary concept for the front end energy management system was a volumetric structure. A "volumetric" structure is a large volume, low density material (foam) mounted in the front of the vehicle. Such a structure has the advantage of light weight, high efficiency, and insensitivity to direction of impact. The single disadvantage is the lack of current usage in automobile structures. This could lead to an increase in cost until the producibility problems had been satisfied. Ultimately, volumetric structures will show relatively little impact in the retail price of automobiles.

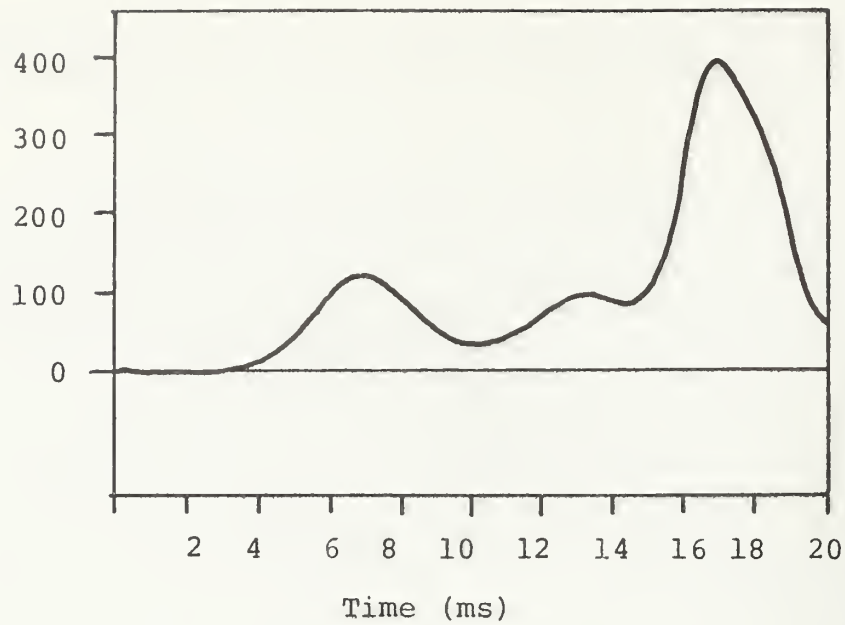


FIGURE 3.14 ACCELERATIONS PULSE OF SCALE MODEL CRUSHABLE TUBE FRONT STRUCTURE

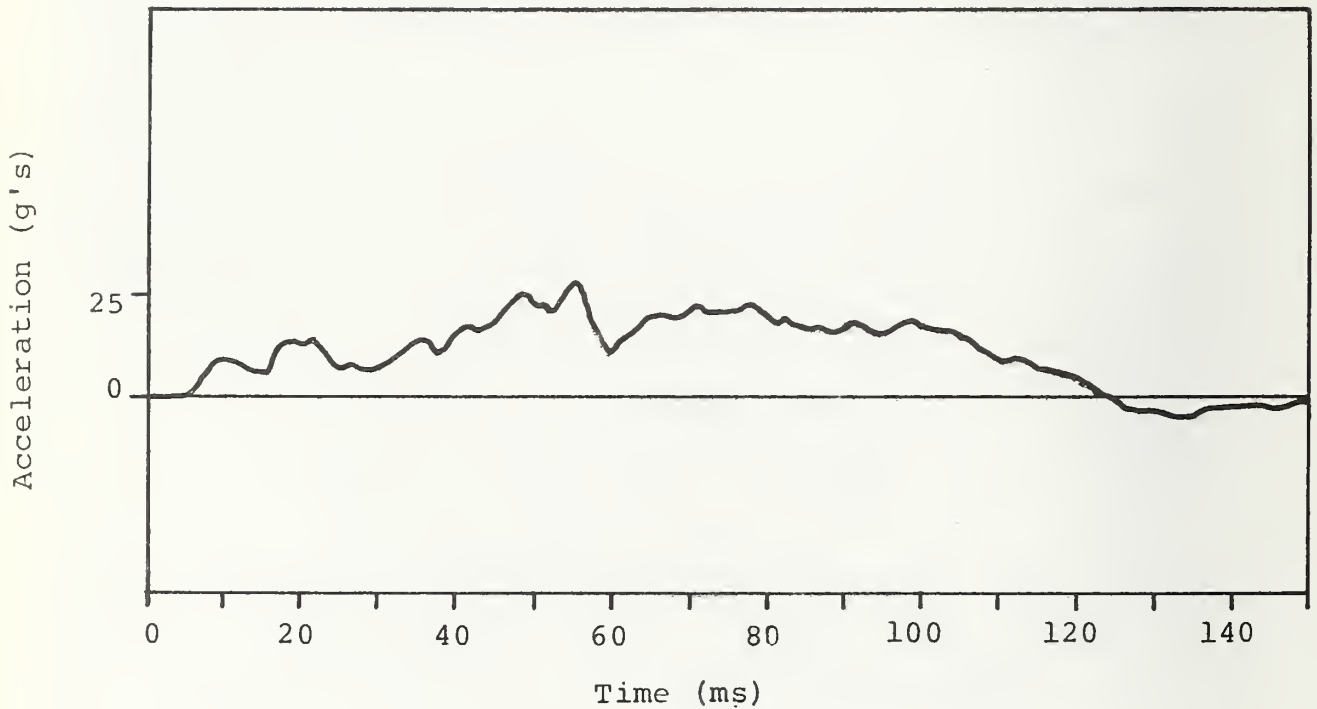


FIGURE 3.15 ACCELERATION PULSE OF FULL SCALE CRUSHABLE TUBE FRONT STRUCTURE (D3)

Volumetric structures (foam) are extremely stroke efficient, with up to 80 percent of the length of the member available for energy absorption. Their high strength to weight ratio has been verified through their extensive use in the aerospace industry. This is particularly true when low density material is combined with thin sheetmetal sections: the foam provides stiffness and the metal provides strength. The omnidirectional character of volumetric structures, vital in oblique crashes, is evident by considering the geometry. The volumetric structures are designed to crush instead of buckling or grossly deforming. With suitable backing, the foam can crush in any direction, thus providing energy management in all impact modes.

The use of volumetric structures was first evaluated by a series of dynamic component tests with prospective designs mounted on the front of a bogey vehicle. A total of six candidate concepts were tested. Table 3.3 details the structure types and the test results. In the first four tests the specimens burst on impact, providing relatively little energy absorption. Tests 1 and 2 were run on uncontained foam blocks. Test 3 used a specimen contained in an "ensolite" blanket, while the fourth test specimen was a sample of paper honeyfoam. Test 5 was a multiple purpose test for three different containment materials. While the specimens behaved satisfactorily, the wrapping techniques did not lend themselves to producibility.

It was apparent from the first four tests that unconfined or weakly confined monolithic foam structures could not accomplish the desired energy management. Test 6 was of a foam-filled aluminum sheetmetal front structure. Its behavior was as predicted except for tearout failure of two rows of rivets along the top of the section. Further designs used all welded construction for the outer surface of the section. The average crush strength of the section was 48 psi. A total crush of 19 inches was measured at an initial velocity of 20.0 mph. The weight of the test article was 2,725 pounds.

TABLE 3.3 TESTS OF CANDIDATE VOLUMETRIC STRUCTURES

<u>Test No.</u>	<u>Type of Structure</u>	<u>Results</u>
1	2# Polyurethane foam block	Sample exploded on impact.
2	5# Polyurethane foam block	Sample exploded on impact.
3	2# Polyurethane foam billet enclosed with ensulite	Sample exploded on impact.
4	Paper honeycomb filled with 2# polyurethane foam	Sample exploded on impact.
5	Three styrofoam (2#) blocks one wrapped with fiberglass tape one wrapped with copper wire one wrapped with steel bands	Wraps contained the foam but the sample did bend slightly in the middle.
6	Aluminum sheet metal sections filled with 2# polyurethane foam	Aluminum contained the foam; some rivets failed.

Based on the result of the component tests, a trial front end volumetric structure was designed for full scale testing. Two vehicles were built and tested as development tests D4 and D5. Table 3.4 contrasts the two designs.

The design of the test article forward structure was based on the following three premises:

1. The upper structure must provide an anti-pitch capacity as well as a method of handling the oblique impact problem. It is important to treat the oblique impact problem with the upper structure, since the engine prevents use of lateral energy absorption material between the lower frames.
2. The lower frames must elastically carry the 10-mph bumper loads and also provide significant energy absorption after start of crush.
3. The engine/drive-train/suspension assembly must separate from the compartment and not load the compartment.

It must be noted that there are many alternative methods of achieving the pulse shape selected in Section 3.2.1. The above approach was selected after considering the effect of the secondary design parameters, such as pedestrian impact, aggressivity, etc.

The upper structure of the test articles used a foam and sheetmetal section to replace the hood and fenders of the production vehicle. Figure 3.16 shows the modified hood section. The lower structure of D4 and D5 each used a different technique of separating the engine and suspension assembly from the compartment mass. In the interest of economy, the vehicles were not raised for tests D4 and D5. The doors were stabilized as discussed in Section 3.2.2.

The configuration of the D4 lower frame weakened the sub-frame in the areas of the lightening holes (Figure 3.17). The engine mounts and engine cross members were separated from the lower frame member. The cross member and engine mounts were then integrated and reattached to the lower

TABLE 3.4  
COMPARISON OF TEST ARTICLES D4 & D5

	<u>D4</u>	<u>D5</u>
Upper Structure	Foam Filled Hood	Foam Filled Hood
Firewall	Enlarged Tunnel	Enlarged Tunnel
Aft Frames	Z-Shaped Plastic Hinge	Weakened Stock Frame
Engine Stroking Mechanism	Radius Struts	Breakaway Mounts

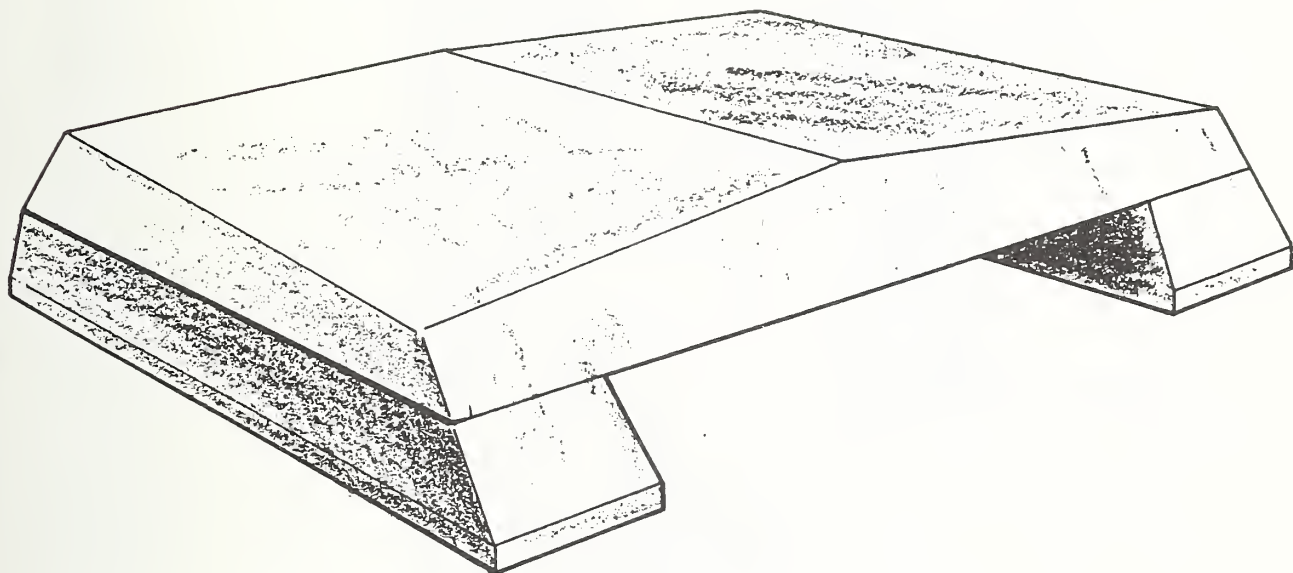


FIGURE 3.16 VOLUMETRIC HOOD MODIFICATIONS

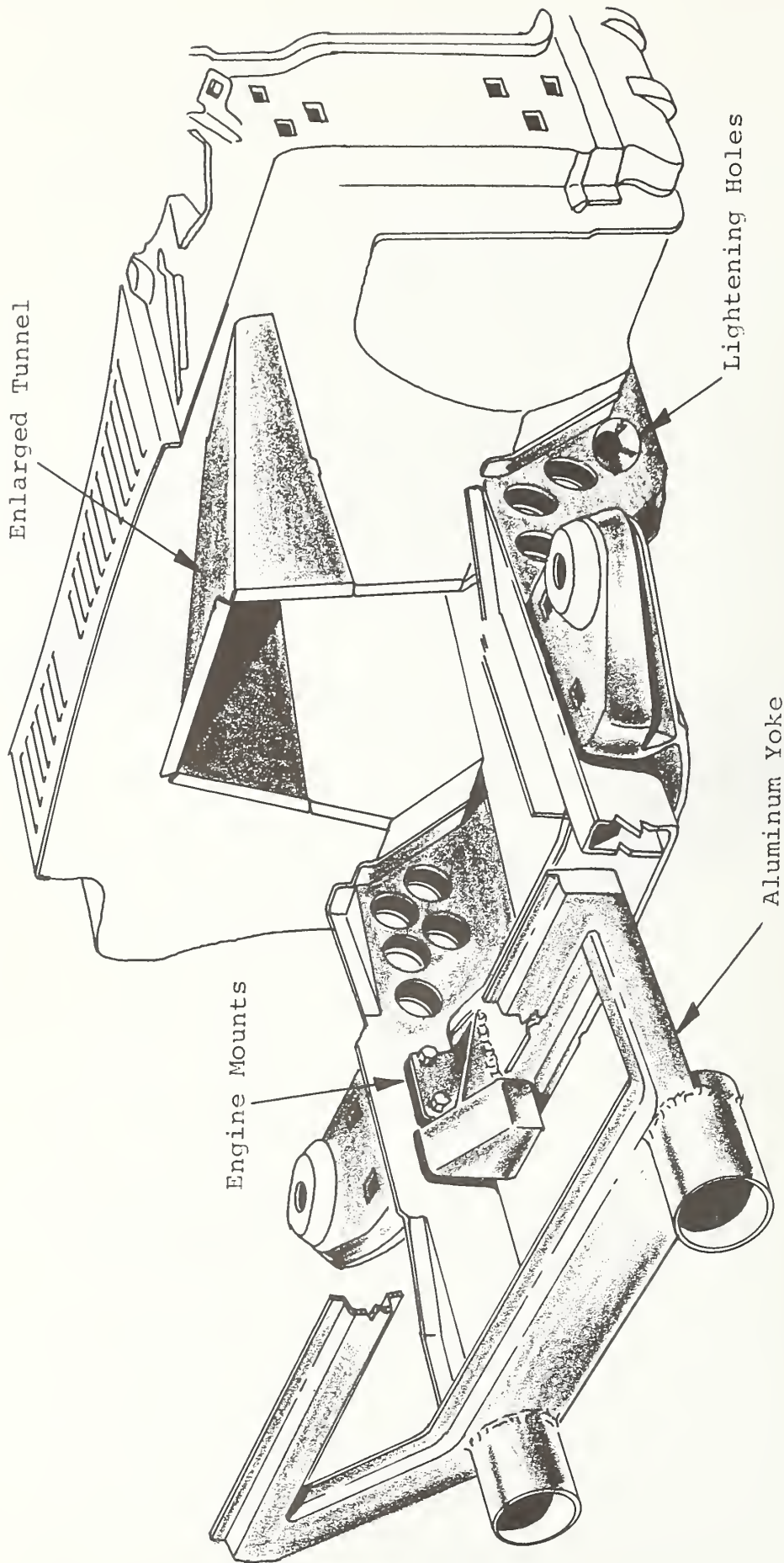


FIGURE 3.17 FRONT LOWER STRUCTURE FOR TEST ARTICLE D4

frame member by shear bolts, so that the engine, cross member, and wheels could be driven under the compartment while the frame member collapsed to a minimum volume.

The configuration of D5 increased the tunnel volume to accept the rearward stroke of the engine. The production lower frame member was cut away in the form of a "Z" shaped plastic hinge and then resupported by radius tubes to the plenum area (Figure 3.18). The lower frame was extended with short tubes forward of the reinforced core support. This configuration should maximize the stroke lengths. The "Z" section was to fail immediately after the 10-mph bumper units were stroked, thereby bringing the lower frame, engine, and front wheels under the compartment with the assistance of the pivoting radius tubes.

Test D4 was a 40-mph frontal barrier impact. The upper structure behaved as predicted with a crush of 22 inches. The lower structure, which consisted of weakened stock frames, penetrated the firewall and may have been a hazard to the legs of the occupants. The engine-cross member assembly separated from the frame but did not drop. The driveshaft probably prevented engine movement, indicating a need for a design with a breakaway driveline. The test demonstrated a satisfactory design for the upper structure. The lower structure, however, must be prevented from penetrating the firewall.

Test D5 was a 40-mph 30° barrier test. The vehicle impacted left side first, crushing the upper structure to a 30° angle. The vehicle remained parallel to its original velocity vector during the early portion of the crush, sliding parallel to the barrier. Then the left wheel stuck in the plywood barrier face and the vehicle rotated parallel to the barrier. It came to rest parallel to the barrier about 6 feet from its initial impact point. As with Test D4, there was no pitch of the vehicle. The crush on the left side was 37 inches, and in the center it was 6 inches. The left A post moved 4.5 inches aft. The lower structure did not behave completely as desired. The Z section in the aft frame collapsed as predicted, but the radius arms did not rotate downward. Thus the engine did not deflect as

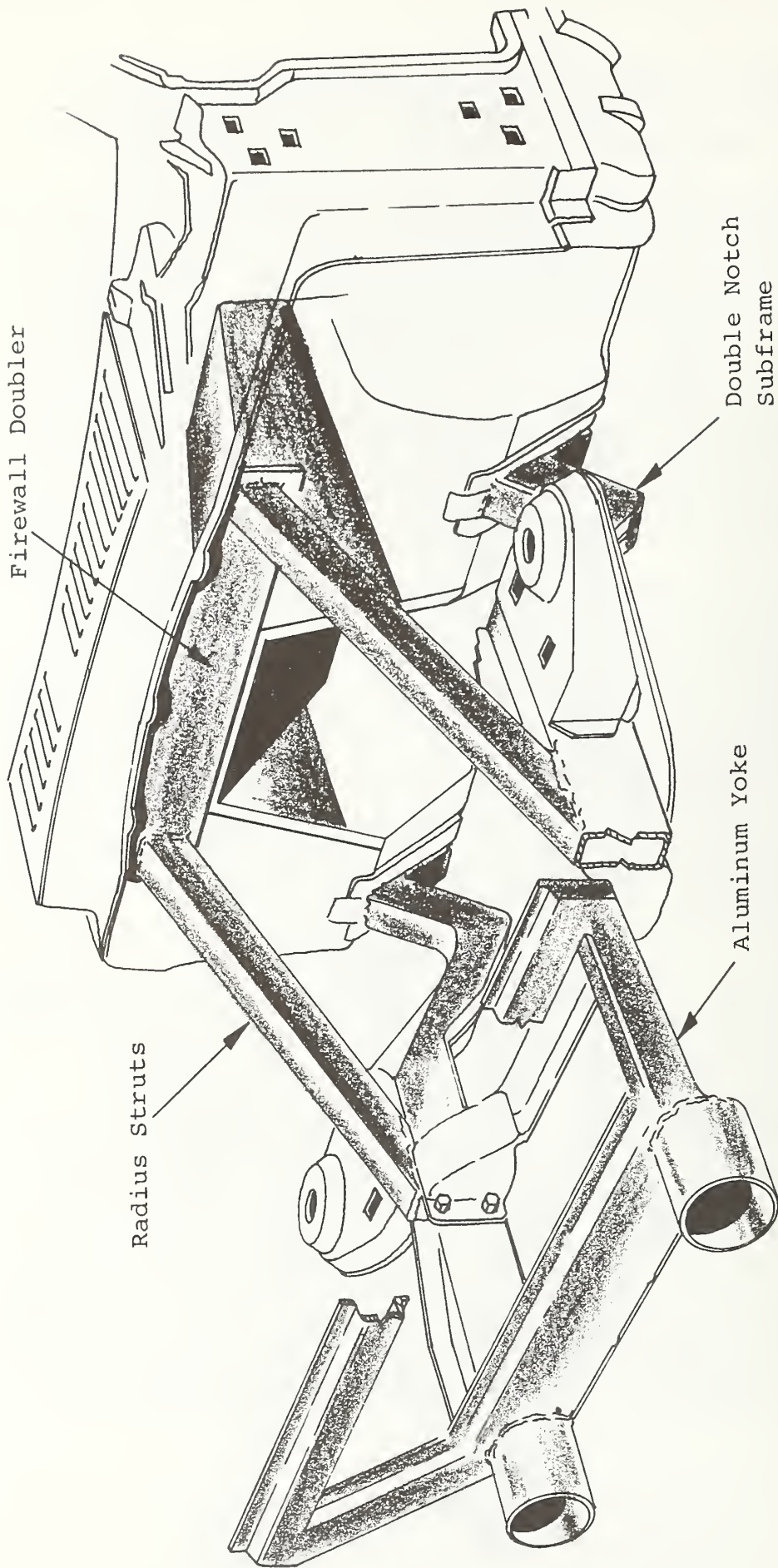


FIGURE 3.18 LOWER FRONT STRUCTURE FOR TEST ARTICLE D5

desired. Test D5 showed the suitability of the foam sheet-metal concept for angular loads; however, the design was still not adequate to guarantee survivability of the occupants. Crash pulses of D4 and D5 are shown in Figures 3.19 and 3.20.

### 3.2.6 Design of Evaluation Test Vehicles

The development tests discussed in Sections 3.2.3, 3.2.4, and 3.2.5 provided the necessary background to proceed with the design of the evaluation test vehicles. As the evaluation series of tests proceeded, it became necessary to alter the original design. Thus, there were a total of four front end energy management system designs. The fourth design was verified by Test E1B and frozen thereafter. The designs are referred to by the test designation number of the evaluation test: e.g., design E1 was the structure design used on the test hardware for Test E1. Table 1.4 lists the component modifications and the designs to which they apply.

The basic front structure was established for design E1. The upper structure configuration selected uses a foam-filled sheetmetal section. A preliminary section drawing is presented in Figure 3.21. The section is in two parts with the parting line as shown. The lower portion of the section comprises the inner fender panels and is rigidly attached to the firewall. The upper section is a hinged hood which opens from the front conventionally. Frontal load is transmitted directly down the member into the firewall. Oblique load is transmitted across the compression surface at the parting line, bringing the entire section into operation. The average frontal area of the design is 525 inches with an average dynamic crush strength of 48 psi; the total force carried by the upper structure was predicted to be 25,200 pounds. This corresponded to a desired force level from the computer run of 22,500 pounds. The discrepancy was considered to be within the accuracy of the estimate. The average crush strength was obtained from the bogey tests reported in Section 3.2.3. All sheetmetal was 3003-0 aluminum, .032 inch thick. The foam was 2 lb/ft<sup>3</sup> polyurethane.

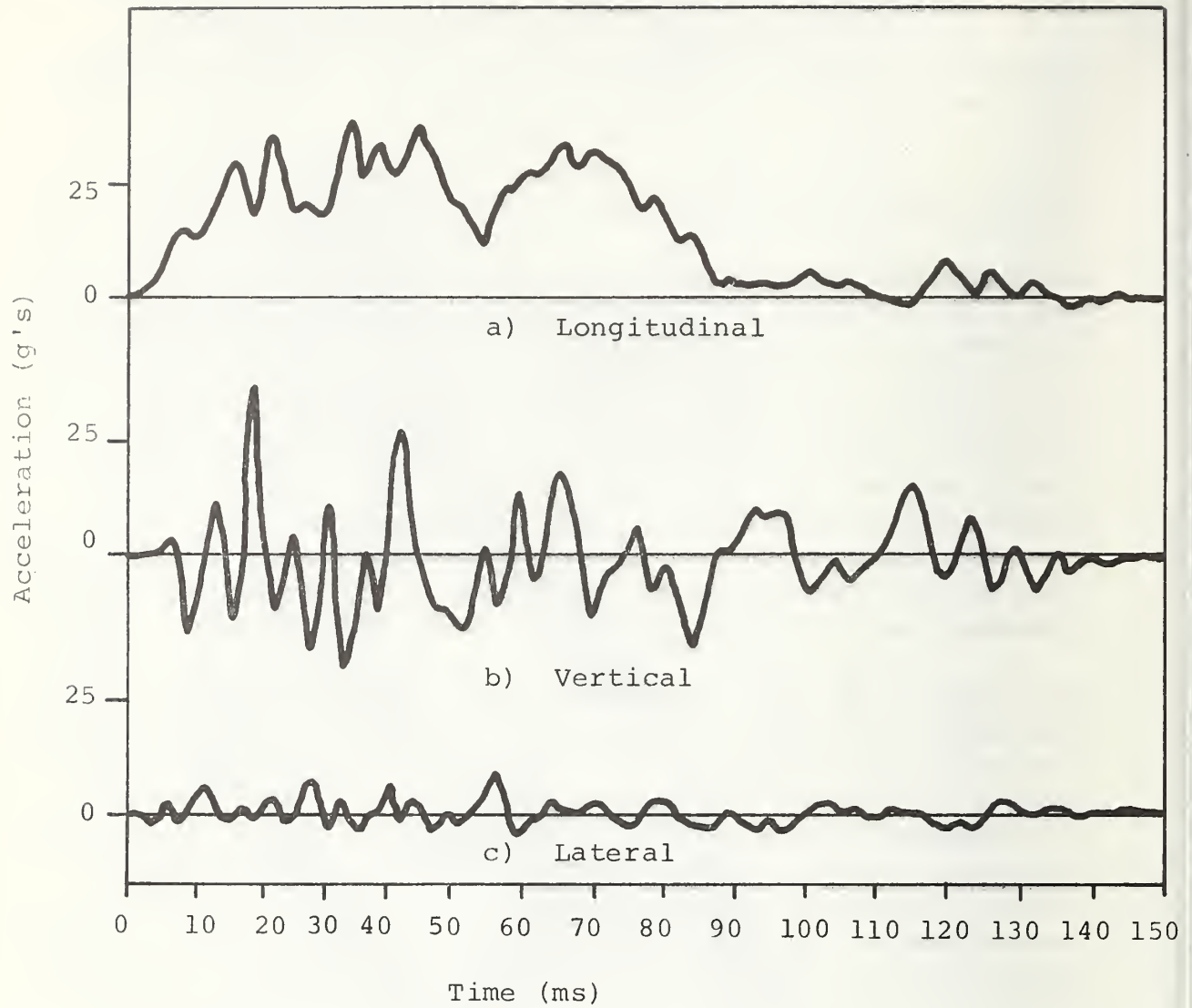


FIGURE 3.19 CRASH PULSE (D4)

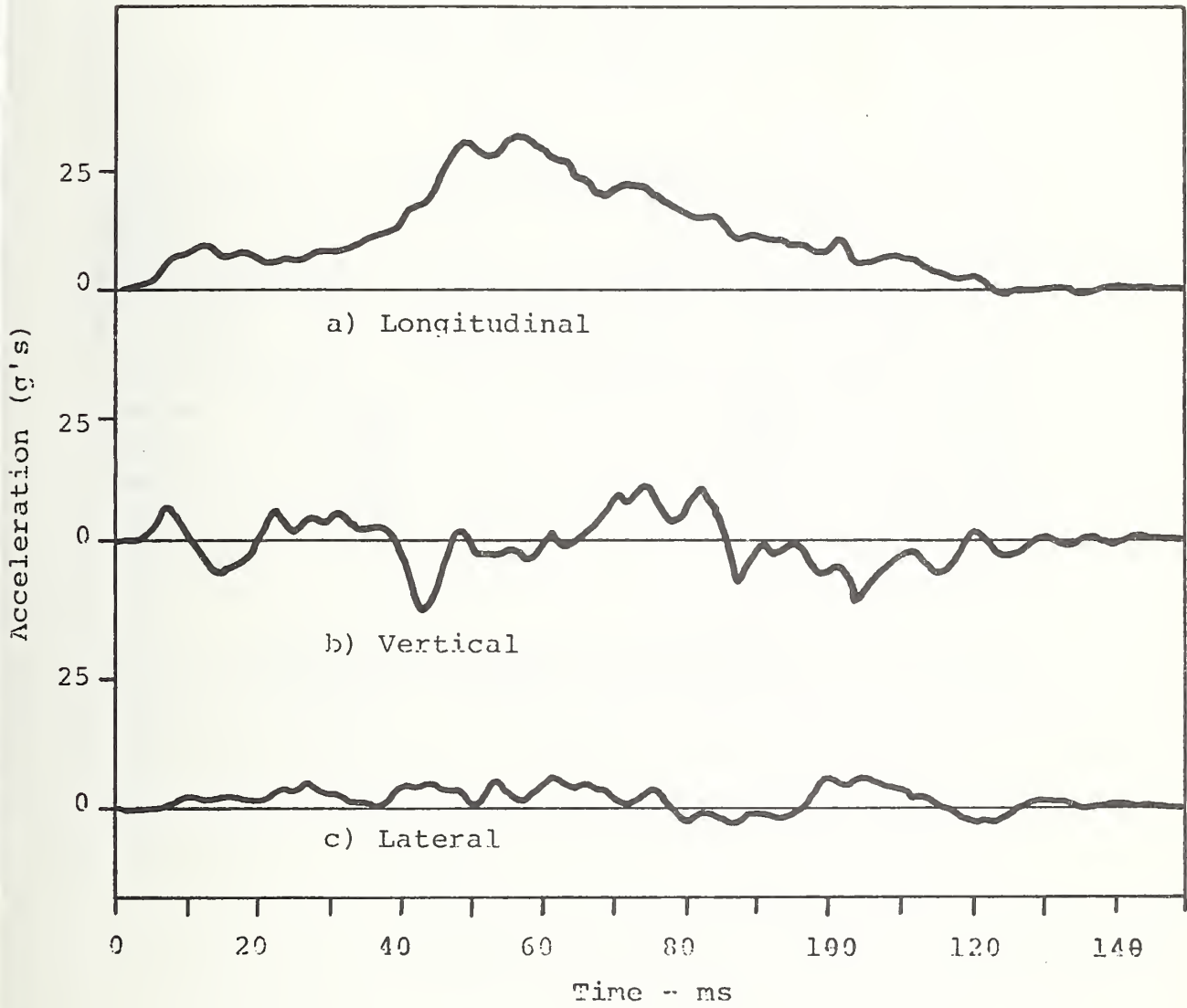
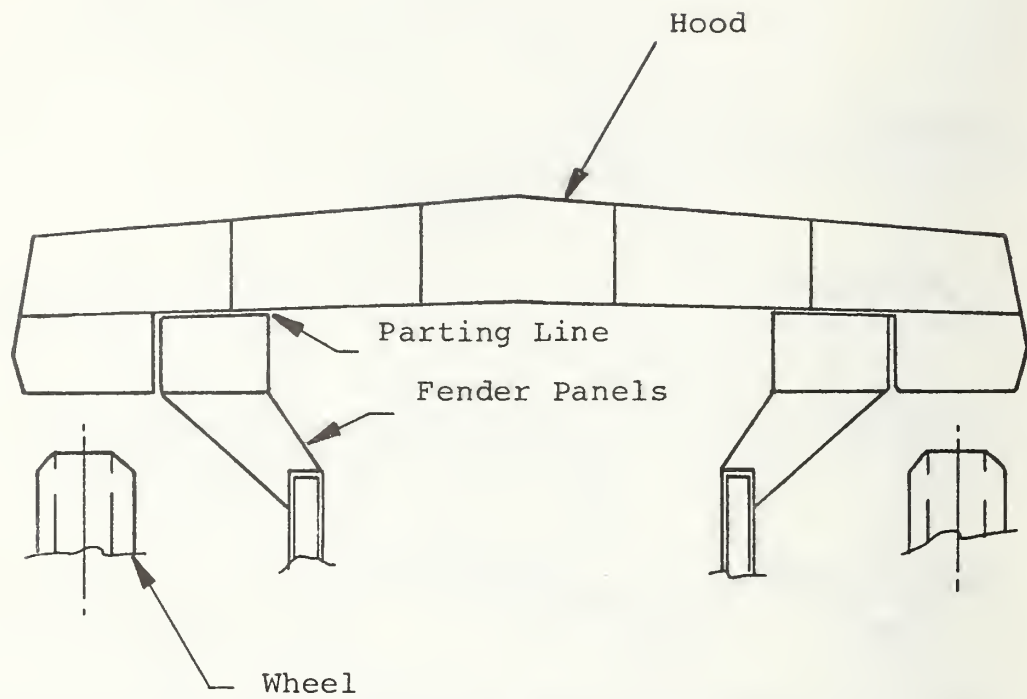


FIGURE 3.20 D5 CRASH PULSE



Section Through Vehicle at Wheel Centerline

FIGURE 3.21 SECTION VIEW OF MODIFIED UPPER STRUCTURE

The lower frame was a rectangular steel tube, 2 x 4 x .063 inches. The size and thickness were based on crush tests of various candidate tubes. The desired force level from the computer run is 20,000 pounds, while the tests indicate a total of 18,000 pounds from both sides. Additional support is provided by the connection to the inner fender panel along its entire length and by the weakened original aft frame. The first 6 inches of the foreframe deflection curve represent the 10-mph bumper units at a load of 17,500 pounds.

The engine/drive-train/suspension assembly breakaway mountings were effected by altering the firewall, engine mounts, transmission mounts, and driveline. The firewall opening at the transmission hump was raised 6 inches by raising the compartment with respect to the engine. The increase in height increases the horizontal distance before striking the firewall, while the slope of the transmission hump will push the engine down and under the compartment. The engine was removed from the frame and mounted to the cross member. The cross member was then mounted to the frame by a bolted connection designed to break at 5,000 pounds. All of the remaining structural load paths were unchanged.

The results of Test E1 indicated a need to modify the lower structure. For Test E1A, the bumper support tubes were increased to a thickness of .083 inches. The bumper unit slide bars were lengthened from 12 inches to 18 inches. The engine mounts were redesigned, and the toeboard area was sloped to enlarge the footwell region. The tunnel section was enlarged to facilitate engine movement.

For design E2, the major changes were the reinforcement of the A post by foam filling aft of the wheel well and rigidizing the plenum chamber by foam filling. The toeboards were also changed to the vertical design, and the engine mount reverted to the E1 design. The foam in the A post fender boxes was increased to 5 lb/ft<sup>3</sup> density.

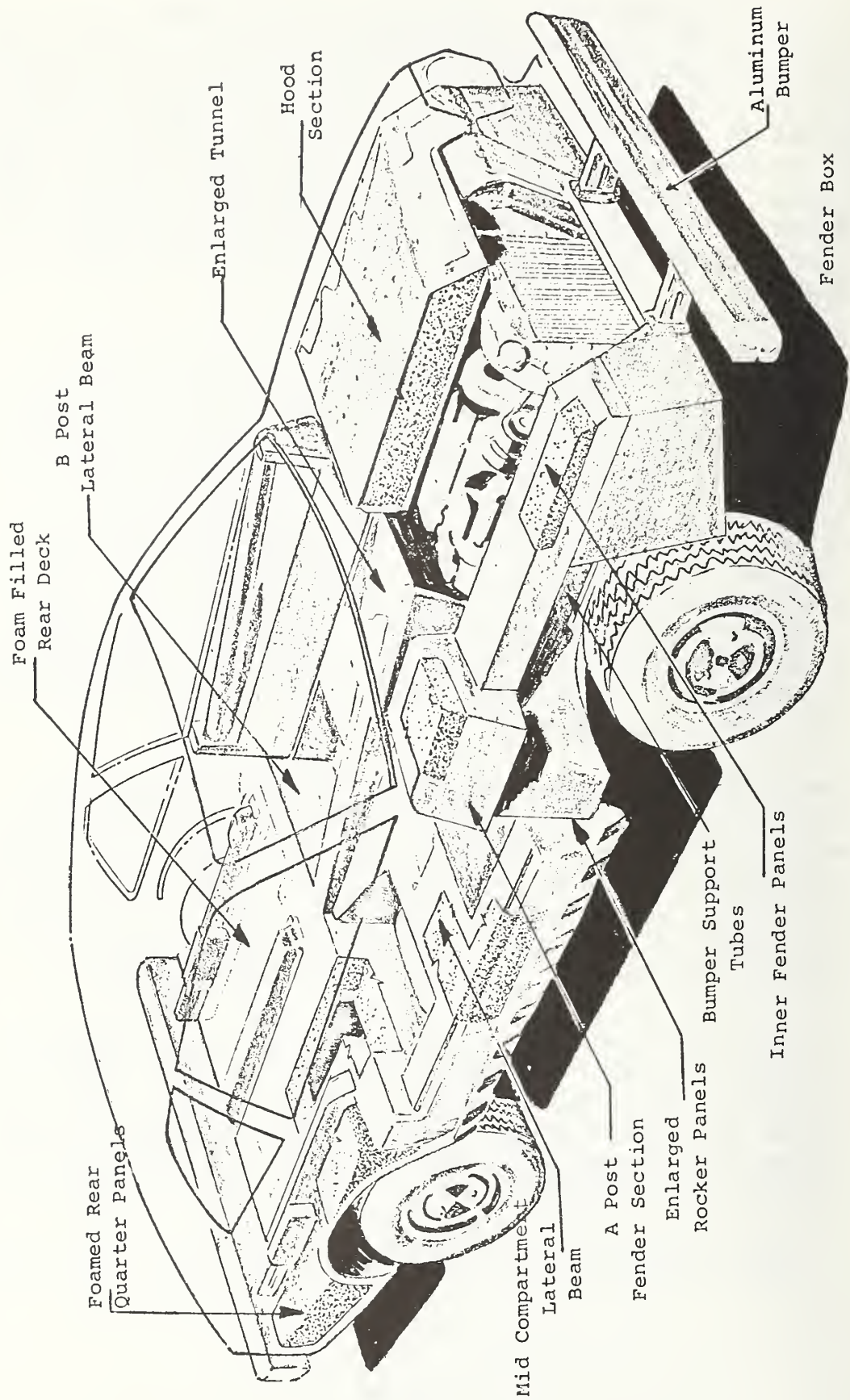


FIGURE 3.22 MODIFIED PINTO STRUCTURE

The design for E15 included the addition of foam-filled aluminum boxes forward of the tires. It was identical to E2 in all other respects.

The final design was mandated and frozen by contract change 3713-75-2582. The following modifications to the E15 design were required:

1. The stock aftframe between the cross member and the toeboard was removed and replaced with an equivalent section in the toeboard box. The bumper unit slider bars were shortened to the minimum possible length.
2. The foam in the wheel boxes, plenum chamber, and fender sections will be adjusted to a uniform density of 2 lb/ft<sup>3</sup>.
3. The B post support is to be strengthened by providing a 4-inch corner gusset to the B post lateral member.

It is appropriate at this time to discuss in detail each of the component modifications listed in Table 1.4. The complete drawing package has been submitted under separate cover, and therefore, the specific details of each design will not be reviewed. Refer to Figure 3.22 for identification of the structural elements.

1. Bumper Support Tubes - These are 4 x 2 x .083 steel tubes extending from under the toeboard area to the bumper. The portion of the tube forward of the cross member is preformed at the corners every 2 inches to encourage the crush tube type of failure. The 10-mph bumper units are mounted inside the tubes. The principle function of the tube is to provide elastic support for the bumper up to a 10-mph impact. Above that level it provides additional energy absorption by the crush tube mode of failure.
2. Inner Fender Panels - These are the foam and aluminum closed sections, inboard of the wheels and connecting the bumper support tubes to the hood section. The

skin is 3003-0 aluminum, .032 inches thick. The section is formed by intermittent welding and is riveted to the steel bumper tubes. The principle function is to provide energy absorption structure.

3. Hood Section - The hood is the main energy absorber in the upper structure. It is a closed aluminum volume with 3003-0 aluminum skin and filled with 2 lb/ft<sup>3</sup> polyurethane foam. Longitudinal baffles are riveted inside the outer shell to form nearly square individual elements. The exterior surface is intermittently seam welded. The hood is attached to the dash by the standard production hinges. The hood lips over the inner fender panels to form an interlocking shear connection. For production, a linear latch would be designed, but for test purposes the hood is held to the inner fender panels with widely spaced rivets. The structural portion of the hood has been recessed below the standard Pinto outline to allow styling of the vehicle.
4. Toeboards - The entire firewall and toeboard of the production vehicle is removed and replaced. The toeboards are closed box sections made of 18 gage cold rolled steel. The forward surface follows the general contour of the production vehicle. The aft (inside) surface forms a sloping toeboard as the forward portion of the foot well. A local stiffener is placed at the location of the bumper support tubes. The purpose of the modified toeboards is to rigidize the compartment and prevent excessive intrusions into the foot area.
5. A Post Fender Section - These are the portions of the fenders aft of the firewall back to the A post. They are closed and filled with foam. The primary function is to provide longitudinal support for the outer part of the hood. They also add rigidity to the passenger compartment.
6. Enlarged Tunnel Section - The production underbody was removed and replaced with an enlarged tunnel approximately 10 inches wide at the top and 18 inches wide at the bottom and 20 inches high at the firewall.

The new tunnel section is made of 18 gage cold rolled steel. The increased tunnel size is to provide space for the rearward movement of the engine-transmission assembly.

7. A Post Reinforcement - The lower portion of the fender just forward of the A post is closed and filled with foam. The modified section gives extra strength at the base of the A post.
8. Midcompartment Lateral Member - A closed box section (16 by 9 inches), extending from the rocker panels laterally to the tunnel, is placed under the front seats. The box is foam-filled and acts as the walls of the footwells. The purpose is to rigidize the compartment for lateral impact conditions.
9. B Post Lateral Member - A closed box section (7 x 9 inches), extending laterally across the compartment at the B posts, is placed under the forward edge of the rear seat. The section is bent up from 18 gage cold rolled steel and filled with 2 lb/ft<sup>3</sup> polyurethane foam. Its purpose is to add lateral rigidity to the compartment for side impact resistance.
10. Enlarged Rocker Panels - The production rocker panels are extended approximately 6 inches downward, closed, and foam-filled. This provides a rigid outboard member to carry the side loads by beam action and the longitudinal loads by compression.
11. Engine Mounts - The production engine mounts are removed from the subframes and mounted to the cross member. The cross member is attached to the subframes with a bolted breakaway connection. This allows the entire drivetrain assembly to act independent of the compartment mass. The ultimate crush limit for frontal impacts occurs when the cross member assembly bottoms at the boards.
12. Transmission Mounts - The production transmission mounts are removed and replaced with bolted breakaway attachments to the underbody of the vehicle.

13. Driveline Modifications - The production drive shaft is cut 14 inches forward of the differential. The rear section is replaced with a 2-7/8 by .05 inch tube riveted to the forward portion of the shaft. The rivets are designed to shear at 5,000 pounds and allow the drive shaft to slide inside the tube. Approximately 10 inches of free stroke is allowed before the drive shaft bottoms out on the end fitting.
14. Foam Fill the Plenum - The stock plenum chamber is filled with 2 lb/ft<sup>3</sup> polyurethane foam. This provides support for the center section of the hood. It becomes effectively a beam across the vehicle from upper A post to upper A post.
15. Fender Boxes - Closed aluminum boxes are added forward of the wheels and outboard of the inner fender panels. Their purpose is to provide additional energy absorption for the offset and oblique impact accident modes.
16. The remaining modifications are addressed to design conditions other than the front structure, and will be discussed in the appropriate sections of the report.

### 3.3 Frontal Barrier Impact

#### 3.3.1 Baseline Impacts

##### 3.3.1.1 20 mph Frontal Aligned Barrier Baseline Test, 01

Baseline Test 01 was a 20-mph frontal barrier impact of a production model 1974 Pinto two-door sedan. The vehicle was prepared in accordance with the baseline test plan (Appendix A). The instrumentation was modified from the basic test plan definition to include six uniaxial accelerometers on the subframe in the engine compartment. These locations were selected in lieu of the vertical and lateral channels on three of the compartment accelerometers. The

purpose of the modification was to provide data for the determination of strain rate effect. Recorded data also included photographic coverage of the event. All instrumentation functioned properly during the test. The data is summarized in Table 3.5. The entire data package was presented in the test report included as an attachment to the December 1973 progress report. (An index of the baseline test reports is given in Table 1.1.) An overview of the photographic coverage is shown in Figure 3.23.

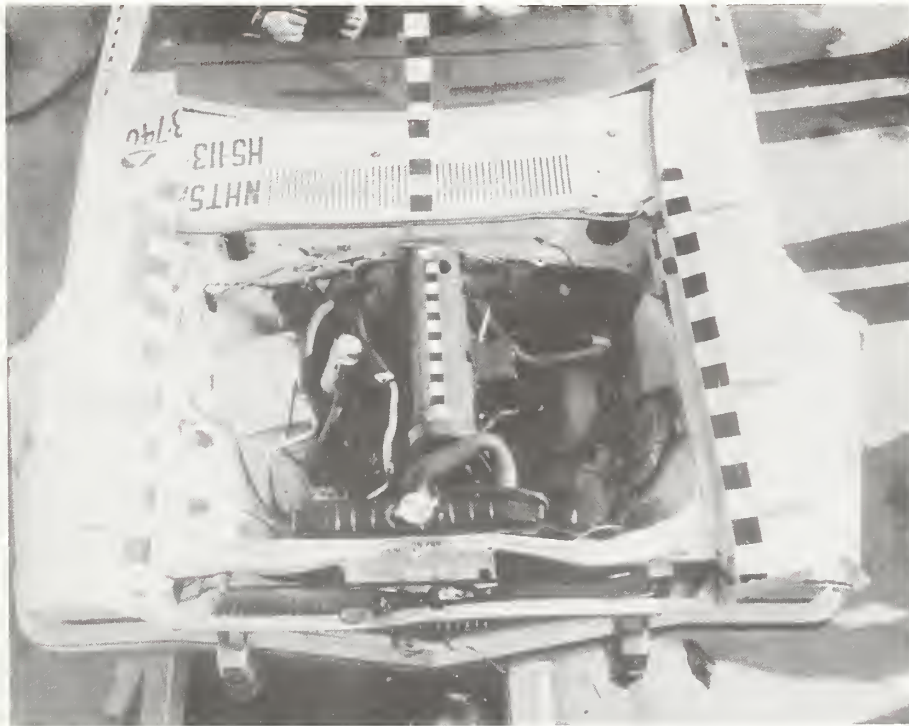
Structural Damage: Damage/deformation was confined to the front sheetmetal and forward bumper/frame substructure. The bumper energy absorbers had not completed their full stroke before the frame rails forward of the engine cross member began to deform. This bending, together with the compression of the structure in front of the engine and an engine stroke of approximately 1 inch, accounted for a static crush of 10.3 inches. Engine stroke was taken up by the engine mounts and driveline universal joints. There was no measurable damage to the engine cross member or steering system as a result of the foreframe deformation or engine stroking. Major visible damage was to the fenders, which were buckled and displaced rearward.

Passenger Compartment Intrusion: No observable change in passenger compartment configuration resulted from the impact. Belt/harness systems seemed to function as designed to restrain the dummies, and there was no measurable steering-wheel/column deformation or stroke. Slight door binding resulted from fender buckling.

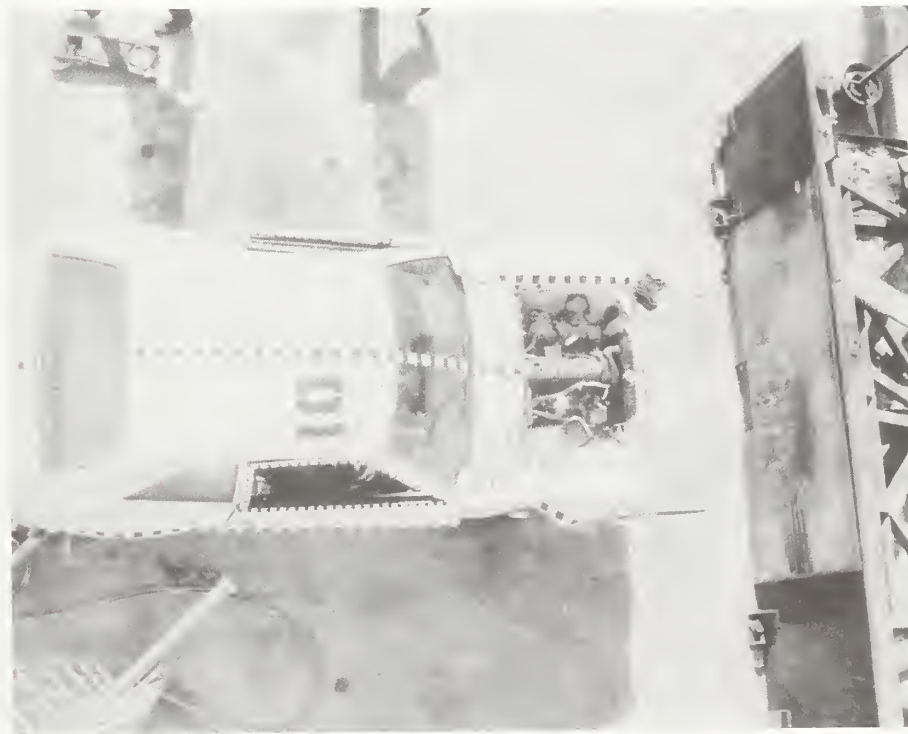
Vehicle Behavior: Impact velocity of 21.3 mph was somewhat in excess of the desired nominal velocity due to the difficulty of regulating towing energy at low speeds. Vehicle rebound reflected the fact that no braking systems were used and minimal front end damage did not lock up the front tires, so that the vehicle was still free to roll.

TABLE 3.5 BASELINE TEST DATA  
FRONTAL BARRIER TEST

	01	02	03	09
Test Date	11/30/73	12/3/73	1/9/74	3/27/74
Impact Velocity (mph)	21.3	40.1	30.9	48.7
Static Crush (inches)	10.3	29.0	21.0	33.8
Dynamic Crush (inches)	14.2	32.4	25.5	41.0
Pitch Angle (degrees)	3.0	14.0	5.5	14.5
A Post Movement	0.0	0.1	0.9	2.3
Peak Acceleration	19.9	30.0	27.2	38



A. Post-Test Engine Overhead



B. Post-Test Overall Overhead

FIGURE 3.23 BASELINE TEST NO. 001



C. Impact



D. Post-Test Driver's Side

### 3.3.1.2 40 mph Frontal Aligned Barrier Baseline Test, 02

Baseline Test 02 was a 40-mph frontal barrier test of a 1974 Pinto two-door sedan. The test was essentially identical to Test 01 (Section 3.3.1.1) except for the higher impact velocity. The data summary is given in Table 3.5, with the complete data package reported in the test report (December 1973 progress report). An overview of the photographic data is shown in Figure 3.24.

Structural Damage: Damage/deformation was severe throughout the forward two-thirds of the vehicle. The bumper energy absorbers were completely stroked, sheared from their frame mounts, and driven back to the cross member under the engine, where they deformed components of the steering system. The front subframe members were buckled both fore and aft of the engine cross member and suffered plastic bending where they joined the firewall, resulting in toeboard and firewall distortion. The front cross member, though it was moved rearward, showed little deformation and seemed to be, together with the engine block, the strongest front-end structure. As a result of the high impact energy, the "soft" structures in front of the engine were completely crushed, and the block itself struck the barrier, with the resulting high force level exerted on the entire drivetrain. The motor mounts were displaced inward and to the rear, and the engine block was pushed a significant distance into the firewall. The bell housing was cracked in several places and the transmission moved down and to the rear to such a degree that the transmission vibration damper struck the ground. The differential showed noticeable damage, with the right leaf spring and shock absorber bent and the left axle tube broken on the inboard end. Firewall deformation was marked, due to the engine and front frame bending. Front end sheetmetal deformation was severe, with the fenders being buckled and sheared from the wheel wells and associated inner panels. In addition to the frame bending at the firewall, a line of lateral bending developed immediately behind the front seats, resulting in door frame distortion, roof buckling, and passenger compartment deformation.



A. Impact



B. Post-Test Driver's Side

FIGURE 3.24 BASELINE TEST NO. 002



C. Post-Test Engine Overhead



D. Post-Test Overall Overhead

FIGURE 3.24 CONT'D

Passenger Compartment Intrusion: Some compartment intrusion resulted from the impact. Although there was little deformation of either the A or B posts, firewall stroke and chassis bending near the B post caused both doors to jam tight. The toeboards were displaced rearward due to engine stroke and lower firewall buckling with associated front footwell buckling. Although the steering column was stroked only slightly, dummy "driver" impact deformed it up and to the left of the vehicle. The harness/belt system seemed to have limited effect on the dummy "driver," since the dummy struck the steering column with some force and was also allowed to contact the windshield header. The crash bolster on the dummy "passenger's" side seemed to have been of some benefit. Seat damage was most severe on the passenger side, possibly as a result of dummy rebound from the stiff crash bolster. Buckling was also in evidence in the rear footwells, due to chassis bending at that point.

Vehicle Behavior: Impact velocity of 40.1 mph was well within the desired nominal velocity range. Vehicle rebound reflected the fact that no braking systems were used; extensive front end damage locked up the front tires, so that the rebound was in the form of skid.

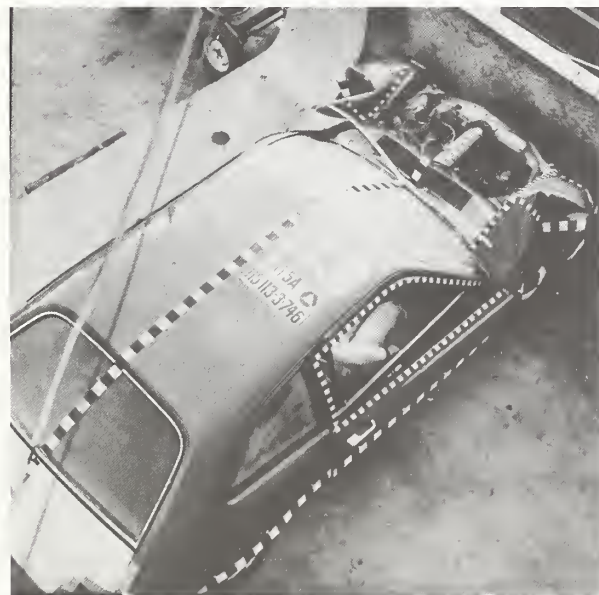
#### 3.3.1.3 30 mph Frontal Aligned Barrier Baseline Test, 03

Baseline Test 03 was a 30-mph frontal barrier test of a 1974 Pinto two-door sedan. This was similar to Tests 01 and 02. The instrumentation of the subframes was deleted from the final instrumentation in accordance with the baseline test plan. The data summary is presented in Table 3.5, with the complete data package presented as an attachment to the April 1974 progress report. Photographic coverage of the test is shown in Figure 3.25.

Structural Damage: Damage/deformation was concentrated in the front half of the vehicle. The bumper energy absorbers were completely stroked, sheared from their frame mounts, and driven rearward to the steering system. The front subframe members were severely deformed forward of the engine

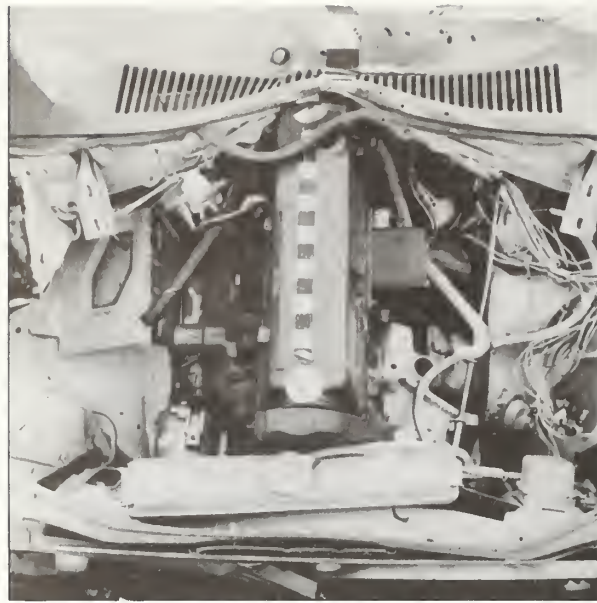


A. Post-Test Passenger's Side



B. Post-Test Overhead

FIGURE 3.25 BASELINE TEST NO. 003



C. Post-Test Engine Overhead



D. Post Test Dummy Position

FIGURE 3.25 CONT'D

cross member. The cross member showed little distortion but was displaced toward the rear. All "soft" structures ahead of the engine were completely crushed, and the engine itself was moved rearward into the firewall. Engine displacement was approximately 6 inches, producing significant deformation of the firewall itself, but, due to rotation of the engine, caused minimal driveline damage. Front end sheetmetal deformation was severe, with the fenders being buckled and sheared from the wheel wells and associated inner panels. The fender displacement also caused jamming of both doors; in the case of the right-hand door, forces were large enough to shear off the outer door skin.

Passenger Compartment Intrusion: Minimal compartment intrusion resulted from the impact. There was little deformation of either the A or B posts, even though the doors were jammed by sheetmetal crushing. The toeboards adjacent to the transmission tunnel were displaced rearward due to engine stroke into the firewall. The dummy "driver" hit the steering wheel with enough force to bend it down and toward the left door, preventing the column from achieving any significant stroke. The dummy "passenger" was allowed to go the full travel of the shoulder harness, where a rapid rotation into the dash was induced. Marked dash damage was sustained, and the rebound of the dummy "passenger" broke its seat.

#### 3.3.1.4 50 mph Frontal Aligned Barrier Baseline Test, 09

Baseline Test 09 was a 50-mph frontal barrier impact of a 1974 Pinto two-door sedan. This test was identical to Test 03 (Section 3.3.1.3) except for the higher impact velocity (48.7 mph). The data is summarized in Table 3.5, and an overview of the photographic coverage is shown in Figure 3.26. The complete test report is presented as an attachment to the April 1974 progress report.

Structural Damage: Damage/deformation was severe throughout the forward two-thirds of the vehicle. The bumper energy absorbers were completely stroked, sheared from their frame mounts, and driven back to the cross member



A. Side View



B. Overhead Engine Compartment

FIGURE 3.26 PHOTOGRAPHIC SUMMARY OF TEST 09

under the engine, where they deformed components of the steering system. The front subframe members were buckled both fore and aft of the engine cross member and suffered plastic bending where they joined the firewall, resulting in energy transfer into, and distortion within, the compartment. The front cross member was both bent rearward and displaced rearward by the movement of the engine and the buckling of the subframe and energy absorbers. Bending failure of this frame member resulted in severe toe-in of the front wheels. The engine was once again the "hard" member in the front end but showed considerably more displacement rearward into the firewall/plenum than had been seen in previous tests. As a result of the massive engine displacement, the entire driveline suffered severe damage. The bell housing was cracked in several places, and the transmission was moved down and to the rear to such a degree that the transmission vibration damper struck the ground. The differential showed noticeable damage, with both axle tubes bent and the universal joint broken. Firewall deformation was marked due to the engine stroke and front frame bending. Front end sheetmetal deformation was severe, with the fenders being buckled and compressed toward the A post.

An interesting result of this test was that the vehicle rotated clockwise during the impact, due possibly to the slight displacement of the engine toward the right of the vehicle and uneven crush of the structural and sheetmetal components.

Passenger Compartment Intrusion: Significant compartment intrusion resulted from the impact. Although there was little deformation of either the A or B posts, firewall stroke and chassis bending near the B posts caused both doors to jam tight. Additional compartment damage resulted from the marked displacement of the engine. The transmission "hump" and the toeboards adjacent to it were severely deformed, and the driveline tunnel showed deformation along its entire length. Marked buckling of both the front and rear floor boards was also noted. Although the steering column was stroked only slightly,

the high-speed movies revealed that the column was displaced rearward into the dummy "driver." Then the column moved to the left when the dummy hit it. This displacement occurred early enough in the event to allow the driver's head to strike the dash. The crash bolster on the dummy "passenger's" side seemed to have been of little benefit. This is probably due to the dummy submarining under the restraint. Seat damage was most severe on the passenger side, possibly as a result of dummy rebound from the stiff crash bolster.

#### 3.3.1.5 Discussion of Baseline Tests

These baseline tests served two functions. First, they provided a standard of performance for comparison with the modified design. Second, they yielded valuable insight into the behavior of vehicles and possible modifications for improvement of crashworthiness. The critical parameters of dynamic crush, static crush, peak acceleration, and pitch angle are given in Table 3.5; crush data are plotted in Figures 3.27, acceleration in 3.28, and pitch angle in 3.29. Figure 3.30 compares the accelerations recorded at the trunk for these baseline tests.

From the data, it is apparent that the baseline Pinto shows good crashworthiness in the frontal barrier impact mode up to a velocity of 40 mph, and except for intrusion up to 50 mph. This is in close agreement with the compatibility studies, which indicated a limit of 53 mph. The major concern for the Pinto sedan in this mode of accident is the large pitch angle and compartment intrusion. The pitch angle reached a maximum value of 14 degrees at 40 mph and did not increase significantly at 50 mph. The intrusion, as measured in the toeboard area, reached a maximum value of 7 inches at 40 mph. At 50 mph the intrusion was 5 inches, but the data is questionable.

The dynamic crush of the baseline vehicle is approximately linear with respect to velocity up to 50 mph. The static crush is linear up to 40 mph, then flattens out between 40 and 50. The change in static crush is due to increased

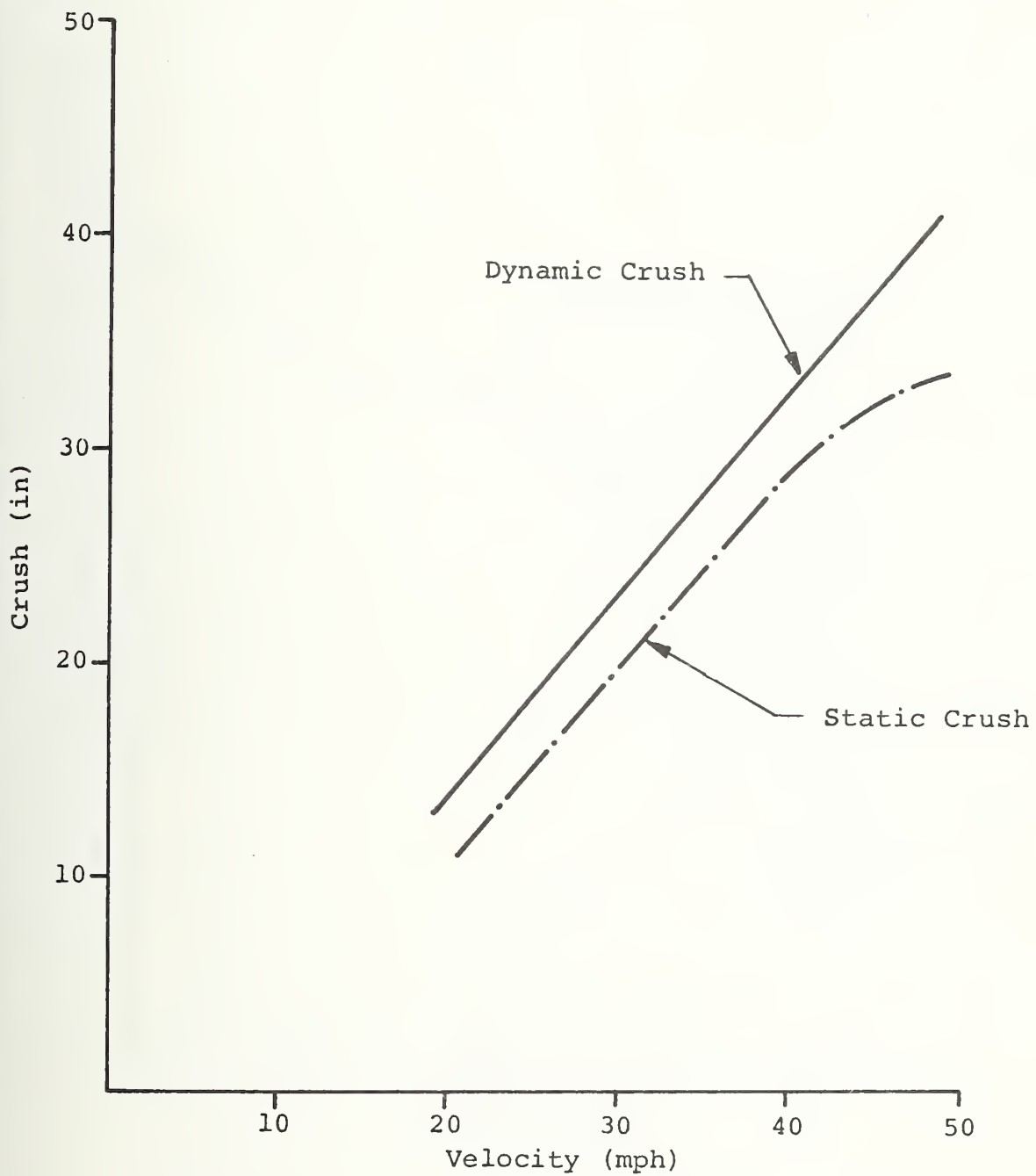


FIGURE 3.27 STATIC AND DYNAMIC CRUSH OF BASELINE PINTO AS FUNCTION OF VELOCITY



FIGURE 3.28 PEAK ACCELERATION OF BASELINE PINTO AS FUNCTION OF VELOCITY

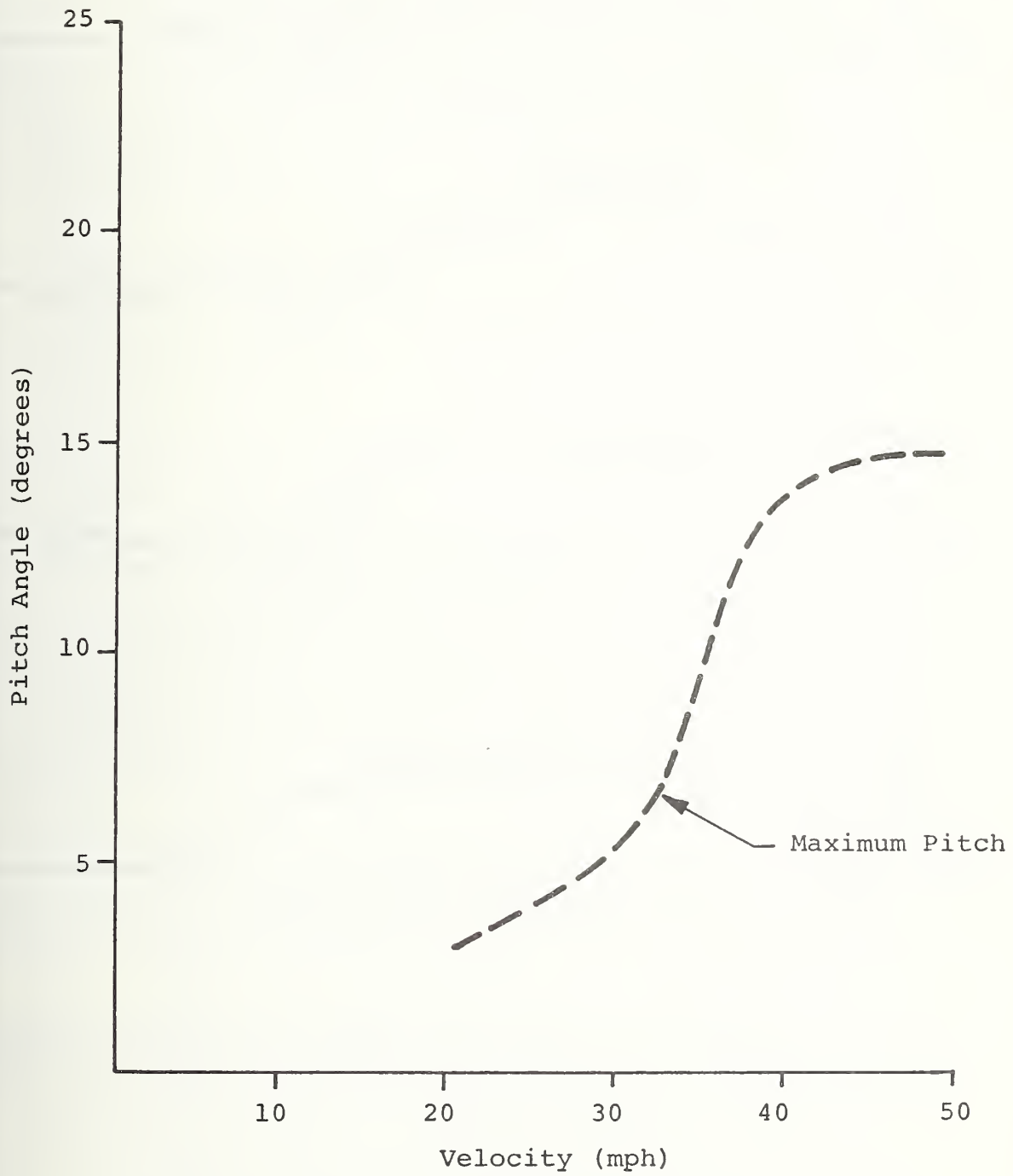


FIGURE 3.29 MAXIMUM PITCH OF BASELINE PINTO AS FUNCTION OF VELOCITY

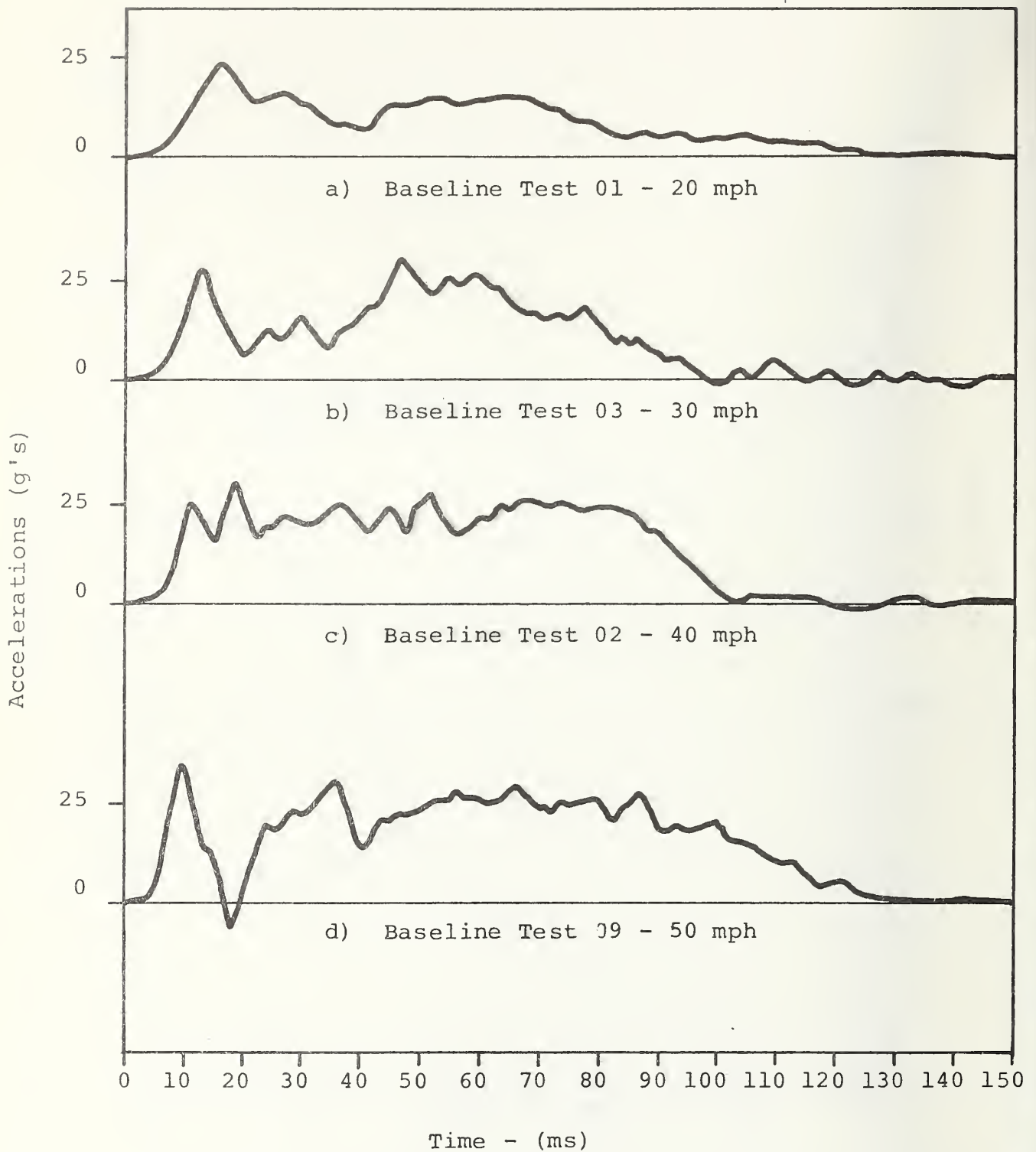


FIGURE 3.30 TRUNK ACCELERATION OF BASELINE FRONTAL BARRIER TESTS 01, 02, 03, 09

elastic energy stored as the structure becomes harder near the passenger compartment.

The peak acceleration measured at the trunk accelerometer shows an unusual curve. It is steep from 20 to 30 mph, then flat between 30 and 40 mph, increasing rapidly again above 40 mph. The shape of this curve is reasonable, since at 20 mph relatively little hard structure has been crushed. At 30 and 40, the crush is between the bumper and the firewall, with fairly constant force levels. Above 40, the firewall is crushed enough to stiffen and increase the acceleration level again.

### 3.3.2 Evaluation Tests

#### 3.3.2.1 50 mph Frontal Aligned Barrier Evaluation Test, E1

Evaluation Test E1 was the first test conducted on the complete front end energy management system. The design of the vehicle was discussed in detail in Section 3.2.6. The test was conducted in accordance with the evaluation test plan (Appendix C) with a nominal test velocity of 50 mph. Instrumentation consisted of the seven basic triaxial accelerometers, with five in the passenger compartment and one each on the engine and in the trunk. Photographic coverage consisted of four high-speed cameras, a real time camera, and 35 mm still photographs, both pre and post test. The actual test velocity was 48.7 mph.

The complete data package was presented in the test report as an attachment to the August 1974 progress report. A summary of the data is given in Table 3.6. An overview of the photographic coverage is shown in Figure 3.31.

Exterior Structural Damage: The major extent of the exterior damage was located forward of the A post. The bumper energy absorption units were completely stroked and behaved as predicted. The bumper itself was undamaged except for local deformation on the rear surface caused by the water-pump shaft. The frame sections started to form the desired collapse mode of progressive tube buckling. However, after 6 inches of crush, the bumper unit slider bars apparently

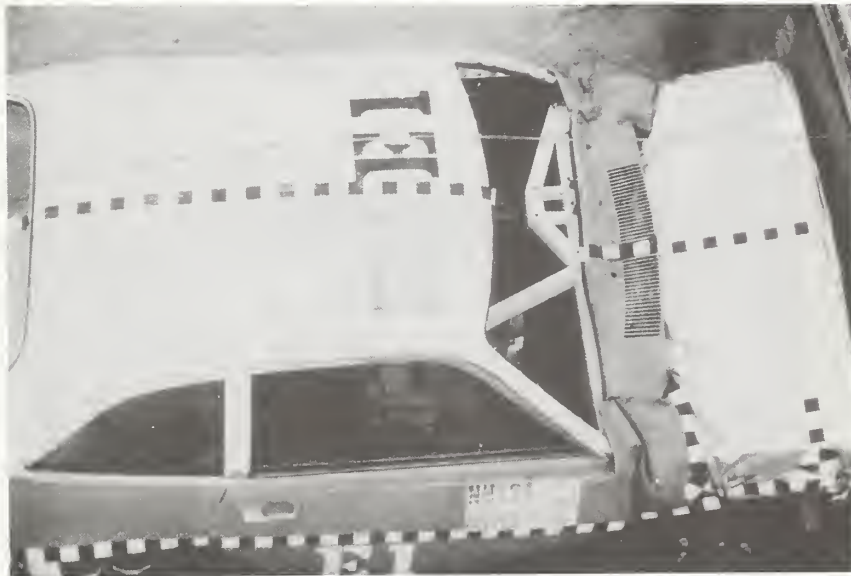
TABLE 3.6 BASELINE AND MODIFIED TEST DATA  
FRONTAL BARRIER IMPACT

	<u>09</u>	<u>EI</u>	<u>EIA</u>	<u>EIB</u>
Test Data	3/27/74	5/24/74	7/2/74	11/13/74
Test Description	50 mph	Frontal Barrier Impact		
Impact Velocity (mph)	48.7	48.5	49.3	50.1
Test Vehicle	Baseline 74 Pinto	Modified 74 Pinto	Modified 74 Pinto	Modified 74 Pinto
Static Crush (Inches)	33.8	38.5	37.3	35.2
Dynamic Crush (Inches)	41.0	39.7	38.3	Not Available
A Fast Movement (Inches)	2.3	0.8	1.8	0.8
Pitch Angle (Degrees)	14.5	-4.0	7	0.0
Peak Acceleration (g's)	38	48	36	44
Driver HIC	*	*	*	692
Driver Chest Accel (g's)	*	*	*	75

\* Data not taken per NHTSA

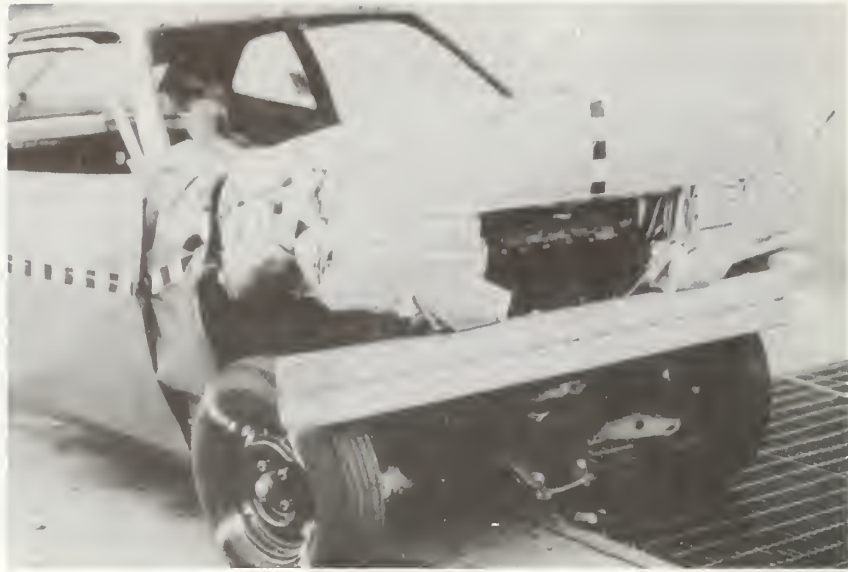


A. Post Test Side View

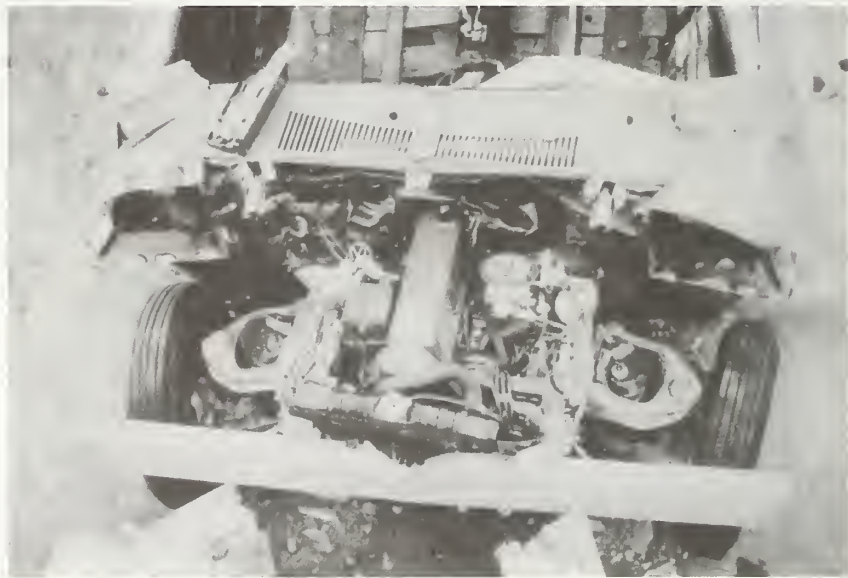


B. Post Test Overhead

FIGURE 3.31 PHOTOGRAPHIC COVERAGE OF EVALUATION TEST E1



C. Post Test Front View



D. Post Test View of Engine Compartment

FIGURE 3.31 CONT'D

glanced off a step in the tube wall at the cross member and caused a general instability failure. The forward portion of the tube bent inside and slid inside past the aft frame, forming an S shape. The engine supports and driveline separated as planned. The engine itself started into the enlarged tunnel section but contacted the firewall on the top. The hood and fender section collapsed as expected. The plenum chamber and firewall did fail in the center of the vehicle, due to engine impact. Total crush of the hood was 15 inches. One minor sheetmetal buckle formed in the roof section but was not pertinent to the final result. Sheetmetal deformation caused jamming of the doors and prevented opening. The doors themselves served their function of load transfer and structural rigidity.

Passenger Compartment Intrusion: Relatively little intrusion was noted in the passenger compartment. The toeboard area suffered some weld failures but moved relatively little. The tunnel section showed distortion and crush due to the engine impact, and the tunnel crush caused the floor boards to buckle. The ballast weight also caused local deformation of the front seat lateral member, but this is considered an anomaly of the test and not attributable to the vehicle design.

A comparison of the trunk acceleration of Test E1, the desired shape, and computer simulation is shown in Figure 3.32. The large peak acceleration occurring after 30 inches in Test E1 is due to the engine impacting the firewall. The pulse did not rise as rapidly as desired in the early stages of the crash. After 20 inches, the acceleration was 25 g's instead of the design value of 35 g's. Overall, the vehicle behaved acceptably.

#### 3.3.2.2 50 mph Frontal Aligned Barrier Evaluation Test, E1A

Since the design was modified after Test E1, a second 50-mph frontal barrier evaluation test (E1A) was conducted. The test was identical to Test E1, with the

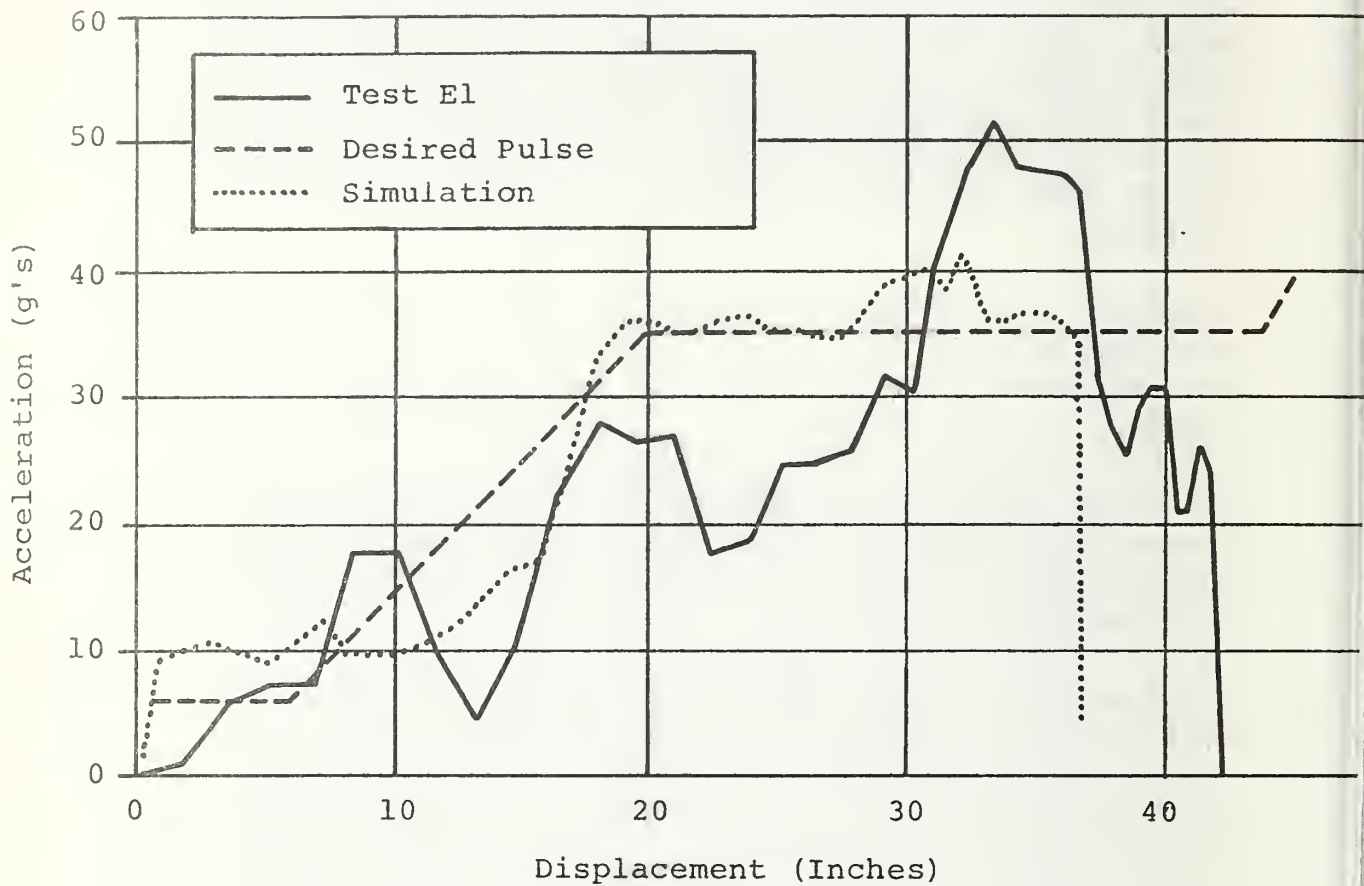


FIGURE 3.32 TRUNK ACCELERATION OF TEST E1 VS DESIRED PULSE AND SIMULATION

exception of the hardware changes discussed above. An actual velocity at impact of 49.3 mph was attained. The test results are summarized in Table 3.6, with the complete test report included as an attachment to the August 1974 progress report. Photographic coverage is shown in Figure 3.33.

Exterior Structural Damage: The total crush of the vehicle was 37.3 inches, including complete crush of the plenum chamber. The bumper units stroked as predicted, with the bumper itself undamaged except for local deformation on the back surface. The frame members formed three lobes of the desired accordion fold for approximately 5 inches of crush. They then bent upward in the middle with the bumper unit slider bars forced through the tube walls. The hood section crushed a total of 19 inches. It rotated with the front end rising and the firewall dropping. The fender section aft of the firewall bent downward. The engine cross member assembly broke free as desired, but the aft end caught the plenum and crushed it. The plenum, crushing under the engine impact, did not contact the restraint mounting bar. The doors did not suffer noticeable deformation, but sheetmetal damage prevented post test opening. Some minor sheetmetal buckling occurred in the roof.

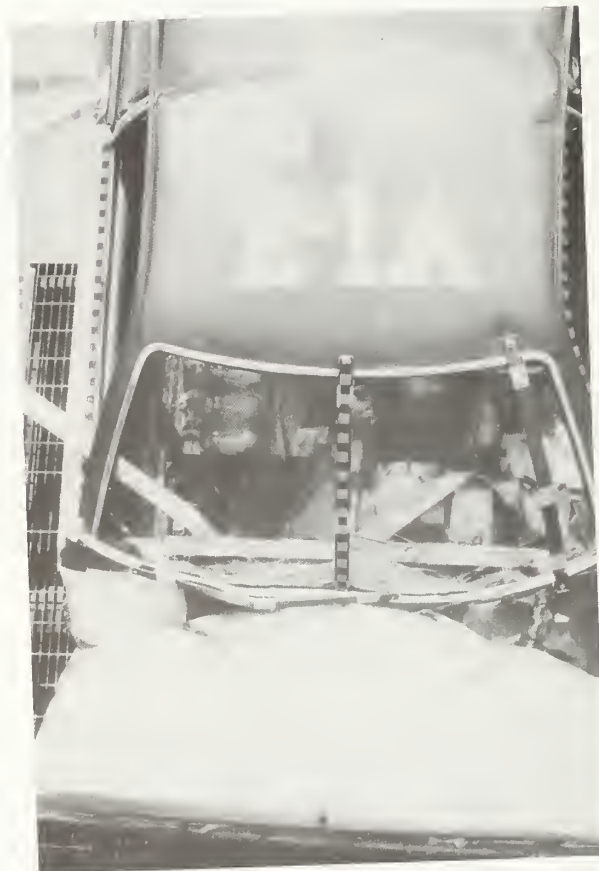
Passenger Compartment Intrusion: The upper A posts moved rearward 1.3 and 1.8 inches. The toeboard region suffered damage and intruded into the footwell, yet there was still sufficient room for the feet in the footwell. The movement of the toeboard caused a rotation of the driver restraint system. The tunnel buckled as it was pushed rearward by the engine. No damage was noticeable aft of the mid-compartment lateral member.

#### 3.3.2.3 50 mph Frontal Barrier Evaluation Test, ElB

This test provided data for the evaluation of the modified Pinto in the frontal aligned crash mode. The actual test velocity was 50.1 mph. A test of improved subcompact driver restraint was piggybacked on this test; results of that test were reported under contract DOT-HS-113-3-742.



A. Side View



B. Top View

FIGURE 3.33 PHOTOGRAPHIC COVERAGE OF EVALUATION TEST E1A



C. Driver Foot Well Area



D. Engine

FIGURE 3.33 CONT'D

To accommodate the restraint test, the test article carried a driver restraint system, instrumented driver dummy, and vehicle-mounted camera aimed at the dummy, in addition to items carried for the sake of the structural test.

The test vehicle carried seven accelerometers, five in the compartment and one each in the trunk and on the engine. Data were also gathered by five high-speed cameras, one real-time camera, and pre- and post-test stills. Automatic timers, terminal speed indicator, and an instant-of-impact indicator were also used. Test results were reported in the progress report dated November 1974 under this contract, and are summarized in Table 3.7. Photo coverage is represented in Figure 3.35. All equipment functioned properly except one left front compartment lateral accelerometer.

#### Structural Damage

The total static crush of the vehicle was 35.2 inches, including crushing of a large portion of the plenum chamber. The bumper units stroked as predicted, with the bumper itself undamaged except for local deformation on the back surface. The frame members formed 6 lobes of the desired accordion fold for about 8 inches of crush, then bent into S shapes. The hood section crushed a total of 17.25 inches and folded in the middle. The engine cross member assembly did not break completely free as desired, but the aft end stroked back to the footwells, causing an average deformation of 1 inch. The forward fender boxes drove the wheels aft, but some parallelogramming of the front end displaced the cross member so that the right front tire moved outboard of the rear fender section. This accounted for a difference in crush of 2 inches from one side of the vehicle to the other. The doors did not suffer noticeable deformation, and sheet metal damage was so minor as to allow post-test opening. Some minor sheet metal wrinkling occurred in the roof.

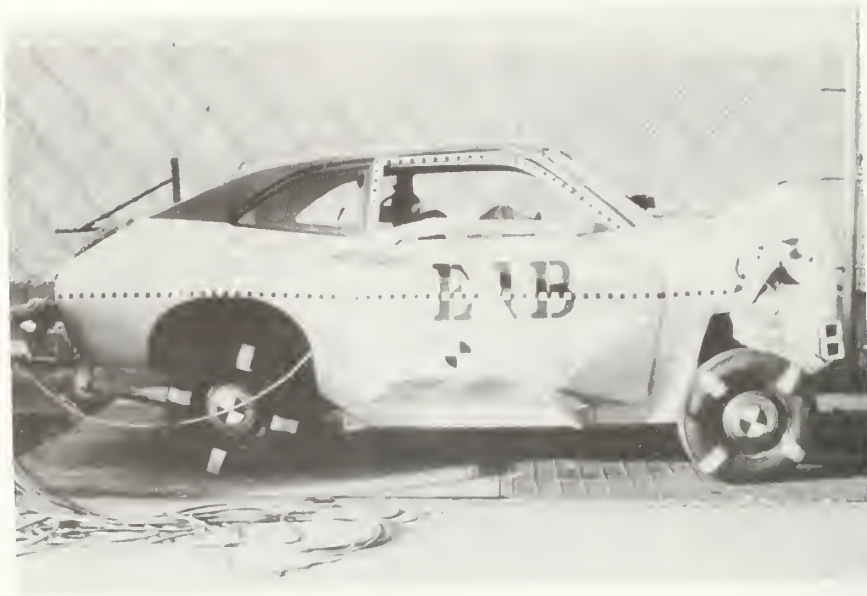
#### Passenger Compartment Intrusion

The left and right upper A posts moved rearward .5 and .9 inches, respectively. The toeboard region suffered less

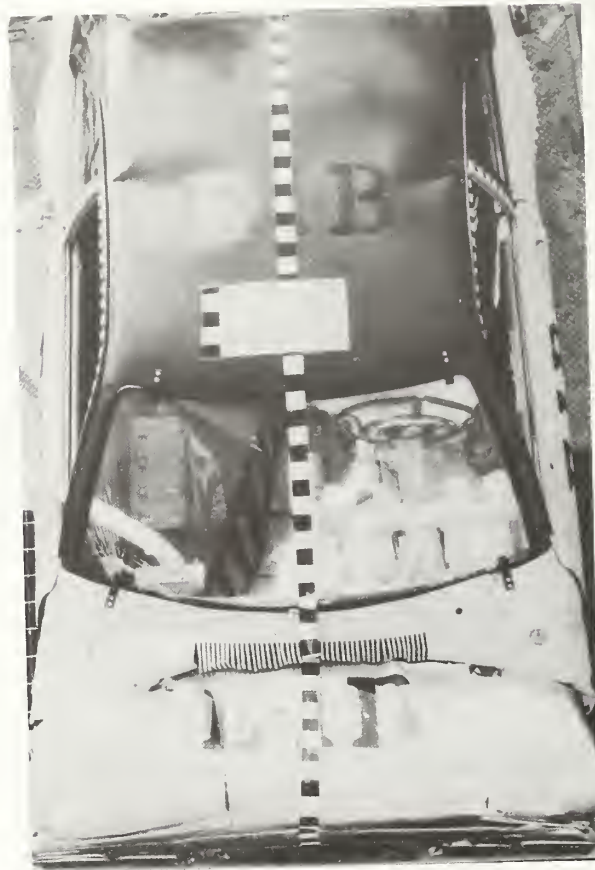
TABLE 3.7

PEAK LONGITUDINAL ACCELERATION OF E1, E1A, E1B, 09

<u>Location</u>	<u>E1</u> (g's)	<u>E1A</u> (g's)	<u>E1B</u> (g's)	<u>09</u> (g's)
Right Front Compartment	49	30	55	30
Left Front Compartment	49	35	60	40
Right Rear Compartment	53	35	45	54
Left Rear Compartment	51	33	63	50
Center Compartment	46	36	72	40
Trunk	48	36	38	44



A. Side View



B. Overhead View



C. Underside View

FIGURE 3.35 CONT'D

Discussion of Results: The comparison of the trunk crash pulses for E1, E1A, E1B, and Baseline Test 09 is shown in Figure 3.34. It can be seen that all these pulse shapes are similar. The intrusion levels are lower in the modified tests, E1, E1A, and E1B with three vehicles showing adequate living space. The acceleration levels are generally lower in the E1, E1A and E1B vehicles (Table 3.7) than in the baseline. The moderate value indicated by the trunk accelerometer for Test E13 may be misleading, since it is not consistent with readings at the other accelerometer locations. The results of Test E1A and E1B proved the crashworthiness of the modified Pinto for 50 mph frontal barrier impacts.

### 3.4 Frontal Aligned Subcompact-to-Standard Impacts

#### 3.4.1 80 mph Frontal Aligned Large Car to Small Car Baseline Test, 08

Baseline Test 08 was a nominal 80 mph frontal aligned impact between an unmodified 1974 Pinto and a 1968 Plymouth Fury sedan. The nominal velocity of 80 mph represents a barrier equivalent velocity of 50 mph.

Although the closing velocity is lower than the contract specifications, it was selected with CTM concurrence as more representative of the contract goals. The test was conducted in accordance with the baseline test plan. Both vehicles were instrumented with seven triaxial accelerometers in the standard locations. Photographic coverage included four high-speed cameras, 35 mm stills, and a real-time camera. The test data is summarized in Table 3.8. The dynamic crush and pitch data could not be obtained from the films due to lack of a fixed reference line. The complete data package was submitted as a separate report.

A comparison of the failure mode observed in the 50 mph barrier versus the 80 mph car-to-car (Test 08) yields the following conclusions:

1. The foreframe and sheetmetal follow the same collapse mechanism for both vehicles.

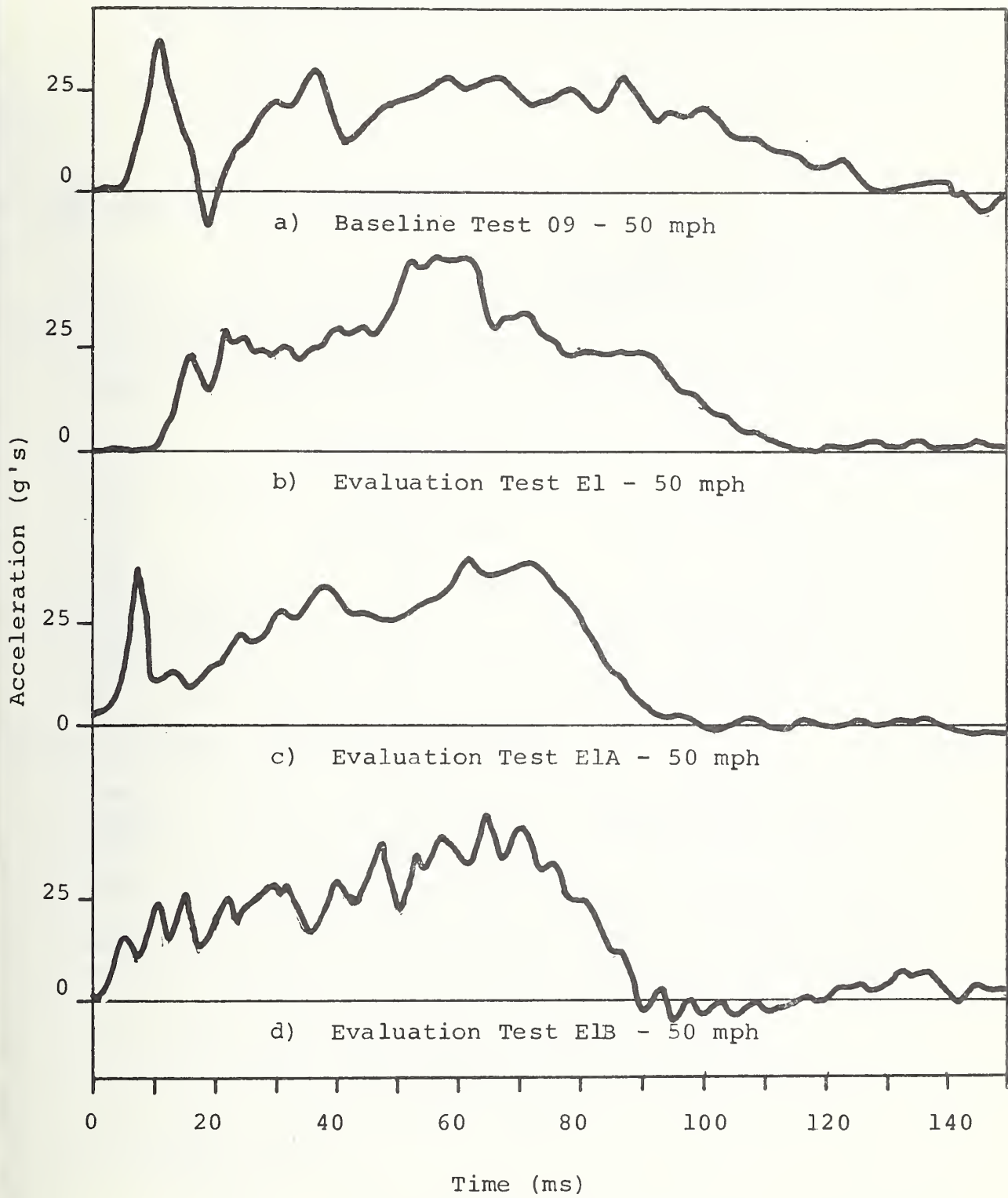


FIGURE 3.34 TRUNK ACCELERATION FOR FRONTAL BARRIER TESTS E1, E1A, E1B, 09

TABLE 3.8  
 BASELINE AND MODIFIED 80-MPH FRONT TO FRONT

<u>Test Description</u>	<u>Test 08</u>	<u>Test E25</u>
80 mph, Aligned large car front to subcompact front		
Test Date	Jan. 10, 1974	April 18, 1975
Impact Velocity (mph)	78.8	78.7
<u>Large Car</u>	'68 Plymouth	'74 LTD
Static Crush (in)	27.8	34.3
Peak Trunk Accel. (g's)	Not Available	30.1
A Post Movement (in)	0.0	0.4
Driver HIC	*	956
Driver Chest Accel. (g's)	*	Not Available
Passenger HIC	*	549
Passenger Chest Acc. (g's)	*	73
<u>Small Car</u>	Baseline '74 Pinto	Modified '74 Pinto
Static Crush (in)	31.0	30.8
Peak Trunk Accel. (g's)	43.1	56.1
A Post Movement (in)	Not Available	1.3
Driver HIC	*	563
Driver Chest Accel. (g's)	*	45
Passenger HIC	*	549
Passenger Chest Acc. (g's)	*	44

\* Data not taken per NHTSA direction

2. The aft frame is damaged more severely in the barrier test, indicating a higher load transfer through that member.
3. The firewall is more severely crushed by the engine in the car-to-car test.
4. The occupant survival space in the Pinto is adequate to about 50 mph BEV.

Based on this comparison, it appears that the two-car impact places a more severe condition on the lower frame and engine than a barrier impact with comparable BEV. The obvious difference is that the lower structure of the other car constitutes the major portion of the resistance.

#### 3.4.2 80 mph Frontal Aligned Large Car to Small Car Evaluation Test, E25

Evaluation Test E25 was conducted in accordance with Contract Modification 3. It included instrumented driver and passenger restraint systems. The other impacting vehicle was a 1974 Ford LTD at a nominal closing velocity of 80 mph. The cars were ballasted to yield a nominal BEV on the Pinto of 50 mph.

The vehicles were instrumented with two triaxial accelerometers, one in the trunk and one on the rear tunnel, two biaxial accelerometers, one on each side at the B posts, and a uniaxial on the engine. The dummies were instrumented with triaxial in the head and chest, and the Pinto driver also had instrumented femurs. Photographic coverage included five high-speed cameras, a real-time camera, and 35 mm pre and post test stills. The complete test report is presented as an appendix to the April 1975 progress report. The physical data is summarized in Table 3.8, with photographic data in Figure 3.36. The actual test velocity of 78.7 mph was well within acceptable limits.

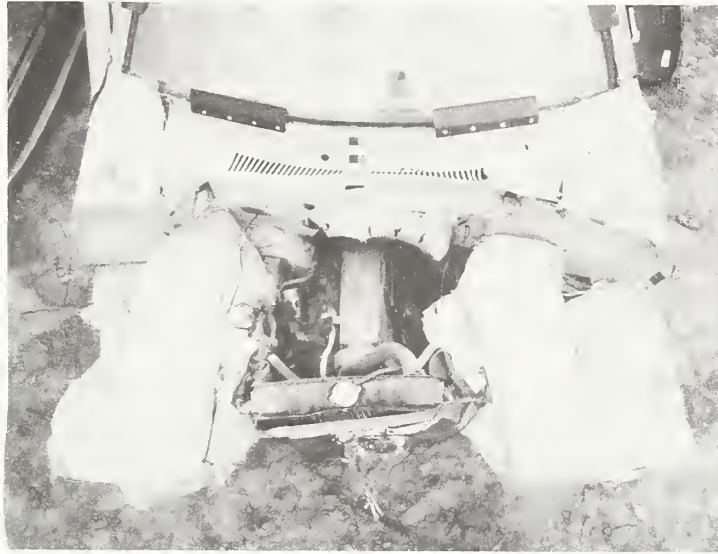


A. Post-Test Pinto



B. Post-Test LTD

FIGURE 3.36 PHOTOGRAPHIC COVERAGE  
OF TEST E25



C. Post-Test Damage Pinto Engine Compartment



D. Pinto Interior Damage

FIGURE 3.36 CONT'D

Exterior Structural Damage: The LTD struck the front of the Pinto aligned, resulting in almost 31 inches of static crush to the Pinto's forward structure, with slightly more distortion on the right hand side than on the left. The measurement of static crush is difficult because the interface between the two vehicles is so irregular. The Pinto appears to have overridden the LTD bumper assembly, forcing the lower Pinto structure -- the fender boxes, the inner fender panels, and forward frame tubes -- to absorb most of the energy. The engine stroked into the enlarged tunnel without striking the tunnel walls. The slightly higher deflections of the passenger side caused this door to be difficult to open, but the driver's door readily opened. The LTD also suffered a generally symmetrical frontal crush. Behind the A post, there was no evident damage.

Interior Compartment Damage: The interior of the Pinto remained essentially undamaged with the exception of minor aft motion, estimated at 2.3 inches, high on the firewall, and some localized buckling of the forward tunnel. No interior damage other than a collapsed upper and lower steering wheel rim and knee/dash contact was noted in the LTD.

Dummy Restraint Analysis: In Test E25, the Minicars wheel-mounted airbag driver restraint system, developed under NHTSA Contract DOT-HS-113-3-742, was installed in the driver position in the modified Pinto. On the passenger side, the airbelt restraint system, developed under NHTSA Contract DOT-HS-4-00917, was installed.

In this test, the modified Pinto underwent a change in velocity of 50 mph. Both restraint systems worked extremely well, with dummy injury measures substantially lower than the allowable criteria. Figure 3.37 shows the relationship between chest g's and crash pulse g's. In this figure, it is obvious that the restraints transmitted very low g amplification over the crash pulse g's, i.e., generally less than 1.0. The final post-crash position of the dummies was very similar to their pre-crash position.

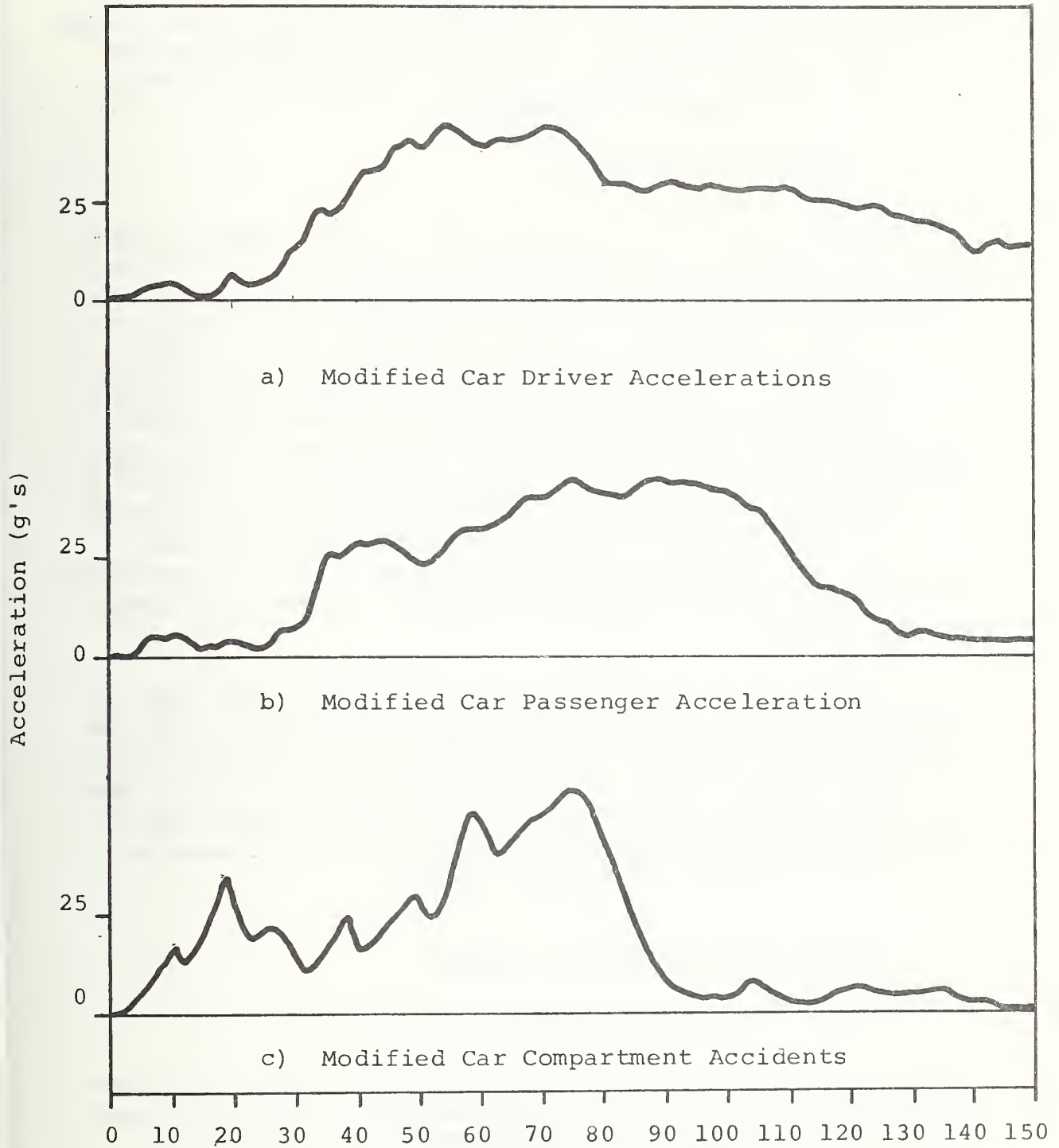


FIGURE 3.37 CHEST AND VEHICLE ACCELERATION FOR 80 MPH  
LARGE CAR - MODIFIED PINTO IMPACTS

A side-by-side examination of the head and chest traces of the driver and passenger of the LTD indicates a head spike of the passenger at about 100 milliseconds and a chest spike at about 65 milliseconds. These are more representative of a driver-wheel impact, and it is felt that these data sets may have become interchanged.

### 3.4.3 Comparison of Results

Figure 3.38 compares the crash pulses of the baseline and modified vehicles. The difficulty in drawing conclusions from the comparison is that the differences in "other" vehicles are reflected in the Pinto pulse. The compatibility study discusses in detail the effect of varying structures for the same total vehicle weight. It is seen that the pulse in the baseline vehicle hitting the 1968 Plymouth Fury reaches about 40 g's and falls rapidly, with the pulse essentially over by 120 milliseconds. On the other hand, the pulse of the modified vehicle when hitting the 1975 LTD reaches a higher level (~54 g's) but also has a shorter duration (87 milliseconds). It is interesting to note that the two crashes resulted in almost the same static crush.

The passenger and driver HIC's and chest SI's were completely acceptable in the Pinto, with HIC's of 563 and 549 and SI's of 677 and 658. The LTD passenger received a high HIC value of 1441. Based on the survivability of the occupants and the limited intrusion into the compartment, the modified design satisfied the contract requirements for head-on vehicle-to-vehicle crashes.

## 3.5 Oblique Barrier Impact - 50 mph

### 3.5.1 50 mph 30° Oblique Barrier Baseline Test, 10

Baseline Test 10 was a 30° oblique barrier crash of an unmodified 1974 Pinto sedan at a nominal velocity of 50 mph. The test was conducted in accordance with the baseline test plan. The vehicle was fully instrumented with seven triaxial accelerometers, and the photographic coverage followed the standard procedure. The test data is summarized

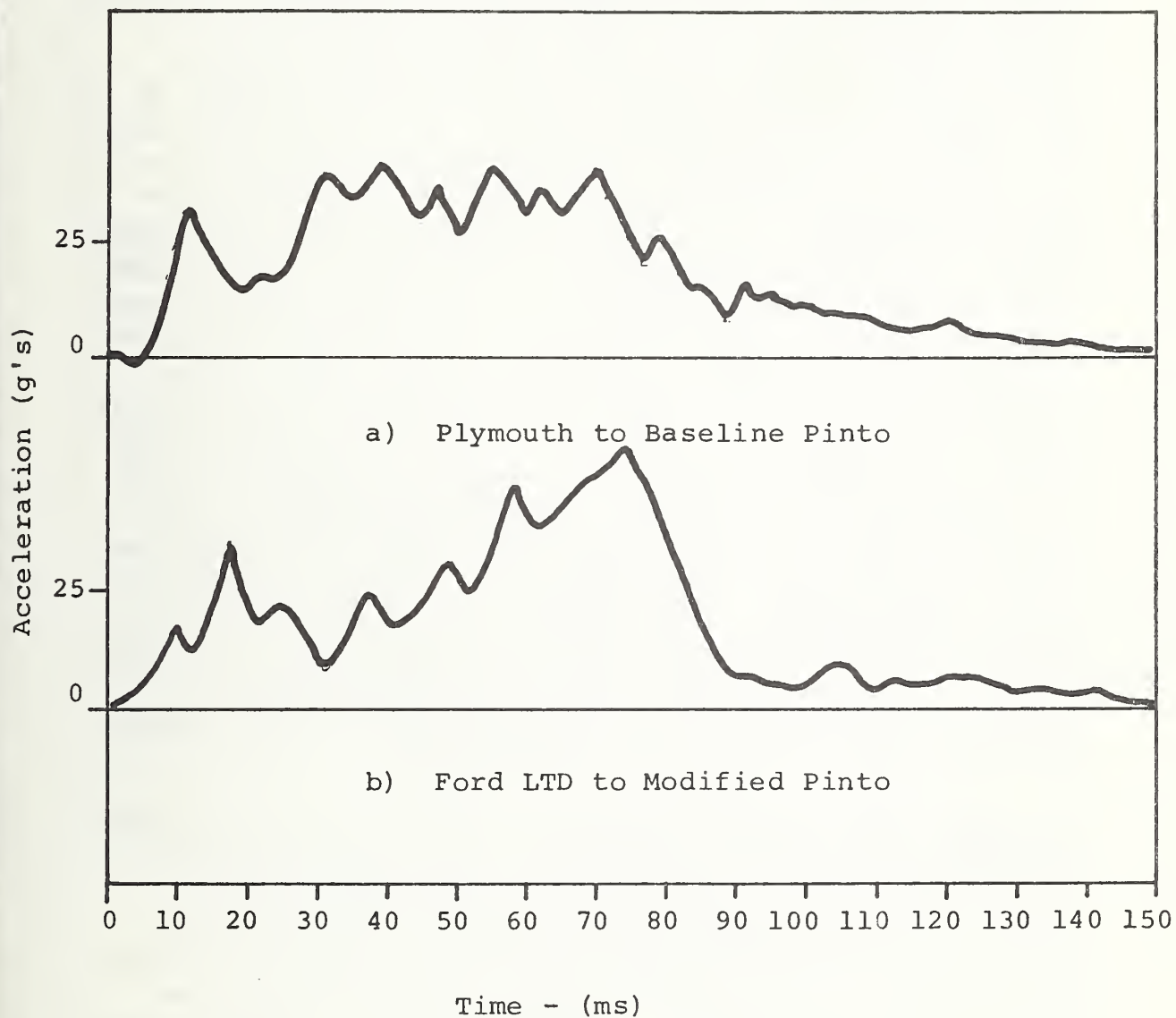


FIGURE 3.38 TRUNK ACCELERATION OF 80 MPH ALIGNED LARGE CAR TO SMALL CAR TESTS 08 AND E25

in Table 3.9, and the photographic coverage is shown in Figure 3.39. The complete test report was submitted as an attachment to the May 1974 progress report. Accelerations of Baseline Test 10 and Evaluation Tests E15 and E24 are compared in Figure 3.40.

Structural Damage: Damage/deformation was severe throughout the forward portion of the vehicle, with the most extreme damage being seen on the left, or initial impact, side. The bumper energy absorbers were completely stroked, sheared from their frame mounts, and driven back to the engine cross member. The front cross member was both deformed and rotated toward the left by the movement of the engine and the crush of the vehicle on the left side. The front subframe member on the left was buckled up to the firewall and was displaced inward, while the right-hand subframe was also buckled and bent around toward the left. As could be expected, the engine was moved to the right of the vehicle and showed considerable displacement rearward into the firewall/plenum. The entire driveline suffered severe damage as a result of the large engine displacement. The bell housing was damaged and the transmission was moved down and to the rear. The differential showed noticeable damage, with both axle tubes bent and the universal joint broken. Firewall deformation was marked due to the engine stroke and front frame bending. Front end sheetmetal deformation was severe on the left side of the vehicle and somewhat less so on the right. There was also buckling of the roof behind the windshield header. Rotation of the vehicle following impact was limited, probably due to the fact that much of the left side was in contact with the impact pad.

Passenger Compartment Intrusion: Significant compartment intrusion resulted from the impact, concentrated mainly on the left side of the vehicle. The right door was jammed due to deformation of the A post, while on the left the severe crush caused the door to split and open. Because most of the impact energy was absorbed by the left side of the vehicle, deformation of the toeboard and floor boards was most severe on that side. The dash on the left side was also displaced rearward a significant amount, reducing the available room for the dummy "driver."

TABLE 3.9

## BASELINE AND MODIFIED OBLIQUE FRONTAL BARRIER TEST DATA

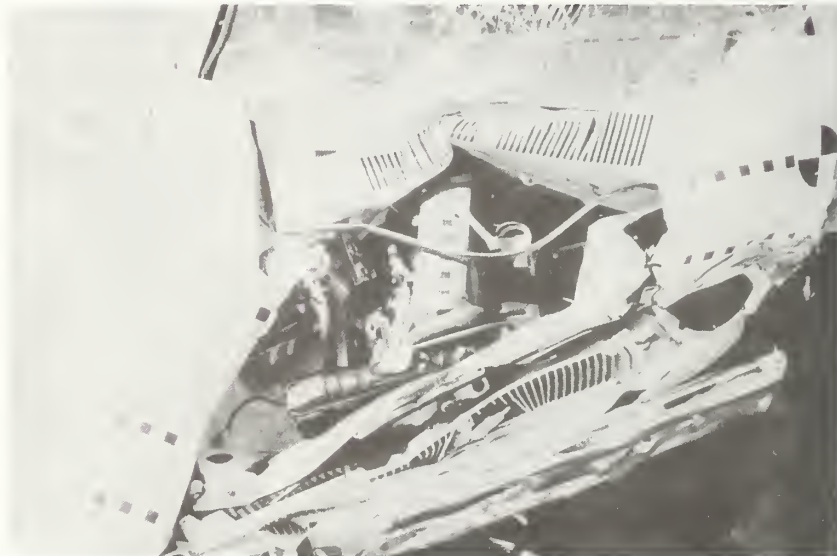
Test No.	010	E15	E24
Test Date	4/12/74	8/2/75	8/20/75
Test Description	330° Oblique Barrier Impact		
Impact Velocity (mph)	50.1	45.2	49.4
Impact Angle (degrees)	330	330	330
Static Crush (inches)	43.5*	45.2	50±
Pitch Angle, Max.(degrees)	36.3	-7.5	
A Post Deflection(inches)	5.5	1.7	.5
Peak Accel. (g's)	30	36	37
Post Impact Behavior		Rotate parallel	Rotate Parallel
Rebound	12.0"	to Barrier	to Barrier & Continue Travel
Driver HIC	**	**	187
Driver Chest Accel. (g's)	**	**	46

\* Crush measured on left side of vehicle.

\*\* Data not taken per NHTSA direction.

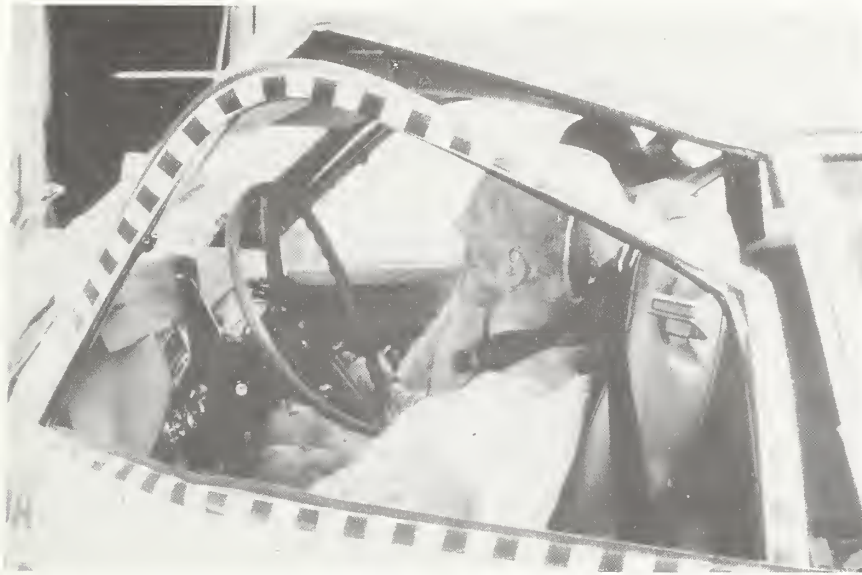


A. Post-Test Overhead

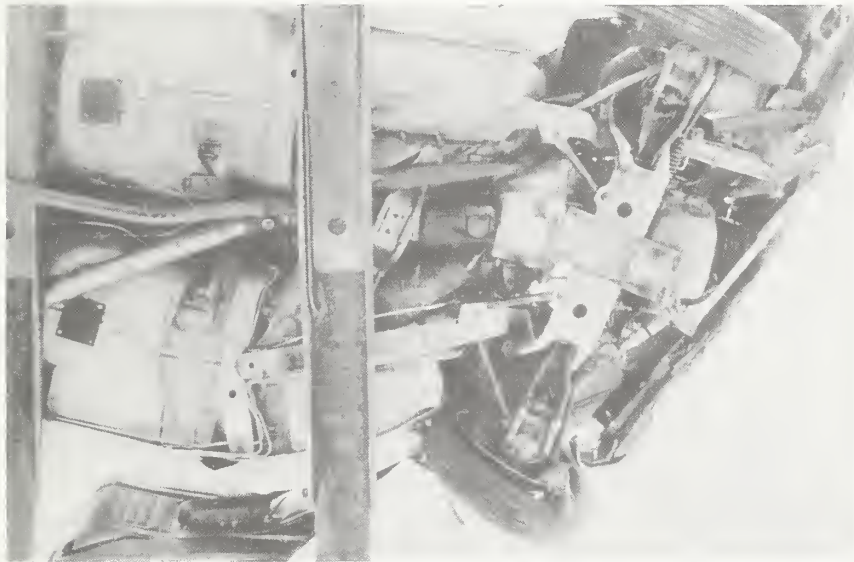


B. Post-Test Engine Overhead

FIGURE 3.39 PHOTOGRAPHIC COVERAGE OF  
BASELINE TEST 10



C. Post-Test Dummy "Driver" Position



D. Post-Test Front Underbody

FIGURE 3.39 CONT'D

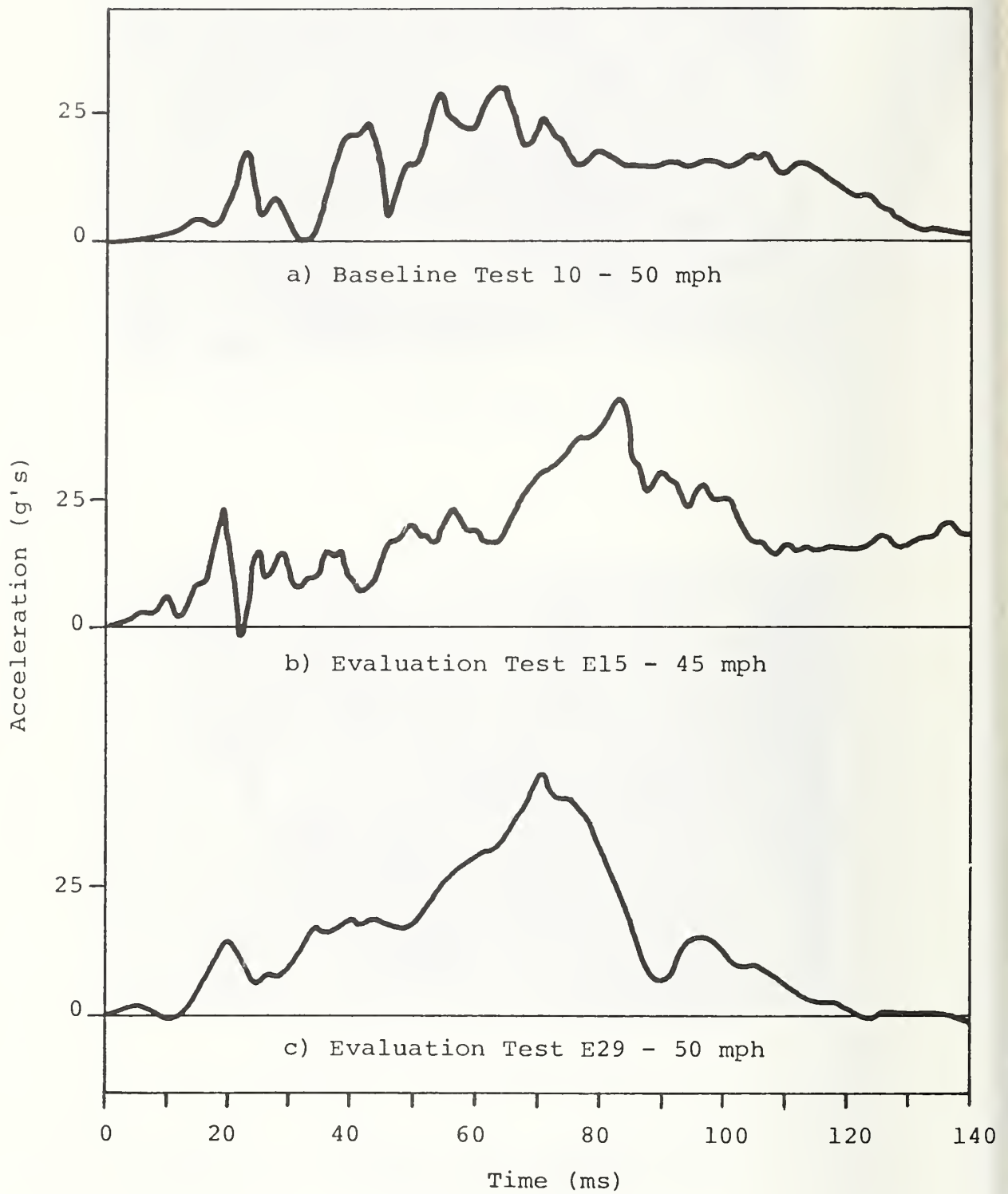


FIGURE 3.40 TRUNK ACCELERATIONS OF 30° BARRIER TESTS 10, E15, AND E24

### 3.5.2 45-mph 30° Oblique Frontal Barrier Evaluation Test, E15

This test was in support of evaluation of the modified design in the oblique frontal mode. Actual test velocity was 45.2 mph. The test vehicle carried seven accelerometers; test data are summarized in Table 3.9. Photographic coverage included high-speed and real-time motion pictures and pre- and post-test stills; photo coverage is summarized in Figure 3.41. Automatic timers, terminal velocity speed trap, and visual instant-of-impact indicator were also used.

#### Exterior Structural Damage

Most of the damage occurred forward of the firewall and along the left (impacted) side of the vehicle. The bumper stroked as desired on the left. The wheel box was crushed between the barrier and the wheel, forcing it over the wheel. The hood crushed approximately 12 inches before the wheel box and tire pushed it into a bending failure directly over the tire. The left lower frame started to collapse in the accordion mode but then buckled upward and inward in the middle. The right lower frame buckled outward about 21 inches aft of the bumper. The engine was pushed sideways by the impact and did not enter the enlarged tunnel. The foam-filled fender sections aft of the firewall and plenum showed slight crushing. The roof buckled just forward of the B pillar. Sheet metal deformation prevented the door from opening, but the door fulfilled its purpose in rigidizing the compartment. The total static crush on the left side was 45.5 inches.

#### Compartment Interior Damage

Damage inside the vehicle was limited to deformation of the tunnel and toeboards. The tunnel deformed at the change in section just forward of seat lateral member. The toeboards were bent in the middle approximately two inches. The front foot wells buckled slightly. The A post movement was 1.7 inches.

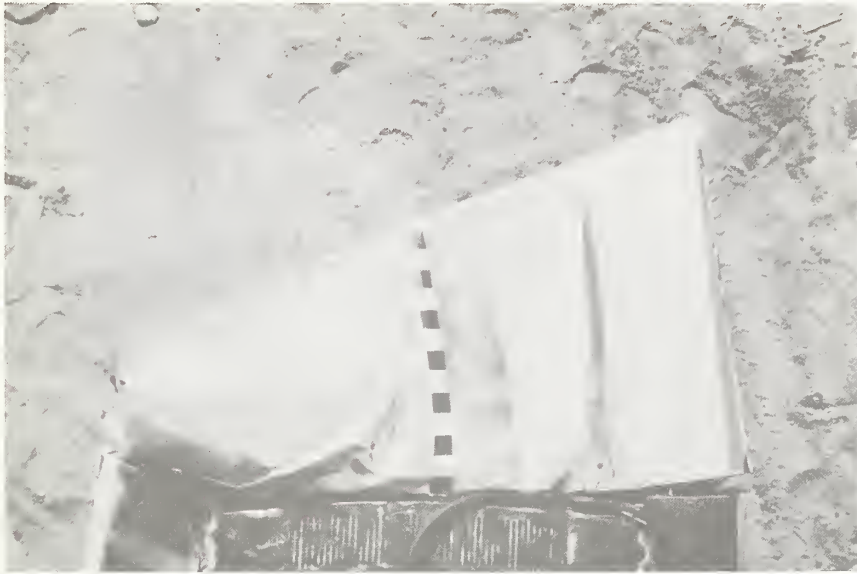


A. Post-Test Left Front Quarter View

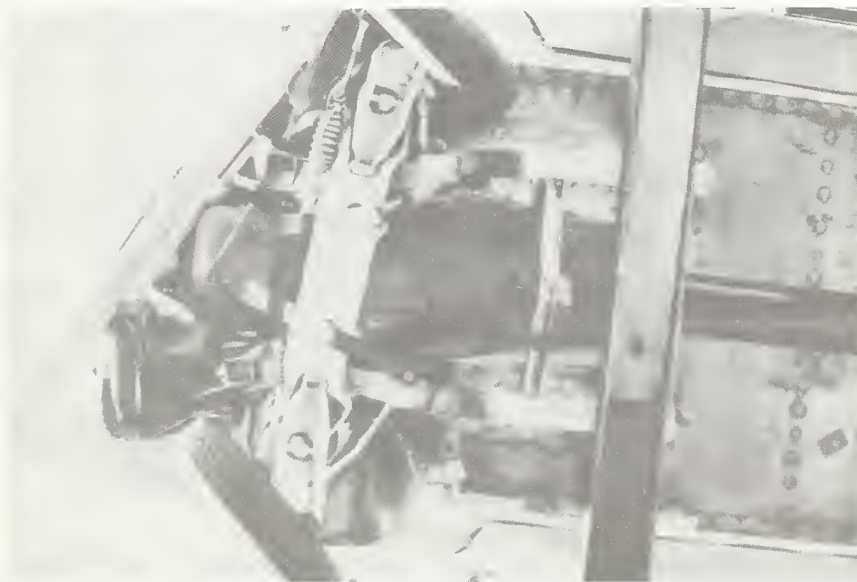


B. Post-Test Right Side View

FIGURE 3.41 PHOTOGRAPHIC COVERAGE OF TEST E15



C. Post-Test Overhead View



D. Post-Test Underneath View

FIGURE 3.41 CONT'D

### 3.5.3 50 mph 30° Oblique Frontal Barrier Evaluation Test, E24

This test supported the evaluation of the modified design in the frontal oblique crash mode. Instrumentation included seven accelerometers, high-speed and real-time motion pictures, etc. Data are summarized in Table 3.9; photo coverage is represented in Figure 3.42. This test was reported on in the August progress report under this contract. This vehicle was equipped with an advanced restraint system and instrumented dummies in connection with another contract; some dummy test results were lost through operator error, but available data indicated that the occupants were successfully protected. Actual impact velocity was 49.4 mph.

#### Structural Damage

Damage and deformation was severe forward of the vehicle "A" posts, being largely concentrated on the left (first impact) side. Both energy absorbers stroked fully, and neither stub frame collapsed in the accordion mode. The left frame was driven back through the toeboard.

The engine detached, translated to the right, and successfully entered the enlarged tunnel area. The driveline sheared, leaving the rear suspension intact.

All foam components, particularly the left side, were fully engaged in the barrier and crushed in a uniform mode. The left front tire was involved in the crash and was detached from the wheel after the crash.

#### Passenger Compartment Intrusion

Beyond the perforation of the left toeboard and some denting of the right toeboard, the interior of the vehicle was essentially undamaged. Incipient buckling was noted at the junction areas of the tunnel and on the left front roof.

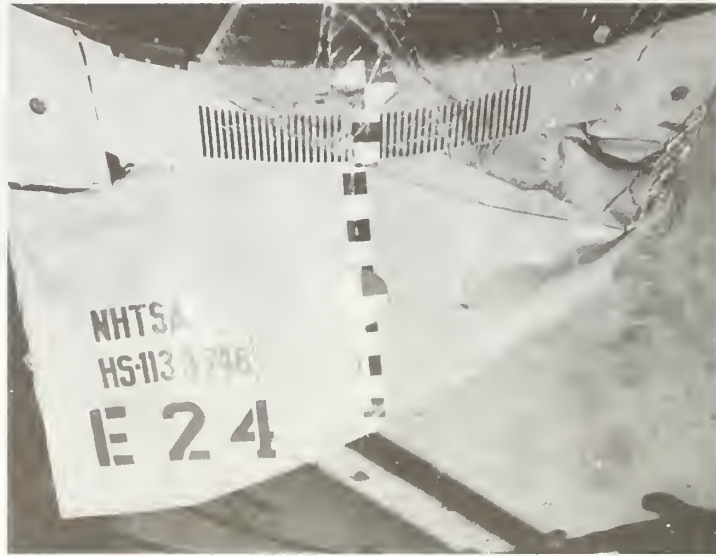


A. Left Front Quarter



B. Left Front

FIGURE 3.42 PHOTOGRAPHIC COVERAGE OF TEST E24



C. Overhead



D. Left Toeboard

The recorded intrusion of 14 inches at the upper inside left toeboard reflects the final position of a light gage sheet metal cover over the toeboard foam which was deflected some 4 to 6 inches further than the structure as the left stub frame detached. Thus a final intrusion of 8 to 10 inches at this point is probably more accurate.

### 3.6 Offset Subcompact-to-Standard Impacts

#### 3.6.1 80 mph Frontal Offset Large Car to Small Car Baseline Test, 06

Baseline Test 06 was an offset frontal impact between a 1974 Pinto sedan and a 1968 Plymouth sedan. The nominal closing velocity was 80 mph. The cars' velocity vectors were parallel but offset 50 percent of the width of the vehicle. Thus the fender of one vehicle lined up with the centerline of the other car. Both vehicles were fully instrumented with seven triaxial accelerometers, and complete photographic coverage was provided. The test data is summarized in Table 3.10. The test velocity was 80.4 mph. The complete test report was presented to the CTM under separate cover and included Tests 04, 07, and 08. Figure 3.43 presents the photographic data for Test 06. The accelerations are presented in Figure 3.44 and contrasted with Test E17 and E21.

The left side of the vehicle pulled inward toward the impact. This created an apparent curvature, convex on the left side of the vehicle. The right side was crushed to the A post, with the right door separating and the A post becoming vertical above the belt line. The right door opened and the dummy rotated out, sustaining broken ribs and shoulder and fatal head strikes.

The Plymouth sedan overrode the Pinto, with the final position of the Plymouth bumper near the dash of the Pinto. It is highly unlikely that the occupants could survive this crash.

TABLE 3.10  
 BASELINE AND MODIFIED TEST DATA  
 OFFSET SUBCOMPACT FRONT TO LARGE SEDAN FRONT

<u>Test Description</u>	<u>Test 06</u>	<u>Test E17</u>	<u>Test E2</u>
50% offset, large sedan front to subcompact front			
Test Date	1/4/74	8/21/74	7/8/75
Impact Velocity (mph)	80.4	70.9	80.8
<u>Large Car</u>	'68 Plymouth	'68 Plymouth	'74 LTD
Static Crush (in)	15.8	21.8	39.5
Peak Trunk Accel. (g's)	not available	not available	34
A Post Movement (in)	not available	1.5	6.5
Driver HIC	*	*	687*
Driver Chest Acc. (g's)	*	*	64
Passenger HIC	*	*	1274*
Pass. Chest Acc. (g's)	*	*	47
<u>Small Car</u>	Baseline '74 Pinto	Modified '74 Pinto	Modified '74 Pinto
Static Crush (in)	52	37.0	not availa
Peak Trunk Accel. (g's)	43	24.7	34
A Post Movement (in)	not available	0.5	.08
Driver HIC	*	*	924
Driver Chest Acc. (g's)	*	*	43
Passenger HIC	*	*	457
Passenger Chest Acc. (g's)	*	*	41

\* Data not taken (per NHTSA direction)

\*\* Data questionable



A. Post-Test View Along Plymouth Travel Direction

FIGURE 3.43 PHOTOGRAPHIC COVERAGE OF BARRIER TEST 06



B. Post-Test View Along Pinto Travel Direction



C. Post-Test Overall View

FIGURE 3.43 CONT'D

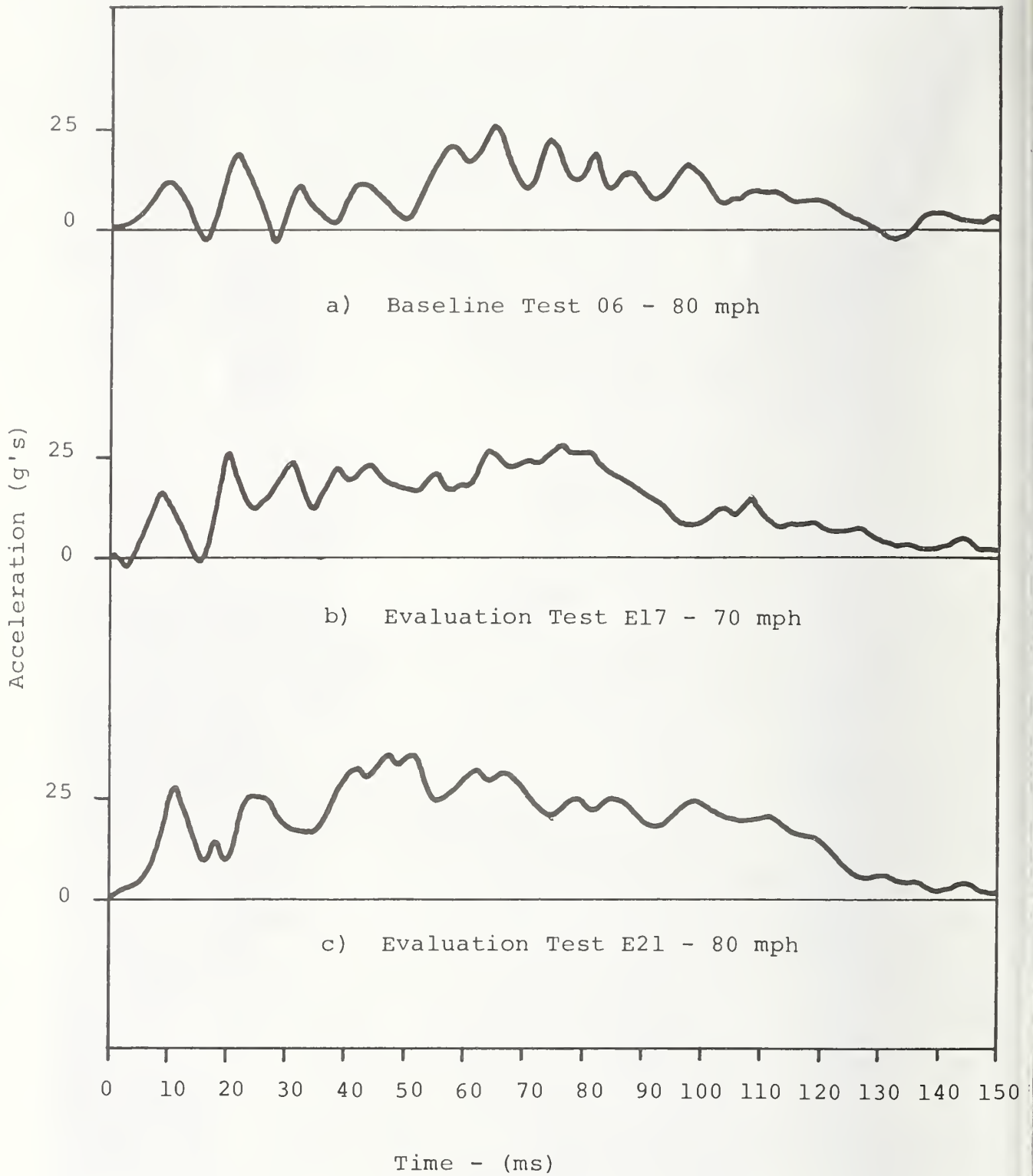


FIGURE 3.44 TRUNK ACCELERATION FOR OFFSET LARGE CAR TO SMALL CAR TESTS 06, E17, E21

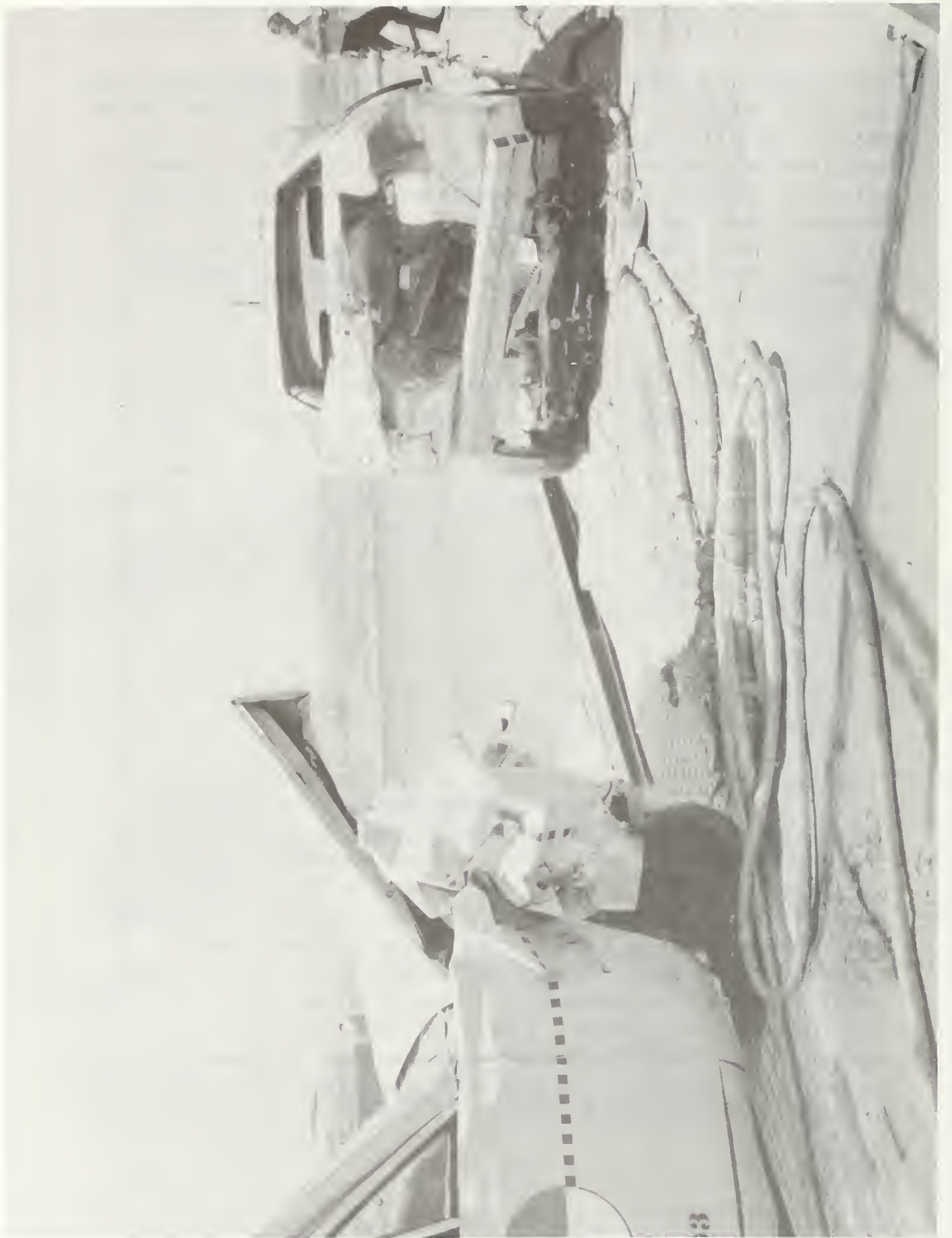
### 3.6.2 70 mph Frontal Offset Large Car to Small Car Evaluation Test, E17

Evaluation Test E17 was similar to Baseline Test 06 except the test vehicle was a modified Pinto sedan and the nominal closing velocity was reduced to 70 mph. As before, the vehicles were offset 50 percent of the width with parallel velocity vectors. The instrumentation and photographic coverage were the same as used in Baseline Test 06. The data is summarized in Table 3.10, with photographs in Figure 3.45. The complete test report was presented as an attachment to the September 1974 progress report.

It is important to note that the greatest value of the modified design is in the offset and oblique impact conditions. The baseline vehicle showed satisfactory performance in the frontal aligned conditions up to a very high velocity. The baseline design, however, breaks down when subjected to the offset or oblique loadings. Minicars has strived to improve the offset and oblique crash-worthiness without sacrificing the behavior in the pure frontal condition. The results of Test E17 have verified the success of the design.

### 3.6.3 80 mph Offset Large Front to Small Front Evaluation Test, E21

This test supported evaluation of the modified design in the frontal offset impact mode against an unmodified full size car (Ford LTD). Instrumented dummy driver and front passenger in the Pinto were protected by an advanced Minicars restraint system, driver and occupant of the LTD by standard 3-point belts. Pinto and LTD were fitted with five accelerometers each. The impact was recorded by high-speed and real-time cameras, with pre- and post-test stills. Data are summarized in Table 3.10; photo coverage is represented by Figure 3.46. Actual closing velocity was 80.8 mph, with the Pinto experiencing a change in velocity of 55 mph. Results were reported in the progress report dated July 1974 under this contract.



A. Post Impact Position of Vehicles



B. Right Front Quarter Post-Test View of Pinto  
FIGURE 3.45 CONT'D



C. Right Side Post-test View of Pinto



A. Left Front Quarter Damage



B. LTD Damage

FIGURE 3.46 PHOTOGRAPHIC COVERAGE  
OF TEST E21



C. Right Front Quarter Damage

FIGURE 3.46 CONT'D

## Exterior Structural Damage

### Pinto

The LTD struck the left front of the Pinto with 28 inches of centerline offset, effectively crushing the entire left side of the structure.

Neither bumper EA unit stroked, and the left stub frame was bent upwards after some accordion failure. The left frame was crushed rearwards about 9-1/2 inches into the toeboard support area, which also showed evidence of considerable tire pressure.

The engine separated and appeared to rotate to the left and nose down, failing to enter the tunnel opening.

The left hood and A post box suffered a general crush of about 22 inches at which time the hood opened. The right hood area was effectively undamaged, and the right fender box detached from the vehicle.

Both doors remained closed during the test. The left door required force to open.

The left roof was slightly buckled at the B post. The windshield remained undamaged. The drive train detached at the slip joint, and the rear suspension remained intact and undamaged.

### LTD

The LTD left front corner was generally crushed back to a line drawn between the right fender and the left A post. Both left doors were sprung, and the left rear fender buckled.

## Interior Compartment Damage

### Pinto

The upper corner of the toeboard was pushed rearwards 10 inches on the left side, and the left sill was buckled

outwards at a point about 9 inches aft of the A post where it was weakened to allow foaming. The left forward tunnel was wrinkled consistent with the deflection of the toeboard area.

LTD

No interior damage, other than a collapsed upper and lower steering wheel rim and knee/dash contact, was noted in the LTD.

### Dummy Restraint Analysis

In Test E21 we installed the Minicars wheel mounted airbag driver restraint system developed under NHTSA Contract DOT-HS-113-3-742 in the driver position in the modified Pinto. On the passenger side we installed the airbelt restraint system, NHTSA Contract DOT-HS-4-00917.

Since this test was a frontal offset test, the amount of structure active in absorbing energy in the crash was substantially less than would be the case in a full frontal test. This structural difference produces two major effects that affect restraint performance. First, the crash pulse g-level is lower since less structure is deforming. Second, the total crush is greater since less resistance to crush is generated by the structure.

The first effect, lower crash pulse g-levels, means that the fixed force portions of the driver and passenger restraint (the energy absorbing column and anchor point force limiters for the driver and passenger, respectively) are too high to allow the vehicle occupants to stroke the normal amounts in the vehicle. This was borne out since the column stroked only 3/8 inch and the anchor point force limiters stroked only about 3/4 inches average. Thus, due to the soft crash pulse, the stroke of the driver and passenger was lower than normal. Even so, however, the measured injury levels were -- for the most part -- relatively low. The only exception was the driver HIC, which was 924.

It should be mentioned that the right front passenger dummy received a broken clavicle in the crash event in spite of the fact the g-levels on the dummy were relatively low. It is impossible to speculate on how this may have affected the dummy kinematics and/or injury levels.

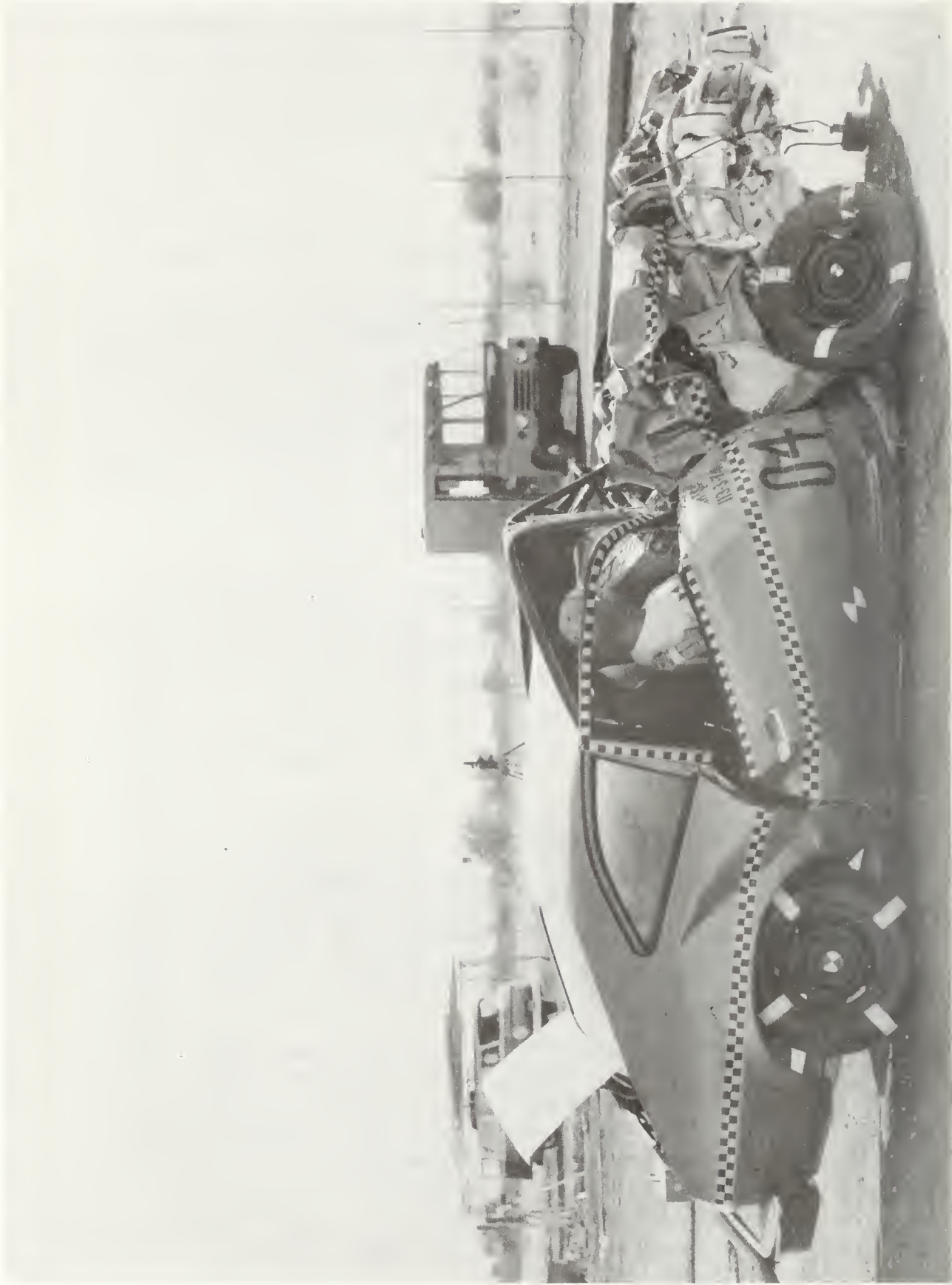
### 3.7 Subcompact-to-Standard Vehicle Oblique Impact, 04

The baseline test plan originally called for an 80 mph vehicle-to-vehicle test with the velocity vectors intersecting at 30°. Such a condition would simulate an accident with two 40 mph vehicles approaching at 30°, as might occur on an undivided highway. During the preparation for conducting the test, the subcontractor determined that it would be impossible to perform the test as required. The best alternative was to place the stationary Pinto at 30° to the line of approach of the Plymouth. The maximum possible velocity for these test conditions was 72.7 mph. The test, as run, represents a more severe condition than originally planned. From the Pinto's point of view, the original condition would see the Plymouth approaching in a crabbing motion with a side velocity of

$$V_S = 40 \sin 30^\circ = 20 \text{ mph.}$$

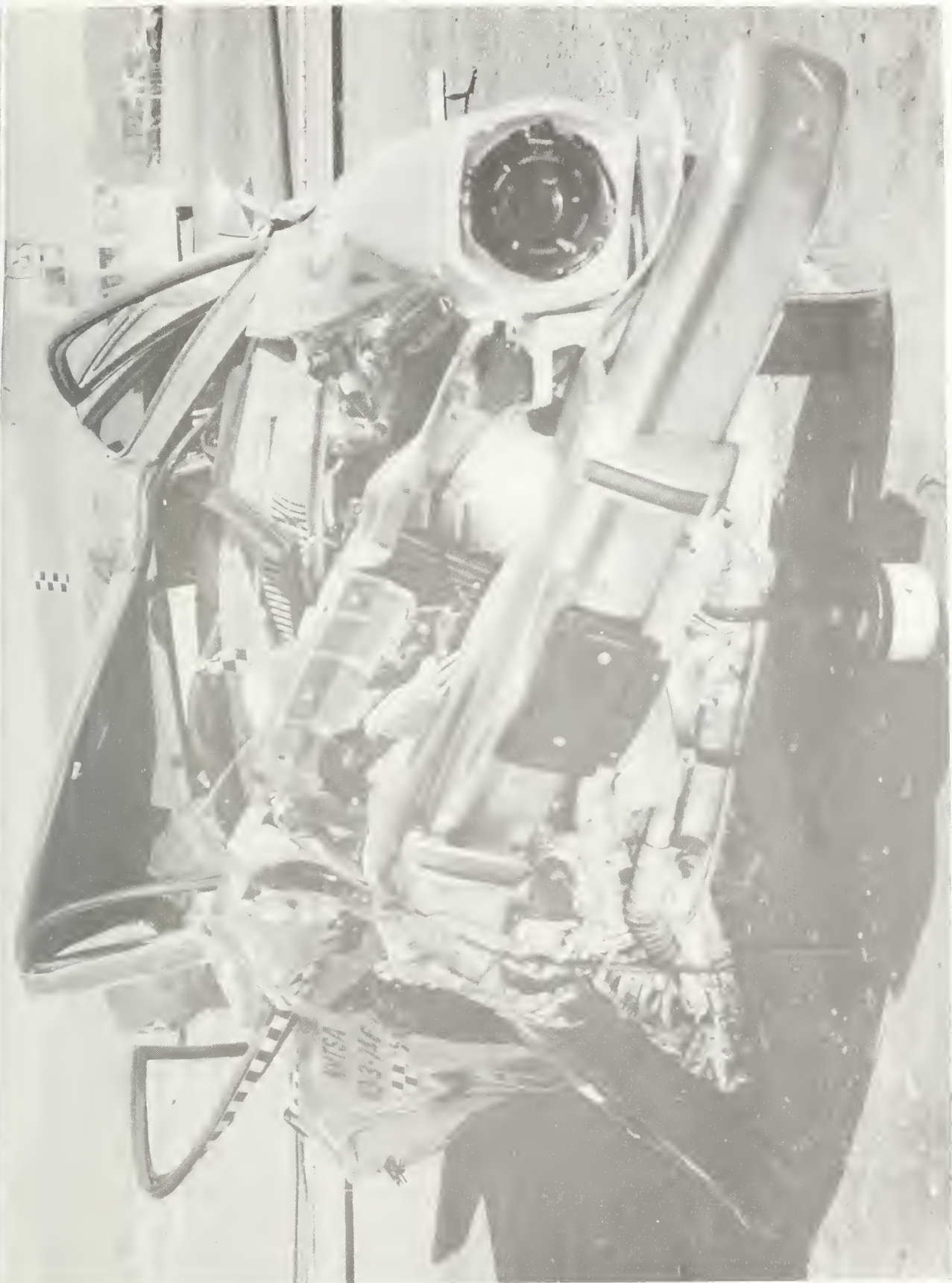
The actual test velocity resulting from the test conditions was  $V_S = 72.7 \sin 30^\circ = 36.4$  mph. The increased side velocity increases the rotation of the impact, with more energy going into rotatory movement. As conducted, the test does not represent any reasonable real world accident. Thus the modified vehicle was not tested under these conditions.

Baseline Test 04 used a 1974 Pinto sedan and a 1968 Plymouth sedan as the test vehicles. Both cars were fully instrumented with seven triaxial accelerometers. The photographic coverage consisted of the standard four high-speed cameras, one real time camera, and the 35 mm stills. The physical data is summarized in Table 3.11, with the photographs shown in Figure 3.47. The complete test report was presented to the CTM under separate cover along with Tests 06, 07, and 08.



A. Post-test Side View of Pinto

FIGURE 3.47 PHOTOGRAPHIC COVERAGE OF BASELINE TEST 07



B. Post-test Front View of Pinto

FIGURE 3.47 CONT'D

TABLE 3.11

BASELINE TEST DATA (TEST 04)

30° OBLIQUE LARGE SEDAN FRONT TO SUBCOMPACT FRONT

Test Date	12/27/73
Test Description	Large Sedan Front to Stationary Subcompact Front at 30°
Impact Velocity	72.7
<u>Large Car</u>	68 Plymouth
Static Crush (inches)	32.8
Peak Acceleration (g's)	Not Available
A Post Movement (inches)	1.2
<u>Small Car</u>	74 Pinto
Static Crush (inches)	40.8
Peak Acceleration (g's)	30.2
A Post Movement	Not Available

The structural damage to the Pinto was similar to the results of Test 06. The left side of the vehicle bent away from the impact, making the vehicle concave on the left side. This is the reverse of the curvature due to the offset impact. Based on preliminary data, the acceleration levels experienced by the dummy are below the critical levels. There appears to be adequate living space between the seat and dash in the vehicle after the crash, although the door opening allowed the dummy to rotate out of the compartment and caused probably fatal head strikes. The Plymouth sedan overrode the Pinto, making a spectacular visual effect. Based on the results of Tests E15 and E17, it is believed that the modified vehicle would have proved crashworthy under the accident conditions.



#### 4.0 SIDE IMPACT CRASHWORTHINESS

The crashworthiness of the baseline side structure was investigated in a series of dynamic impacts, including side pole tests and normal and oblique front-to-side impacts. The baseline vehicle had a maximum survivable velocity of approximately 12 miles per hours. A modified design of the door and compartment was developed which increased the survivable velocity to over 30 mph.

The results of baseline study indicate two basic crashworthiness problems associated with side impacts. First, the production vehicles have their primary structure aligned longitudinally, with relatively little lateral structure. Thus, this lateral strength and energy-absorption capability is very low. Second, stock bumpers are higher than stock rocker panel members. In front-to-side impacts, the bumper overrides the only side structure capable of offering significant resistance. In order to satisfy the crashworthiness criteria, vehicle structures must be strengthened laterally and located in the plane of the impacting surface.

Modifications of the compartment included raising the rocker section to bring it nearer to the height of an impacting vehicle's bumper. In addition, foam filled lateral members were installed under the front and rear seats, and the rocker panel was made deeper and foam filled. The doors were stiffened both longitudinally and laterally by filling with foam and adding a longitudinal compression strut.

The effectiveness of the modified design was verified in a series of evaluation tests conducted in the same impact modes as the baseline tests. The final oblique front-to-side tests included instrumented anthropomorphic dummies in both front and rear seats. The evaluation of the modified design was based on the response of the dummies during the crashes.

## 4.1 Evolution of Design

### 4.1.1 Design Approach

The side impact design goals specified in the contract are as follows:

1. Side pole impact at 20 mph.
2. Front-to-side impact at 40 mph by baseline, modified, and large car.

The side pole impact condition mandates that all kinetic energy be absorbed by the side energy management system. The pole will contact all of the longitudinal members including the rocker panel, roof rail, and door beam. The pole acts as a rigid support, causing combined beam bending and local crush of the side structure. Figure 4.1 depicts the type of deformation caused by side pole impacts. The kinetic energy of the distributed mass of the forward and aft portions of the vehicle must be transmitted by shear and bending. As in all beam bending problems, the cross section must be maintained to provide maximum stiffness. This requires transverse members at several locations.

The local crush of the vehicle directly against the pole must be limited to prevent excessive intrusion into the compartment. Since compartment intrusion is only a problem at the location of the occupants, these are the points where the lateral supports must be located. The logical locations are under the front seat and under the rear seat. Thus, to satisfy the side pole impact criteria, the modified design should have stiff compartment lateral members, strong rocker panels, and crushable doors.

The vehicle-to-vehicle side impact crashworthiness presents a completely different problem from the frontal impact criteria. The crush distance available in the subcompact vehicle for side impact is, at most, 10 inches. Some of

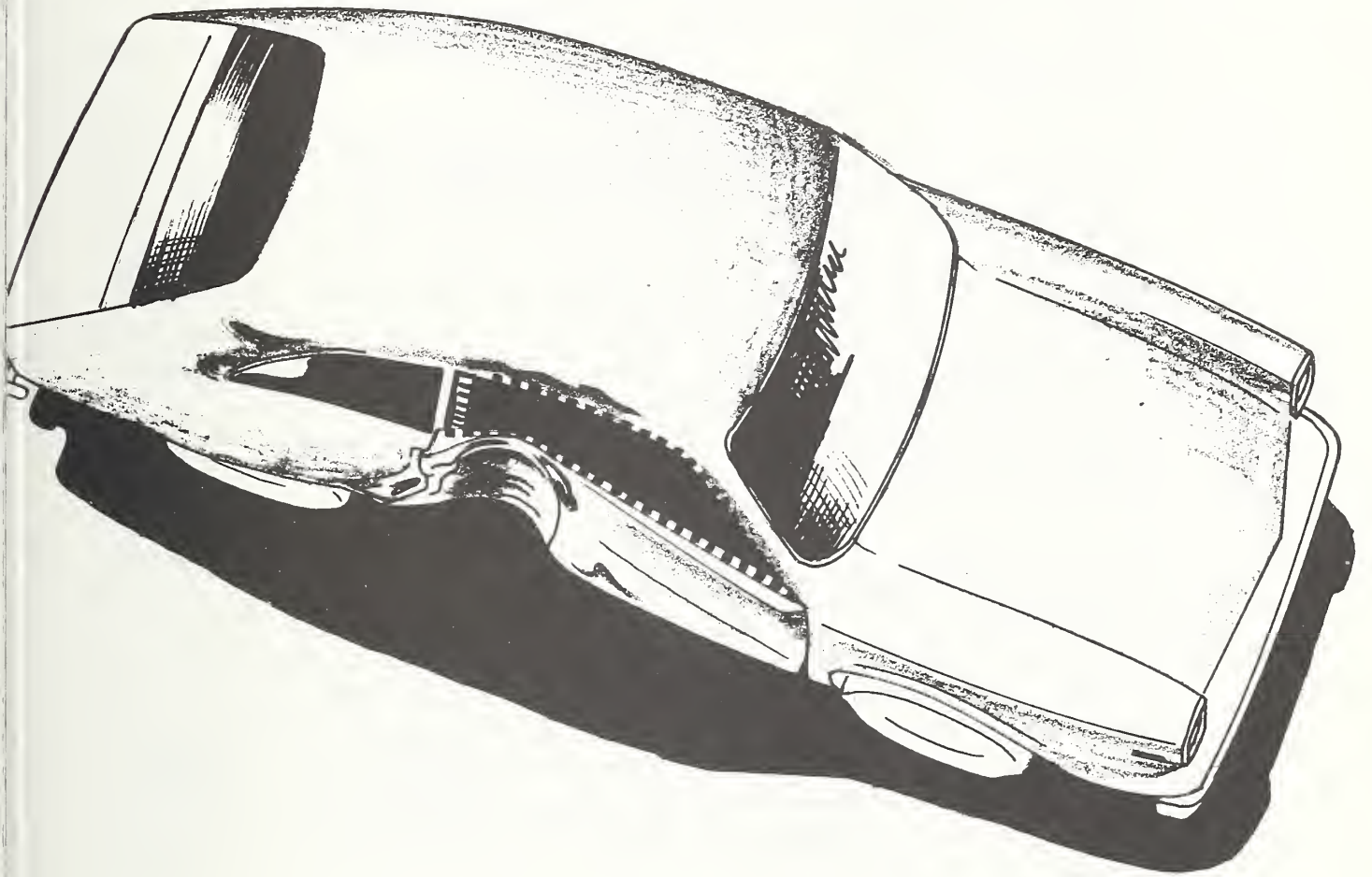


FIGURE 4.1 TYPICAL SIDE POLE IMPACT DAMAGE

this available crush distance must be used as padding to attenuate the acceleration and jerk levels of the occupant, i.e., the occupant stroking distance. The remainder, about 7 inches, is all that can be used for a side energy management system.

In order to increase the crashworthiness, the additional crush distance must be obtained from the impacting vehicle. To accomplish this, the side of the struck vehicle must provide a force level greater than the crush force of the impacting vehicle front structure. The maximum crush forces of the nine vehicles used in the compatibility study are shown in Table 4.1. Using these values as guides, the side structure of the subcompact must reach a minimum force of 70,000 pounds before significant crush occurs in the impacting vehicle.

The impacting vehicle does not contact the entire vertical plane of the side, but instead contacts it along a horizontal line. In most instances, the contact line is above the primary structure of the struck vehicle (i.e., the rocker panel). The bumper hits the soft door and pushes inward until either the A post or the B post is contacted. The present production door parts are generally weaker than the front structure of the impacting car. They must absorb the major portion of the energy of impact.

The simplest and most direct solution to the front-to-side impact problem is to locate the bumper of the bullet car in the same horizontal plane as the rocker panel of the target vehicle. The present design standards prevent complete adoption of this solution. The most

TABLE 4.1  
FRONT END CRUSH FORCE OF VARIOUS  
VEHICLES IN THE TRAFFIC MIX

<u>Vehicle Weight</u> <u>(lbs)</u>	<u>Maximum Crush Force*</u> <u>(kip)</u>
2500	82
2570	61
2958	68
3406	72
4324	80
5728	78
6170	115

\*Maximum force based on computer simulations of  
a 100 mph impact with a 1974 Pinto sedan.

that can be accomplished is to raise the subcompact enough so that the rocker panels catch at least part of the oncoming bumper.

In addition to raising the car, the A and B posts must be stiffened at the base to provide a better load path when they are contacted by the bumper. The compartment lateral members described for the side pole impact will also support the rocker during the front-to-side impact.

Overall, the modified design should include compartment stiffeners, raised and strengthened rocker panels, stiffened door posts, and front and rear shear members.

#### 4.1.2 Final Design of the Side Structure

The design process for the side structure proceeded concurrently with and was similar to the design process for the front structure. A rational design was selected based on baseline tests and literature review. The component testing phase was deleted, since individual tests could not provide a true indication of the system behavior. Subsystem tests were conducted with excellent results, and the design was finalized for incorporation on the evaluation test articles.

The only change in design of the side structure resulted from Contract Modification 3, which required increased B post stiffness to handle oblique side impacts.

The final modifications include the following items and apply to all evaluation test articles except as noted:

1. Doors - Stock door beams and window mechanisms removed. Longitudinal door beam added, door enlarged at the H-point location, and the lower portion foamed in place.
2. Rocker Panels - Rocker panels raised 6 inches; new facing sheet added extending the panel downward 5 inches. The entire panel was foamed with 2 lb/ft<sup>3</sup> polyurethane foam.

3. Compartment Laterals - Two lateral members added, one under the front seats and one at the B post.
4. B post closed and foamed.
5. B post gusseted at the intersection with the B post lateral. This modification applied only to test articles E20, E21, E24, and E25.
6. Other modifications affecting the side are discussed in the sections dealing with their primary functions, e.g., toeboards are discussed in Section 3.2.6.

The modified door design is shown in Figure 4.2. The modifications were accomplished in the following manner. The doors were removed from the vehicle and completely disassembled. The inside and outside skins were removed, leaving just the door frame intact. The door latch mechanism was replaced and a steel housing built over it. A new longitudinal door beam, a 2-1/2 inch diameter x .065 inch thick steel tube, was welded in place running from the upper A post hinge to the housing over the latch. The new inside skin (18 gage steel) was welded to the door frame and the horizontal partition. The final step in the door modification was to fill the lower portion of the door with 2 lb/ft<sup>3</sup> polyurethane foam.

The rocker panels in the evaluation test articles were raised as a part of the overall raising of the compartment. The total increase in height of the rocker was 6 inches. An outer skin of 18 gage steel extending from the top of the rocker to the bottom of the footwells is welded in place. Thus a new rocker panel 10-5/8 inches deep is formed. The entire panel is foamed in place with 2 lb/ft<sup>3</sup> polyurethane foam. Figure 3.7 showed a section of a modified rocker panel.

The compartment laterals, at the B post and under the front seat, are formed as an integral part of the new underbody. The front seat lateral is 9 x 16 inches and is made from 18 gage steel. It runs laterally from the rocker to the tunnel on each side of the vehicle. The top of the

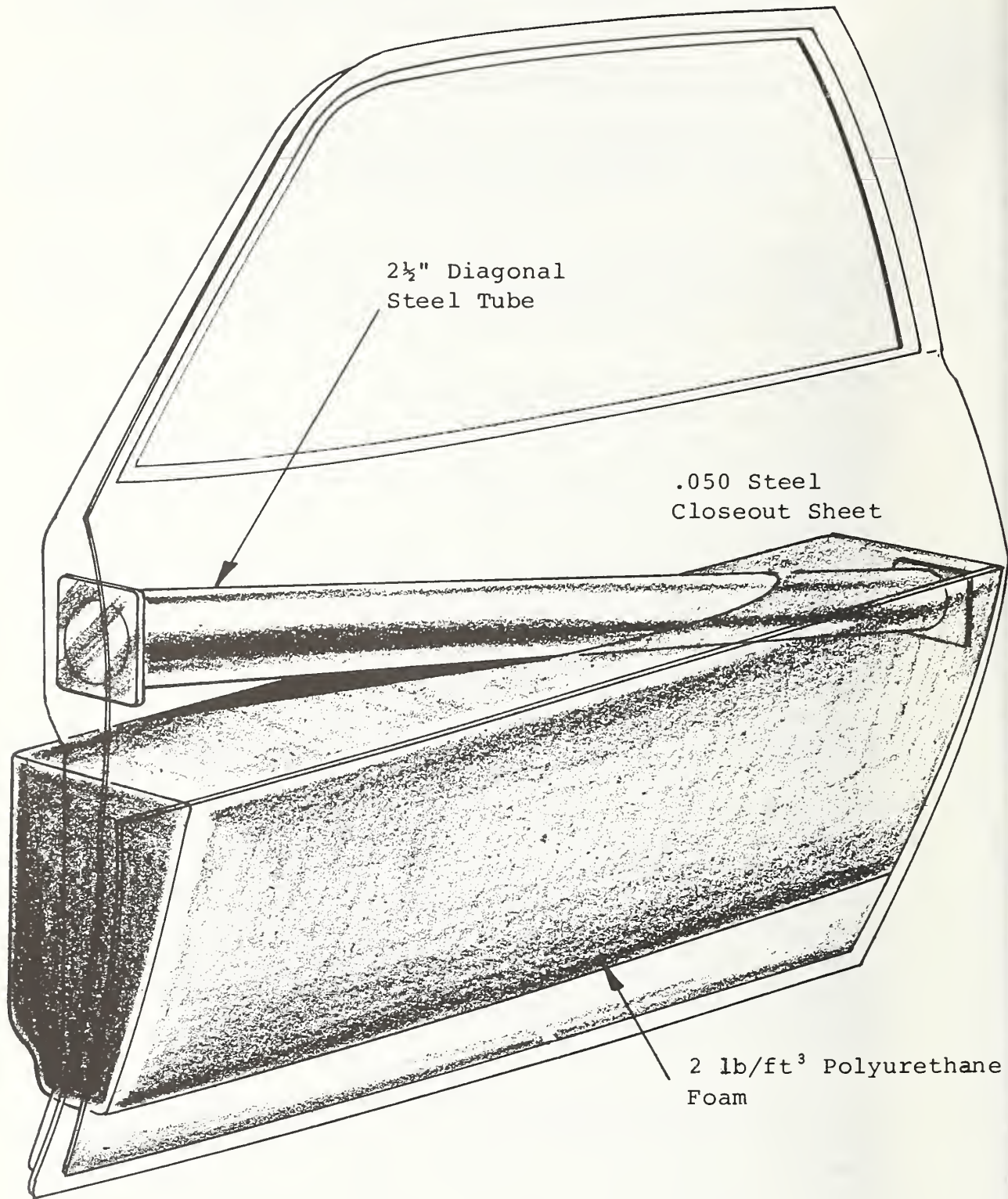


FIGURE 4.2 DOOR MODIFICATIONS

lateral provides the support structure for the front seats. The vertical sides of the lateral form part of the front and rear footwells. The B post lateral is a 7 x 8 inch member running laterally across the vehicle between the B posts. It is an integral part of the underbody and is fabricated from 18 gage steel. This member supports the forward edge of the rear seats. Both of the compartment laterals are foamed in place with 2 lb/ft<sup>3</sup> polyurethane foam. Both compartment laterals are shown in Figure 4.3.

For test articles E20, E21, E24, and E25 the design of the B post lateral included a 4 inch gusset at the intersection of the B post and the B post lateral. The purpose of the gusset was to stiffen the B post against lateral bending during an oblique front-to-side impact.

Other design modifications which affect the crashworthiness of the vehicle during side impacts include the toeboards, the tunnel design, the trunk deck, and the rear fenders. These members, as do all the modifications, serve several purposes for the various design goals. The intent throughout this report is to discuss the design of a component in the section covering its primary purpose. The toeboards and the tunnel are discussed in Section 3.2.6. The trunk deck and the rear fenders are discussed in Section 5.1.

#### 4.1.3 Development testing

##### 4.1.3.1 Introduction

Four side subsystem development tests were conducted during the course of the contract. Two of the four were static crush tests of unmodified Pinto compartments and two were dynamic tests of a modified and an unmodified side subsystem. The purpose of the static tests was to provide the force deflection properties for the compartment under both pole impact (D7) and front-to-side impact (D11) conditions for later use in dynamic modeling.

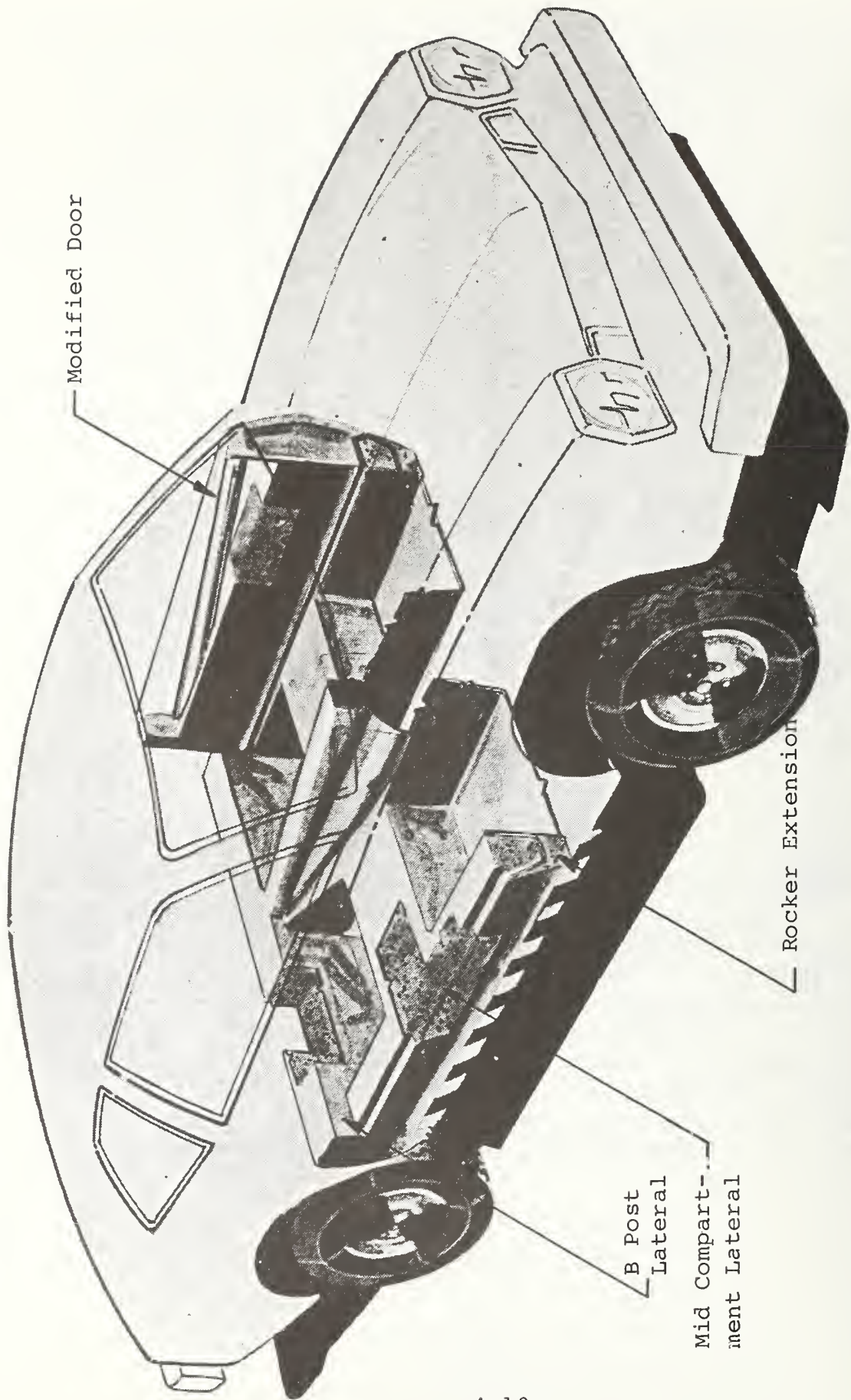


FIGURE 4.3 COMPARTMENT MODIFICATIONS

#### 4.1.3.2 Static Crush Tests

The static crush tests were performed on the Minicars hydraulic crusher. Both test articles were the undamaged compartments of previously crashed Pinto sedans. The vehicles were stripped forward of the firewall and aft of the rear window shell. Contact was on the left side of the compartment.

The impact surface for the pole test (D7) was a 14-inch diameter pole mounted on the hydraulic ram and extending above the roof rail and below the rocker panel. The front-to-side crush test (D11) used a steel plate to simulate the impacting surface of a 1968 Plymouth sedan. The plate was mounted on a sliding fixture which was actuated by the ram.

The basic problem of static crush tests is the difficulty in providing supports which simulate the inertial effects of dynamic loading. In the first test, the pole impact test, this problem was approached by reinforcing the right side of the compartment, thus forcing the failure to occur on the impacted side, as is noted in the dynamic side pole tests. For the front-to-side test, the problem of simulation was approached by symmetrically loading the test article. The support plate on the right side was identical to the loading plate on the left side. It was hoped that failure mechanisms would simulate a true dynamic failure mode.

The tests were run at loading rates of 3 inches/minute for the pole test and 4 inches/minute for the front-to-side test. The data included load cell measurement, displacement measurement, and photographic coverage. Four load cells were used to support the reaction plate of the crusher. The sum of these cells is the total resistance force of the compartment. A linear displacement transducer was used to record the crush distance. Photographic coverage included slow motion film and 35 mm slides taken during the test, as well as pre and post test shots. Figure 4.4 presents the force-deflection data obtained from both D7 and D11. The pole test

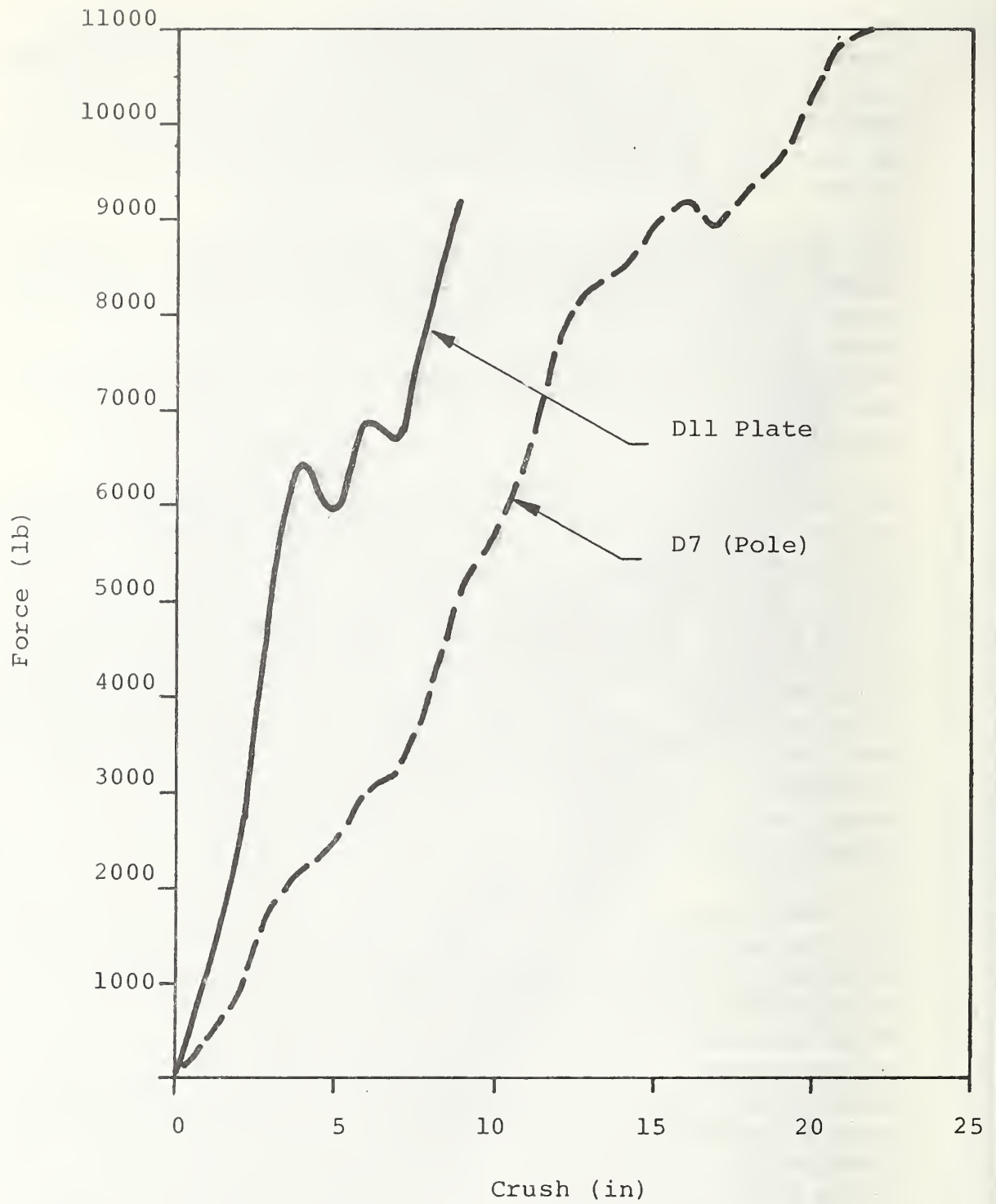


FIGURE 4.4 STATIC FORCE DISPLACEMENT FOR BASELINE  
74 PINTO SIDE STRUCTURE

was run to 22 inches. The front-to-side test was stopped at 9 inches due to interference between the vehicle and the crusher walls. Photographic data from tests D7 and D11 are summarized in Figures 4.5 and 4.6, respectively.

The static crush development tests were considered only partially successful. Neither system of support provided the exact crush mode desired. Based on these two tests, it is apparent that a more sophisticated method of support is required to gather side crush data. A system of progressive supports such as is used for frontal static crush tests may be required. Much additional experimentation is required before completely satisfactory results can be obtained.

The data obtained in these two development tests should be considered a first step in thoroughly investigating side structures. A library of data similar to the Minicars' data bank on frontal crush characteristics is required for adequate dynamic modeling.

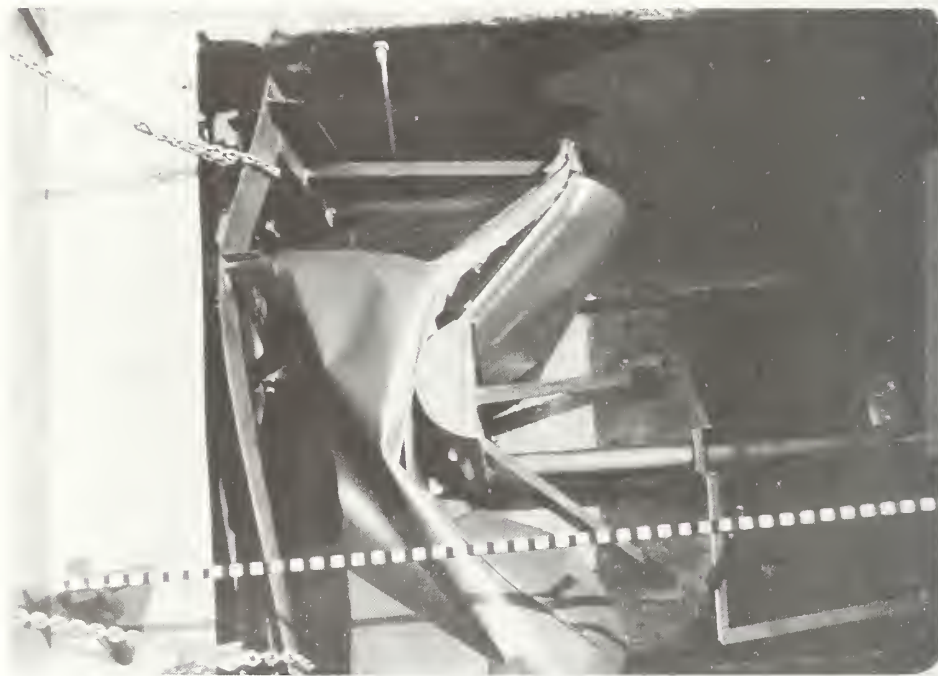
#### 4.1.3.3 Dynamic Tests

The dynamic development tests were simulations of a 20-mph side pole impact. These tests were not included in the original plan of work. They were added in order to evaluate the behavior of the early side modification concepts for Pintos under side pole impacts. Previously crashed 1972 Pintos were used as the test articles. The side structure of the 1972 and 1974 Pintos are almost identical, thus allowing the substitution of the older model vehicle.

The tests were conducted with the Pinto stationary, with the left side facing the impacting bogey vehicle. A 14-inch diameter pole was mounted on the front of the bogey. The mass and velocity of the bogey were adjusted to give an energy of impact equivalent to the 20-mph rigid pole test. The data included two triaxial accelerometers, photographic coverage, and pre and post test measurements. The significant data is summarized in

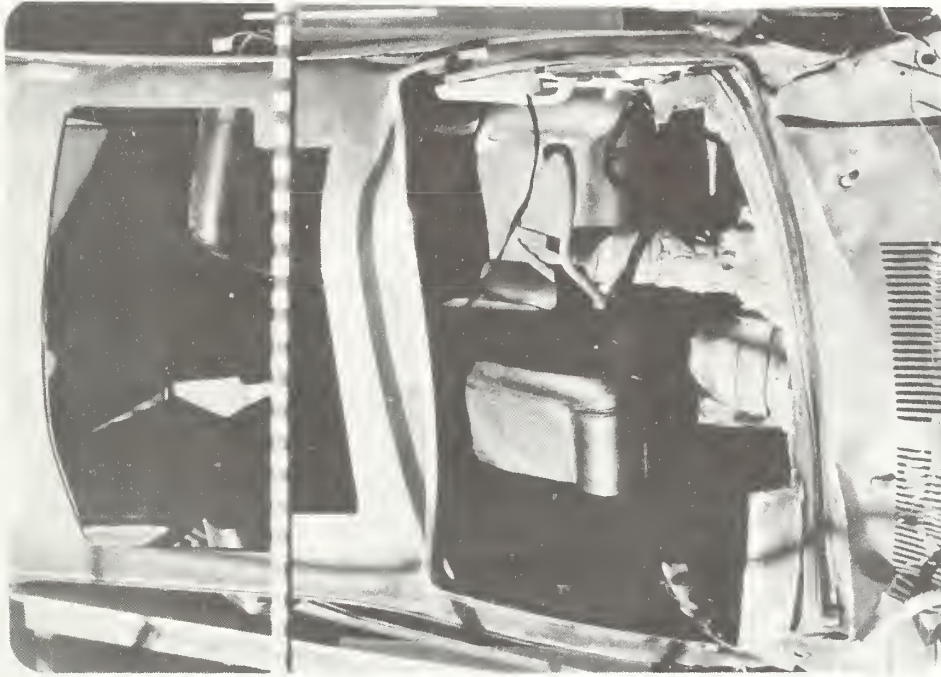


A. Pre Test

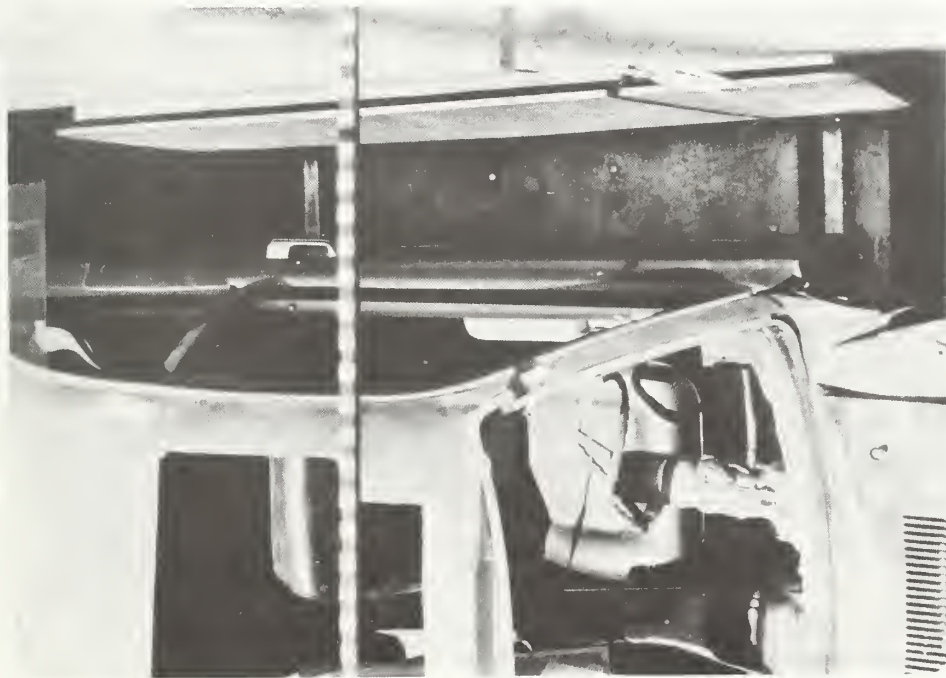


B. Post Test

FIGURE 4.5 SIDE POLE CRUSH TEST D7



B. Post Test



A. Pre Test

FIGURE 4.6 SIDE CRUSH TEST D.11

Table 4.2, with the photographic coverage presented in Figure 4.7. The location of impact, selected by the CTM, was 6 inches forward of the B post. This placed the pole between the proposed lateral stiffening members.

Test D1 was a baseline test of a 1971 Pinto which had been previously crashed in a 30 mph frontal barrier test.

The modified test article (D2) for the dynamic test of the side structure was fabricated from a previously crashed Pinto. It was stiffened laterally by a 16 x 6 inch foam-filled sheetmetal box extending across the vehicle from rocker panel to rocker panel under the front seat. The section at the B post was stiffened laterally by a foam-filled sheetmetal member running from B post to B post. A modified door, as described previously, was installed using standard hinges and was bolted closed.

The validity of the proposed concept was completely verified by the results shown in Table 4.2. The intrusion reported in the table is defined as the difference in internal space before and after the impact. The unmodified vehicle showed an intrusion of 17 inches, while the modified subsystem allowed only 6 inches of intrusion. The improvement in occupant acceleration levels, due to the presence of interior padding, illustrates that increased compartment stiffness is not detrimental to an occupant with a properly designed restraint system. The actual design of the restraint system was beyond the scope of the crashworthiness program.

## 4.2 Front-to-Side Impact

### 4.2.1 30 mph 270° Large Front to Small Side, Baseline Test, 05

Baseline Test 05 was a dynamic front-to-side impact of a 1968 Plymouth Fury sedan impacting the left side of a stationary 1974 Pinto sedan. The target point was the center of the Pinto door. A deceleration device was attached to the Plymouth to prevent secondary strikes. It stopped the vehicle 5 feet past the point of impact. An actual test velocity of 30.3 mph was obtained.

The instrumentation for the test consisted of seven triaxial accelerometers placed in each vehicle at the standard locations

TABLE 4.2  
 BASELINE AND MODIFIED TEST DATA SIDE  
 POLE IMPACT DEVELOPMENT TESTS

	<u>Intrusion</u>	<u>Chest Acc.</u>	<u>Head Acc.</u>
Unmodified	17 in.	46 g's	121 g's
Modified	6 in.	42 g's	78 g's



A. Test D1 Unmodified



B. Test D2 Modified

FIGURE 4.7 DYNAMIC SIDE POLE TESTS D1 AND D2

according to the baseline test plan. The quantity of data dictated the use of transducers with a past history of poor performance. These units were rewired for this test and were placed in locations of less significant data value. Photographic coverage included four high-speed movie cameras and 35 mm pre and post test stills. In addition, pre and post test physical measurements were taken of both vehicles. The test data is summarized in Table 4.3, with the photographic coverage in Figure 4.8. The complete test report was presented as an attachment to the September 1974 progress report.

Exterior Structural Damage: The bumper and front sheetmetal of the Plymouth impacted the Pinto above the rocker panel over the main structure of the Pinto. The exterior surface of the door and the A and B posts were pushed inward. The production door beam was apparently of little benefit in this type of accident. The A and B posts suffered major damage, bending inward and crushing completely at the height of bumper impact. The fender and rear quarter both suffered extensive sheetmetal crush along the entire length of the car. The forward end of the vehicle showed shear deformation of 8.5 inches. The rocker panel rotated up but did not crush. The roof rail bent at the junction of the A and B pillars with metal separation occurring at the B pillar. The roof suffered slight buckling.

Damage to the Plymouth was light. The left front fender showed local damage just aft of the headlight housing. The only other effect of the impact was scratches on the bumper and grill. The Plymouth was usable for later tests.

Passenger Compartment Intrusion: Extensive damage was noted to the interior of the Pinto. The inner surface of the door reflected a maximum intrusion of 11.5 inches. The seat was forced against the tunnel, crushing at the line of the H point. The seat back collapsed in the middle. The A post collapse buckled the dash and plenum chamber upward. The floor boards were buckled along the entire length of the compartment. The rear shelf buckled upward in the center and showed metal separation at the ends.

TABLE 4.3

## BASELINE TEST DATA 270° LARGE FRONT TO SMALL SIDE IMPACT

	<u>Test 05</u>	<u>Test E9</u>
<u>Test Description</u>		
Large sedan front to sub-compact side at 270° at door centerline		
Test Date	7/17/74	7/19/74
Impact Velocity (mph)	30.3	29.7
<u>Impacting Car</u>	68 Plymouth	68 Plymouth
Static Crush (inches)	None	0.5
Peak Accelerations (g's)	5	15
<u>Struck Car</u>	74 Pinto	Modified 74 Pinto
Intrusion (inches)	11.5	8.5
Peak Acceleration (g's)	22.5	15
Centerline Displacement (inches)	8.5	3.5



A. Post Test Left Rear Quarter View

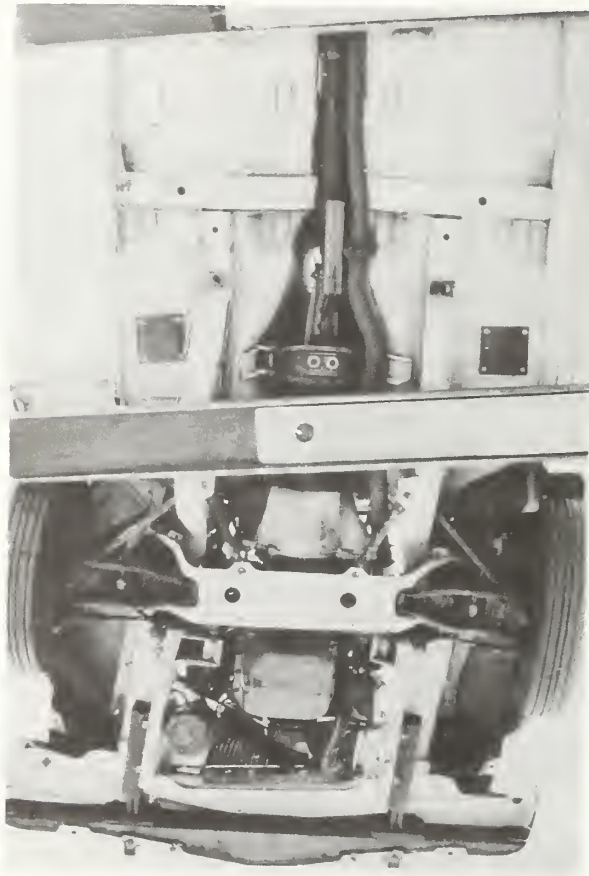


B. Post Test Left Front Quarter View

FIGURE 4.8 PHOTOGRAPHIC COVERAGE OF  
BASELINE TEST 05



C. Post Test Dummy Position



D. Post Test Underside View

FIGURE 4.8 CONT'D

#### 4.2.2 30 mph 270° Large Front to Small Side Evaluation Test, E9

Test E9 was an evaluation test of the modified Pinto under a 30-mph front-to-side impact with a 1968 Plymouth sedan. The test was identical in organization and operation to Baseline Test 05 (Section 4.2.1). The actual test velocity was 29.7 mph. The test data is summarized in Table 4.3, with Figure 4.9 showing the photographic coverage.

Exterior Structural Damage: The bumper of the Plymouth impacted the A post, door surface, and B post, bending these sections inward. The door received major structural damage along its length. The frame of the door and the foam filler were both crushed. The bumper apparently overrode the rocker panel without extensive damage, but the rocker was pushed inward and slightly rotated. The left front fender and left rear quarter were badly crushed. Total static crush, as measured on the outside of the door at the beltline, was 5.0 inches. The front structure of the vehicle suffered shearing deformation with a maximum displacement of 3.5 inches.

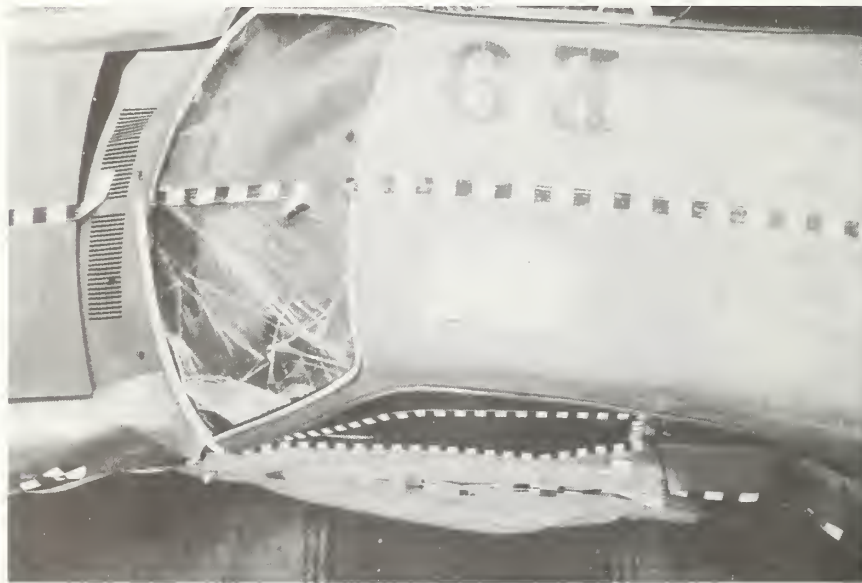
Compartment Intrusion Damage: The inward movement of the rocker deformed the outboard end of the seat lateral member with metal separation occurring along the weld-joint. The interior portion of the fender well was crushed against the toeboard. The bending of the A post buckled the dash and plenum chamber. The seat back was broken along a vertical line down the center of the back. The B post lateral was crushed at the outboard end and the close out panel for the left rear quarter was pushed into the compartment. Some minor sheetmetal damage was present in the left footwell floors. The right side of the compartment was not affected.

#### 4.2.3 Evaluation of Results

The relative intrusions of the baseline and modified vehicles present the best evaluation of the improved crashworthiness of the vehicle. The modified vehicle showed an improvement of 55 percent in the intrusion



A. Post Test Left Front Quarter View

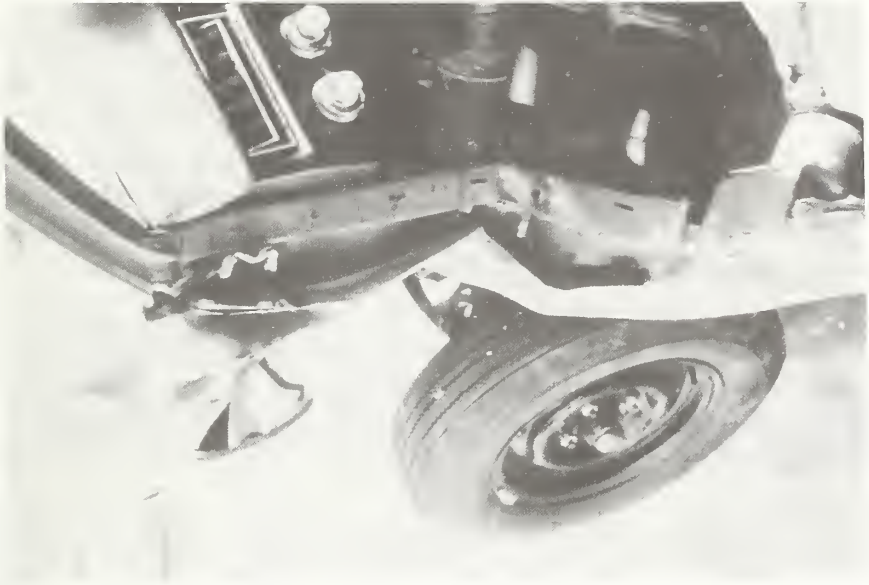


B. Post Test Overhead View

FIGURE 4.9 PHOTOGRAPHIC COVERAGE OF TEST E9



C. B-Post Damage



D. A-Post Damage

FIGURE 4.9 CONT'D

at the windowsill. The improvement at the upper B post was 26 percent. These measurements are of the most critical regions of the compartment, since the occupant's head and upper torso are near these points.

Figure 4.10 compares the acceleration traces of the mid-compartment for Baseline Test 05 and Evaluation Test E9. The peak acceleration for the baseline vehicle was 43 g's, occurring at 50 milliseconds, as opposed to a peak acceleration of 27 g's at 30 milliseconds in the modified vehicle. This represents an improvement of 37 percent. The change in pulse shape is also significant in the assessment of crashworthiness. The baseline pulse is sawtooth with several severe spikes over the total duration of 70 milliseconds. The modified pulse shape is much smoother, showing only minor irregularities over the 70 millisecond duration.

The structural modifications have significantly improved the crashworthiness of the Pinto sedan in front-to-side impacts. The intrusion is 55 percent less and the peak acceleration is 26 percent less, with an improved pulse shape.

### 4.3 Side Pole Impact

#### 4.3.1 20 mph Side Pole Evaluation Tests, E3 and E3A

Evaluation Tests 3 and 3A were side pole impact tests of the modified side structure at 20 mph. A rigid 14-inch diameter pole was mounted to the face of the barrier. The test vehicles were mounted on a wheeled dolly fabricated from rectangular steel tubing. The line of impact was 6 inches forward of the B post. Instrumentation included the 7 basic triaxial accelerometers, photographic coverage of high-speed films and stills, and pre and post test physical measurements.

Test E3 was conducted with the impact occurring on the left side of the vehicle. All of the electronic instrumentation functioned properly, but the high-speed cameras

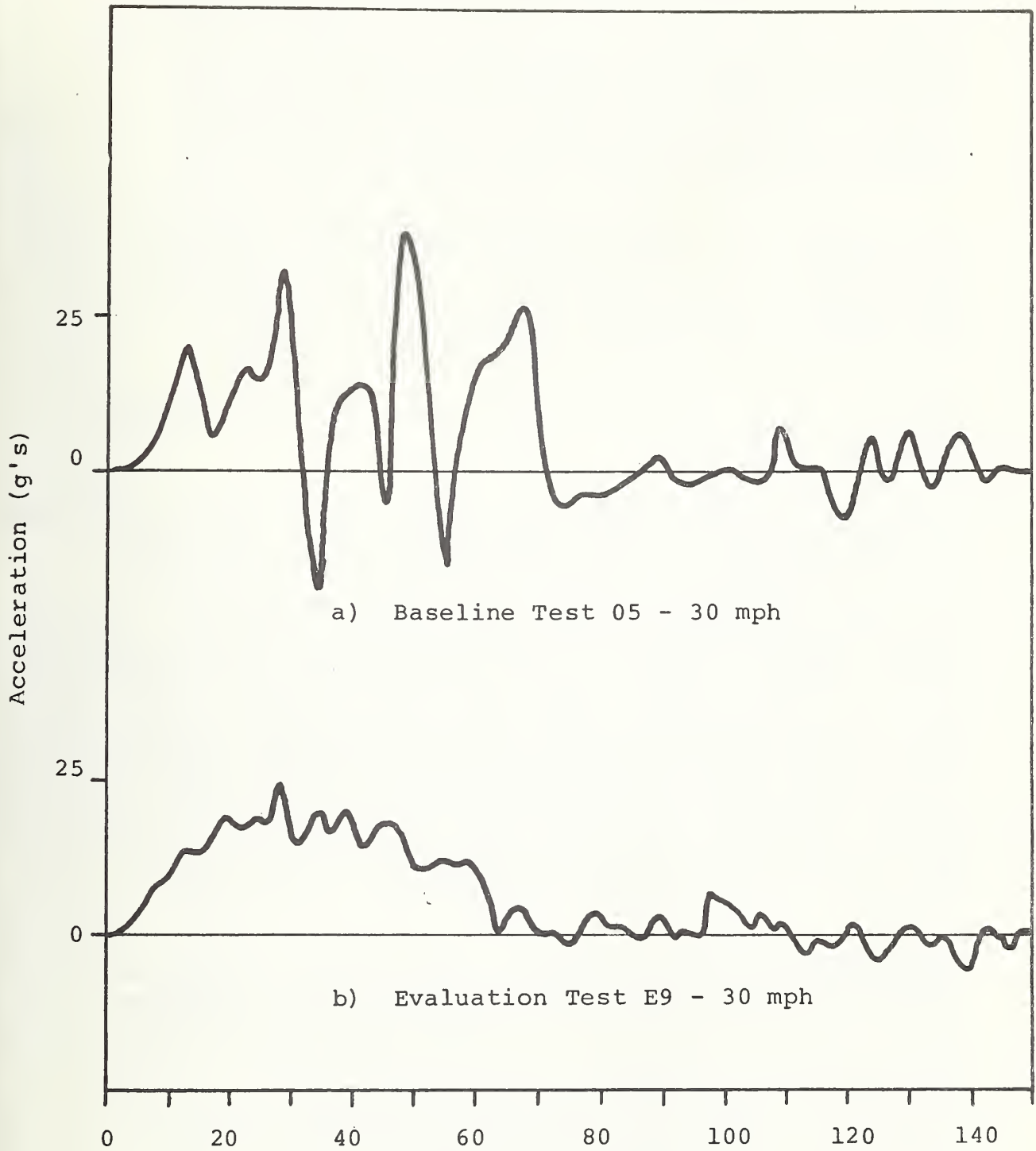


FIGURE 4.10 COMPARTMENT ACCELERATIONS FOR 90° FRONT TO SIDE TESTS 05 & E9

failed to function for the overhead and pit views. The test article was remeasured and used for an identical test, E3A, with impact occurring on the right side of the vehicle. Reuse of the vehicle was acceptable, since the physical damage was essentially limited to local failure on the impacted side of the test article. A comparison of the accelerometer traces of E3 and E3A verifies the appropriateness of this decision.

The complete test reports for E3 and E3A were presented as attachments to the September 1974 progress report. The physical data is summarized in Table 4.4, with the photographic stills shown in Figure 4.11. Impact velocity of E3 was 18.2 mph and E3A was 18.9 mph.

Damage in tests E3 and E3A were similar and are reported by one description.

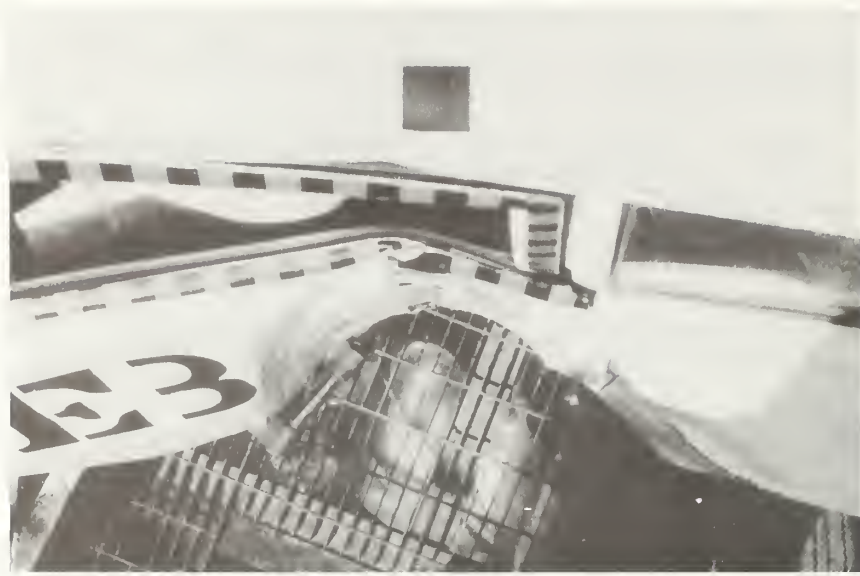
Exterial Structural Damage: The pole first contacted the outer surface of the door, crushing the foam in the lower portion and bending the steel tube in the upper portion. The rocker panel was impacted next, crushing the section and pushing it into the compartment between the two lateral members. The roof rail was contacted by the pole as the vehicle stopped, thus causing indentation in the rail. The rear quarter panel aft of the B post and the B post itself both suffered extensive sheetmetal crush. In the later stages of the crash, the vehicle rotated about 8.5 degrees. The vehicle also underwent beam bending with a total deformation of 6.3 inches for test E3A. No roll of the vehicle was apparent in the crash films.

Passenger Compartment Intrusion: The maximum compartment intrusion was 5.8 inches directly behind the pole impact point. The inside surface of the door was pushed inward. The rocker panel deformation caused local failure at the ends of the lateral members next to the tunnel. The rear footwell floor buckled slightly and the tunnel section suffered only minor damage. The opposite side of the compartment was unaffected by the crash.

TABLE 4.4  
DEVELOPMENT AND EVALUATION TEST DATA  
SIDE POLE IMPACT

	<u>D1</u>	<u>E3</u>	<u>E3A</u>
Test Date		6/10/74	6/14/74
Test Description	Moving Pole Bogie into Side Station- ary Vehicle.	Moving Vehicle Im- pacting Fixed Pole in Side.	
Impacting Velocity (mph)		18.2	18.9
Static Crush (in)	Not Available	Not Available	13.8
Dynamic Crush (in)	Not Available	Not Available	14.2
Intrusions (in)	17	6.5	5.7
Peak Acceleration (g's)	13	17	14
Head Acceleration (g's)	121	*	*
Chest Acceleration (g's)	46	*	*
Bogie Vehicle Weight(lbs)	3285	Not Applicable	Not Applicable

\* Data not taken per NHTSA direction.



A. Damaged Area



B. Final Vehicle Position

FIGURE 4.11 PHOTOGRAPHIC COVERAGE OF TEST E3A



C. Overall View



D. Side Pole Impacts

FIGURE 4.11 CONT'D

#### 4.3.2 Evaluation of Results

Since no baseline side pole impact test was included in the baseline test plan, Development Test D1 (Section 4.1.3.3) provided the comparative data base. Table 4.5 contrasts the results of D2 with E3 and E3A tests. It is seen that the intrusion into the occupant compartment was reduced from 17 inches to approximately 6 inches. The acceleration levels in E3 and E3A were negligible except at the locations nearest the point of impact. At these sensors, the maximum accelerations were about 45 g's. Test D1 showed a maximum acceleration on the vehicle of 13 g's. The tests prove that the modified side structure limits the intrusion into the compartment without creating serious acceleration hazards.

#### 4.4 Front-to-Side Oblique Impact

##### 4.4.1 30 mph 300° Small Front to Small Side Baseline Test, E22

This test determined the aggressivity of the unmodified Pinto when colliding at an angle into the side of another unmodified Pinto. The vehicle to be struck was set across the path of the towed vehicle, angled so that the striking vehicle hit with its left front corner on a point just aft of the front edge of the left door of the struck vehicle (3 inches aft of Door Opening Reference Point, SAE J972a). Both cars carried accelerometers. In addition, instrumented dummies occupied the driver and front passenger seats of the struck car, to measure aggressivity in terms of occupant reaction. Data including occupant accelerations are summarized in Table 4.5; photo coverage is represented in Figure 4.12. Acceleration traces for this and related tests are compared in Figure 4.13.

Structural Damage - Striking Car: The left frame collapsed, and front left sheet metal damage was extensive. Struck Car: The incoming bumper overrode the sill, forcing the door to absorb most of the crash energy. Some sheetmetal aft of the door was also involved as the cars rotated to 220° late in the event.

TABLE 4.5  
 BASELINE AND MODIFIED TEST DATA, 300° FRONT TO SIDE IMPACT

	<u>E22</u>	<u>E20</u>	<u>E19</u>	<u>E23</u>
Test Date	7/75	5/15/75	9/23/75	7/75
Test Description	Front to side impact at 300° striking aft of A post.			
Impacting Velocity (mph)	29.9	29.8	29.4	30.4
<u>Impacting Car</u>	'74 Pinto	'74 LTD	'68 Plymouth w/LTD bumper	Modified '74 Pinto
Static Crush (in)	not available	8.6	23	not available
Peak Accel (g's)	13	6	low	15
<u>Struck Car</u>	'74 Pinto	Modified '74 Pinto	Modified '74 Pinto	'74 Pinto
Intrusion (in)	10.5	5.6	4.5	12.6
Peak Accel. (g's)	13	12	24	17
Driver HIC	63	43*	1110	225
Driver Chest Accel. (g's)	32	26	15	30
Rear Passenger HIC	151	29*	not available	245
Rear Pass. Chest Acc(g's)	20	20	not available	35

\* Head accelerations - HIC not calculated.



FIGURE 4.12 DAMAGE TO STRUCK CAR, E22

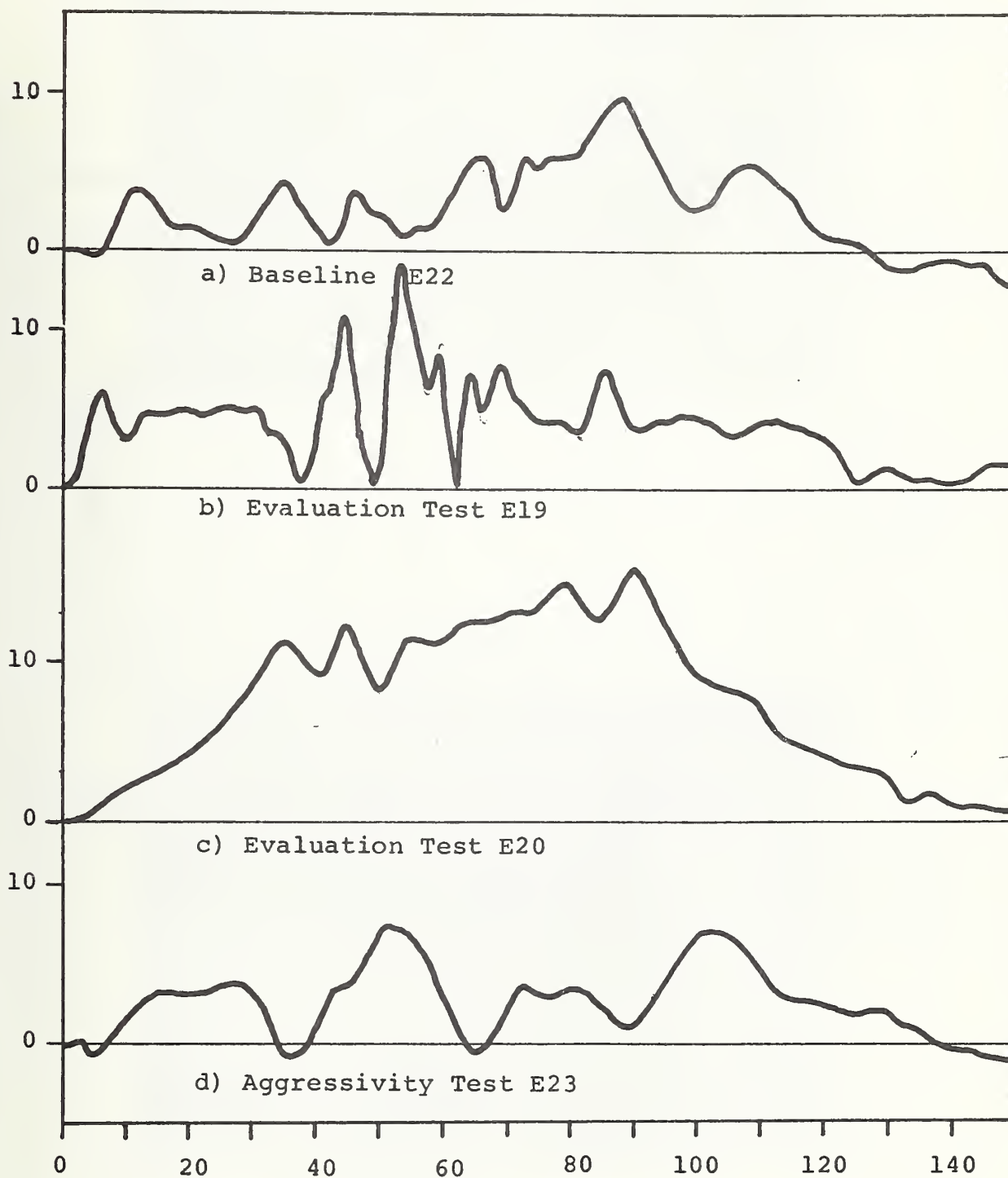


FIGURE 4.13 BASELINE AND EVALUATION TESTS OF SIDE STRUCTURE

Compartment Intrusion: The struck door intruded into the passenger living space. The floor pan started to buckle at the left edge of the tunnel. The striking car compartment was not intruded upon.

#### 4.4.2 30 mph 300° Oblique Large Front to Small Side Evaluation Test, E19

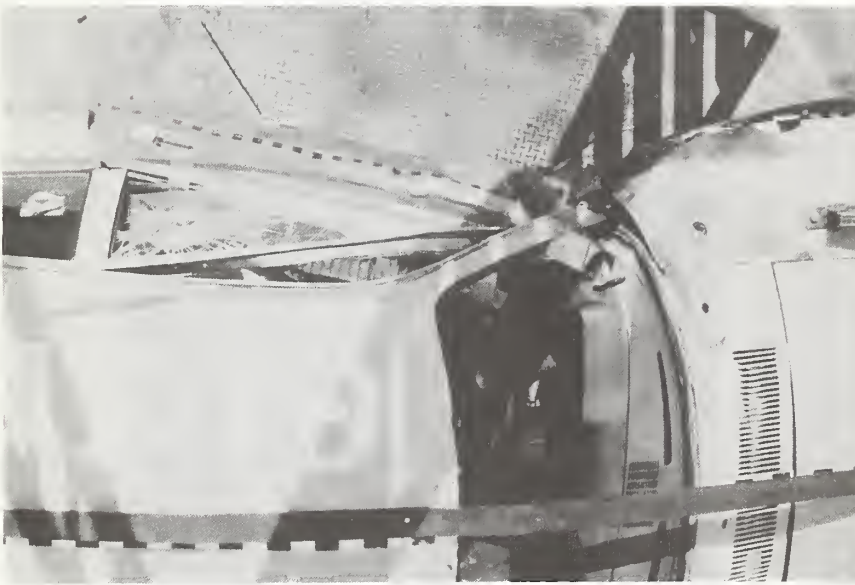
Evaluation Test E19 was a 300° oblique front-to-side impact test with a 1968 Plymouth Fury impacting the side of a modified 1974 Pinto. The nominal velocity was 30 mph with the point of impact located so that the Plymouth bumper just missed the left A post of the Pinto.

The Plymouth bumper was replaced with a 1974 Ford bumper at the direction of the CTM. A 50th percentile male dummy was installed and instrumented, also at the request of the CTM. Dummy instrumentation consisted of triaxial accelerometers mounted in the head and chest. Since there is a maximum of 42 data channels available, some channels were deleted from the impacting car. The deleted channels were the right front compartment triax and the left rear compartment triax. The camera locations were also changed from the Evaluation Test Plan with CTM approval. The pit camera was deleted and an onboard camera to observe the dummy behavior was substituted.

In all other respects, the data acquisition system corresponded to the Evaluation Test Plan. The test report for E19 was presented in the October 1974 progress report. Table 4.5 summarizes the physical and electronic data. The photographic data is reviewed in Figure 4.14. The actual velocity of impact was 29.4 mph.

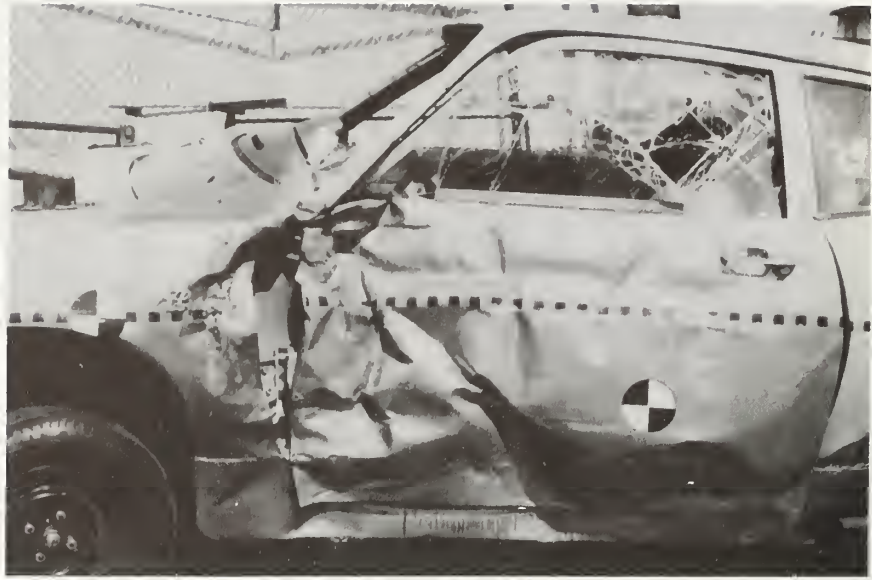


A. Impact



B. Post Test Overhead View of Pinto

FIGURE 4.14 PHOTOGRAPHIC COVERAGE OF TEST E19



C. Post Test Side View of Pinto



D. Post Test Closeup Side View of Pinto

FIGURE 4.14 CONT'D

Exterior Structural Damage: The Plymouth struck the Pinto so that the left edge of the Plymouth just missed the aft surface of the A post. The bumper did not seriously override the rocker. The exterior surface of the door was badly crushed and the window frame distorted, breaking the glass. The rocker panel was crushed and pushed inward. The A post was twisted and pushed inward by the door hinges. The front fender and plenum chamber both suffered sheet metal failure. The roof buckled forward of the B pillar.

The 1974 Ford bumper mounted on the Plymouth was damaged locally at the left mounting point. It bent downward and deformed the mounting structure. The lower left frame was also bent down and aft at the end. The left front fender and the hood suffered extensive sheetmetal buckling. Fender sheetmetal crush interfered with the left door opening but did not prevent it. Total crush of the Plymouth was 23.0 inches.

Compartment Intrusion Damage: The left outboard end of the seat lateral member and the toeboard were crushed. The floors of the front and rear footwells were buckled. The dash buckled at the location of the instrument cluster. The dummy remained in the seat but did suffer a head strike on the window. The right side restraint was bent but remained in place. The seat did not suffer major damage. The interior surface of the door was pushed inward, and the padding was crushed to nearly full depth. No interior damage was noted in the Plymouth.

No baseline test was performed for the oblique front-to-side impact condition. However, post test inspection of the vehicles showed less damage than was anticipated. The maximum compartment intrusion of 4.5 inches was well below the intrusion experienced in the 270° front-to-side impact. The difference in behavior can be attributed to two factors. First, the Plymouth, when impacting at an angle, is much weaker than in an aligned longitudinal crash. This is verified by the greater extent of crush in the Plymouth in E19 over E9. Second, the 1974 Ford bumper has a flatter face with less tendency to override the rocker panel. The rocker panel in E19 showed more crush and less rotation than was noted in Test E9.

The vehicle acceleration levels were reasonable, as is shown in Table 4.5. The chest g levels are also acceptable. The head did not fare as well, since a head strike into the window glass resulted in an HIC of 1110 and an HSI of 1358. Post test evaluation indicates the window was safety plate glass rather than safety sheet. The increased thickness may have caused higher acceleration levels and thus generated the high HIC value.

In summary, the vehicle performed adequately for this side impact, primarily due to good bumper-rocker panel contact. The driver did not survive, due to a head strike into the side window.

#### 4.4.3 30 mph 300° Large Front into Small Side Evaluation Test, E20

This test supported evaluation of the compatibility of the modified design when struck in the non-aligned front-to-side crash mode. The modified Pinto was set at an angle across the tow path of an unmodified 1974 Ford LTD, so that the LTD struck with its left front corner the modified car just aft of the front edge of the left (driver) door (4" aft of the door opening reference point per SAE J072a). Actual impact velocity was 29.75 mph.

Both vehicles carried accelerometers, and full photographic coverage was provided. In addition, instrumented dummies occupied the driver's seat and left rear seat of the Pinto. Cameras mounted on the Pinto records dummy behavior. Data are summarized in Table 4.5. Photo coverage is represented in Figure 4.15. This test was reported on in the progress report dated May 1975 under this contract.

#### Exterior Structural Damage

Pinto: The LTD struck the Pinto behind the A post. The door skin was crushed inwards but remained intact except where the LTD fender ornamentation perforated it. The door glazing cracked but remained in place. The rocker panel was crushed slightly, suggesting uniform lateral



A. Door Sill Area



B. Door of Target Vehicle

FIGURE 4.15 PHOTOGRAPHIC COVERAGE OF TEST E20



C. Location of Head Strike on Glass

FIGURE 4.15 CONT'D

pressure applied by the door. Forward and aft of that portion of the side covered by the door, the car appeared essentially undamaged. Both doors of the Pinto could be opened after the test without force, but the left door required a hard slam to relatch it.

LTD: The LTD bumper stroked aft on its left mount and moved into the fender front hardware. Damage appeared confined to this hardware and to about one-half inch deflection of the left hood and fender.

#### Interior Compartment Intrusion

Pinto: The left outboard end of the seat lateral member and the toe-board were crushed. The floors of the front and rear foot wells were buckled. The dash buckled upwards at the location of the instrument cluster. The driver dummy remained in the seat without benefit of restraint. Evidence of a head strike was noted at two points on the door glazing. A third head strike occurred on the padding over the forward edge of the door. The rear seat dummy also remained seated and showed general head contact with the roof behind the rear window. Both right side restraints were bent but remained in place. The interior surface of the door was pushed inward and the padding was crushed to nearly full depth.

#### 4.4.4 30.4 mph 300° Modified Front into Modified Small Side Evaluation Test, E23.

This test supported the evaluation of the compatibility of the modified design in the non-aligned side impact crash mode. An unmodified Pinto was set at an angle across the towpath of a modified Pinto, so that the towed car struck with its left front corner at a point just aft of the front edge of the struck car's left (driver) door (3" aft of the door opening reference point per SAE J972a). Actual impact velocity was 30.4 mph.

Both cars carried accelerometers, and full photographic coverage was provided. In addition, instrumented dummies occupied the driver's seat and rear left passenger seat of the struck car. Cameras mounted on the struck car recorded dummy behavior.

Data are summarized in Table 4.5. Photographic coverage is represented in Figure 4.16. This test was reported in the progress report dated August 1975 under this contract.

#### Exterior Structural Damage

Struck Vehicle: The modified Pinto struck the side of the unmodified Pinto behind the "A" post. The bumper overrode the sill, forcing the door to absorb the bulk of the energy, without benefit of support along its lower edge except for whatever resistance was furnished by the seat pans.

The crush was largely confined to the door except that the sheet metal directly ahead of the rear wheel was involved and the trailing edge of the front fender also became involved, probably late in the event as the two cars rotated into an almost parallel alignment.

Bullet Vehicle: The modified car (E23) showed almost no damage except for incipient crush of the rightmost 12 inches of the hood and fender box where the crush was limited to a triangular volume about 3" deep at the rightmost corner of the hood.

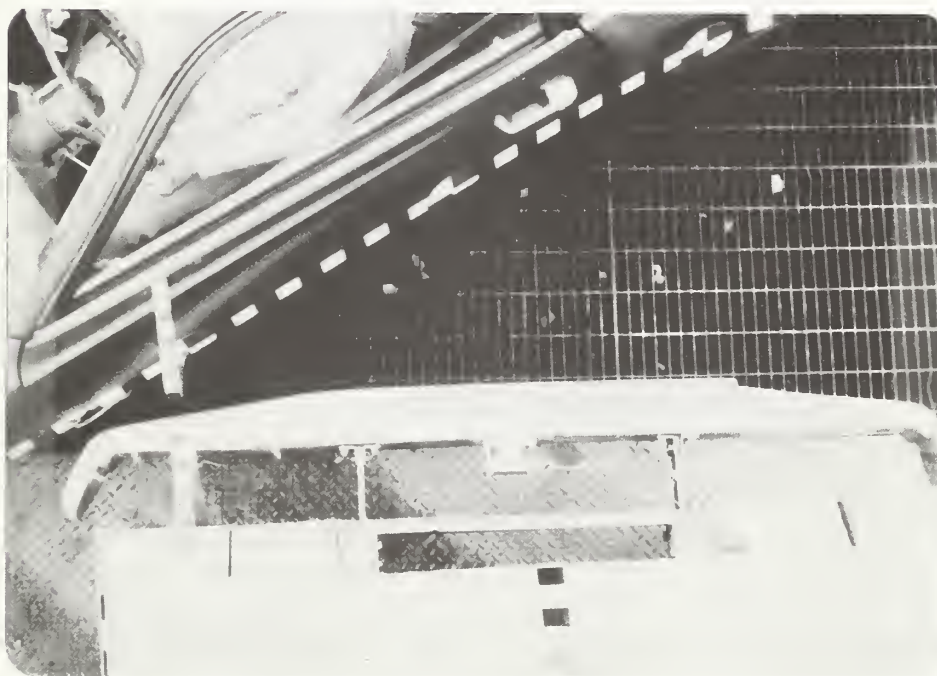
#### Interior Compartment Intrusion

Struck Car: The door intruded into the passenger volume, the intrusion being more severe in this than when the striking car was unmodified (E22). The floor pans showed an incipient buckle on the left tunnel.

Bullet Car: No compartment intrusion occurred in the modified car.



A. Left Rear Quarter



B. Overhead Pre-Crash

FIGURE 4.16 PHOTOGRAPHIC COVERAGE OF TEST E23



C. Overhead Post Crash

FIGURE 4.16 CONT'D

## 5.0 REAR IMPACT CONDITION

### 5.1 Evolution of Design

#### 5.1.1 Design Goal

The design goal, as specified in Contract Modification One, is a front-to-rear impact at 50 mph with the front of a large car striking the rear of the subcompact on center-line at 180°. The accident analysis of Section 2.1 has shown that nearly all of the societal cost of front-to-rear accidents is below 40 mph. Increasing the crashworthiness capability to 50 mph will provide for very little additional reduction of societal cost.

The relatively low societal costs for front-to-rear impacts at high velocities can be largely attributed to the following conditions. First, there is a low occupancy rate for the rear seats. Intrusion into the rear seat area does not create the same probability of injury as intrusion into the front seat living space. Second, the occupants are supported by the seat backs and head rests for rearward acceleration. There is little free flight space to build up high relative velocities between the vehicle and the occupant, thus guaranteeing good "ride down." In addition, the hard contact points are minimized by the soft seat cushions. The final factor is that the nature of the accident limits the relative velocity of two vehicles. Front-to-rear accidents must occur between two vehicles facing in the same direction. A relative velocity of 50 mph would require the car in back to be traveling 50 mph faster than the car in front (or some freak situation in which the car in front is backing up). Such conditions, although they do occasionally occur, are rare and contribute a small portion of the already small societal cost of front-to-rear accidents.

Based on these findings, it can be seen that the benefit-cost ratio does not justify crashworthiness at high velocity in front-to-rear impacts. Nevertheless, Minicars has developed a modified rear structure design which will satisfy the 50-mph front-to-rear crashworthiness criteria.

### 5.1.2 Final Design of Modified Rear Structure

The rear structure of the baseline Pinto sedan is composed of two 1" x 3" channel sections extending from the end of the vehicle to the rear of the compartment. These are on each side of the vehicle and are connected by the deck of the trunk area. Minor additional strength is obtained from the roof and fenders. The baseline rear structure is much lighter and weaker than the baseline front structure. It is not required to support heavy subsystems, such as the engine and steering mechanism, which must be carried by the front structure. The road loads are lighter and, consequently, the frame members are lighter.

The modified design of the rear structure has greatly increased the crush strength of the vehicle at a relatively little increase in weight of 50 pounds. The baseline structure from the B post aft weighed 540 pounds and the modified structure weighs 590 pounds. The modifications use the volumetric structure principle to increase both longitudinal strength and oblique crush strength. Many of the component energy absorbers considered for application to the front end structure were reviewed for their applicability to the rear structure. The two most promising were the honeyfoam members and the sheetmetal-foam structures. The foam and sheetmetal combination was selected for the final design, since the use of honeyfoam resulted in excessively high crush strengths and production costs.

The final design is illustrated in Figure 5.1. There are three main components to the design, as follows:

1. Three longitudinal sheetmetal beams, 3" x 5", extend from the aft of the vehicle to the B post lateral beam. The two outside beams are just inboard of the rear wheel wells. The third beam is on the centerline of the vehicle. All were filled with 2 lb/ft<sup>3</sup> polyurethane foam.
2. The original rear deck is replaced with a 2" thick sheetmetal-foam sandwich panel.

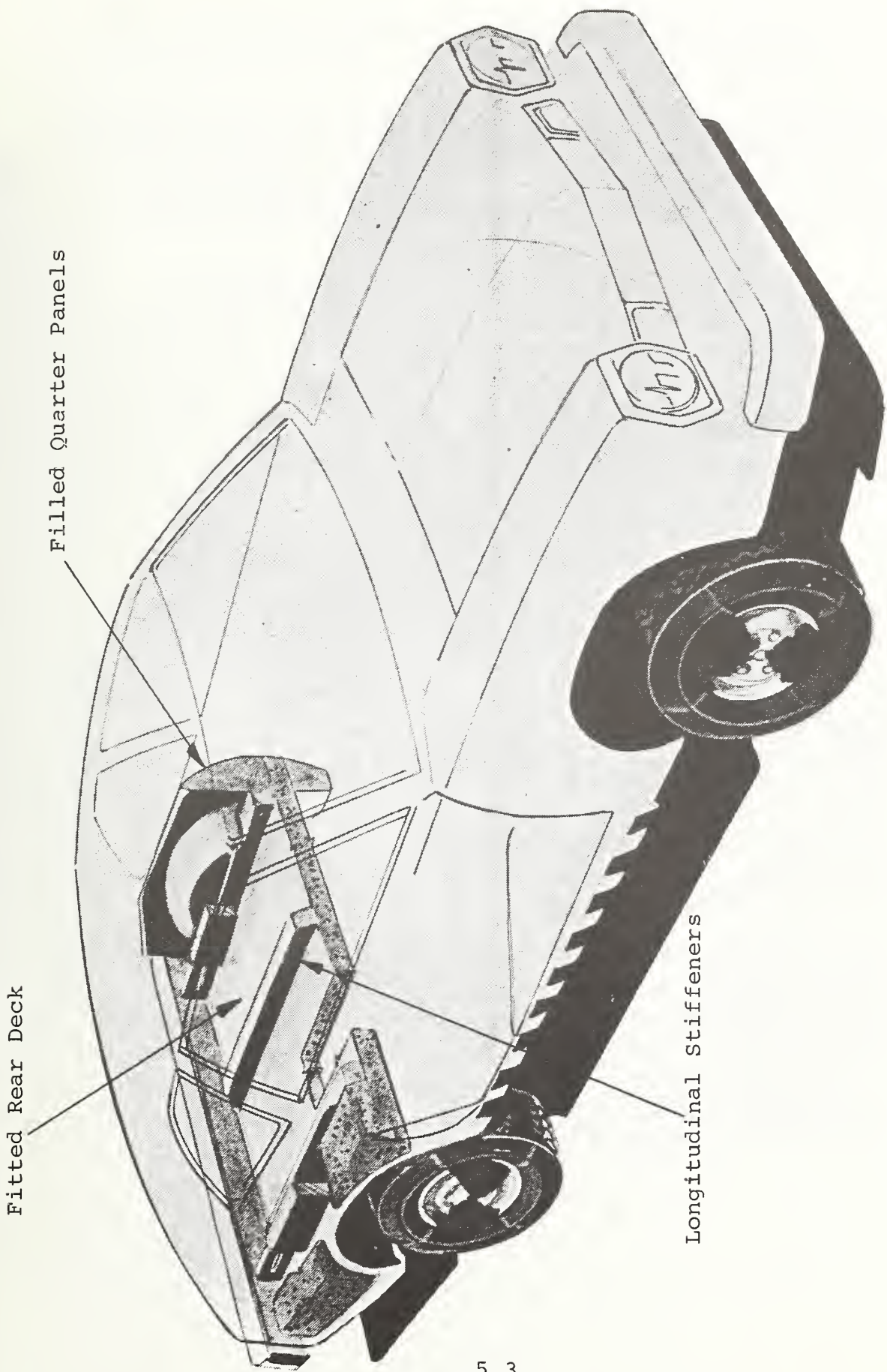


FIGURE 5.1 REAR MODIFICATIONS

3. The rear quarter panels are closed and filled with 2 lb/ft<sup>3</sup> foam.

The longitudinal beams constitute the primary components of the rear structure. They transmit the impact loads to the compartment structure where the B post lateral distributes them to the rocker panels and the tunnel.

The modified trunk deck provides additional lateral stiffness and acts as a shear tie for the longitudinal members. It helps distribute the lateral loads under an oblique rear impact. The closing and filling of the rear quarter panels provides crush capability above the plane of the trunk deck. It absorbs energy in the case of bumper override and resists bending of the primary structure.

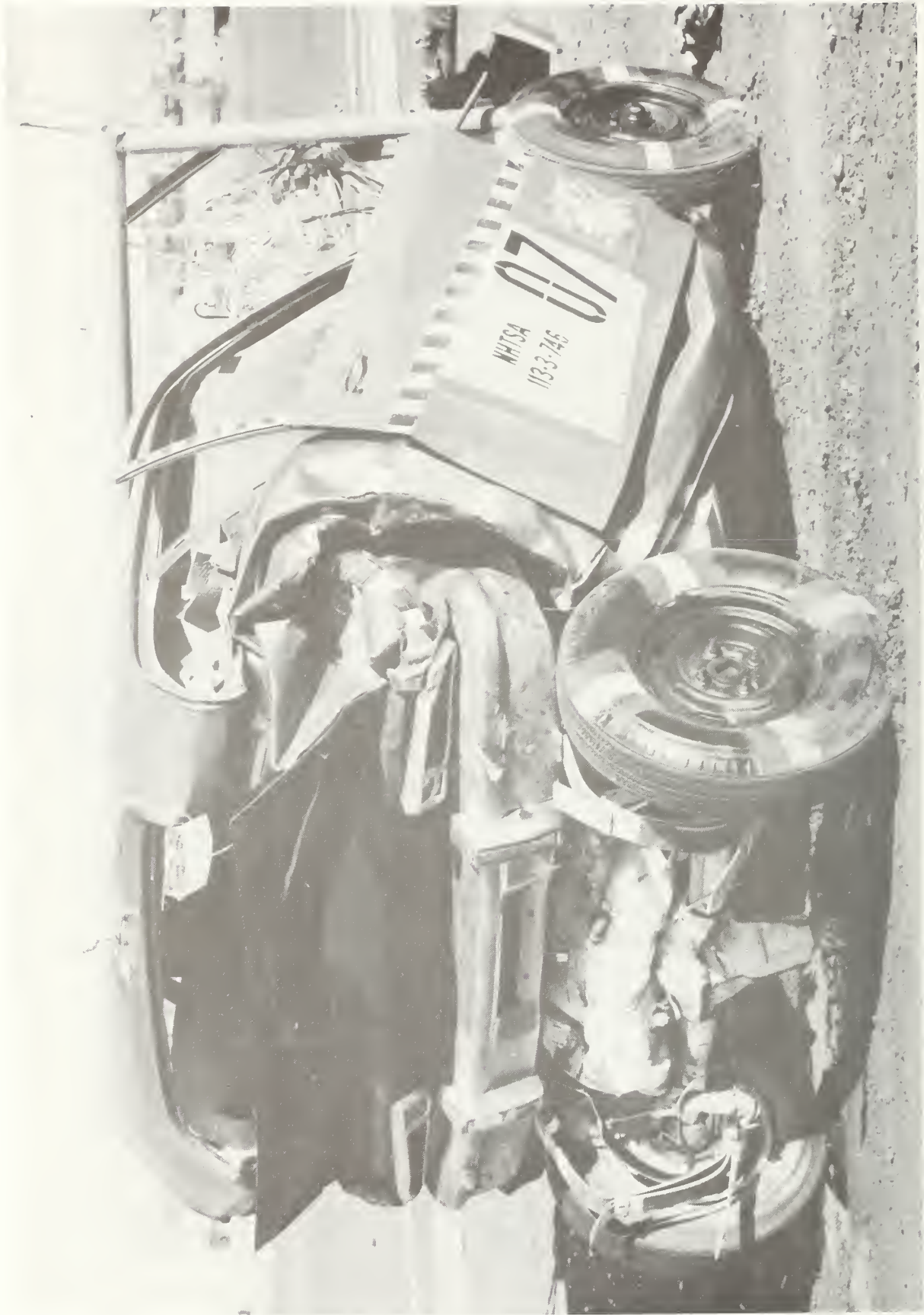
#### 5.2 60-mph Large Front to Small Rear Baseline Test, 07

Baseline Test 07 was a dynamic front-to-rear test of a production 1974 Pinto sedan impacted by a 1968 Plymouth Fury sedan. The target vehicle was the test article used in the 30-mph frontal barrier baseline test. Although damage to the front end was heavy, it did not affect the use of the vehicle for the rear end impact. The target vehicle was placed stationary along the test track and the bullet vehicle (1968 Plymouth) was accelerated to 60.2 mph, impacting the Pinto on centerline at 180°. The 60-mph velocity was in accordance with the design goals in effect at that time.

Both vehicles were fully instrumented with seven triaxial accelerometers located as shown in the baseline test plan. Both vehicles were measured before and after the tests. Photographic coverage included four high-speed cameras, a real-time camera, and pre and post test 35mm slides. The physical test data is summarized in Table 5.1, with an overview of the photographic data shown in Figure 5.2.

TABLE 5.1  
 BASELINE TEST RESULTS FRONT TO REAR IMPACT

	<u>Test 07</u>
Test Date	1/15/74
Test Description	Large sedan front into stationary subcompact rear
Impact Velocity (mph)	60.2
Large Car	'68 Plymouth
Small Car	'74 Pinto (previously used in 30 mph frontal barrier impact)
Static Crush (in)	51.0
Peak Acceleration(g's)	21



A. Post-test Rear Quarter View of Pinto

FIGURE 5.2 PHOTOGRAPHIC COVERAGE OF BASELINE TEST 07



B. Post-test Side View of Pinto

FIGURE 5.2 CONT'D

The results of Test 07 were visually spectacular. The Plymouth contacted the Pinto bumper squarely, crushing the rear frame and trunk. The front wheels of the Plymouth rode up on the rear wheels of the Pinto, forcing the crush upward into the compartment. The rear seat area was completely demolished with metal pushed as far forward as the front seat. The true extent of the damage can only be appreciated by viewing the pictures of Figure 5.2. Acceleration traces at the front seat locations, forward of the damage area, were about 21 g's. The total crush due to the rear impact was 51.0 inches.

Structural damage to the Plymouth was relatively minor. The bumper and front sheet metal were destroyed, but damage did not extend past the engine compartment area. The crush force levels developed in the baseline Pinto were not sufficient to force significant crush in the Plymouth.

## 6.0 BUMPER SUBSYSTEM

### 6.1 Evolution of Design

#### 6.1.1 Design Approach

The contract design goals for the bumper subsystem are as follows:

1. The bumper must sustain a 10-mph barrier impact with no damage.
2. The vehicle must be crashworthy under a 50-mph front pole impact.

Each of these goals presents different problems to the bumper system. The no-damage criterion reflects most strongly on the bumper support system. It establishes minimum force levels for elastic design of the subframe and toeboard. Also, the energy level associated with a 10-mph vehicle impact requires a new approach to the design of the energy absorber.

On the other hand, the 50-mph front pole impact sets a minimum design level for the bumper itself. The bumper must transmit the concentrated force of the pole to the energy management system. The bumper may suffer inelastic deformation but must not collapse under the impact forces.

The emphasis under this contract has been on the function of the bumper and not on styling. The best shape for a bumper should satisfy the following criteria:

1. Sharp points should be avoided, to prevent presenting a hazard during pedestrian impact and to prevent load concentration during vehicle impact.
2. The surface should be vertical, to decrease the tendency to override or underide the opposing vehicle.
3. The bumper should curve around the vehicle, to provide extra protection for the 11 and 1 o'clock accidents.
4. The face of the bumper should be high and deep enough to contact bumpers of all other vehicles on the road.

Most present production bumpers have been designed by styling departments, with little concern for the basic function of the bumpers. Only under pressure from the Department of Transportation have auto manufacturers recently improved the strength of the bumper and its support system. In the case of the Pinto sedan, compliance with the 5-mph no-damage criterion dictated an increase in strength of both the bumper and the frame. The changes took the form of an add-on channel section to the bumper and increased support for the subframe. The trouble with add-on modifications is that they are seldom efficient. They are generally makeshift fixes that increase both the weight and the price of the vehicle. The Pinto bumper, modified for the 5-mph criterion, weighs 136 pounds.

Stylists have also shown a strong tendency to fit the shape of the bumper to the contour of the car. The results are usually free flowing curves with points at very inopportune locations. The points present hazards to pedestrians as well as providing concentrated loading points into an impacted vehicle. A flat vertical surface across the face of the vehicle is the best surface for all frontal or rear impacts. The vertical surface is extremely important in discouraging override and underride, either of which will direct the crush of the vehicles away from the principle energy management systems. An override situation will cause excessive crush in the vehicle whose frame is underneath. If the modified subcompact were to override, this could also cause the hood to be above the crush and thus not function as an energy absorber. Test E25 illustrates this point (Figure 3.36).

Override can also occur if the two impacting bumpers are not at the same height above the ground. In spite of the bumper height regulations, many vehicles on the road have bumpers well above or below the 20" specifications. To insure good contact with these bumpers, it is important for a crashworthy bumper to have a deep face surface. Although such a large flat surface does not meet the currently acceptable styling designs, it could be properly packaged and sold to the public. A minimum of 6" was selected for the modified subcompact bumper, giving a face from 17" to 23" above the ground. This is a minimum acceptable value and could be much larger. The choice was based on perturbing the design as little as possible.

The one area where styling and function could be compatible is the curving of the bumper around the 11 and 1 o'clock positions. A bumper with this feature will help to spread the impact energies of oblique vehicle-to-vehicle impacts. Since these types of accidents were not part of the design goals of the contract, the curving feature was not included in the design of the modified bumper.

#### 6.1.2 Design of the Low-Speed Energy Absorbers

The increase from the present 5-mph no-damage bumper criterion to a 10-mph requirement constitutes a fourfold increase in the energy level the bumper system must survive. Thus the new system must either provide four times the stroke or four times the force, or some combination of these. Also, the criterion must be applied to both front and rear bumpers, doubling the problem.

Two types of low-speed energy absorbers are used on the majority of new cars. These are an elastomeric pad type and a short stroke hydraulic unit. The first type operates by shear deformation of an elastomeric pad as the energy absorption mechanism. The second type absorbs energy by hydraulic action. Both of these mechanisms weigh in the 15-pound range. To increase their capacities by fourfold would raise the weight by at least 300 percent. Thus the units for a 10-mph capability would weigh between 45 and 50 pounds! With two units on the rear and two on the front, the total component weight would be nearly 200 pounds. A new approach to the problem had to be developed or the bumper system would become ruinously heavy.

Minicars considered many possible alternatives during the conceptualization stage but, ultimately, selected two possibilities for fabrication and test. The first was a linear friction device with a  $\frac{1}{4}$ " thick steel bar sliding between two friction pads mounted on the inside of the foreframe. Figure 6.1 shows the EA unit. The slider is mounted to the bumper by angle brackets. The friction force is set by bolt pressure. The friction material is Raybestos disc brake pad material.

The second device was a coiled friction spring as shown in Figure 6.2. The resisting force is generated by the metal coils

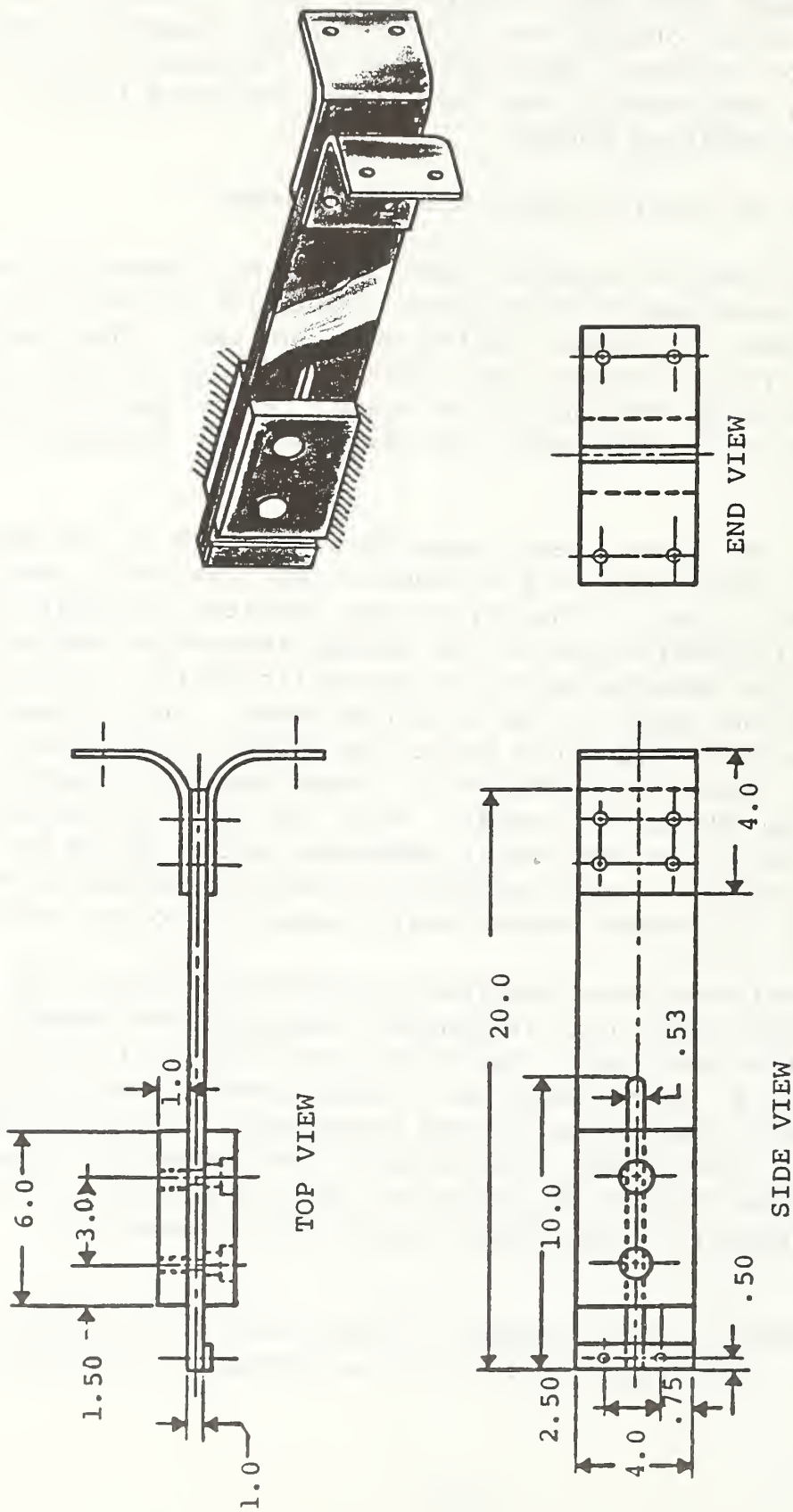


FIGURE 6.1 FRICTION PAD BUMPER ENERGY ABSORBER

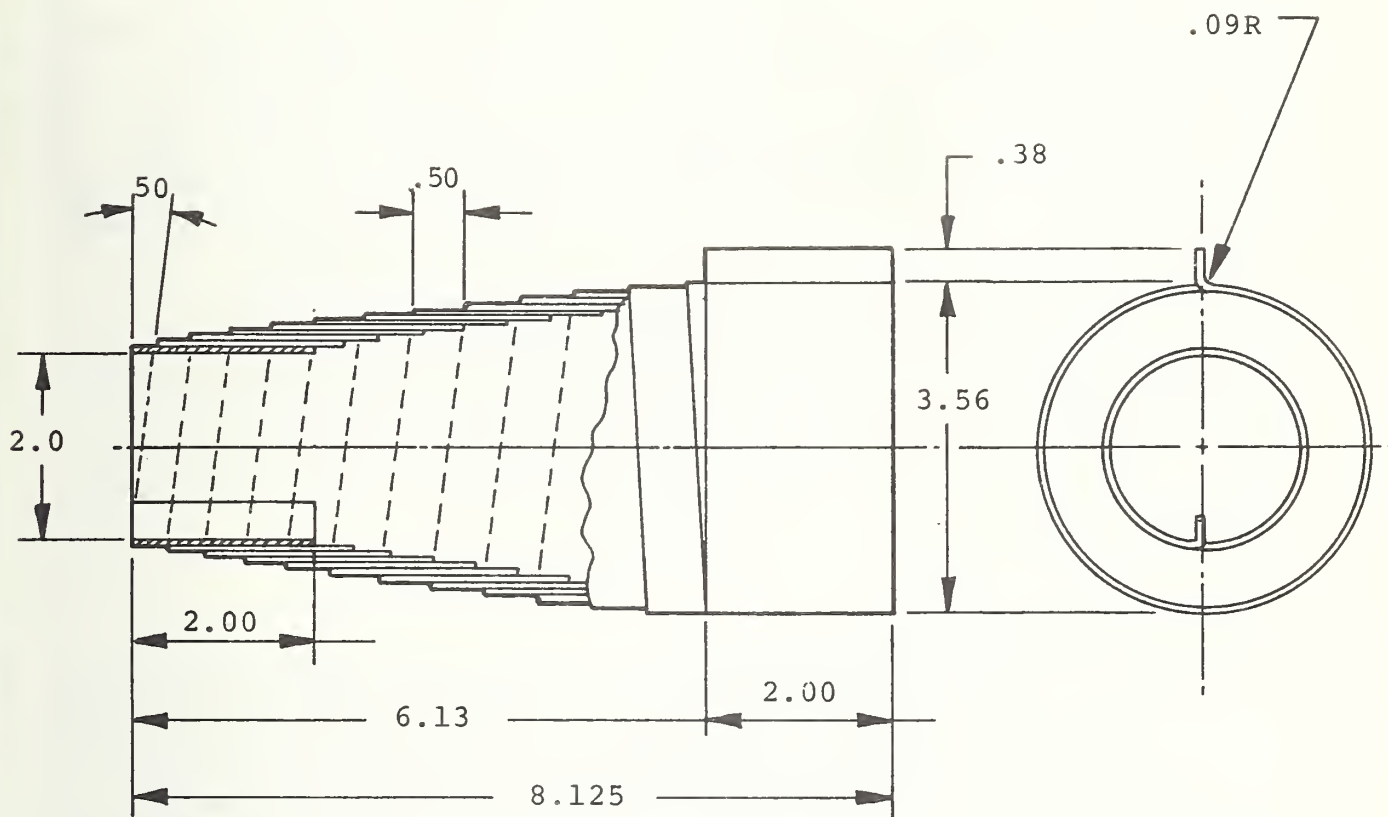


FIGURE 6.2 COIL TYPE BUMPER ENERGY ABSORBER

sliding against each other as the spring collapses. Coils are formed by spirally wrapping aluminum or steel strips around a mandrel. The force of collapse is adjusted by tightening the spiral by turning one end with respect to the other. Mounting to the bumper and frame must be accomplished by end blocks.

Both of these units were tested on the Minicar sled. The runs were at 10 mph with a weight of 1,000 pounds. The linear friction device worked as anticipated. An average force of 8,000 pounds was attained through a displacement of 5". The initial peak acceleration seen in Figure 6.3 is probably due to the effect of static friction as opposed to dynamic friction.

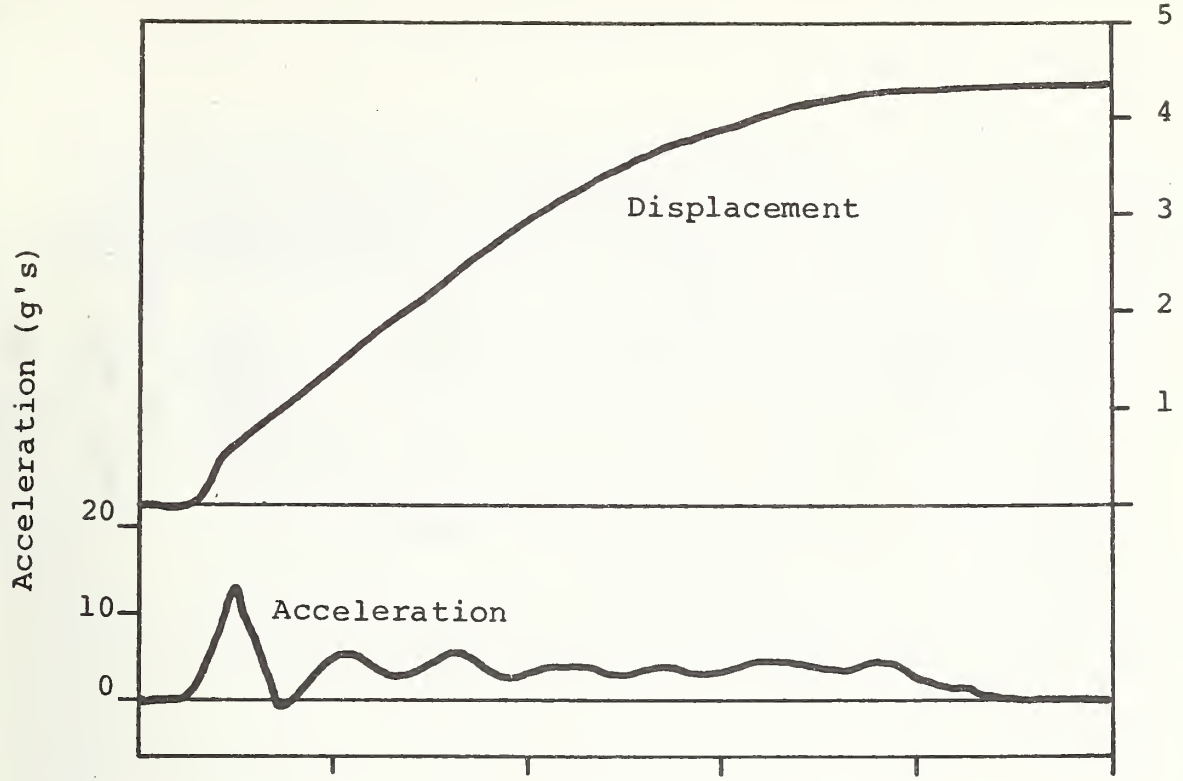
The coiled friction device developed extremely erratic behavior with very low average values. The anomaly in behavior of this unit was due to geometrical irregularities inherent in the fabrication procedure. These difficulties could be overcome, but the success of the linear absorber, combined with its simple fabrication and installation, made it the selection for final design.

### 6.1.3 Design of Bumper

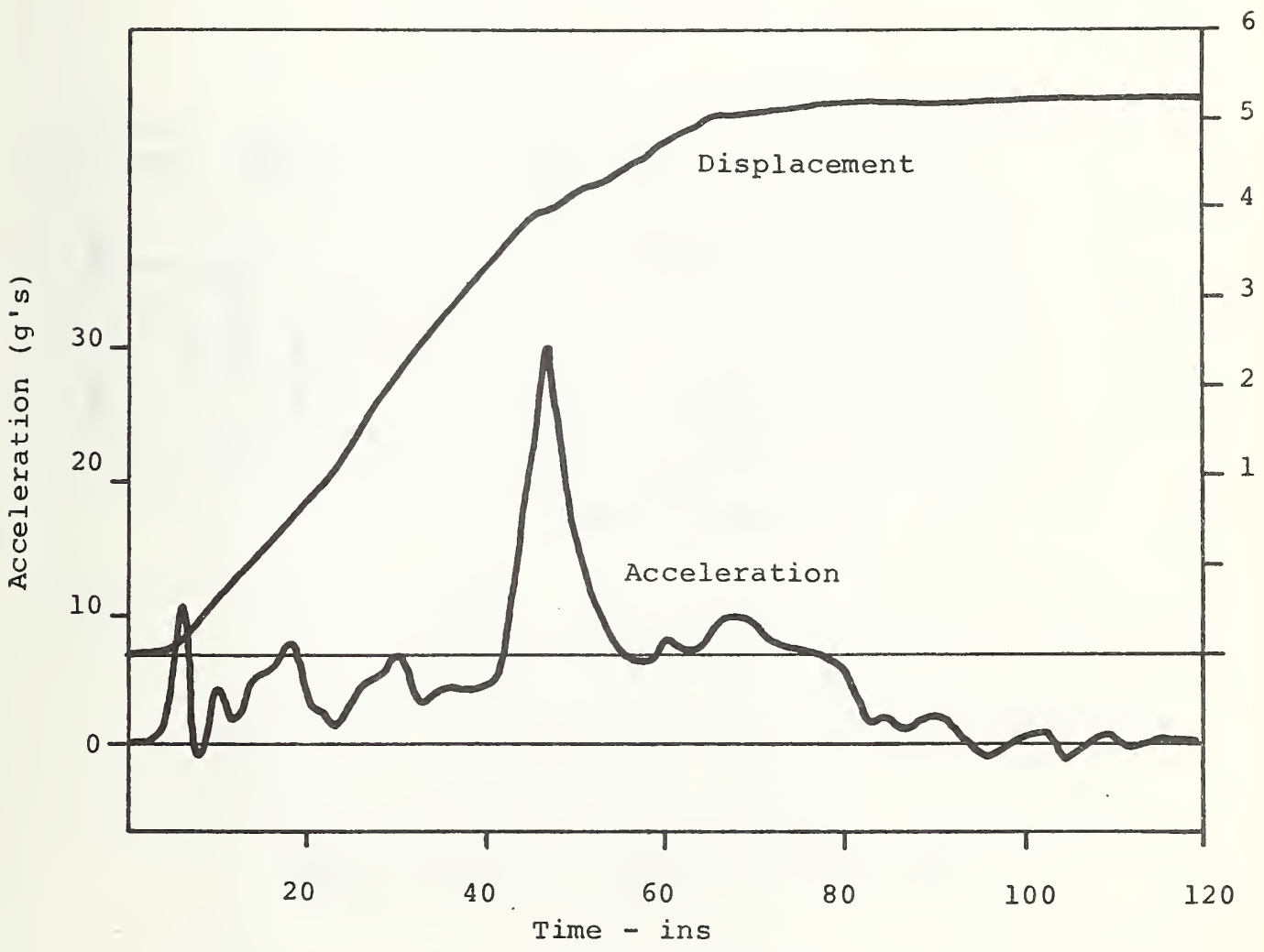
The design of the bumper itself was a combined effort of Minicars and Stanford Research Institute. SRI has had considerable experience in auto safety bumper design, beginning with the Ford ESV and continuing with NHTSA scale modeling contracts. Based on Minicars' established criteria, SRI selected several trial designs including both steel and aluminum sections. These trial designs were tested on SRI's scale model test facility. The tests corresponded to a 50-mph frontal pole impact.

Two designs were recommended to Minicars as possible candidates for use on the modified subcompact vehicle. One of the designs consisted of two 3" x 3/8" square aluminum tubes welded together to form a 6" x 3" section with a 3/4" middle web. The second design was a 5.25 x 2.6 inch 4130 steel tube, 1/4" thick. These two designs are shown in Figure 6.4.

Minicars selected the aluminum design because of its light weight of 30 pounds, as opposed to 43 pounds for the steel bumper. The failure mode for a bumper under pole impact is



a) 10 mph Impact Test



b) 15 mph Impact Test

FIGURE 6.3 FRICTION PAD ENERGY ABSORBER TEST DATA

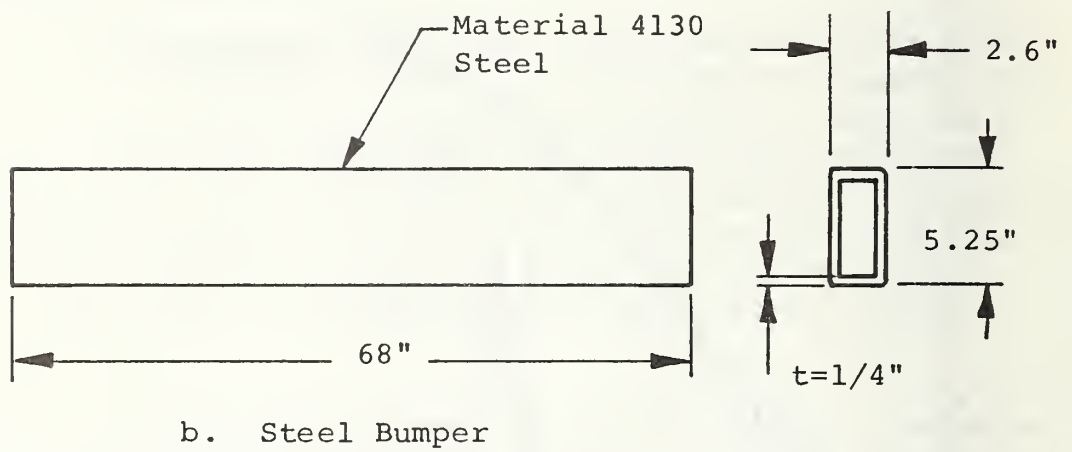
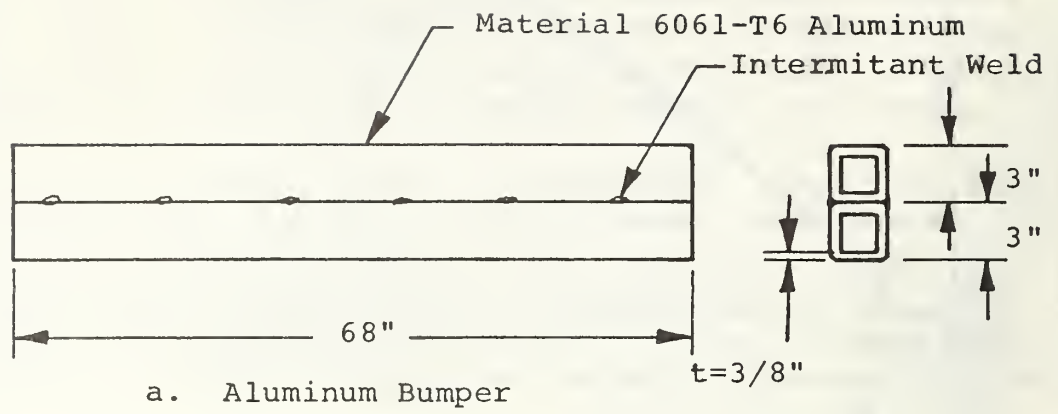


FIGURE 6.4 ALTERNATIVE BUMPER DESIGNS

a local failure directly under the load. The webs fail by crippling, allowing the flanges to move together decreasing the section modulus of the member. It is important in bumper design to provide adequate web area to prevent crippling. Since crippling is a function of thickness more than strength, it is weight efficient to use aluminum rather than steel.

## 6.2 Evaluation Tests

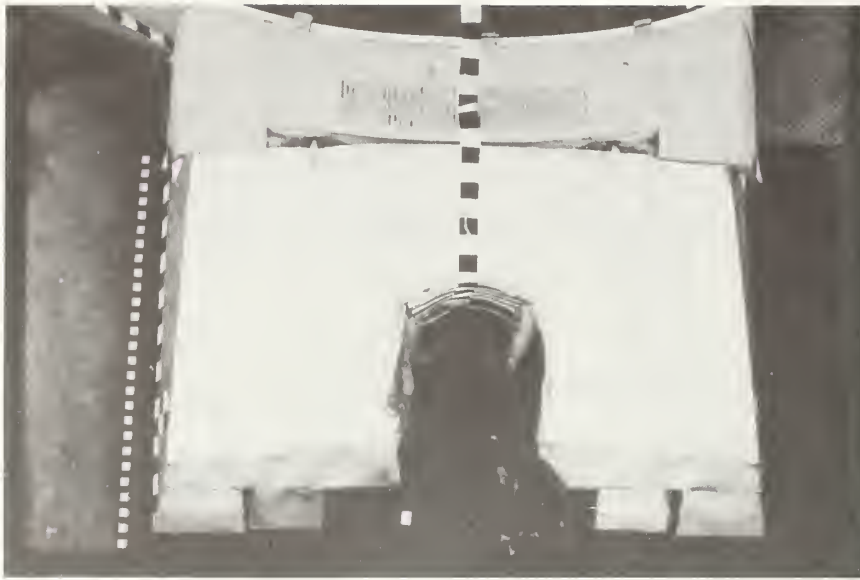
### 6.2.1 10-mph Bumper Test, D6

The 10-mph no-damage impact capability was demonstrated by Test D6. This test was run using the vehicle designated for Test E1B. It was run as a preliminary to that test with the instrumentation and test hardware as described in Section 3.3.2.3. The actual test velocity was 9.5 mph. The bumper behaved as anticipated, with a stroke of 5 1/2". No damage was observed on the bumper or the vehicle.

### 6.2.2 40 mph Front Pole Test, E2

Test E2 was a 40-mph frontal pole impact test of the modified subcompact vehicle. The test was conducted at a lower velocity than the design goal, at the discretion of the CTM. It was felt that more valuable information could be obtained at this impact level. The test article was instrumented with the standard seven triaxial accelerometers. Photographic coverage included four high-speed cameras, a real-time camera, and 35mm still photographs both pre and post test. Physical measurements of the vehicle were taken both before and after the test to determine the crush distances. The photographic data is summarized in Figure 6.5 and the physical data is presented in Table 6.1. The complete test report is presented as an attachment to the October 1974 progress report.

Exterior Structural Damage: The rigid pole contacted the bumper about 1-1/2" left of center. The EA units stroked the full 6". The bumper bent under pole impact to approximately a 20° angle. The left lower frame formed 4 complete accordian folds and developed an S shaped failure, with the forward portion sliding inside the aft portion. The right lower frame started to form the S shape failure, with the forward portion outside the aft portion, and then bent upward at the S Section.



A. Top View With Hood In Place

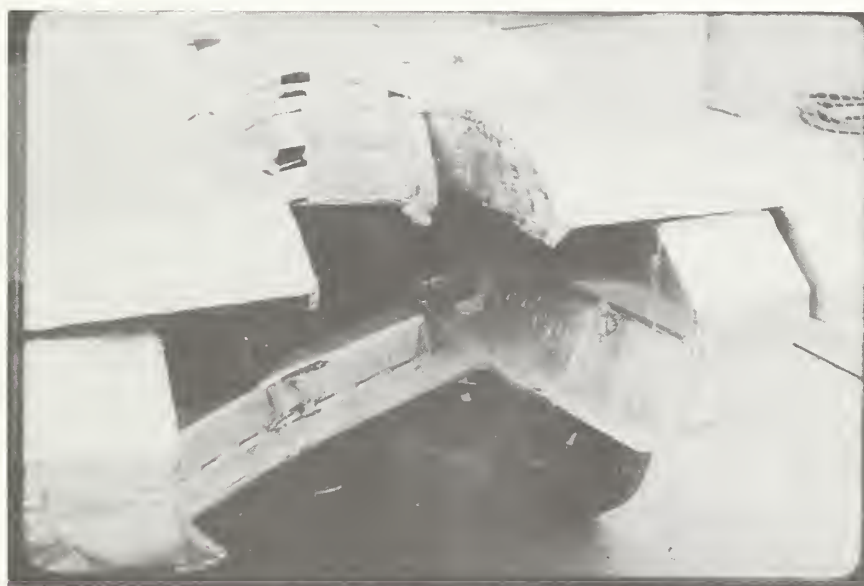


B. Top View of Engine Compartment

FIGURE 6.5 PHOTOGRAPHIC COVERAGE OF TEST E2



C. Front View



D. View of Hood Damage

FIGURE 6.5 CONT'D

TABLE 6.1 EVALUATION TEST DATA  
FRONTAL POLE IMPACT

Test Date	8/29/74
Test Description	Subcompact Front to a Fixed Pole at Centerline of Vehicle
Impact Velocity (mph)	39.0
Static Crush (inches)	33.3
A Post Movement (inches)	0.7
Peak Acceleration (g's)	24

The engine cross member assembly separated from the frames and moved aft on the right side. The cross member hit and crushed the stock aft frames at the toeboards. The engine hit the right side of the firewall under the plenum and pushed rearward. The aft end of the transmission impacted the tunnel forward of the seat lateral. The center portion of the hood under the pole crushed 18.5", but the outer edges were not affected. Slight sheetmetal damage occurred on the left rear corner of the hood. The roof buckled just forward of the B posts. The doors were not damaged and opened after the crash. Total static crush was 33.3".

Interior Compartment Damage: Interior damage was limited to the tunnel, toeboards, and front foot wells. The tunnel was crushed at the change in section located on the forward edge of the seat lateral member. Sheetmetal buckling also occurred in the tunnel walls. The toeboards were pushed in by the aft frame about 2". The footwell floors showed sheetmetal buckling. Total A post movement was 0.7".

The acceleration trace for the trunk accelerometer is shown in Figure 6.6. The vehicle developed a long low pulse with a peak value of approximately 25 g's and a duration of over 100 ms. Based on these results, the 50-mph velocity would not have created any significant problems. The bumper subsystem design was validated by this test.

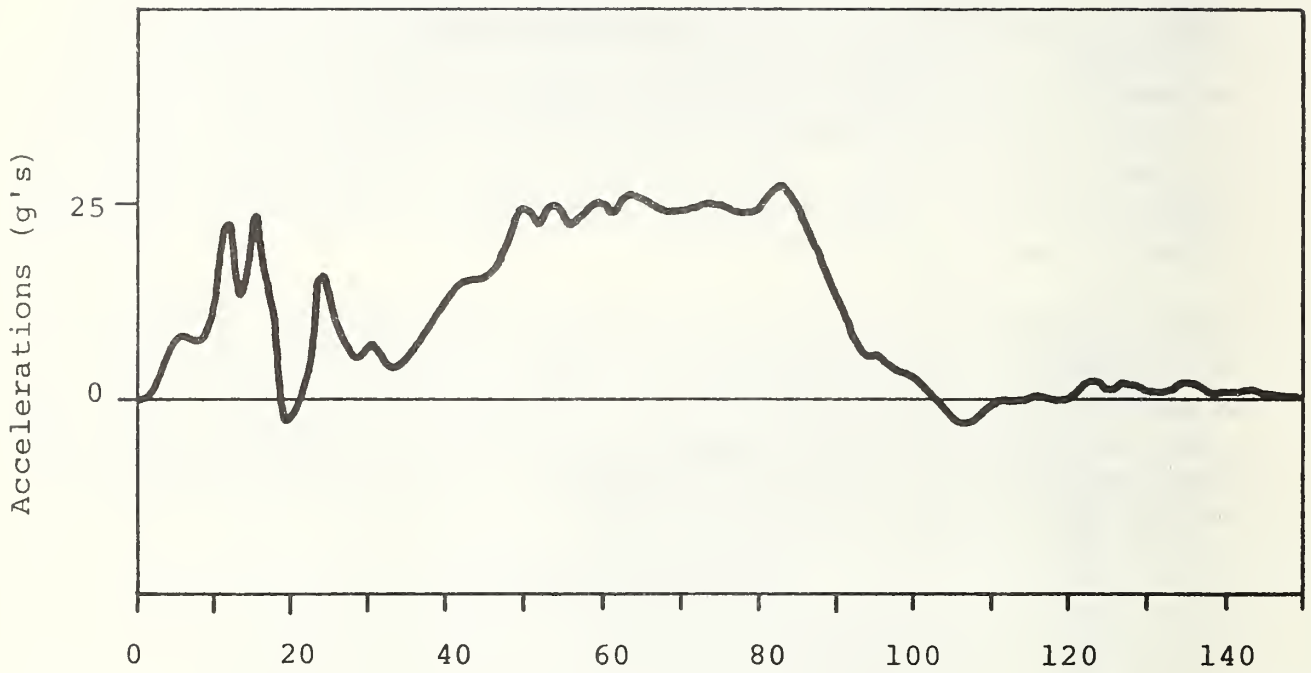


FIGURE 6.6 FRONTAL ACCELERATION FOR  
FRONTAL POLE TEST E2

TL 242 .T27

CRASHWORTHY  
SUBCOMPACT

*Handwritten signature*

Form DOT F 1720  
FORMERLY FORM DOT 1

DOT LIBRARY  
  
00092673